Grafted cellulose acetate derivatives for the purification of biofuels by a sustainable membrane separation process

Faten Hassan Hassan Abdellatif

▶ **To cite this version:**

Faten Hassan Hassan Abdellatif. Grafted cellulose acetate derivatives for the purification of biofuels by a sustainable membrane separation process. Chemical and Process Engineering. Université de Lorraine, 2016. English. NNT : 2016LORR0015 . tel-01673821

HAL Id: tel-01673821

https://theses.hal.science/tel-01673821

Submitted on 1 Jan 2018

HAL is a multi-disciplinary open access archive for the deposit and dissemination of scientific research documents, whether they are published or not. The documents may come from teaching and research institutions in France or abroad, or from public or private research centers.

L'archive ouverte pluridisciplinaire **HAL**, est destinée au dépôt et à la diffusion de documents scientifiques de niveau recherche, publiés ou non, émanant des établissements d'enseignement et de recherche français ou étrangers, des laboratoires publics ou privés.

AVERTISSEMENT

Ce document est le fruit d'un long travail approuvé par le jury de soutenance et mis à disposition de l'ensemble de la communauté universitaire élargie.

Il est soumis à la propriété intellectuelle de l'auteur. Ceci implique une obligation de citation et de référencement lors de l'utilisation de ce document.

D'autre part, toute contrefaçon, plagiat, reproduction illicite encourt une poursuite pénale.

Contact : ddoc-theses-contact@univ-lorraine.fr

LIENS

Code de la Propriété Intellectuelle. articles L 122. 4
Code de la Propriété Intellectuelle. articles L 335.2- L 335.10
http://www.cfcopies.com/V2/leg/leg_droi.php
http://www.culture.gouv.fr/culture/infos-pratiques/droits/protection.htm

UNIVERSITE DE LORRAINE (UL)
ECOLE NATIONALE SUPERIEURE DES INDUSTRIES CHIMIQUES (ENSIC)
LABORATOIRE DE CHIMIE PHYSIQUE MACROMOLECULAIRE (LCPM)
ECOLE DOCTORALE SCIENCE ET INGENIERIE ED 410 :
Ressources, Procédés, Produits, Environnement (RP2E)

THESE

Présentée pour obtenir le titre de

DOCTEUR DE L'UNIVERSITE DE LORRAINE
Spécialité : Génie des Procédés et des Produits

Par

Faten HASSAN HASSAN ABDELLATIF

Grafted cellulose acetate derivatives for the purification of biofuels by a sustainable membrane separation process.

Soutenance confidentielle le mercredi 9 mars 2016

COMPOSITION DU JURY

Mme Anne JONQUIERES	Université de Lorraine/ENSIC	Directeur de thèse
Mme Eliane ESPUCHE	Université Claude Bernard Lyon 1	Rapporteur
Mr Jean-Jacques ROBIN	Université Montpellier 2	Rapporteur
Mme Carole ARNAL-HERAULT	Université de Lorraine/ENSIC	Co-directeur de thèse
Membre invité :		
M. Jérôme BABIN	Université de Lorraine/ENSIC	Membre invité

Laboratoire de Chimie Physique Macromoléculaire UMR CNRS-UL 7375, ENSIC,
1 rue Grandville, BP 20451, 54001 Nancy Cedex.

ACKNOWLEDGMENTS

First of all, I am grateful to **Almighty God** for giving me the strength to fulfill this work.

I would like to express my sincere gratitude to my supervisor **Prof. Anne Jonquieres** for her continuous support, her patience, motivation, immense knowledge, aspiring guidance, invaluably constructive criticism and friendly advices during my PhD study. Her guidance helped me in all the time of research and writing of this thesis. The enjoyment and passion she has for scientific research was infectious and motivational for me, even during tough periods in the Ph.D. quest. I could not have imagined having a better supervisor and mentor for my Ph.D study.

I would like to express my deepest gratitude to my Co-supervisor, **Dr. Carole ARNAL-HERAULT,** and **Dr. Jérôme BABIN** for their excellent guidance, patience, and providing me with excellent ideas, explanations and suggestions throughout my study. I am extremely grateful for their assistance and support.

I would also like to thank both Reviewers, **Prof. Eliane ESPUCHE** and **Prof. Jean-Jacques ROBIN** for having accepted and taken their time to review my manuscript, and for fruitful discussions during my PhD defense.

I would like to thank the **Université de Lorraine** and **Erasmus mundus ELEMENT Programme** for giving me the opportunity to fulfill my PhD.

Very special thanks goes out to Laboratory Physical Chemistry of Macromolecules (LCPM) in Nancy, where this work was accomplished. I would like to thank **Prof Alain Durand**, director of LCPM, for hosting me in this laboratory.

My deepest thanking to **Prof Laurent David** for his contribution in the determination of the morphology of the synthesized membranes by synchrotron SAXS.

My thanks to **Mr. Olivier Fabre**, Engineer at LCPM for NMR analyzes and **Mr. Henri Lenda** former technician at LCPM for pervaporation analysis for their appreciated assistance during my PhD.

I would like also to thank **Mrs. Marie-Christine Grassiot, Mrs. Mathilde Achard, Mr. Jean-Claude Silvaut** for their help and technical support throughout my work. Also thank **to Mrs. Jeanine Fourier, Mrs. Amélie Trottman** and **Mrs. Nathalie Brenon** for their administrative assistance and usual kindness.

I am much thankful to all my current and former colleagues with whom I had a great time and were able to put a good friendly atmosphere in the laboratory: **Dr.Mohamed Mehawed, Dr. Soliman Soliman, Asma, Xavier**.

Last but not the least, I would like to thank my family: **my parents** and **my husband** who were waiting for this moment and to **my brothers, sisters**, and **my beautiful Kids** for supporting me spiritually throughout this thesis and during my life in general.

Grafted cellulose acetate derivatives for the purification of biofuels by a sustainable membrane separation process

Abstract

During the industrial production of ethyl *tert*-butyl ether (ETBE) biofuel, this ether forms an azeotropic mixture containing 20 wt% of ethanol. Compared to the ternary distillation currently used for ETBE purification, the pervaporation membrane process could offer an interesting alternative and important energy savings. Cellulosic membranes have been mainly reported for this application. In particular, the selectivity of cellulose acetate (CA) was outstanding but its flux was too low. In this work, different grafting strategies were developed for improving the CA membrane properties for ETBE purification. The first strategy used "click" chemistry to graft CA with polylactide oligomers leading to original bio-based membranes for the targeted application. The grafting of ionic liquids onto CA was then investigated first by "click" chemistry (unsuccessful due to side reactions) and then by another two-step strategy implying simple nucleophilic substitution. A second series of cellulosic materials was obtained by grafting different ionic liquids containing the same bromide anion and different cations (imidazolium, pyridinium or ammonium) with increasing polar feature. A third series of new membrane materials was finally developed by exchanging the bromide anion with different anions Tf_2N^-, BF_4^-, and AcO^-. The membrane properties of all grafted CA membranes were finally assessed on the basis of the sorption-diffusion model, which revealed that both sorption and pervaporation properties were improved by the different grafting strategies.

Key words: cellulose acetate, grafting, "click" chemistry, polylactide, ionic liquids, membranes, bio-fuel, permeability, structure-property relationships

Dérivés greffés de l'acétate de cellulose pour la purification d'un biocarburant par un procédé de séparation membranaire dans une politique de développement durable

Résumé

Lors de la production industrielle du biocarburant éthyl *tert*-butyl éther (ETBE), cet éther forme un azéotrope contenant 20 % d'éthanol. Comparé à la distillation ternaire utilisée pour la purification de l'ETBE, le procédé membranaire de pervaporation pourrait offrir une alternative intéressante et d'importantes économies d'énergie. Des membranes cellulosiques ont principalement été décrites pour cette application. En particulier, la sélectivité de l'acétate de cellulose (CA) était extrêmement élevée mais son flux trop faible. Dans cette thèse, différentes stratégies de greffage ont été explorées pour améliorer ses propriétés membranaires. La première a mis en œuvre la chimie "click" pour le greffage d'oligomères polylactide, conduisant à des membranes bio-sourcés originales pour cette application. Le greffage de liquides ioniques (LIs) a ensuite été étudié, initialement par chimie "click" (échec dû à des réactions secondaires) puis par une autre stratégie en 2 étapes impliquant une simple substitution nucléophile. Une seconde série de matériaux cellulosiques a été obtenue avec des LIs contenant un même anion bromure et différents cations (imidazolium, pyridinium ou ammonium) de polarité croissante. Une troisième série de nouveaux matériaux membranaires a ensuite été développée en échangeant l'anion bromure par différents anions Tf_2N^-, BF_4^-, and AcO^-. Les propriétés membranaires de tous les matériaux greffés ont finalement été évaluées sur la base du modèle de sorption-diffusion, révélant que la sorption et la pervaporation étaient conjointement améliorées par les différentes stratégies de greffage développées.

Mots clés : acétate de cellulose, greffage, chimie "click", polylactide, liquides ioniques, membranes, biocarburant, perméabilité, relations propriétés-structures

Laboratoire de Chimie Physique Macromoléculaire UMR CNRS-UL 7375, ENSIC, 1 rue Grandville, BP 20451, 54001 Nancy Cedex.

Résumé étendu de la thèse en français

Dérivés greffés de l'acétate cellulose en vue de la purification d'un biocarburant par un procédé de séparation membranaire dans une politique de développement durable

I. Contexte de l'étude

Les perspectives d'épuisement des réserves pétrolières mais aussi les contraintes environnementales incitent les gouvernements à développer des politiques favorisant les nouvelles ressources énergétiques. Ainsi, il a été montré par exemple que les émissions de gaz à effet de serre sont actuellement principalement liées à la combustion incomplète des carburants. De ce fait, l'amélioration de la combustion de l'essence est un enjeu très important. A ce jour, l'utilisation de biocarburants représente l'une des meilleures alternatives à l'emploi de carburants issus du pétrole bien qu'elle soit parfois controversée.

Dans ce contexte, l'éthyl *tert*-butyléther (ETBE) est considéré comme l'un des biocarburants les plus prometteurs à l'heure actuelle et entre dans le cadre de la politique française des filières de carburants pour un développement durable. En raffinerie, ce composé est obtenu à partir de l'éthanol, dont l'origine peut être agricole, et de l'isobutène (Figure 1).

Incorporé à l'essence, l'ETBE présente deux avantages majeurs. Il permet augmenter l'indice d'octane, et d'autre part, mélangé à l'essence, il permet d'en améliorer la combustion par l'apport d'oxygène conduisant ainsi à une combustion quasi-complète du carburant, ce qui contribue à réduire de manière significative les émissions toxiques dans l'environnement.

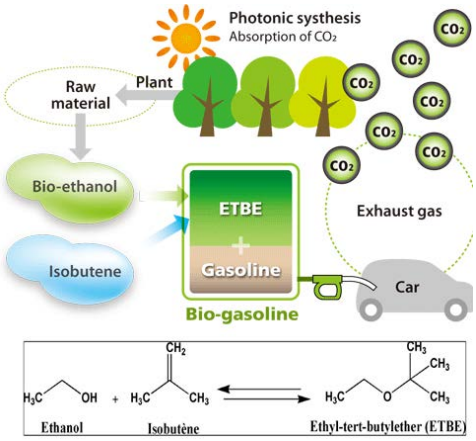

Figure 1 : Synthèse et utilisation de l'ETBE

Pour éviter les inconvénients liés à la présence d'éthanol et surtout d'eau associée dans les carburants, la purification de l'ETBE s'avère indispensable. Le procédé de production de cet éther se heurte néanmoins à la difficulté de séparer le mélange azéotropique éthanol/ETBE (contenant 20% en masse d'éthanol) qui est généré lors de ce procédé. Actuellement, les procédés les plus utilisés font appel à la distillation ternaire qui est très coûteuse en temps et en énergie. L'Institut Français du Pétrole (IFP) a par ailleurs montré que l'utilisation d'un procédé hybride couplant la distillation à un module de séparation membranaire pourrait permettre une économie pouvant aller jusqu'à 54 millions d'euros par an en fonction des propriétés des membranes utilisées. Ainsi, pour que la purification de l'ETBE par le module de séparation membranaire soit efficace, il est primordial de développer des membranes très sélectives et perméables vis-à-vis de l'éthanol. Les propriétés de sélectivité et de perméabilité variant généralement de manière opposée, l'enjeu est de s'affranchir de la limitation classique perméabilité/sélectivité pour ces nouvelles membranes organosélectives.

Parmi les matériaux membranaires décrits dans la littérature pour la séparation EtOH/ETBE, les polymères esters cellulosiques sont très largement utilisés pour la purification de l'ETBE. Les membranes préparées à base d'acétate de cellulose ont montré une excellente sélectivité avoisinant les 100%, mais une perméabilité relativement faible, généralement autour de 0,08 kg/m^2 h à 40°C pour des épaisseurs de 5 µm. Les propriétés membranaires varient fortement selon la nature de l'ester cellulosique utilisé. En effet, la sélectivité diminue avec le nombre d'atomes de carbone contenus dans le motif ester alors que la perméabilité varie en sens inverse.

Des équipes de recherche ont montré que des mélanges d'esters cellulosiques conduisent à de meilleures perméabilités pouvant varier de 0,6 jusqu'à 3 kg/m^2 h par comparaison avec un seul dérivé cellulosique. Des mélanges d'un ester cellulosique avec un autre polymère de type poly(vinyl pyrrolidone) (PVP), polyméthacrylate etc… ont également été étudiés. Cependant, ce type de

matériaux membranaires a parfois posé un problème de vieillissement physique, en raison de l'extraction de composants présents dans la membrane par le mélange liquide à séparer.

Afin d'éviter ce problème, plusieurs chercheurs ont travaillé sur le développement de membranes à partir de réseaux de polymères semi-interpénétrés (s-IPN). Ces s-IPNs correspondent à des mélanges de deux polymères, dont l'un est réticulé chimiquement sous forme d'un réseau tridimensionnel et l'autre y est emprisonné. Bien que la réticulation chimique engendre une stabilisation des membranes, des problèmes de reproductibilité des propriétés de séparation obtenue ont été rencontrés, liés au procédé de fabrication.

Un travail réalisé au LCPM sur des copolymères greffés à base d'acétate de cellulose et de poly(méthoxy(diéthylène glycol) méthacrylate) (PMDEGMA) d'architectures différentes a par ailleurs conduit à des matériaux performants pour la purification visée avec une sélectivité élevée (autour de 94%) et une perméabilité (jusqu'à 0,87 kg/m^2 h) fortement augmentée comparativement à celle de l'acétate de cellulose. Ces copolymères ont été obtenus par une méthode de "*grafting from*" par polymérisation radicalaire contrôlée par transfert d'atome (ATRP) à partir d'un macroamorceur cellulosique. Les résultats obtenus ont permis de montrer que le greffage contrôlé de l'acétate de cellulose permettait d'en améliorer fortement les propriétés membranaires et de les optimiser sur la base de relations propriétés-structures pour la purification de l'ETBE.

Par ailleurs, depuis une dizaine d'année, la chimie "click" a permis de développer de nouvelles voies de modification de la cellulose et de ses dérivés dans des conditions particulièrement douces. Dans le cadre d'une chimie durable, la chimie "click" a largement contribué à étendre les perspectives et la fonctionnalité des matériaux cellulosiques pour différentes applications. Dans cette thèse réalisée grâce à une allocation de recherche du Programme international Erasmus Mundus ELEMENT, nous avons étudié la possibilité de tirer partie d'une chimie "click" pour l'élaboration de nouvelles membranes polymères pour la purification de l'ETBE.

II. Bibliographie sur le greffage de la cellulose et ses dérivés par chimie click catalysée par le cuivre.

La chimie « click » définie par Sharpless correspond à une famille de réactions de couplage sélectif avec de hauts rendements et sans formation de produit secondaire. La chimie « click » présente des tolérances élevées vis-à-vis de groupes fonctionnels et permet de coupler deux fonctions complémentaires par une liaison hétéroatomique (C-X-C) en conditions douces. Parmi les différentes réactions de chimie click décrites, nous avons considéré plus particulièrement la réaction qui met en jeu une fonction azoture (N_3) et une fonction alcyne, aussi appelée cycloaddition 1,3 dipolaire de Huisgen, catalysée par du cuivre (CuAAC). La cycloaddition entre la fonction azoture et la fonction alcyne conduit à la formation d'un cycle triazole. Cette réaction, malgré la dangerosité potentielle des substances organo-azidées, reste la réaction de chimie click la plus utilisée de part la stabilité du cycle triazole vis-à-vis à de l'eau et de l'oxygène, mais aussi dans la plupart des conditions de synthèse organique.

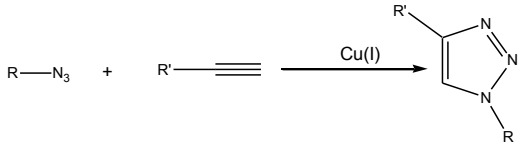

Figure 2 : La réaction de chimie "click" entre une fonction azoture et une fonction alcyne (CuAAC).

Récemment, de nombreux progrès ont été réalisés dans le domaine de la modification chimique de la cellulose et de ses dérivés par chimie click. Dans le chapitre 1, nous avons réalisé une analyse bibliographique des différentes approches de greffage conduisant à des architectures macromoléculaires complexes et variées à partir de dérivés cellulosiques porteurs de groupements fonctionnels clickables pour conduire à des matériaux de nature variée comme des réseaux réticulés sous forme de gels par exemple, des copolymères à blocs, des copolymères greffés, de la cellulose « dendronisée » etc … ou pour la modification de surface de la cellulose aux échelles macro et nano.

Ainsi, le développement de ces nouveaux matériaux a donc nécessité, dans un premier temps, la pré-modification des polysaccharides afin d'introduire, de manière régiosélective ou non, des fonctions azoture ou alcyne. Classiquement, si la position à fonctionnaliser importe peu, la modification du polymère est réalisée en deux étapes. La première étape consiste à activer des hydroxyle portés par les cycles glucosidiques, souvent par une réaction de tosylation. Dans une deuxième étape, la fonction chimique désirée est introduite par une réaction de substitution nucléophile. Néanmoins, si la fonction clickable doit être située sur une position précise du sucre, une stratégie de protection-déprotection des autres fonctions hydroxyle sera utilisée.

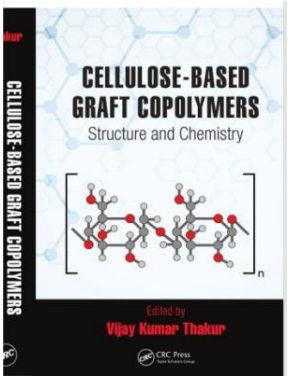

Figure 3 : "Grafting of cellulose and cellulose derivatives by CuAAC click chemistry", F. Hassan Hassan Abdellatif et al., in "Cellulose-based Graft Copolymers : Structure and Chemistry", edited by Vijay Kumar Thakur, CRC Press, chapter 25, pp. 569-597, 2015.

Dans ce contexte, l'objectif de la thèse a été de contribuer à l'élaboration de nouveaux matériaux membranaires pour la purification de l'ETBE par pervaporation. Pour obtenir une séparation efficace du mélange azéotropique éthanol/ETBE, il est nécessaire de développer des membranes organosélectives capables d'extraire l'éthanol de façon rapide et sélective. Pour ce faire, deux grandes familles de matériaux ont été synthétisées à partir d'un polysaccharide leader dans le domaine des matériaux membranaires : l'acétate de cellulose. Dans le chapitre 2, la chimie "click" CuAAC a ainsi été mise en œuvre pour le greffage d'oligomères polylactides (PLA) en proportion variable et contrôlée. Dans le chapitre 3, nous avons ensuite étudié le greffage de liquides ioniques présentant une forte affinité pour l'éthanol. Les propriétés de sélectivité et perméabilité de tous les matériaux obtenus ont été étudiés en termes de relations propriétés-structures pour permettre leur optimisation pour la purification de l'ETBE.

III. Greffage du PLA sur l'acétate de cellulose pour la purification d'un biocarburant par un procédé de séparation membranaire.

III.1 Synthèse et caractérisation des matériaux polymères

L'acide polylactique (PLA) est un polymère biodégradable de la famille des polyesters qui est issu de ressources naturelles renouvelables comme l'amidon de maïs. Il est utilisé dans de nombreux domaines tels que la délivrance de principes actifs, l'ingénierie tissulaire, dans les emballages alimentaires grâce à ses propriétés barrières liées à son taux de cristallinité ou encore en perméation gazeuse. En rapport avec l'application visée, le PLA présente également plusieurs avantages comme un caractère polaire, une bonne affinité pour l'éthanol et une faible température de transition vitreuse (T_g) conduisant à un effet plastifiant dans un matériau cellulosique. Cependant, très peu de travaux rapportent l'utilisation du PLA pour la séparation de mélanges de liquides. En 2011, Zereshki et al. ont montré que des mélanges de PLA et de poly(vinyl pyrrolidone) (PVP) conduisent à des propriétés intéressantes pour la séparation du mélange EtOH/ETBE par pervaporation, ce qui confirme l'intérêt du PLA pour l'application visée.

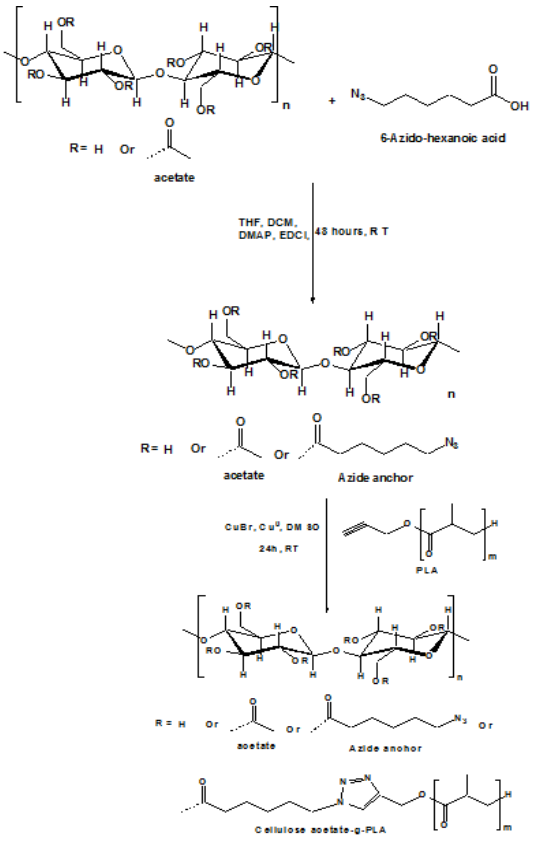

Figure 4:Schéma de synthèse de la modification de l'acétate de cellulose par le PLA

Dans la thèse, nous avons développé de nouveaux matériaux membranaires bio-sourcés à partir du greffage d'un oligomère PLA porteur à son extrémité d'une fonction alcyne (alcyne-PLA) sur un dérivé de l'acétate de cellulose portant des fonctions azoture complémentaires pour la chimie "click" selon une stratégie en deux étapes (Figure 3).

La synthèse a débuté par l'introduction de fonctions clickables azoture sur l'acétate de cellulose via une estérification avec l'acide 6-azidohexanoique. En parallèle, la préparation des greffons de PLA portant une fonction alcyne terminale a été réalisée par polymérisation contrôlée par ouverture de cycle de D,L-lactide selon un protocole mis au point au laboratoire à partir de l'alcool propargylique (amorceur fonctionnel) en présence d'un catalyseur $SnOct_2$ (Collaboration : Jean-Luc Six, Cécile Nouvel, LCPM). La seconde étape a été le greffage "onto" de l'alcyne-PLA sur le dérivé azidé de l'acétate de cellulose par chimie "click" CuAAC. La stratégie développée a ainsi permis de contrôler à la fois le nombre et la longueur des greffons de PLA introduits. Par ailleurs, le contrôle de la proportion des greffons a permis d'ajuster précisément la structure de ces matériaux polymères pour une efficacité optimale vis-à-vis de l'application ciblée.

La structure de l'ensemble des polysaccharides modifiés a été caractérisée par spectroscopie infrarouge (ATR-FTIR) et par spectroscopie RMN du proton ^{1}H. Des caractérisations physiques par calorimétrie différentielle à balayage (DSC) et diffraction des rayons X aux petits angles (SAXS) à l'European Synchrotron Radiation Facility à Grenoble (collaboration: Laurent David, IMP, Lyon) ont également permis d'étudier les transitions thermiques et la morphologie des nouveaux matériaux, qui jouent un rôle très important pour l'application visée.

Alcyne-PLA : La caractérisation en RMN ^{1}H et en ATR-FTIR des greffons PLA a mis en évidence la présence de la fonction alcyne terminale. Par ailleurs, la masse molaire moyenne en nombre (M_n) a été déterminée par SEC-MALLS et calculée également par RMN ^{1}H. Les résultats en SEC-MALLS montrent que l'oligomère de PLA a une M_n=1640 g/mol correspondant à un degré de polymérisation moyen en nombre X_n= 22 avec une dispersité Đ= 1,27, ce qui confère à l'échantillon une homogénéité de la taille des greffons. Ces résultats sont en accord avec les calculs réalisés à partir des spectres RMN ^{1}H (Mn=1769 g/mol).

Azido-acétate cellulose : Le degré de substitution en fonction azoture (DS_{N3}) de l'acétate de cellulose déterminé par RMN ^{1}H est égal à 0,39, ce qui correspond à un taux de modification relativement élevé pour des polysaccharides, sachant que le degré de substitution des groupements hydroxyle par cycle glycosidique est DS_{OH}= 0,54. Par ailleurs, l'ATR-FTIR a révélé la signature caractéristique de la fonction azoture vers 2100 cm^{-1}.

Acétate de cellulose greffé par différents taux de PLA : Les spectroscopies RMN ^{1}H et ATR-FTIR ont confirmé la formation du cycle triazole caractéristique de la réaction de chimie click. Par ailleurs, la RMN ^{1}H a été exploitée pour calculer les différents taux de greffage. Les résultats ont montré qu'il est possible de faire varier la fraction massique de phase souple de 23 à 40,5%. De plus, d'une manière générale, les résultats obtenus par DSC ont mis en évidence la diminution de la T_g lorsque le taux de greffage augmente, ce phénomène étant lié à la plastification du polysaccharide par les greffons PLA. Les analyses SAXS ont révélé que les matériaux sont homogènes et ne présentent pas de nano-structuration, ce qui témoigne d'une bonne dispersion des greffons PLA au sein du polymère.

III.2 Principaux résultats en séparation membranaire

La pervaporation, ainsi nommée par Kober en 1917, est une technique de séparation de mélanges liquides homogènes à travers une membrane dense. Le transfert de matière est réalisé en conservant une basse pression à l'aval de la membrane (inférieure aux pressions de vapeur saturante des constituants du mélange), ce qui crée un gradient de potentiel chimique entre les deux faces de la membrane. Les espèces ayant migré à travers la membrane et s'étant vaporisées au niveau de la face aval sont recueillies par condensation sur une paroi froide et constituent le pervaporat, comme le montre la figure 5. La fraction du mélange liquide qui n'est pas transférée est nommée rétentat.

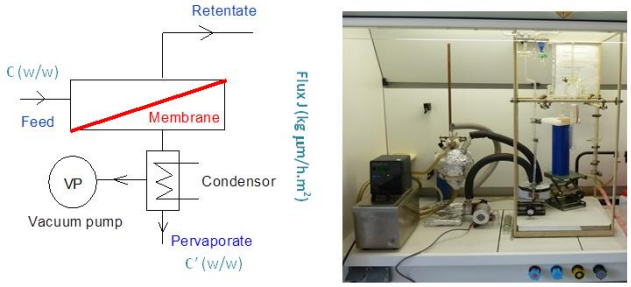

Figure 5:Schéma du principe de la pervaporation et montage utilisé

La pervaporation est principalement utilisée en industrie pour extraire ou récupérer des espèces minoritaires à partir d'un mélange liquide. En comparant avec des méthodes telles que la distillation, la pervaporation présente des avantages significatifs en termes énergétiques. En effet, dans ce procédé de séparation membranaire, seule la fraction du mélange transférée à travers la membrane va consommer de l'énergie en se vaporisant, contrairement à la distillation où tout le mélange à traiter doit être vaporisé. De plus, les interactions spécifiques entre la membrane et les espèces à extraire conduisent généralement à un enrichissement supérieur du perméat par rapport à la distillation simple. Pour les mélanges azéotropiques qui sont très difficiles à séparer, la pervaporation est ainsi un procédé alternatif très efficace et simple, grâce à la membrane de pervaporation capable d'interagir spécifiquement et fortement avec les espèces ciblées.

L'ensemble des copolymères synthétisés a tout d'abord fait l'objet d'une étude en sorption, qui correspond à la première étape du transfert membranaire d'après le modèle de sorption-diffusion (Figure 6 a). Les propriétés de sorption contribuent ainsi aux performances globales des membranes en pervaporation. Les expériences de sorption ont permis de caractériser les aspects thermodynamiques du transfert en mesurant la solubilité des différentes espèces du mélange dans les membranes pour le mélange azéotropique à séparer EtOH/ETBE (20/80 % en masse).

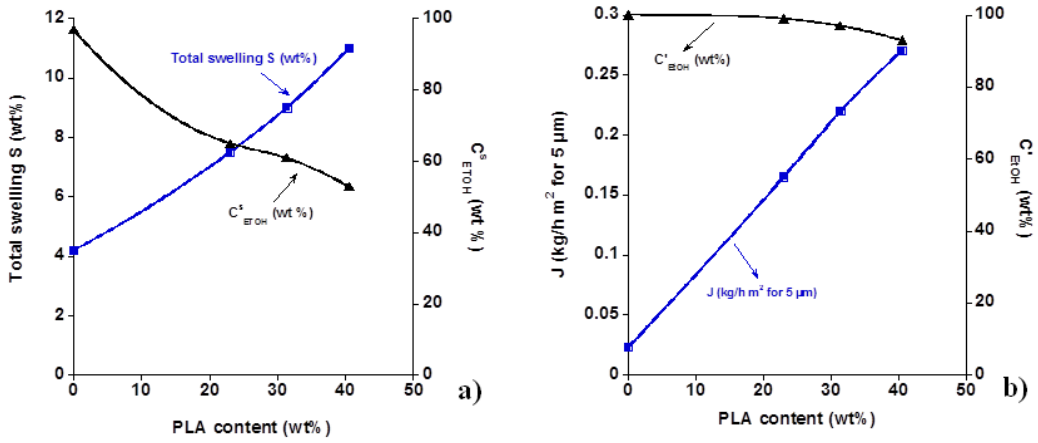

Figure 6:Influence de la fraction massique de PLA sur les propriétés de sorption a) et de pervaporation b)

Ces expériences de sorption (Figure 6 a), qui ont permis de caractériser la capacité des matériaux à absorber le mélange liquide à séparer et leur sélectivité pour l'éthanol, ont montré un facteur de séparation très élevé β_s= 129 et un gonflement faible S= 4,2 % en masse pour l'acétate de cellulose non modifié. Ce résultat est lié à la présence de fonctions hydroxyle libres qui possèdent une très forte affinité pour l'éthanol et la grande rigidité des chaînes polymères qui limite le gonflement.

Lorsque la proportion massique de greffons PLA varie entre 23 et 40,5%, le gonflement augmente linéairement de manière modérée de 7,5 à 11%. Ce comportement s'accompagne d'une forte diminution de l'affinité des membranes pour l'éthanol, avec une variation de β_s de 129 à 4,5 pour les matériaux les plus greffés. Toutefois, l'ensemble des membranes préparées conserve une bonne sélectivité vis-à-vis de l'éthanol lors de l'étape de sorption, le mélange absorbé par les membranes contenant au moins 50% d'éthanol.

Par la suite, les propriétés de pervaporation des membranes ont été évaluées pour la purification de l'ETBE à partir du mélange azéotropique EtOH/ETBE. Deux grandeurs essentielles ont été déterminées : le flux global et la composition du perméat relevant de la sélectivité de la membrane (Figure 6 b). La figure 6 b montre que l'ensemble des matériaux testés conduit à une extraction très sélective de l'éthanol, avec des fractions massiques en éthanol dans le perméat ne descendant pas au-dessous du seuil de 90%. De plus, l'augmentation de la fraction massique du PLA a permis d'augmenter le flux jusqu'à un facteur 12 pour le plus fort taux de greffage.

Globalement, le greffage de PLA sur l'acétate de cellulose par chimie "click" a donc permis une forte amélioration des propriétés membranaires pour l'application visée.

IV. Greffage de l'acétate de cellulose avec des liquides ioniques pour la purification d'un biocarburant par un procédé de séparation membranaire.

IV.1 Introduction

Au cours de ces dernières années, les liquides ioniques ont été proposés comme une alternative aux solvants organiques classiques pour le respect de l'environnement, en raison de leurs propriétés uniques telles que leur stabilité thermique, leurs caractères non-volatil et ininflammable, leur pression de vapeur négligeable et leur capacité à dissoudre une large gamme de composés organiques.

Par ailleurs, un des grands avantages de ces composés réside dans la possibilité d'adapter leur structure en fonction des propriétés désirées. En effet, il est possible de modifier et combiner à volonté la structure du cation ou de l'anion. Au-delà de leur utilisation en tant que solvants «verts», les liquides ioniques ont également ouvert de nouvelles perspectives dans les matériaux pour l'énergie ou en séparation de molécules d'intérêt dans les biotechnologies, en perméation gazeuse, et dans une bien moindre mesure pour la séparation des liquides par pervaporation.

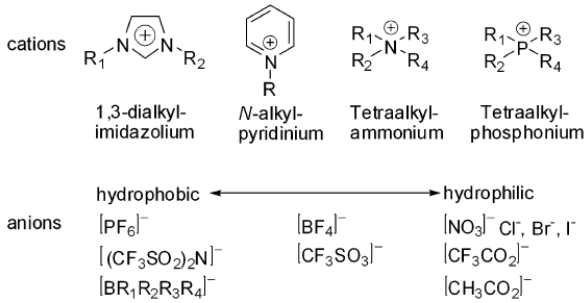

Figure 7: Exemples de structures des cations et anions composant les liquides ioniques d'après J.Yuan et M. Antonietti Polymer, 52 (2011) 1469-1482.

L'incorporation de liquides ioniques dans des membranes polymères a notamment conduit à des avancées majeures pour des séparations du CO_2. En effet, les liquides ioniques ont permis d'augmenter à la fois le flux et la sélectivité des membranes, ce qui est exceptionnel. Néanmoins, cette approche a été très peu étendue à la séparation de liquides, en raison des problèmes d'instabilité dans le temps qui ont été observés dus à l'extraction progressive des liquides ioniques par les mélanges à séparer.

Dans cette thèse, nous avons développé une stratégie de greffage des liquides ioniques sur l'acétate de cellulose afin de s'affranchir de cette limitation et d'ouvrir le champ de la séparation de mélanges de liquides organiques à des membranes organosélectives contenant des liquides ioniques.

IV.2 Développement d'une nouvelle stratégie de greffage des liquides ioniques avec des cations différents et un même anion

IV.2.1 *Synthèses et caractérisations des matériaux*

Le chapitre 3 de la thèse, qui est consacré au greffage de l'acétate de cellulose par des liquides ioniques pour la purification de l'ETBE par pervaporation, s'articule en deux parties. La première partie est consacrée au développement d'une stratégie de greffage efficace pour des liquides ioniques contenant un anion bromure et des cations de structure chimique variable (pyridinium, imidazolium et ammonium) afin de comprendre l'influence du cation sur les performances observées pour la

séparation membranaire ciblée. La seconde partie du chapitre porte sur l'influence de la nature de l'anion sur les propriétés de séparation pour le mélange EtOH/ETBE.

Par extension de l'approche développée pour le greffage d'oligomères PLA, une première stratégie de synthèse par chimie "click" a été étudiée afin de greffer un liquide ionique imidazolium clickable sur un acétate de cellulose clikable. Ces tentatives se sont soldées par la gélification du milieu réactionnel, en raison d'une réaction secondaire d'addition de l'imidazolium sur l'extrémité terminale de la chaîne polysaccharidique. Une seconde stratégie de greffage en deux étapes a alors été développée avec succès (Figure 8).

Dans la première étape, il s'agit d'introduire sur l'acétate de cellulose un bras espaceur possédant à son extrémité un atome de brome facilement substituable.

La seconde étape consiste à faire réagir le dérivé bromé de l'acétate de cellulose en présence d'un réactif nucléophile (pyridine, 1-méthylimidazole ou *N,N*-diethylmethylamine) afin de générer le liquide ionique greffé *in situ*.

Ainsi, par une réaction de substitution nucléophile, il a été possible de greffer simplement sur le polysaccharide des liquides ioniques avec un même anion bromure et des cations de différentes structures, et de faire varier la quantité des liquides ioniques greffés.

La structure chimique des matériaux obtenus ainsi que le taux de greffage des liquides ioniques ont été caractérisés par des analyses en RMN ^{1}H. Les résultats ont montré que l'efficacité du greffage augmente avec la nucléophilie du réactif (pyridine < 1-méthylimidazole < *N,N*-diethylmethylamine). Le greffage est quantitatif avec l'amine secondaire jusqu'à un taux de greffage de 87% qui est élevé pour un polysaccharide. En revanche, pour atteindre des taux de greffage élevés en présence de 1-méthylimidazole ou de pyridine, il est nécessaire de travailler en présence d'un large excès de réactif nucléophile. Dans ce cas, les taux obtenus sont de 83 et 77% pour le 1-méthylimidazole et pour la pyridine, respectivement.

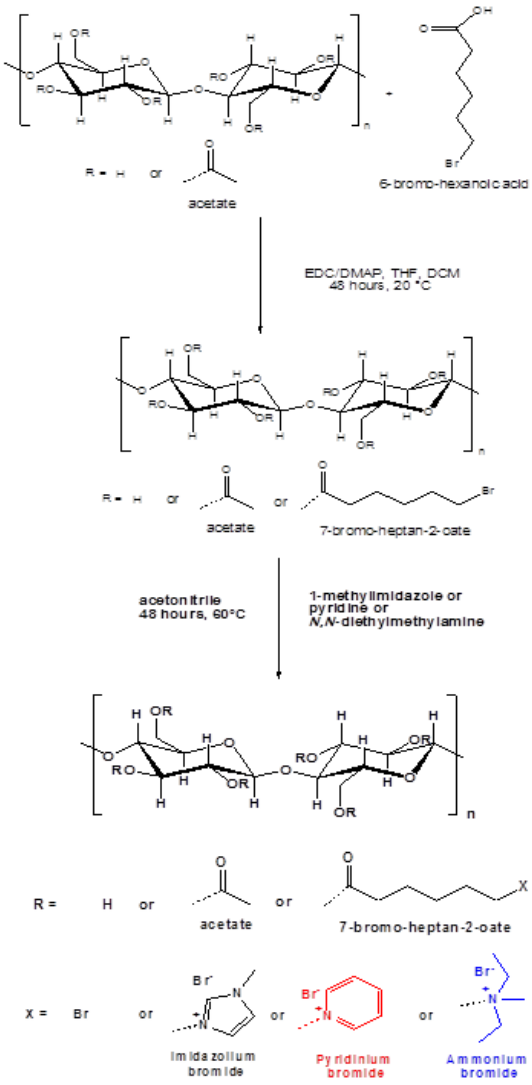

Figure 8: Nouvelle stratégie de greffage de l'acétate de cellulose par des liquides ioniques contenant un même anion bromure et des cations de différentes structures (pyridinium, imidazolium et ammonium)

Des analyses complémentaires en DSC ont montré que le greffage des liquides ioniques s'accompagne d'une diminution importante de la température de transition vitreuse (T_g) du dérivé cellulosique et que la T_g obtenue augmente avec la température de fusion du liquide ionique. En conséquence, l'effet de plastification du liquide ionique augmente avec la mobilité du liquide ionique moléculaire selon l'ordre suivant : ammonium < pyridinium < imidazolium. Les résultats obtenus par synchrotron SAXS (collaboration : Laurent David, laboratoire IMP, Lyon) ont révélé l'absence de nano-structuration des liquides ioniques dans les matériaux obtenus qui sont homogènes.

IV.2.2 *Principaux résultats en séparation membranaire*

Les principales expériences de sorption ont été réalisées pour les cations ammonium et imidazolium. Dans le cas du cation pyridinium, une seule valeur a été déterminée pour le film

possédant le taux de greffage le plus élevé en raison des faibles flux. L'acétate de cellulose pur présente un gonflement faible de 4,2% mais un facteur de séparation élevé dû à la rigidité des chaînes polymères et de la présence des groupes hydroxyle possédant une bonne affinité pour l'éthanol. Lorsque la quantité de liquide ionique augmente, le gonflement du matériau reste relativement faible (< 10% en masse) mais le facteur de séparation β_s augmente fortement avec des teneurs en éthanol dans les mélanges absorbés très élevées avoisinant les 100%.

En comparant des membranes qui correspondent aux plus forts taux de greffage pour les trois cations, le gonflement augmente légèrement (+38%) avec le caractère polaire du cation tandis que la quantité d'éthanol absorbée diminue très légèrement de 99% à 97,5% en raison d'un effet de plastification induit par le gonflement les plus élevé. Dans tous les cas, à notre connaissance, les matériaux obtenus sont les plus sélectifs jamais décrits pour la sorption du mélange azéotropique EtOH/ETBE.

Les résultats obtenus pour les expériences de pervaporation (Figure 9) montrent que quelle que soit la proportion d'imidazolium dans les matériaux, il n'y a pas d'influence sur la perméabilité de la membrane dont le flux reste relativement bas autour de 0,05 kg/m^2/h contre 0,023 kg/m^2/h pour l'acétate de cellulose non modifié. Néanmoins, la sélectivité reste très élevée. En revanche, le cation ammonium permet d'augmenter les flux jusqu'à un facteur 8 pour le matériau le plus greffé (J= 0,182 kg/m^2 h) qui conduit par ailleurs à un perméat ne contenant que de l'éthanol.

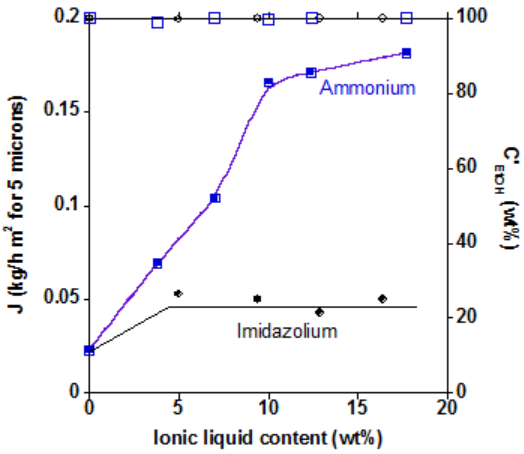

Figure 9: Influence de la quantité de liquide ionique sur les propriétés de pervaporation pour la purification de l'ETBE.

Pour approfondir la compréhension des propriétés des membranes, une analyse a été réalisée à partir des paramètres physico-chimiques de Kamlet et Taft : π^* qui correspond à l'indice de polarité/polarisabilité et α, β qui décrivent respectivement l'acidité (caractère donneur de liaison hydrogène) et la basicité (caractère accepteur de liaison hydrogène). En comparant les propriétés de sorption et de pervaporation pour des matériaux correspondant aux taux de greffage les plus élevés pour les différents cations, le gonflement et le flux augmentent avec le caractère accepteur de liaison hydrogène β des liquides ioniques, qui favorise de fortes interactions avec l'éthanol, qui est fortement donneur de liaisons hydrogène. Ainsi, le cation ammonium entraîne le gonflement le plus élevé, induisant la meilleure plastification et un effet de synergie de sorption.

Finalement, les flux de pervaporation sont également augmentés en renforçant l'aptitude des liquides ioniques greffés à former des liaisons hydrogène et les sélectivités des matériaux les plus greffés sont exceptionnelles, les perméats étant constitués d'éthanol pur.

IV.3 Greffage de l'acétate de cellulose avec des liquides ioniques pour la purification de l'ETBE : Influence de l'anion

Dans cette partie, l'anion bromure des liquides ioniques greffés sur l'acétate de cellulose a été échangé par trois anions (Tf_2N^-, BF_4^-, AcO^-) pour des teneurs massiques quasi-identiques d'environ 17% de liquides ioniques ammonium et imidazolium. Cette teneur correspondait aux taux de greffage maxima obtenus pour les deux séries précédentes. Les 8 matériaux résultants ont ensuite permis d'étudier pour la première fois l'influence de la nature de l'anion sur les propriétés de membranes pour la séparation d'un mélange de liquides à partir de séries *homologues* de liquides ioniques.

IV.3.1 *Synthèses et caractérisations des matériaux*

La figure 10 décrit la procédure générale ayant permis de réaliser l'échange de l'anion en présence d'un large excès de sel inorganique. Une analyse quantitative en RMN ^{19}F a permis de

montrer que cet échange est quantitatif pour les anions fluorés (Tf_2N^- ou BF_4^-). Dans le cas de l'anion acétate AcO^-, la méthode la plus efficace décrite dans la littérature pour des liquides ioniques moléculaires a tout d'abord été testée en utilisant la résine Amberlite® A-26 contenant des anions hydroxyde. Un premier échange de l'anion bromure a ainsi été réalisé par un anion hydroxyde, qui a réagi dans une deuxième étape avec de l'acide acétique. Appliquée aux dérivés cellulosiques greffés par des liquides ioniques, cette méthode a conduit à une dégradation chimique des matériaux, impliquant la coupure des fonctions esters acétate et hexanoate. L'utilisation d'un sel d'acétate a ensuite permis d'éviter ce problème mais le taux d'échange déterminé par RMN ^1H est resté limité à 65%, en raison des conditions hétérogènes de l'échange imposées par la très faible solubilité de ces sels dans les solvants des matériaux étudiés.

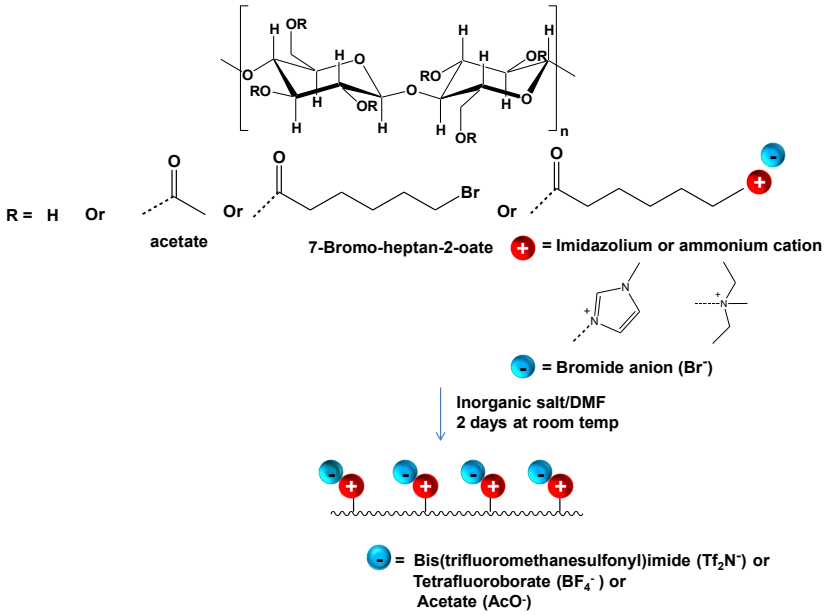

Figure 10: Méthode générale d'échange du contre-ion pour l'acétate de cellulose greffé par des liquides ioniques

Des analyses complémentaires en DSC et en SAXS ont été réalisées afin de comprendre l'influence de l'anion sur les transitions thermiques et la morphologie des nouveaux matériaux. La T_g des polymères est fortement influencée par la nature de l'anion et augmente selon l'ordre suivant : Tf_2N^-< AcO^-<BF_4^-< Br^-. Contrairement à ce qui avait été observé pour l'influence du cation, aucune corrélation n'a pu être trouvée avec la température de fusion des liquides ioniques. Cependant, nous avons montré que la T_g du matériau augmente avec la T_g du liquide ionique greffé dans la série imidazolium pour tous les contre-ions, sauf l'acétate pour lequel la valeur de T_g n'a pas été rapportée. Comparativement à l'acétate de cellulose, la plus forte diminution de T_g de 184°C à 111°C a été enregistrée pour le liquide ionique imidazolium avec un anion Tf_2N^-, qui interagit moins en raison de sa grande taille et de faibles interactions de Coulomb. Comme dans le cas des différents cations, les expériences en SAXS ont révélé que les matériaux sont homogènes avec une bonne dispersion des liquides ioniques.

IV.3.2 *Principaux résultats en séparation membranaire*

Quel que soit le cation, les gonflements mesurés en sorption sont beaucoup moins importants avec les anions hydrophobes fluorés Tf_2N^- et BF_4^- qu'avec les anions hydrophiles AcO^- et Br^- avec des facteurs de séparation β_s également plus faibles. Par ailleurs, curieusement, nous avons observé que l'anion qui comporte le plus d'atomes de fluor (Tf_2N^-) conduit à un gonflement un peu plus important que celui qui en contient moins (BF_4^-). Une analyse grâce aux paramètres de Kamlet-Taft a finalement révélé que le gonflement augmente avec le caractère accepteur de liaison hydrogène β du liquide ionique et sa taille moléculaire.

En pervaporation, toutes ces membranes se sont révélées extrêmement sélectives avec des perméats ne contenant que de l'éthanol. Le flux suit les mêmes tendances que le gonflement global

mais l'amélioration du flux est plus importante, comme prévu par les théories du volume libre rendant compte de la diffusion d'un solvant à travers une membrane polymère dense.

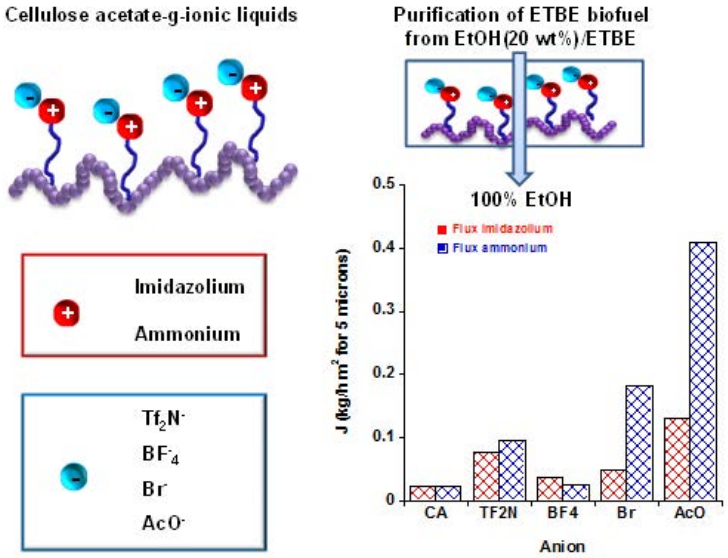

Figure 11:Résultats de pervaporation obtenus pour la purification de l'ETBE

Finalement, en combinant le meilleur caractère accepteur de liaison hydrogène β et une taille moléculaire importante, le liquide ionique ammonium avec un anion acétate a conduit aux meilleures propriétés membranaires pour la purification de l'ETBE avec un flux normalisé de 0,41 kg/m² h (environ 20 fois celui de l'acétate de cellulose non greffé) pour une épaisseur de membrane de 5 µm, une fraction massique en éthanol de 100% dans le perméat, correspondant à un facteur de séparation en pervaporation β_{PV} infini à 50°C.

Table of Contents

Table of Contents

General Introduction

Membrane separation processes are widely used worldwide for water treatment, gas and liquid separations. Compared to other separation processes such as distillation, adsorption and liquid-liquid extraction, membrane processes generally offer important energy savings, modularity and lower environmental impact. In these separation processes, membrane optimization is essential for industrial success. In addition to being resistant to operating conditions, the membrane material should be both highly permeable and selective. Nevertheless, permeability and selectivity usually vary in opposite ways and the corresponding permeability/selectivity trade-off is a real challenge for membrane designers [1-3].

In this work, a membrane separation process is considered for the purification of the ethyl *tert*-butyl ether (ETBE) bio-fuel, which is one of the major European bio-fuels. This ether is an oxygenated additive widely used in gasoline fuels in replacement to the former toxic lead derivatives (Figure 0-1). Compared to ethanol, ETBE offers several advantages for fuel formulations. It has a better octane number, lower vaporization enthalpy and lower hydrophilic character [4]. The latter advantage is often considered as determining for the petroleum industry because it avoids troublesome phase separations in fuel lines and tanks, which usually occur in presence of residual water in ethanol-containing fuels. Furthermore, ETBE can be easily blended to gasoline fuels up to a content of 15 % and it leads to quasi-complete fuel combustion, therefore minimizing toxic emissions and improving air quality. In the United States of America, this ether has also recently been considered as an interesting alternative to the related methyl *tert*-butyl ether (MTBE) formerly banned in California because ETBE is much better biodegradable [4, 5].

The main industrial ETBE process involves the reaction of isobutene with bio-ethanol and leads to an azeotropic mixture EtOH/ETBE (20/80 wt%), which cannot be separated by simple distillation. Therefore, ETBE purification is usually achieved by a highly energy intensive "ternary" distillation process [4, 6]. A few works have reported that the pervaporation (PV) membrane process, alone or in hybrid processes with simple distillation, could offer important energy savings for this separation [7-9]. The French Petroleum Institute has made an estimate of 54 millions of euros for yearly energy savings expected with a hybrid distillation/PV process, depending on the membrane properties, for the French ETBE production capacity of 400 000 metric tons/year [7].

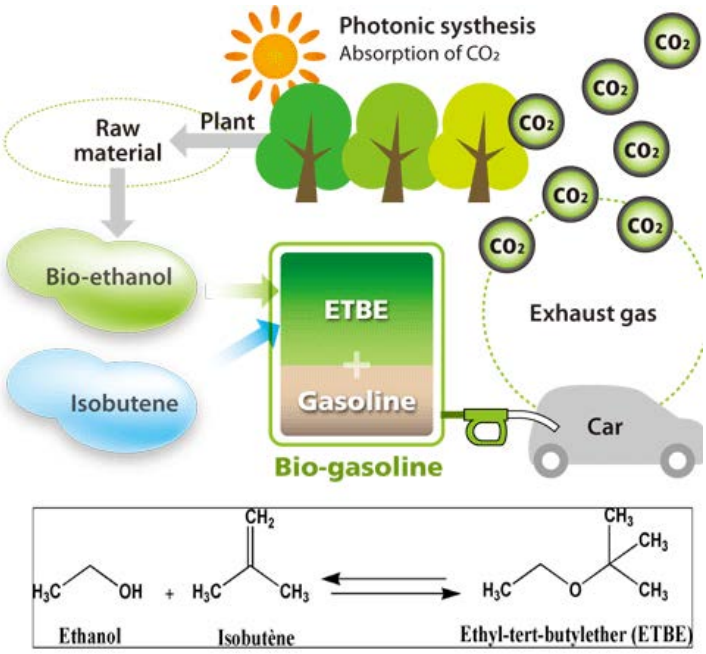

Figure 0-1: Importance of ethyl tert-butyl ether (ETBE) for the petroleum industry

Nevertheless, ETBE purification by pervaporation is quite challenging and requires *organoselective* membranes capable of extracting ethanol from the targeted azeotropic mixture. As it will be reviewed later on, the relatively rare PV membranes reported for ETBE purification were mainly cellulosic membranes and, to a less extent, poly(vinyl pyrrolidone) blends and segmented copolymers [10-12]. In particular, a cellulose acetate (CA) membrane was extremely selective with a permeate ethanol content of 100% but the reported flux of 0.08 kg/m^2 h for a reference membrane thickness of 5 µm was too low at 40°C [13].Cellulosic blends and semi-interpenetrated networks have been reported as interesting alternatives for improving cellulosic membrane properties for ETBE purification. The Laboratory of Macromolecular Physical Chemistry UMR CNRS-UL 7375 in Nancy has also shown that cellulose acetate grafting with PEO-containing polymethacrylate grafts greatly improved the membrane flux while the permeate ethanol content remained in the high range for this application [10]. In the latter work, a "grafting from" approach has been developed from a cellulose acetate macroinitiator for atom transfer radical polymerization (ATRP).

On the other hand, over the past few years, the copper(I) catalyzed Huisgen 1,3-dipolar cycloaddition of azides and alkynes (CuAAC) "click" chemistry has offered new ways of modifying cellulose and its derivatives in particular mild conditions. Within the frame of sustainable chemistry, CuAAC "click" chemistry has already contributed to greatly extend the scope and functionality of cellulose-based materials for several applications in smart packaging, advanced food, drug delivery, biomaterials and composites, biosensors,

bactericidal materials, and biofunctional films. In this work developed thanks to a PhD scholarship of the ELEMENT Erasmus Mundus Programme, CuAAC "click" chemistry has been used for developing new cellulose acetate derivatives for ETBE purification by pervaporation (Figure 0-2).

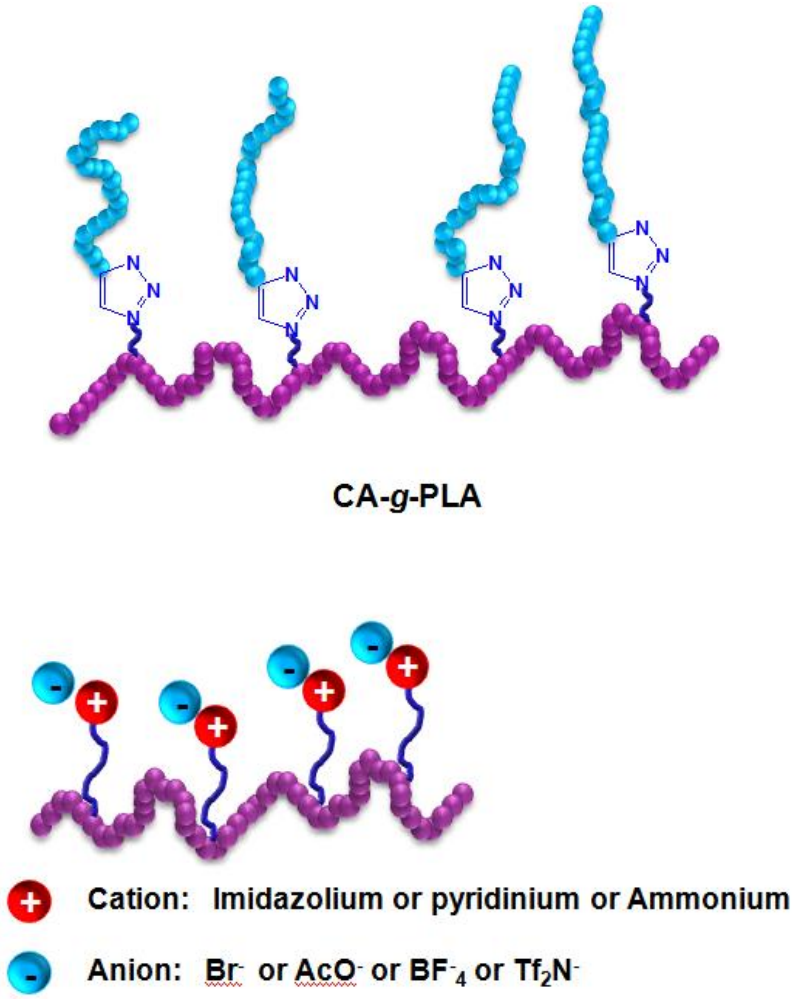

Figure 0-2: The different cellulose acetate derivatives developed in this work for ETBE purification by the pervaporation membrane process

After introducing the main current techniques of "click" chemistries, **Chapter 1** focuses on the CuAAC "click" chemistry and makes a thorough review of its application for modifying cellulose and cellulose derivatives. The second part of Chapter 1 reports the preparation of a wide range of advanced cellulose-based macromolecular architectures (*i.e.* cross-linked networks, block and graft copolymers, dendronised celluloses, and polyelectrolytes) by different CuAAC strategies. The surface modification of bulk cellulosic materials and nano-celluloses is also reviewed, showing the great versatility of CuAAC "click" chemistry in this

field. Our review has recently been published as a book chapter {Hassan Hassan Abdellatif, 2015 #19}.

Chapter 2 reports new bio-based PV membranes obtained by a "grafting onto" strategy of polylactide oligomers (PLA) onto cellulose acetate by CuAAC "click" chemistry in homogeneous conditions. PLA is a biodegradable polyester derived from renewable sources such as corn starch. Its ester groups are H-bonding acceptors, which have been shown to interact strongly with water and ethanol and a former work has already reported the interesting properties of poly(vinyl pyrrolidone)/PLA blends for ETBE purification [11]. The synthesis and characterization of a series of cellulose acetate-*g*-PLA materials is first described, following an original approach for modifying cellulose acetate in a controlled way. The membrane properties are then investigated for ETBE purification on the basis of the sorption-diffusion model accounting for permeability through dense polymer membranes.

The extension of the former strategy is then considered for grafting ionic liquids onto cellulose acetate. For the past ten years, ionic liquids have led to an important breakthrough in gas separation membranes, in particular for CO_2 capture. It has been shown that both permeability and selectivity could be improved *at the same time* by incorporating ionic liquids in polymer membranes [15-17]. Nevertheless, according to a bibliographic study which will be developed later on, the separation of liquid mixtures by ionic liquids-containing membranes is particularly challenging and has been reported rarely so far. The former works focused on the recovery of biofuels from dilute fermentation broths or that of volatile organic compounds (VOCs) from water with *organophilic* membranes. In the latter case, the ionic liquid extraction by the feed mixture has sometimes been reported with a decrease in the membrane properties over time.

Chapter 3 reports different strategies for ionic liquid "grafting onto" cellulose acetate for developing *organoselective* membranes for ETBE purification. These strategies extend the scope of ionic liquid-containing membranes to the challenging separation of purely organic mixtures, in which these ionic liquids are soluble. After a brief part reporting the limitations of the CuAAC "click" chemistry for grafting ionic liquids onto cellulose acetate, the second part describes an original successful 2-step strategy. Cellulose acetate is first grafted with ionic liquids containing the same bromide anion and different cations (imidazolium, pyridinium and ammonium) and the resulting materials are characterized by complementary techniques. The influence of the ionic liquid cation on the membrane properties is then analyzed in terms of structure-property relationships for ETBE purification. According to the best of our knowledge, very little is known about the influence of the ionic liquid anion on membrane properties due to the lack of systematic studies involving homologous series of ionic liquids.

In the last part of Chapter 3, a procedure of anion exchange is used to analyze the influence of the anion structure (Tf_2N^-, BF_4^-, Br^- and AcO^-) on the membrane properties for imidazolium and ammonium ionic liquids after the characterization of the different polymer materials.

References

[1] R.W. Baker, Membrane technology and applications, 2nd ed, John Wiley & Sons, Chichester, 2004.

[2] E. Drioli and L. Giorno, eds. *Comprehensive Membrane Science and Engineering*. 2010, Elsevier Science: Kidlington (UK).

[3] E.M.V. Hoek and V.V. Tarabara, eds. *Encyclopedia of Membrane Science and Technology*. 2013, John Wiley & Sons: Hoboken, New Jersey.

[4] K.F. Yee, A.R. Mohamed, and S.H. Tan, A review on the evolution of ethyl tert-butyl ether (ETBE) and its future prospects, Renewable and Sustainable Energy Reviews, 22 (2013) 604-620.

[5] H. Noureddini, Ethyl tert-butyl ether and methyl tert-butyl ether: status, review, and alternative use. Exploring the environmental issues of mobile, recalcitrant compounds in gasoline, ACS Symposium Series, 799 (2002) 107-124.

[6] E. Weber de Menezes and R. Cataluna, Optimization of the ETBE (ethyl tert-butyl ether) production process, Fuel Processing Technology, 89 (2008) 1148-1152.

[7] C. Streicher, Institut Francais du Pétrole, Ethyl tertio-butyl ether purification process combining a membrane method and distillation, Ethyl tertio-butyl ether purification process combining a membrane method and distillation US Patent 5607557, 1997.

[8] M.S. Chen, R.M. Eng, J.L. Glazer, and C.G. Wensley, Pervaporation process for separating alcohols from ethers, Pervaporation process for separating alcohols from ethers US patent 7,774,365, 1988.

[9] A. Jonquieres, C. Arnal-Herault, and J. Babin, Pervaporation, in E.M.V. Hoek and V.V. Tarabara (Eds.). Encyclopedia of Membrane Science and Technology, John Wiley & Sons, Hoboken, New Jersey, 2013, (3), pp. 1533-1559.

[10] M. Billy, A. Ranzani Da Costa, P. Lochon, R. Clement, M. Dresch, and A. Jonquieres, Cellulose acetate graft copolymers with nano-structured architectures: Application to the purification of bio-fuels by pervaporation, Journal of Membrane Science, 348 (2010) 389-396.

[11] S. Zereshki, A. Figoli, S.S. Madaeni, F. Galiano, and E. Drioli, Pervaporation separation of ethanol/ETBE mixtures using poly(lactic acid)/poly(vinyl pyrrolidone) blend membranes, Journal of Membrane Science, 373 (2011) 29-35.

[12] M. Wang, C. Arnal-Herault, C. Rousseau, A.I. Palenzuela, J. Babin, L. David, and A. Jonquieres, Grafting of multi-block copolymers: A new strategy for improving membrane separation performance for ethyl tert-butyl (ETBE) bio-fuel purification by pervaporation, Journal of Membrane Science, 469 (2014) 31-42.

[13] Q.T. Nguyen, C. Leger, P. Billard, and P. Lochon, Novel membranes made from a semi-interpenetrating polymer network for ethanol-ETBE separation by pervaporation, Polymers for Advanced Technologies, 8 (1997) 487-495.

[14] F. Hassan Hassan Abdellatif, J. Babin, C. Arnal-Herault, and A. Jonquieres, Chapter 25 : Grafting of cellulose and cellulose derivatives by CuAAC click chemistry, in V.K. Thakur (Ed.). Cellulose-based Graft Copolymers : Structure and Chemistry, CRC Press Taylor & Francis Publisher, 2015, pp. 563-591.

[15] R.D. Noble and D.L. Gin, Perspective on ionic liquids and ionic liquid membranes, Journal of Membrane Science, 369 (2011) 1-4.

[16] L.J. Lozano, C. Godinez, A.P. de los Rios, F.J. Hernandez-Fernandez, S. Sanchez-Segado, and F.J. Alguacil, Recent advances in supported ionic liquid membrane technology, Journal of Membrane Science, 376 (2011) 1-14.

[17] P. Scovazzo, Determination of the upper limits, benchmarks, and critical properties for gas separations using stabilized room temperature ionic liquid membranes (SILMs) for the purpose of guiding future research, Journal of Membrane Science, 343 (2009) 199-211.

Chapter 1 Bibliography

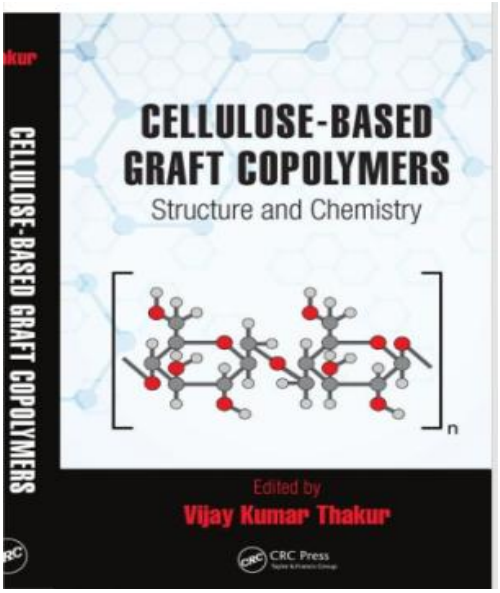

Grafting of cellulose and cellulose derivatives by CuAAC click chemistry

Faten HASSAN HASSAN ABDELLATIF, Jérôme BABIN, Carole ARNAL-HERAULT, Anne JONQUIERES*

Laboratoire LCPM FRE 3564, ENSIC, Université de Lorraine, 1 rue Grandville, BP 20451, 54 001 Nancy Cedex France

Abstract: Click chemistry encompasses a group of powerful linking reactions that are simple to perform, have high yields, require no or minimal purification, and are versatile in joining diverse structures without the prerequisite of protection steps. The orthogonality of click reactions also results in ready access to a large number of compounds as the individual building blocks can be combined in different ways. Cellulose is one of the most abundant and inexpensive polysaccharides. Nevertheless, its supramolecular structure, its insolubility in water and most organic solvents and its poor processability have been limiting for several applications. Over the past few years, the copper(I) catalysed Huisgen 1,3-dipolar cycloaddition of azides and alkynes (CuAAC) click chemistry has offered new ways of modifying cellulose and its derivatives in particular mild conditions. This review with 63 references focuses on this emerging field for the synthesis of advanced cellulose-based materials and gels. The first part reports on cellulose pre-click modification for introducing azide or alkyne groups necessary for the CuAAC click chemistry. Its application is then reviewed for the preparation of different advanced cellulose-based macromolecular architectures: i) crosslinked networks for structural materials and hydrogels, ii) block and graft copolymers, and iii) dendronised celluloses. Recent works on cellulose-based polyelectrolytes are also reviewed before addressing the particular issue of (nano)cellulose surface modification. Within the frame of sustainable chemistry, CuAAC click chemistry certainly contributes to greatly extend the scope and functionality of cellulose-based materials for a wide range of applications in smart packaging, advanced food, health care, drug delivery, biomaterials, biocomposites, biosensors, bactericidal materials, and biofunctional films.

Corresponding author. Email address: anne.jonquieres@univ-lorraine.fr, tel: +33 3 83 17 50 29, fax: +33 3 83 37 99 77.

1. Introduction to click chemistry

1.1. Definition of click chemistry

The introduction of the click chemistry concept by Sharpless and colleagues in 2001 [1] clearly marks a turning point in synthetic chemistry as its fundamental principles have been rapidly adopted and it has served as inspiration for chemists in almost all areas [2].

The term "click" refers to facile, efficient, selective and versatile chemical transformations [3]. Therefore, click chemistry was born to meet the demands of modern day chemistry and be a solution to many problems that have been encountered in polymer science for a long time, such as:

a) A poor degree of functionalization with many conventional methods, especially when involving multiple functional groups (i.e. in graft-, star-, and block copolymers, dendrimers, as well as on densely packed surfaces and interfaces);

b) Purification problems associated with partially functionalized mixtures;

c) Incomplete reactions on surfaces and interfaces; and

d) Harsh reaction conditions of several conventional methods, which can lead to the break-up of auto-assemblies in particular in the newly emerging supramolecular sciences [4].

Click chemistry has led to a significant change in design strategies and the overall approach to synthetic problems. The click philosophy is based on the concepts of modularity and orthogonality: building blocks for a final target are made individually and subsequently assembled by means of click reactions. Such a modular approach is often more efficient than a conventional synthesis strategy involving sequential reactions. Moreover, the orthogonality of click reactions also results in ready access to a large number of compounds as the individual building blocks can be combined in different ways [2].

1.2. General classification of click reactions

Click chemistry encompasses a group of powerful linking reactions that are simple to perform, have high yields, require no or minimal purification, and are versatile in joining diverse structures without the prerequisite of protection steps. To date, four major classifications of click reactions have been identified:

- **Cycloadditions** : They primarily refer to Huisgen azide-alkyne 1,3-dipolar cycloadditions (Fig. 1) but they also include Diels-Alder and hetero-Diels-Alder cycloadditions (Fig. 2).

In particular, the thermally reversible nature of Diels-Alder adducts makes them attractive building blocks for the design of thermoreversible materials [5].

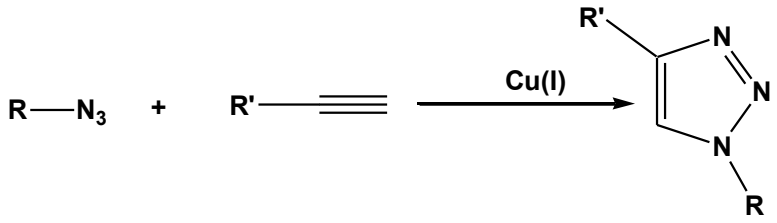

Figure 1: Huisgen 1,3-dipolar cycloaddition of azides and terminal alkynes [3].

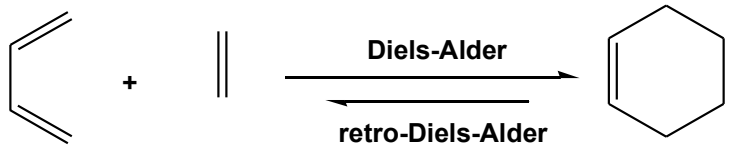

Figure 2: Diels–Alder/retro Diels–Alder reactions [5].

- **Nucleophilic ring-openings:** They refer to the opening of strained heterocyclic electrophiles, such as aziridines, epoxides, cyclic sulfates, etc (Fig. 3).

Figure 3: Nucleophilic ring-openings [3].

- **Carbonyl chemistry of the non-aldol type:** Examples include the formations of ureas, thioureas, hydrazones, oxime, ethers, amides, aromatic heterocycles, etc. Carbonyl reactions of the aldol type generally have longer reaction times and give side products, and therefore cannot be considered click reactions (Fig. 4).

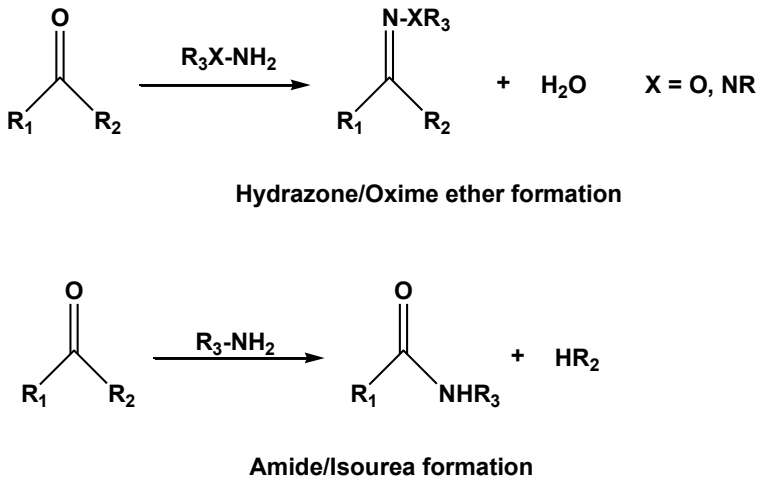

Figure 4: Non-aldol carbonyl chemistry [3].

- **Additions to carbon-carbon multiple bonds:** They include epoxidations, aziridinations, dihydroxylations, and certain Michael additions (Fig. 5) [6],[7].

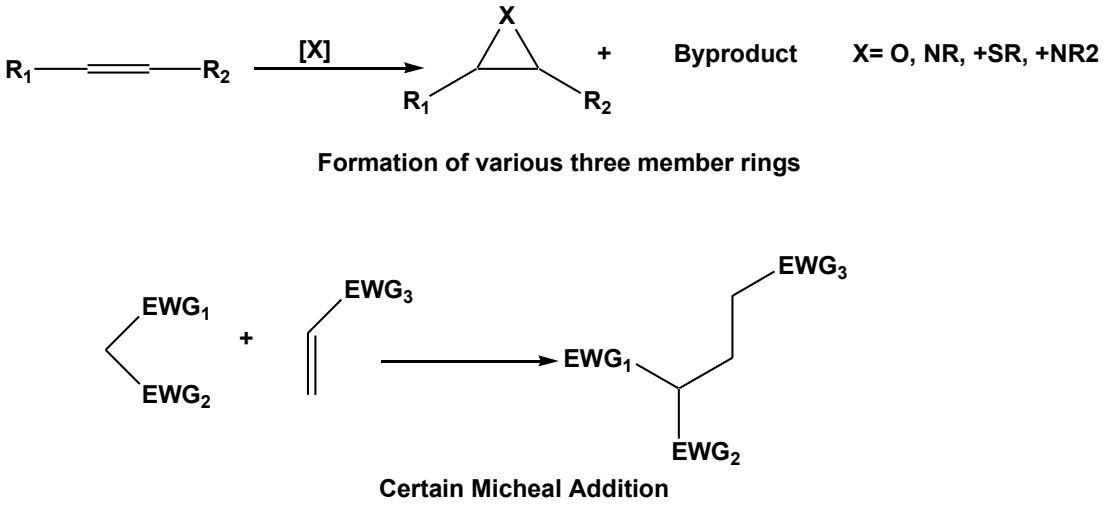

Figure 5: Carbon-carbon multiple bonds additions [3].

Other important examples are thiol based click reactions (Fig. 6) [8]. Thiol based click reactions can proceed by free radical addition of thiols or can involve a number of nucleophilic thiol-X additions, e.g. base catalyzed Michael-type thiol-ene additions, thiol isocyanate additions, thiol oxirane additions and thiol halogen substitutions [9]. Although thiol based click reactions by free radical can be debaited due to the formation of bi-products during thier reaction

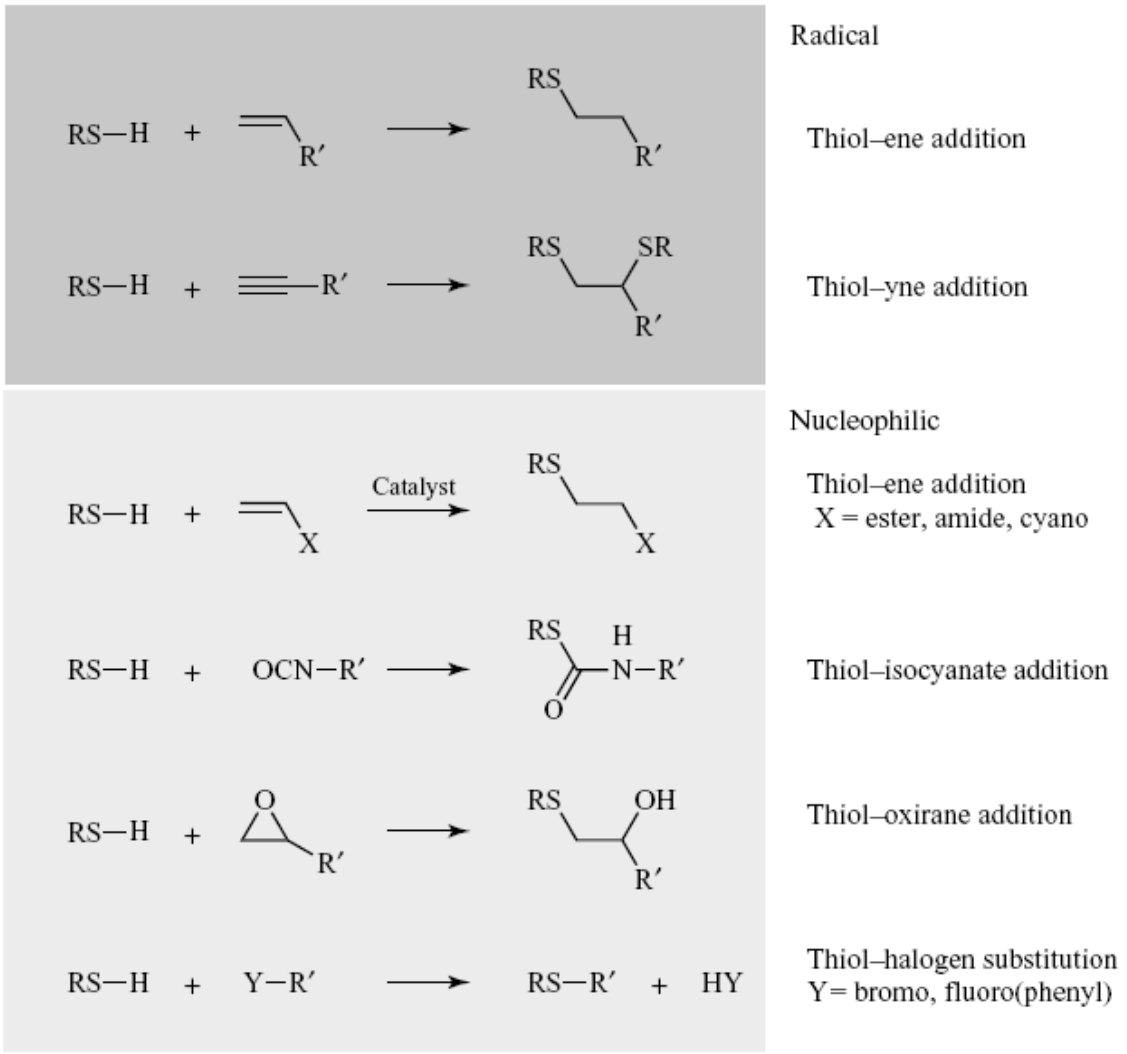

Figure 6: Radical and nucleophilic thiol based click reactions [8].

1.3. Click chemistry based on Cu-catalyzed Azide-Alkyne Cycloaddition (CuAAC)

Although different chemical reactions can be considered as click type reactions as mentioned earlier, Cu(I) catalyzed Huisgen 1,3-dipolar cycloaddition of azides and alkynes (CuAAC) to form 1,2,3-triazoles remains the leading example for click chemistry [10, 11]. Hence, the term “click” has been most generally used to denote this reaction in recent literature. In this part, we will focus on this particular reaction, which will be mainly used in the PhD thesis

1.3.1. Introduction to Cu-catalyzed Azide-Alkyne Cycloaddition CuAAC

Among the cycloaddtion click reactions Sharpless et al used to consider the Cu(I) catalyzed Huisgen 1,3-dipolar cycloaddition of azides and alkynes (CuAAC) as the cream

and crop due to that the azides and terminal alkynes are fairly easy to introduce by chemical functionalization and they are extremely stable at standard conditions in addition to the absence of dimerization problems of the azide group [1]. They both can tolerate oxygen, water, common organic synthesis conditions, biological molecules, a large range of pH, and the reaction conditions of living systems (reducing environment, hydrolysis, etc.) [6].

Among the several advantages of CuAAC, this reaction is particularly attractive for bioscience. Firstly, as aforementioned, CuAAC proceeds well in aqueous medium and therefore may be efficiently performed under physiological conditions. Perhaps even more importantly, CuAAC is an extremely chemoselective reaction and can therefore be used for modifying highly functional biomolecules such as polypeptides, nucleic acids or polysaccharides [3].

In the absence of transition-metal catalyst, 1,3-dipolar Huisgen cycloadditions of azides and alkynes are, in most cases, not regioselective and usually rather slow at room temperature [12]. However, Meldal and coworkers reported that the use of catalytic amounts of copper(I), which can bind to alkynes, leads to fast, highly efficient and regioselective azide–alkyne cycloadditions at room temperature in organic medium [13]. Moreover, CuAAC can be successfully performed in polar media such as tert-butyl alcohol, ethanol or pure water led to a remarkable development of Huisgen cycloadditions in synthetic chemistry. Hence, CuAAC has been exponentially investigated within the last few years in organic synthesis, inorganic chemistry, polymer chemistry and biochemistry [3, 14]. Such rapid adoption of CuAAC in almost all areas of chemistry is rather unique and illustrates the versatility of this click reaction [3]

1.3.2. Mechanism of Cu-catalyzed Azide-Alkyne Cycloaddition (CuAAC)

The role of copper in the catalysis of the triazole formation has been subject to many debates since the discovery of this extremely useful cycloaddition, in which the catalyst accelerates the rate of reaction by 7 orders of magnitude [13].

The mechanism of azide/alkyne click reaction was first proposed by Sharpless et al. [10] and updated by Bock et al.[15] indicating that using of the Cu(I) catalyst improve the regioselectivity of the reaction to get absolute 1,4-triazoles and the reaction is kinetically second order. This means that at least two cupper atoms are probably used as linkage center for two acetylene groups by μ bridge (Fig. 7).

From Figure 7, it was found that in the first step of the reaction, Cu(I) can insert itself into the terminal alkynes. It can coordinate with the π electron of terminal alkynes. This

coordination is responsible for lowering the pKa of the acetylene proton, thus allowing deprotonation of the alkynes in aqueous solvent without the addition of a base. The structure of the resulting Cu(I) acetylide is very difficult to predict and approximately 35 structures have been reported for this intermediate . In the case of using a non basic solvent, a base, has to be added [6].

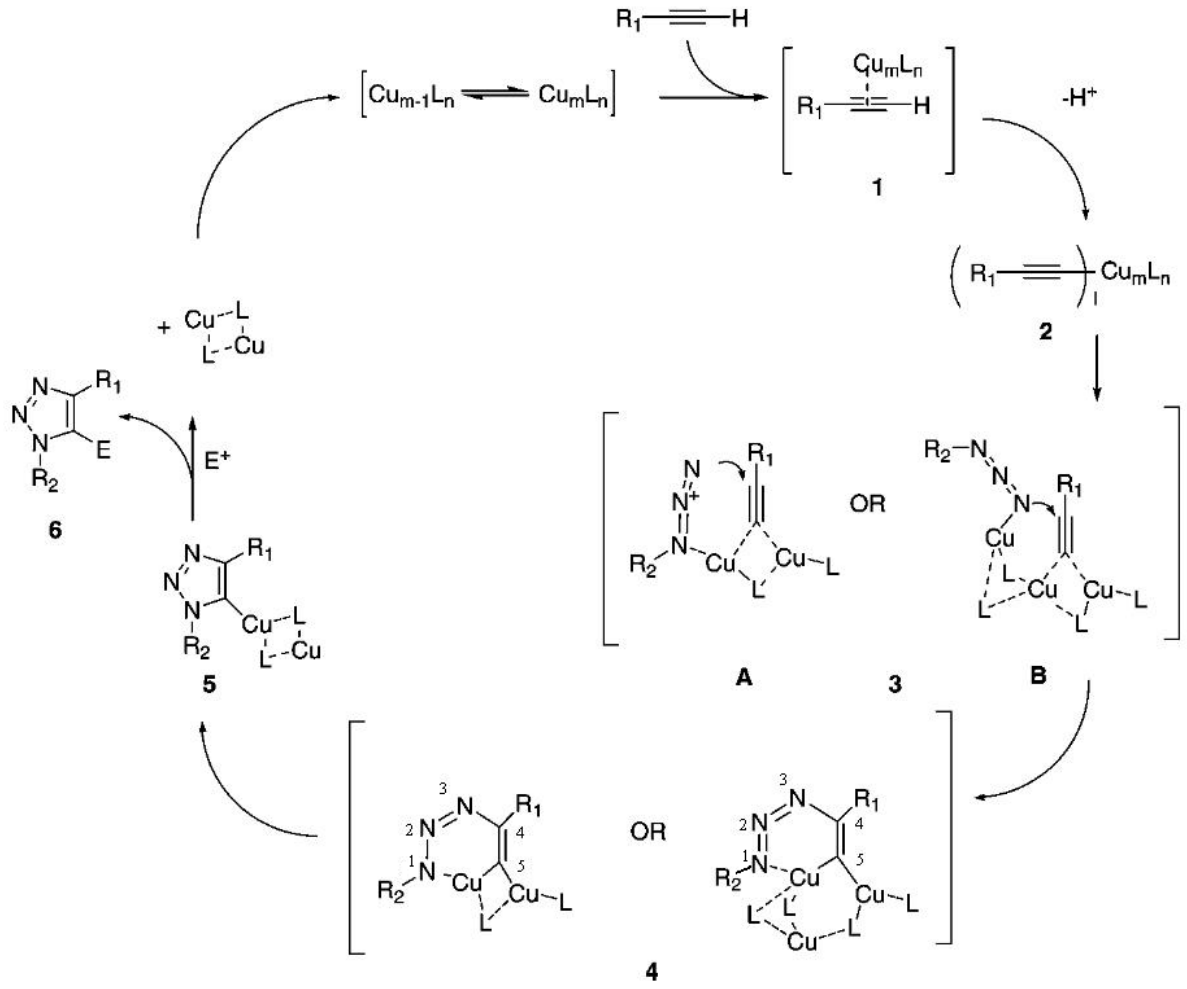

Figure 7: Proposed mechanism for the azyde/alkyne click reaction. Ligands are represented by "L" [4].

In the following step N1 atom displaces one of the ligands from the second Cu to form the species 3, which activates the azide for nucleophilic addition of N3 onto C4 becomes very easy, leading to the formation of metallocycle in step 4. The metallocycle contracts when N1 attacks C5 to form the triazole in step 5. Once the species 5 is formed, the attached Cu dimer immediately complexes to a second terminal alkyne. However, this second alkyne cannot undergo a cycloaddition due to the unfavorable structure of the complex, and it dissociates upon protonation to reform 5. One final protonation releases the Cu(I) catalyst

from the 1,2,3-triazole product 6. Both of these protonations generally occur due to interactions with protonated base or solvent [6].

1.3.3. Catalytic systems for Azide-Alkyne Cycloadditions (AAC)

A variety of methods have been used to generate active catalysts that affect on 1, 3 dipolar cycloaddition reactions. One of the most common methods is the reduction of Cu(II) salts e.g. $CuSO_4.5H_2O$ in the presence of a reducing agent such as sodium ascorbate to obtain the active Cu(I). There are large number of reducing agents that can be used with a reasonable success such as hydrazine and tris(2-carboxyethyl)phosphine. This catalytic system is preferred in many cases because it is very cheap, can be performed in water and does not need deoxygenated atmosphere. But the main drawback of this system is that the reducing agent may also reduce Cu(II) to Cu(0) , this limitation can be overcome by using a proper ratio of the reducing agent to the catalyst and addition of stabilizing agent such as tris(hydroxypropyl triazolyl methyl) [6].

Another source of Cu(I) is the direct addition of Cu(I) salts such as copper halides, CuI and CuBr. Copper halides are largely applicable in polymer and biological reactions. They are soluble in organic solvent and the reaction rate increases comparing to $CuSO_4.5H_2O$. But purity of the catalyst system is a more important criterion, so using of $CuSO_4.5H_2O$ is more reliable than copper halides due to high purity of $CuSO_4.5H_2O$. In case of CuI, it is often selected when special anhydrous condition is required, and can be purified because of its partial solubility in intermediate polar solvent such as acetonitrile, THF, and acetone.

Another catalytic system consists of oxidizing copper metal with an amine salt, but this method has a lot of problems. First, it needs long reaction time and using of large amount of copper, which makes it more expensive comparing to the other methods. In addition, it requires acidic environment that may affect negatively on the acidic sensitive functional groups [6].

Using of Cu(I) modified zeolites as catalytic systems are very promising, since they are high porous, have high surface area, high thermal/hydrothermal stability and high site of selectivity [13].

CuAAC generally yields 1,4-disubstituted 1,2,3-triazole (Fig. 8A). In some cases, however, 1,5-disubstituted triazoles are preferred e.g. for the synthesis of certain enzyme inhibitors. In order to obtain exclusively 1,5-disubstituted 1,2,3-triazoles from organic azides and alkynes, a ruthenium(II) catalyst was used (Fig. 8B). This Ru-catalyzed process, (RuAAC) exhibited a good scope with respect to both azides and terminal or internal alkynes

and functional group tolerance. Nevertheless, in contrast to CuAAC, RuAAC requires more stringent reaction conditions with respect to temperature and solvent, which has generally limited its application to bioconjugation reactions for biologically relevant molecules [16].

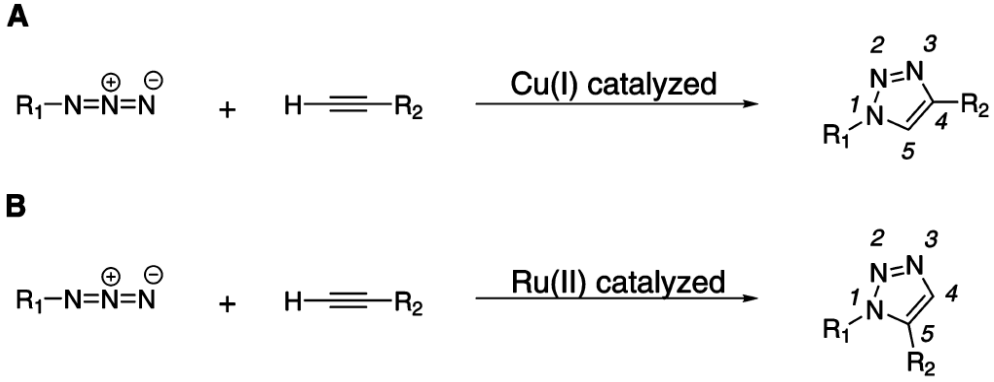

Figure 8: (A) Cu(I)-catalyzed 1,3-dipolar cycloaddition reaction, (B) Ruthenium(II)-catalyzed cycloaddition [16]

1.3.4. Copper free Azide-Alkyne Cycloadditions (AAC)

A potential drawback of the Cu(I) catalyzed cycloadditions for the synthesis of polymers, in particular those aimed for biomedical applications, is the cytotoxicity of Cu(I). This can be especially troublesome because it is difficult to remove the copper catalyst from the synthesized polymers.

Several studies have shown that catalysis is not always required for the cycloaddition to proceed. Strain promoted or Cu(I)free (2,3) cycloaddition strategy relies on the use of cyclooctynes, which decrease the activation energy of the cycloaddition. In this case, the click reaction can be carried out without Cu(I) catalyst at low temperature [17].

However, the first generation of cyclooctynes was hampered with a relatively low reactivity toward azides, as compared to the CuAAC, resulting in long reaction times and lower coupling efficiencies.In addition, the cyclooctynes method produces a racemic mixture of regioisomers, which is not compatible with the concept of click chemistry, requiring click reactions to be regiospecific (Fig. 9) [6].

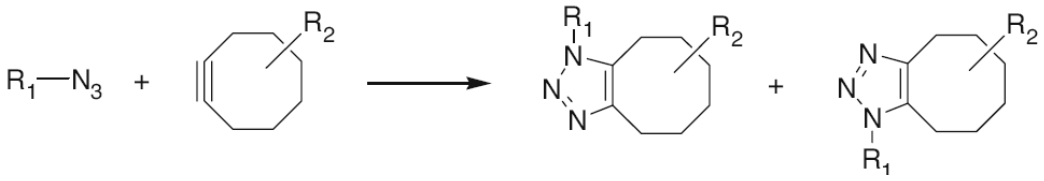

Figure 9: Huisgen 1,3 dipolar cycloaddition of azide and cyclooctyne without Cu(I) catalyst

To improve the cyclooctyne reactivity, several 4-dibenzocyclooctynols were synthesized (Fig. 10). By introducing aromatic moieties to the cyclooctyne, additional ring strain was created, and also better conjugation was achieved as an additional factor to increase the reactivity of the alkyne.[16].

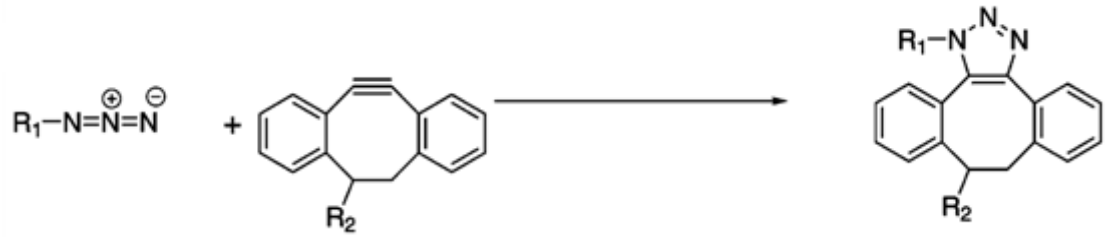

Figure 10: Ring strain promoted cycloaddition with 4-dibenzocyclooctynol

However, the first generation of cyclooctynes and 4-dibenzocyclooctynols was rather insoluble in water, and in an attempt to improve the reactivity and water solubility, a second generation of difluorinated cyclooctynes were synthesized (Fig. 11). These difluorinated cyclooctynes possess similar reaction kinetics as the Cu(I)-catalyzed cycloaddition reaction. Unfortunately, these difluorinated cyclooctynes are rather difficult to synthesize [16].

Figure 11: Second generation of ring strain promoted cycloaddition

2. Grafting of cellulose and cellulose derivatives by CuAAC click chemistry

2.1. Introduction

Cellulose is one of the most abundant and inexpensive polysaccharides. Nevertheless, its supramolecular structure, its insolubility in water and most organic solvents and its poor processability have been limiting for several applications. Chemical modification of cellulose has led to a variety of cellulosic derivatives with a broad property diversity and has opened new scopes to cellulose-based materials. Chemical modifications have also offered new functionalities to cellulose-based materials such as water or oil repellency, antibacterial properties or stimuli-responsive behaviours.

Recently, important progress has been made for cellulose and its derivatives with new modification strategies based on the copper(I) catalysed Huisgen 1,3-dipolar cycloaddition of azides and alkynes (CuAAC) click chemistry (Fig.7). Since the pioneering work of Sharpless et al. on CuAAC click chemistry[1, 18] and its first application to polymer chemistry in 2004,[19] CuAAC click chemistry has become one of the best approaches to complex macromolecular architectures and polymer modification.[2-4, 7, 20-22]

Over the past few years, CuAAC click chemistry has offered new ways of modifying cellulose and its derivatives in particular mild conditions and with hydrolytically stable triazole linkers. Its high reliability, efficiency and tolerance of different functional groups have contributed to developing great structural and functional variety for cellulosic materials. According to the work of Liebert et al. on the first modification of cellulose by CuAAC click chemistry [23] and to related recent reviews on polysaccharides,[22, 24, 25] CuAAC click chemistry still offers opportunities for polysaccharide modification with great potential for a wide range of applications in smart packaging, advanced food, health care, drug delivery, biomaterials, biosensors, bactericidal and antifouling materials, biofunctional films etc.

The following part of this chapter focuses on the emerging field of cellulose/cellulose derivatives grafting by CuAAC click chemistry for the synthesis of advanced materials and gels. The first part reports on cellulose pre-click modification for introducing azide or alkyne groups, which are necessary for CuAAC click chemistry. The chapter then reviews the use of CuAAC click chemistry for the preparation of different cellulose-based macromolecular architectures: i) crosslinked networks for structural materials and hydrogels, ii) block and graft copolymers, and iii) dendronised celluloses. Recent works on cellulose-based polyelectrolytes obtained by CuAAC click chemistry are also reviewed before addressing the particular issue of advanced cellulose (nano) materials by CuAAC surface modification.

2.2. Pre-click modification of cellulose and cellulose derivatives for CuAAC click chemistry

Pre-click modification of cellulose and cellulose derivatives is an essential step for CuAAC click chemistry, which consists of introducing azido or alkyne groups onto the anhydroglucose rings (Fig. 12).[22, 26]

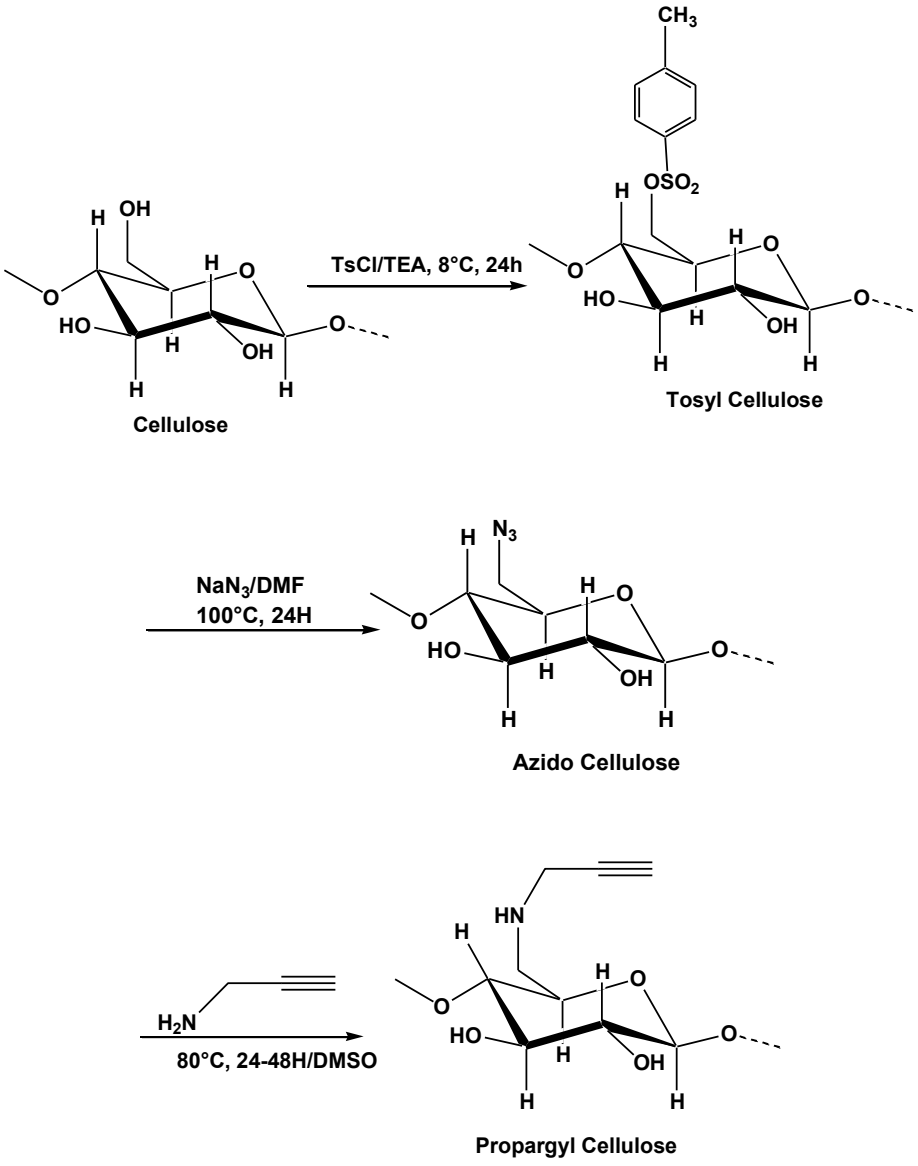

Figure 12: Pre-click modification of cellulose for CuAAC click chemistry. An example according to Faugeras et al.[22, 26]

This functionalisation is mainly achieved after activation of the cellulose hydroxyl groups by tosylation. The resulting *p*-toluene sulfonic ester of cellulose (tosyl cellulose) is one of the most widely used intermediates in cellulose chemistry due to its high reactivity and

its solubility in a wide range of organic solvents.[27] Tosylation of cellulose can be carried out by homogeneous reaction of cellulose with *p*-toluene sulfonic acid in DMAc/LiCl. A wide range of substitution degrees for the tosyl group (DS_{tosyl}) can be obtained by varying the molar ratio of *p*-toluene sulfonic acid to the cellulose hydroxyl groups. Furthermore, cellulose tosylation takes place preferably at position 6, as expected from the better reactivity of the corresponding primary hydroxyl groups. Consequently, cellulose tosylation has been shown to be regioselective for $DS_{tosyl} < 1$.[26, 28] In addition, the tosyl group is an excellent leaving group to perform nucleophilic substitutions with e.g. sodium azide or propargyl amine and introduce azido or propargyl groups, respectively. Other miscellaneous techniques have been reported to a much less extent for cellulose random pre-modification for the CuAAC click chemistry [26, 29-32].

The properties of cellulose derivatives generally differ for randomly or regioselectively substitution of the hydroxyl groups of the anhydroglucose rings. Regioselectivity is thus an important issue in cellulose chemistry. The introduction of the azido or propargyl groups at positions 2 and 3 requires regioselective cellulose modification as initially reported by Koschella et al. for propargyl groups.[33, 34] Regioselective modification involves protecting group chemistry and additional synthetic steps, which are justified only when specific positions are targeted for the azido or propargyl groups.[35] As way of example, Fig.13 shows the regioselective cellulose modification for introducing propargyl groups at position 3 according to Fenn et al.[36] In the later work, thexyldimethylsilyl protecting groups were chosen due to their high selectivity for positions 2 and 6 in homogeneous conditions. 2,6-di-*O*-thexyldimethylsilyl cellulose was then treated with allyl halide (e.g. propargyl bromide) to produce 3-*O*-propargyl cellulose regioselectively. Xu et al. reported the same strategy to prepare an azido amphiphilic regioselective cellulose derivative (3-*O*-azidopropoxy poly(ethylene glycol)-2,6-di-*O*-thexyldimethylsilylcellulose).[37]

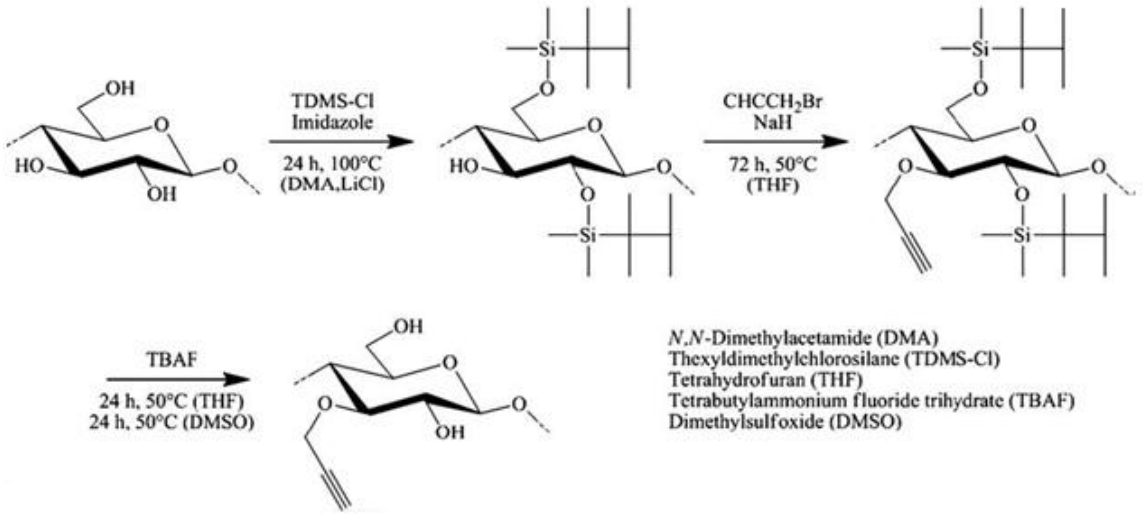

Figure 13: Regioselective pre-click modification of cellulose for CuAAC click chemistry. Example of the synthesis of 3-O-propargyl cellulose using thexyldimethylsilyl protecting groups.[36].

Pre-click modification of the *terminal* reducing or non-reducing ends of cellulose derivatives has been very rarely reported for CuAAC click chemistry and has offered new opportunities for designing original graft or block cellulosic copolymers.[38, 39] Nakagawa et al. prepared methyl cellulose with a terminal alkyne group at the non-reducing end by reacting methyl 1,2,3- tri-*O*-methyl celluloside with propargyl bromide after activation of the terminal hydroxyl group by NaH.[38] Cellulose triacetate derivatives with terminal azido groups at the reducing end were obtained as CuAAC precursors by Nakagawa et al.[38] and Enomoto-Rogers et al.[39] on the basis of a multi-step procedure initially reported by Kamitakahara et al. in a work not related to CuAAC click chemistry.[40]

2.3. Advanced crosslinked cellulose-based networks by CuAAC click chemistry

CuAAC click chemistry has brought new simple ways of crosslinking cellulose and cellulose derivatives on the basis of azido or propargyl-cellulose. Compared to former crosslinking strategies using difunctional agents, the new approaches based on CuAAC click chemistry offered specific advantages for designing crosslinked cellulose-based newtorks.[26]. The chemical stability of the triazole ring formed by reaction of azido with alkyne groups was one of the important advantages compared to the weakness of former ester-containing crosslinking bridges towards hydrolysis. The new strategy also allowed a much better control of network formation by avoiding intramolecular reactions of the azido or alkyne groups. In this new strategy, the azido or alkyne side groups had to react with

complementary groups on other polysaccharide chains to form the crosslinking bridges, leading to improved three-dimensional networks.

2.3.1. Crosslinked cellulose-based structural materials

Over the past few years, new strategies based on CuAAC click chemistry have led to original advanced crosslinked structural materials from cellulose alone or cellulose combined with other polysaccharides. A nice example was reported by Faugeras et al. with a simple approach for cellulose crosslinking (Fig.14).[26] In this work, azido-cellulose with a DS_{azide} of 1.5 was reacted with propargyl-cellulose with a DS_{alkyne} of 1.3. CuAAC click chemistry was performed in DMSO/H_2O with $CuSO_4$, $5H_2O$ in presence of sodium ascorbate (reducing agent) during 7 days at room temperature or activated by microwave irradiation. Scanning electron microscopy revealed very significant differences between the azido- or propargyl-celluloses, and the resulting crosslinked porous networks.

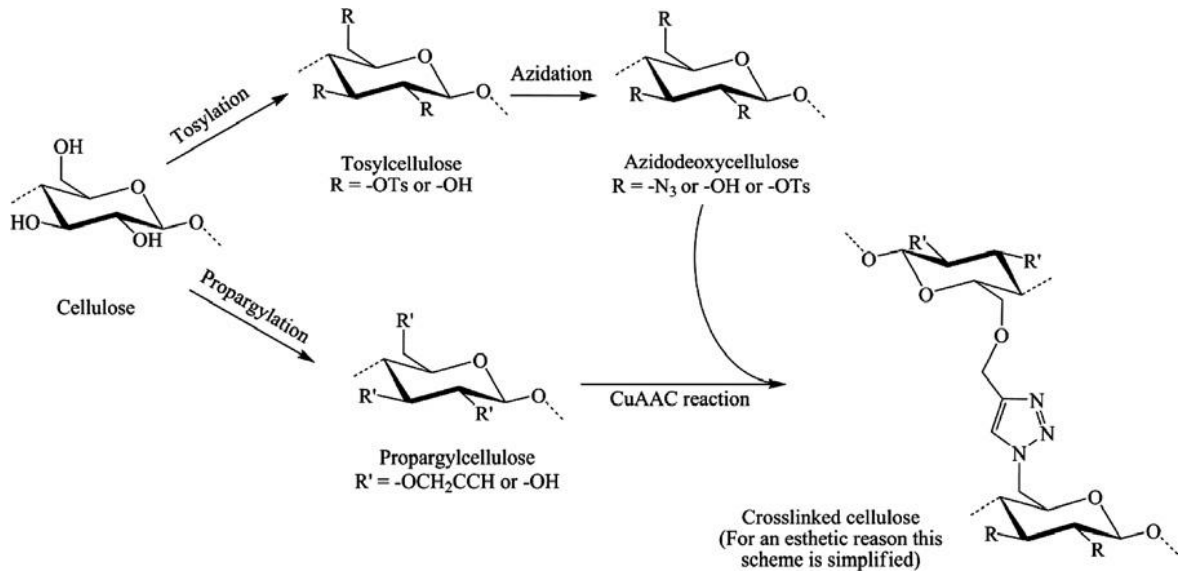

Figure 14: Preparation of crosslinked cellulose by CuAAC click chemistry.[26].

This promising approach was then extended to crosslinking of azido-cellulose with propargylated starch.[41] In the later 4-step strategy, 6-azido 6-deoxy cellulose with a DS_{azide} of 0.4 obtained under microwave irradiation, was reacted with propargylated starch with a DS_{alkyne} of 2.2. The crosslinked cellulose/starch networks were obtained in high yield (83%). SEM characterisation showed the different morphologies obtained after each step and the continuity of the polysaccharide network after crosslinking as shown in Fig.15.

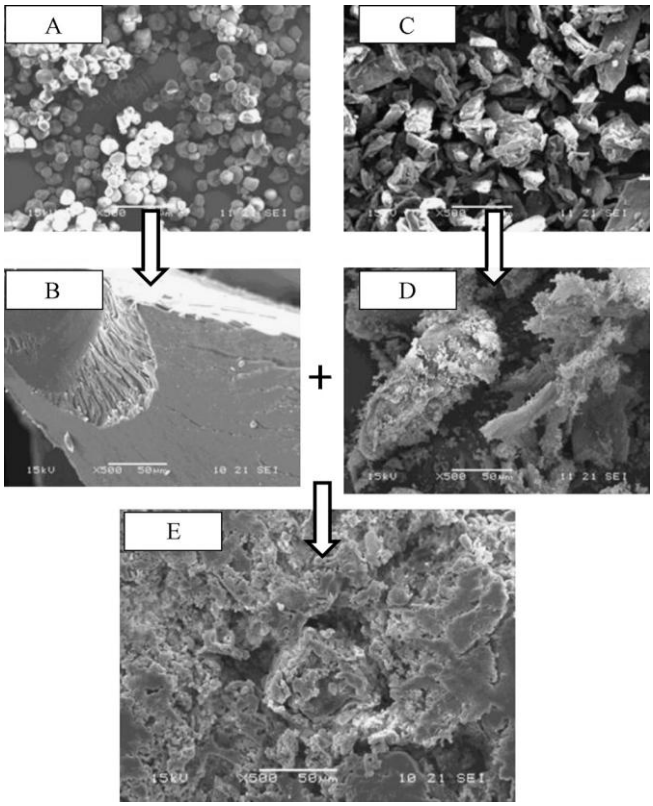

Figure 15: SEM pictures (500×) of: (A) unmodified starch; (B) propargyl starch; (C) unmodified cellulose; (D) azido cellulose; (E) crosslinked cellulose/starch network obtained by CuAAC click chemistry.[41].

In another recent related work by Peng et al., CuAAC click chemistry was reported for crosslinking of cellulose and chitosan, which is another important polysaccharide (Fig. 16).[29]. Propargyl-celluloses with different DS_{alkyne} from 0.25 to 1.24 were reacted with azido-chitosans with DS_{azide} from 0.02 to 0.46 in DMSO/H_2O with $CuSO_4$, $5H_2O$ in presence of sodium ascorbate at room temperature for 48 h. FTIR characterization showed the significant decrease of the alkyne and azido bands after click chemistry. Complementary CP/MAS ^{13}C NMR experiments proved the formation of triazole rings. The crosslinked cellulose/chitosan networks had improved thermal stability compared to cellulose, chitosan and even cellulose/chitosan complex. SEM pictures obtained after fracture of the crosslinked networks revealed the striking presence of hollow tubes of millimiter size, which were not observed for the corresponding cellulose/chitosan complex (Fig. 17).

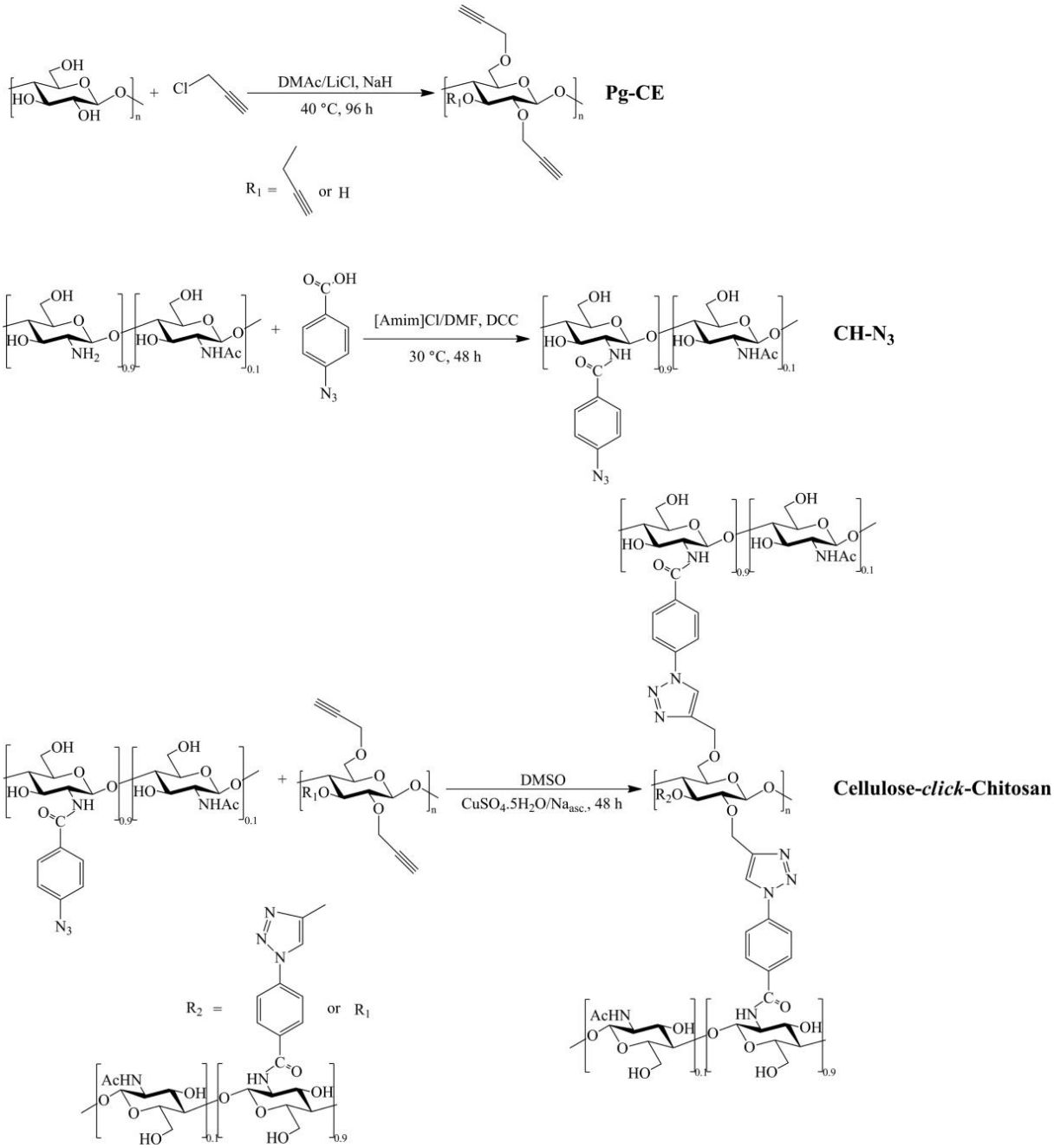

Figure 16: Preparation of crosslinked networks of cellulose and chitosan by CuAAC click chemistry.[29].

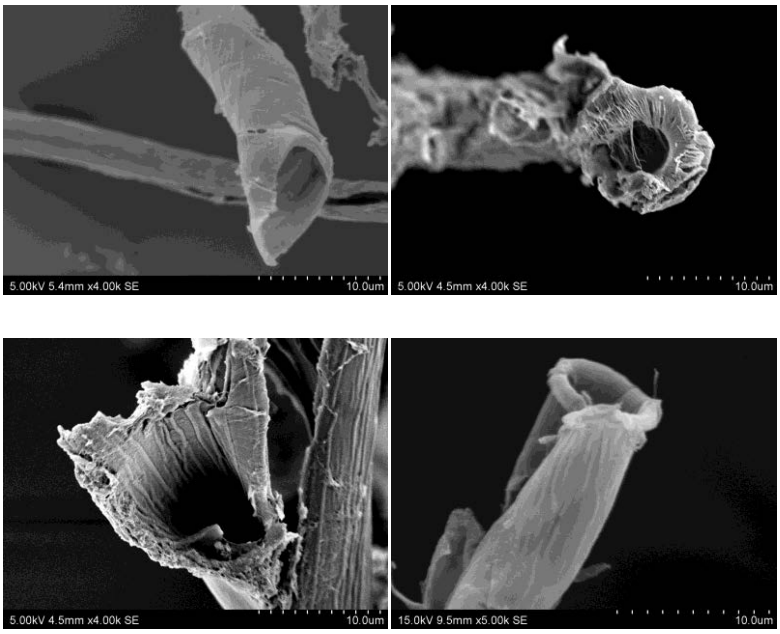

Figure 17: Examples of SEM pictures showing hollow tubes for the crosslinked networks of cellulose and chitosan obtained by CuAAC click chemistry.[29].

Agag et al. prepared original crosslinked networks of cellulose and polybenzoxazine from azido-cellulose and an alkyne-functionalised benzoxazine monomer (Fig.18).[42]. In the later work, benzoxazine monomer units were first grafted onto cellulose by CuAAC click chemistry as confirmed by FTIR and ^{1}H NMR. Thermal curing of this cellulosic derivative at high temperature (200°C/1h) led to the ring opening polymerisation (ROP) of the benzoxazine monomer units. TGA analysis showed that the resulting crosslinked cellulose/polybenzoxazine networks were much more resistant to heat than virgin cellulose, with a residual weight increased by one order of magnitude at 800°C.

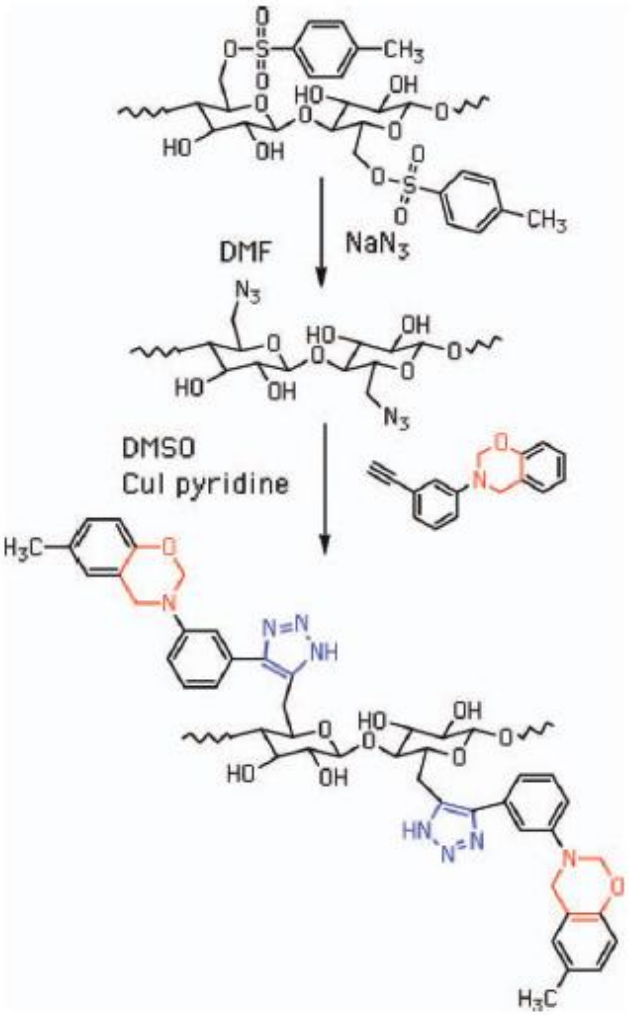

Figure 18: Synthesis of benzoxazine-functional cellulose by CuAAC click chemistry, considered as an interesting intermediate for preparing crosslinked cellulose/polybenzoxazine networks.[42].

2.3.2. Crosslinked cellulose-based hydrogels

CuAAC click chemistry has also offered innovative pathways to crosslinked polysaccharide-based hydrogels, which have been recently reviewed by Elchinger et al. and Uliniuc et al..[22, 25] Amongst them, cellulose-based hydrogels have remained really scarce so far, despite their high potential as crosslinked bio-based hydrogels.

With this respect, Koschella et al. have reported the carboxymethylation of azido- and alkyne-celluloses leading to water soluble cellulose derivatives for CuAAC click chemistry.[43] Transparent hydrogels were then readily obtained by adding $CuSO_4$, 5 H_20 and ascorbic acid to aqueous solutions containing both cellulose derivatives with equimolar

ratio of azido and alkyne groups (Fig. 19). Rheologic measurements showed that the gelation time strongly decreased with increasing DS_{azide}, DS_{alkyne} and copper catalyst concentration. Some of the freshly prepared hydrogels could further swell in water up to a water content of ca. 100%. However, in these challenging conditions, these hydrogels lost their mechanical withstanding and disintegrated. According to the authors, improving click chemistry for these systems could lead to advanced stimuli responsive cellulose-based hydrogels.

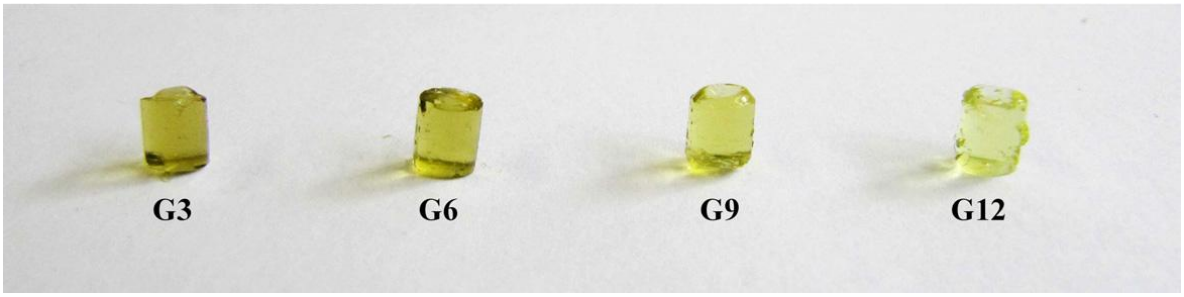

Figure 19: Freshly prepared hydrogels by CuAAC click chemistry of azido- and alkyne-carboxymethyl celluloses in various conditions.[43].

Following another interesting synthetic pathway combining classical radical polymerisation, polymer modification and CuAAC click chemistry, Zhang et al. synthesised a series of original temperature-responsive hydrogels from an azido-cellulose with a DS_{azide} of 0.95 and an alkyne- functionalised thermo-responsive copolymer (poly(N-isopropyl acrylamide-*co*-hydroxyl ethyl methacrylate) P(NIPAM-*co*-HEMA)).[44] The grafting of the alkyne-functionalised P(NIPAM-*co*-HEMA) onto the azido-cellulose was carried out in DMSO in presence of CuBr and *N,N,N′,N″,N‴*-pentamethyldiethylenetriamine (PMDETA) at room temperature with different amounts of the thermo-responsive grafts (Fig. 20). After freeze-drying and cryo-fracture of the crosslinked hydrogels, SEM pictures revealed discontinuous porous inner structures. The average pore sizes decreased from 40 and 10 µm when the amount of the thermo-responsive grafts increased from 50 to 80 wt%, leading to higher crosslinking degrees.

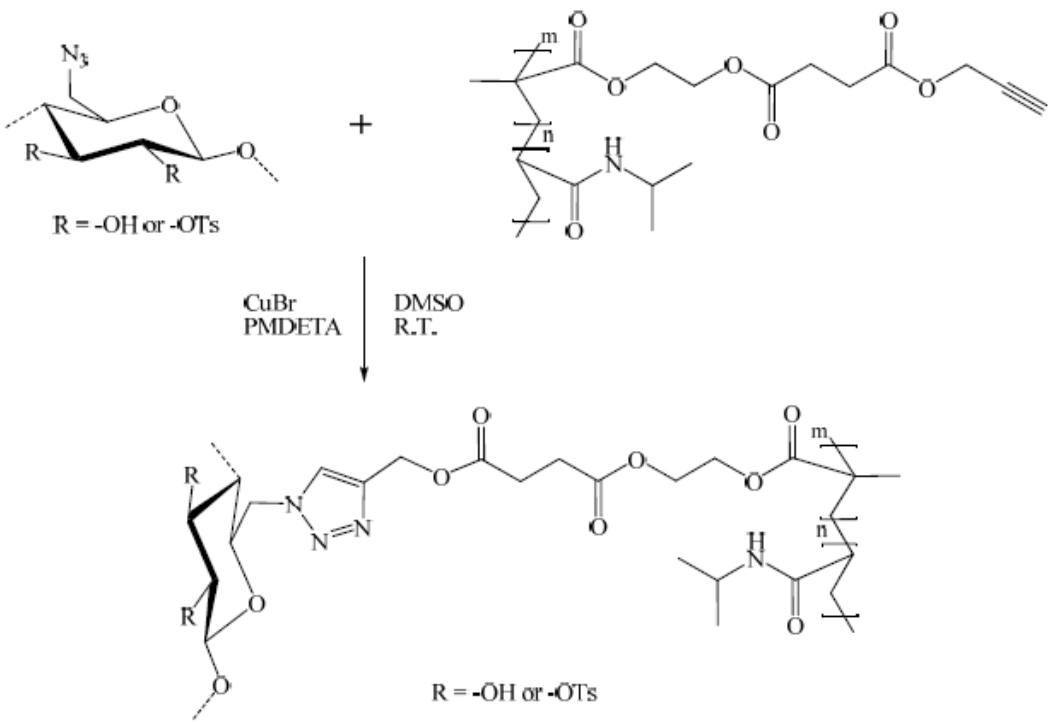

Figure 20: Preparation of thermo-responsive crosslinked hydrogels from an azido-cellulose and an alkyne-functionalised copolymer P(NIPAM-co-HEMA) by CuAAC click chemistry.[44].

2.4. Block and graft cellulosic copolymers by CuAAC click chemistry

To the best of our knowledge, the synthesis of *block copolymers* from cellulose or its derivatives by CuAAC click chemistry has been reported only once so far. In 2012, Nakagawa et al. prepared amphiphilic diblock copolymers from cellulose triacetate with a terminal azido group at position 1 and methyl cellulose with a terminal alkyne group at position 4 (Fig. 21).[38] CuAAC click chemistry in presence of CuBr, sodium ascorbate and PMDETA initially led to diblock copolymers with two *hydrophobic* blocks made of low molecular weight cellulose triacetate and methyl cellulose. After cleavage of the acetate groups by sodium methanolate in organic medium, the cellulose triacetate block was converted into a hydrophilic cellulose block. An amphiphilic diblock copolymer was finally obtained with thermoreversible gelation properties.

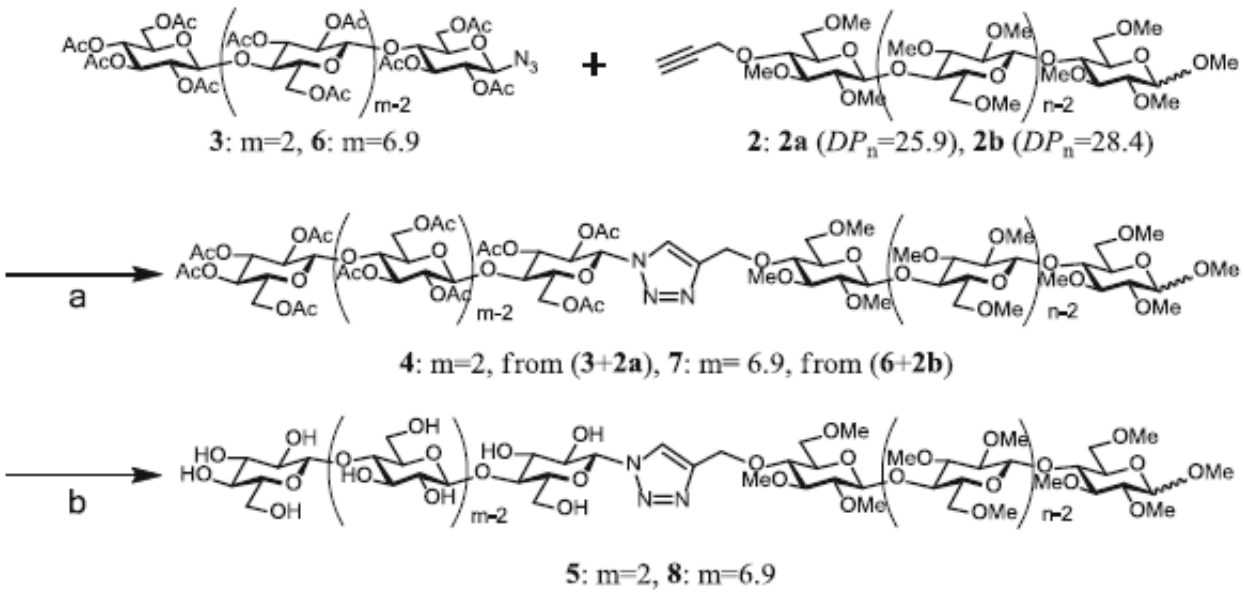

Figure 21: Preparation of amphiphilic cellulose-based diblock copolymers by CuAAC click chemistry.[38].

The preparation of *graft copolymers* from cellulose or cellulose derivatives has been widely investigated and, over the past few years, a few bibliographic reviews have pointed out the recent progress made for controlling this grafting by various techniques.[22, 24, 45-47] Nevertheless, CuAAC click chemistry has been rarely reported for the preparation of graft copolymers from cellulose and its derivatives so far. This click chemistry is currently emerging as a promising method for cellulose grafting and designing original materials with very different properties. Graft cellulosic copolymers are obtained by grafting of cellulosic derivatives in homogeneous solution. The grafting of (nano)cellulose surfaces is considered in a specific following subsection of this chapter.

By combining controlled radical polymerisation (ATRP) with CuAAC click chemistry, Li et al. prepared two closely related series of ethyl cellulose (EC) graft copolymers. For the first series of graft copolymers, an EC macroinitiator with brominated side groups was used for the "grafting from" of polystyrene (PS) grafts with controlled lengths (Fig. 22).[31]

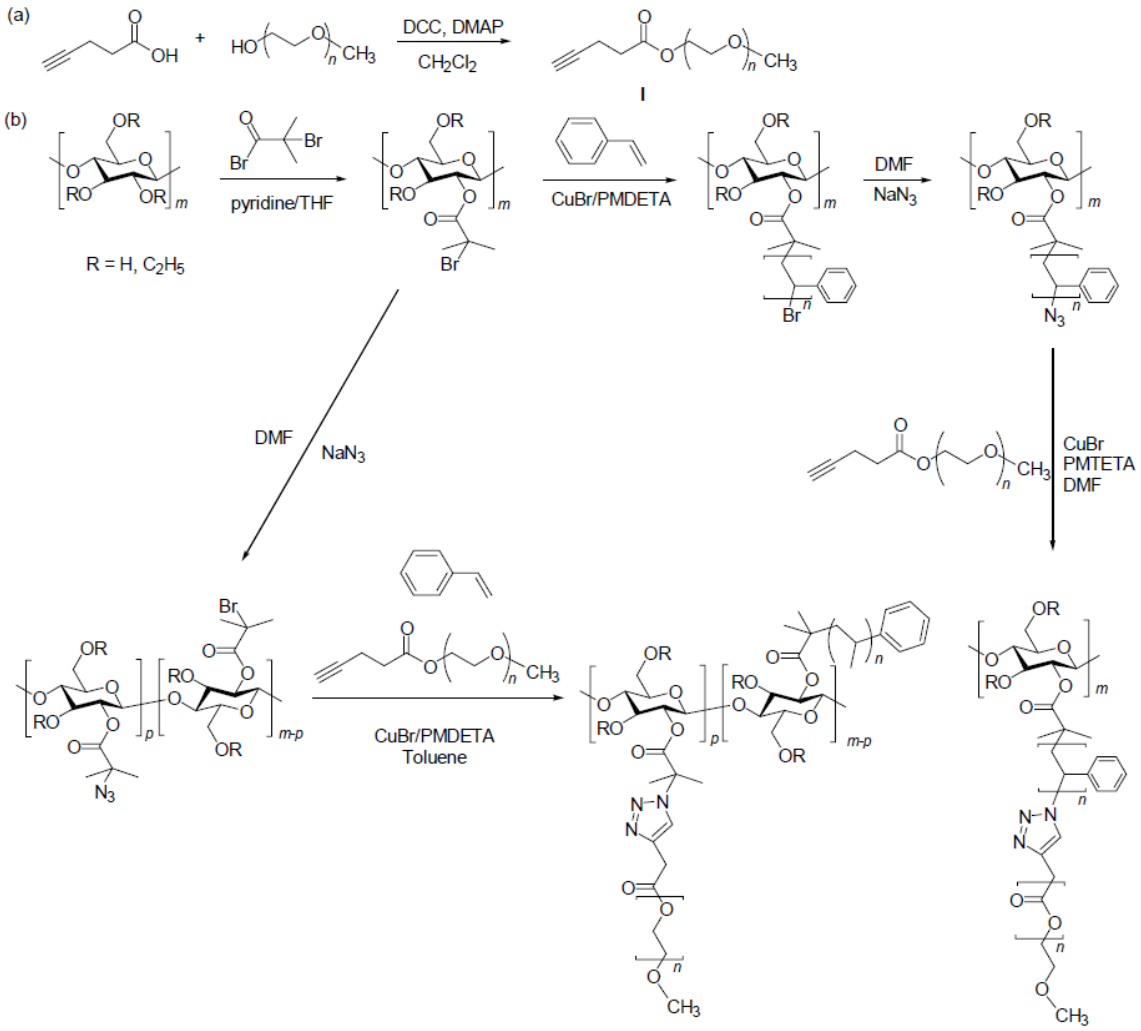

Figure 22: Two strategies for the synthesis of ethyl cellulose graft copolymers with diblock PS-b-PEG grafts or with both PS and PEG grafts by CuAAC click chemistry in homgeneous solution.[31].

The bromine terminal atoms of the PS grafts were then substituted for azido groups. These azido groups were further reacted with an alkyne-monomethoxy poly(ethylene glycol) by CuAAC click chemistry, leading to ethyl cellulose derivatives with diblock grafts PS-*b*-PEG. For the second series of copolymers, the bromine atoms of the EC macroinitiator were partially converted into azide groups. The resulting "clickable" macroinitiator was then used for the one-pot "grafting from" of styrene by ATRP and "grafting onto" of ω-alkyne monomethoxy-PEG by CuAAC click chemistry. This second smart strategy took advantage of the orthogonality of ATRP and CuAAC click chemistry for obtaining EC copolymers grafted by both PS and PEG grafts in a *single* synthesis step.

Amphiphilic cellulosic graft copolymers were obtained by Xu et al. with PEG grafts bearing azido terminal groups for click chemistry.[37] The multi-step synthesis allowed the

regioselective grafting of PEG with allyl terminal groups at position 3 with thexyldimethylsilyl protecting groups at positions 2 and 6. The allyl terminal groups of the PEG grafts were then converted into azido groups in 3 steps. Honeycomb films were then prepared by the breathing figures method and their pore sizes were controlled by the X_n of the functional PEG grafts. The honeycomb films were grafted by biotin by CuAAC click chemistry, leading to advanced functional porous films for bio-applications. Very recently, further studies showed the availability of the grafted biotin for conjugation with fluorescent avidin inside the pores of the honeycomb films (Fig. 23).[32] CuAAC click chemistry also enabled to functionalize the honeycomb films with Quantum Dots (QDs), which were again located inside the pores as shown by confocal fluorescence microscopy. In another related work by the same team, the grafting of an alkynated quaternary ammonium compound led to honeycomb films with antifouling and antibacterial properties for *Escherichia coli* [48].

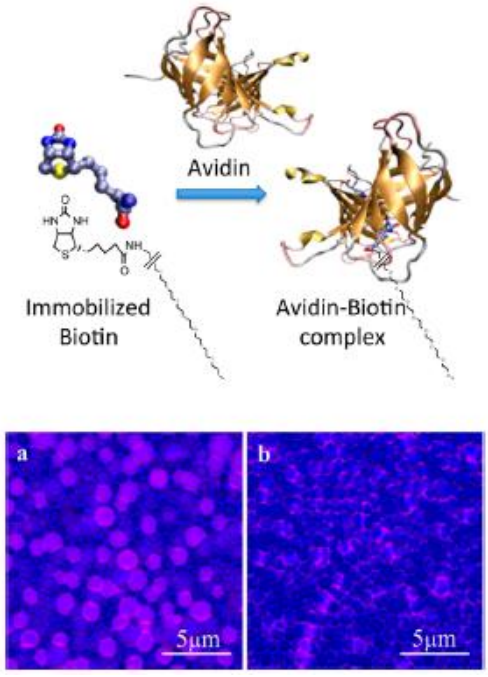

Figure 23: Bio-functional honeycomb films made of an amphiphilic cellulosic graft copolymer with PEG-biotin grafts obtained by CuAAC click chemistry. Comparison of the combined confocal fluorescent (pink) and optical (blue) images (a) before and (b) after conjugation with avidin.[32].

Negishi et al. reported the regioselective grafting of different alkyne-functionalised maltoside (Mal) and lactoside (Lac) oligosaccharides onto azido-cellulose at position 6.[49] The grafting was carried out by CuAAC click chemistry in DMSO in presence of $CuBr_2$, ascorbic acid, and propylamine at room temperature for 12h with yields ranging from 65 to 79%. Water solubility of the grafted copolymers was strongly influenced by the nature of the

spacer between cellulose and the grafted oligosaccharides. The water solubility was much lower in case of a hydrophobic spacer although molecular dynamics simulations showed that hydrophilic and hydrophobic spacers led to the same type of sheet-like structures for the grafted copolymers.

Compared with the former works on cellulosic copolymers grafted by CuAAC click chemistry, another originality of the recent work of Enomoto-Rogers et al. was to consider grafted copolymers with *cellulosic grafts* rather than cellulosic main chains (Fig.24).[39] In this new work, an amorphous polymethacrylate with alkyne side groups was initially prepared in three steps using protecting group chemistry. The "grafting onto" of cellulose triacetate grafts with azido groups at the reducing end was then carried out by CuAAC click chemistry. After cleavage of the acetate groups by sodium methanolate, a polymethacrylate comb copolymer was obtained with cellulosic grafts. An analysis by wide angle X-ray diffraction showed that a film of this grafted copolymer was semi-crystalline with a diffraction pattern corresponding to that of regenerated cellulose.

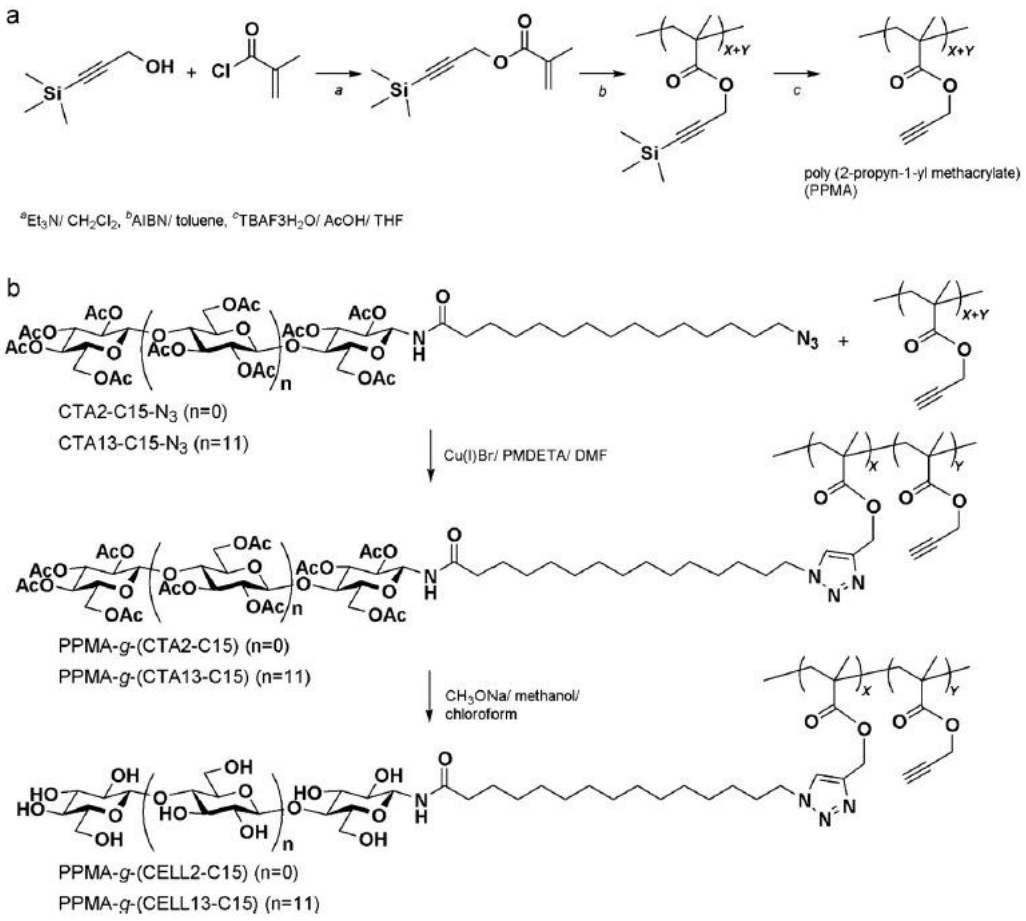

Figure 24: Preparation of polymethacrylate copolymers grafted with cellulosic side chains by CuAAC click chemistry.[39].

2.5. Dendronised celluloses by CuAAC click chemistry

The grafting of dendrons onto cellulose by CuAAC click chemistry has led to a variety of biofunctional materials over the past few years. Dendrons are fractal structures with increasing number of functional groups from one generation to the next one. Dendronization of cellulose can thus increase its chemical functionality tremendously and offer interesting prospects for a wide range of bio-applications (e.g. biosensors, drug delivery systems, biocatalysts etc).

In their first attempt to prepare dendronised cellulose, Pohl and Heinze regioselectively grafted polyamido amine (PAMAM) dendrons of first and second generations, with an azido moiety at their focal point, onto an alkyne-cellulose with a DS_{alkyne} of 0.48 at position 6 (Fig. 25).[28] The grafting rate decreased from 70 to 50 % for the dendrons of first and second generations, respecively, most likely due to strong steric hindrance. All the dendronised cellulose derivatives were soluble in aprotic dipolar solvents (DMSO, DMF, DMAc).

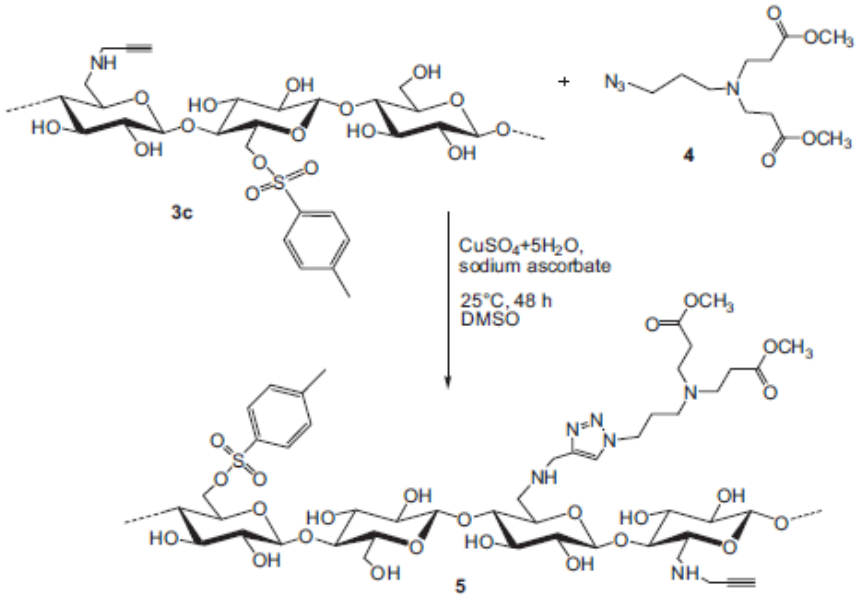

Figure 25: Preparation of dendronised cellulose with PAMAM dendrons of first generation from an alkyne-functionalised cellulose at position 6 by CuAAC click chemistry.[28].

Pohl et al. also investigated the reverse strategy consisting in grafting PAMAM dendrons with an alkyne moiety at their focal point onto an azido-cellulose with a DS_{azido} of 0.75 at position 6. In homogeneous conditions in DMSO, grafting rates of 89, 75 and 41% were obtained for the dendrons of first, second and third generations, respectively. Here again, steric hindrance limited the grafting rate of the bulkiest dendrons but, overall, the new

work greatly improved the number of grafted dendrons and the functionality of the dendronised celluloses. Heterogeneous grafting in MeOH was also remarkably well achieved with comparable grafting rates as those obtained in homogeneous conditions.[50]

The regioselective grafting of PAMAM dendrons onto cellulose at position 3 required more demanding protecting group chemistry.[36] Thexyldimethylsilyl groups were chosen as protective groups due to their high selectivity for positions 2 and 6, leaving position 3 available for introducing alkyne side groups with a DS_{alkyne} of 1. After deprotection, alkyne-cellulose was successfully grafted with azido-functionalised PAMAM dendrons of first and second generations but the grafting rates were fairly low (≤25%).

Water soluble dendronised celluloses were also prepared by Pohl et al. from a carboxymethylated azido-cellulose with a DS_{azide} of 0.81 by CuAAC click chemistry in water at ambient temperature (Fig.26).[51] The grafting of alkyne-functionalised PAMAM dendrons proceeded mainly at position 6 with grafting rates varying from 63 to 48 % from the first to the third generation of dendrons. A thorough physical chemical investigation showed that the grafting of dendrons had no or a weak influence on the cellulosic chain stiffness or conformation in solution.

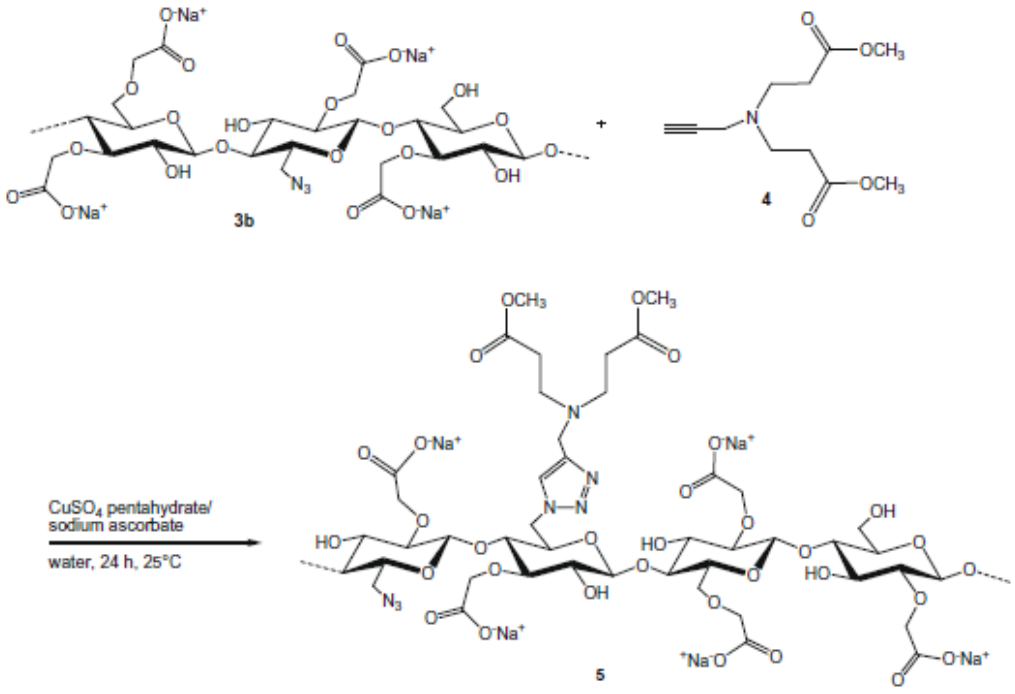

Figure 26: Preparation of dendronised carboxymethyl cellulose with PAMAM dendrons of first generation from an azido-functionalised cellulose at position 6 by CuAAC click chemistry.[51]

Novel biofunctional cellulosic films were also developed by the same team from dendronised cellulose containing a high number of amino groups, which are particularly appropriate for further modification with biomolecules.[52] In a first approach, azido-cellulose was first grafted with alkyne-dendrons containing terminal amine groups in homogeneous solution and the resulting dendronised cellulose was then simply blended with cellulose acetate. The second approach considered simple surface grafting of an azido-cellulose film with the same dendrons in mild conditions. After careful removal of the residual copper ions by complexation with diethyldithiocarbamate trihydrate to avoid any detrimental interference with the targeted biomolecules, the cellulosic films were successfully biofunctionalised with a glucose oxidase enzyme in two steps (Fig. 27).

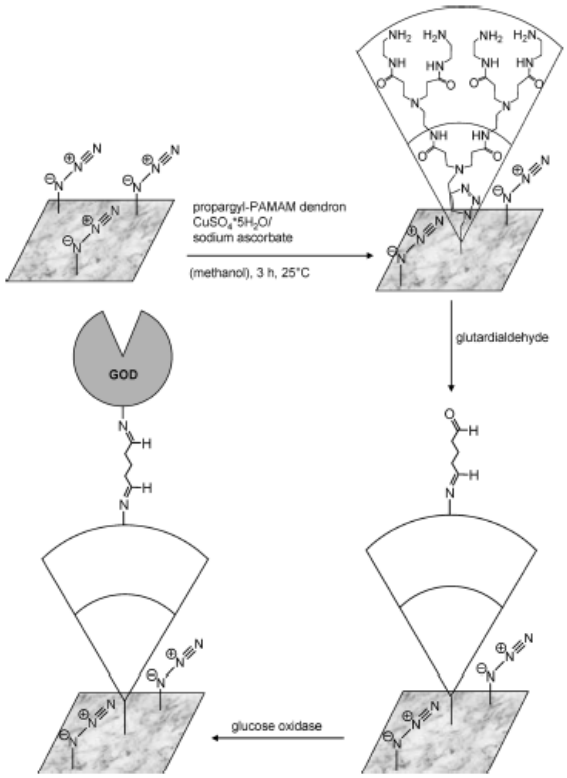

Figure 27: Two-step biofunctionalisation of an azido-cellulose film grafted by alkyne-dendrons containing terminal amino groups with a glucose oxydase enzyme.[52].

Highly versatile dendronised cellulosic surfaces were also developed by Montanez et al..[53] After its functionalization by azido groups, cellulose paper was grafted with functional dendrons of first to fifth generations by CuAAC click chemistry in mild conditions (Fig. 28). The dendron terminal groups were then chemically modified to obtain a very high number of orthogonal chemical functions at the periphery. By this high precision multi-step strategy, each hydroxyl group initially present at cellulose surface eventually led to 64 dendritic OH

and 32 dendritic azido groups. Biofunctionalisation was then successfully achieved with different alkyne-functionalised molecules including amoxicillin and mannose. In the latter case, the biofunctional surface allowed the detection of lectin protein at a concentration as low as 5 nM. This dendronised cellulosic platform is particularly promising for bio- and chemical sensors, with respect to the high number of the orthogonal functions present at the periphery and its versatility to address a wide range of sensing applications.

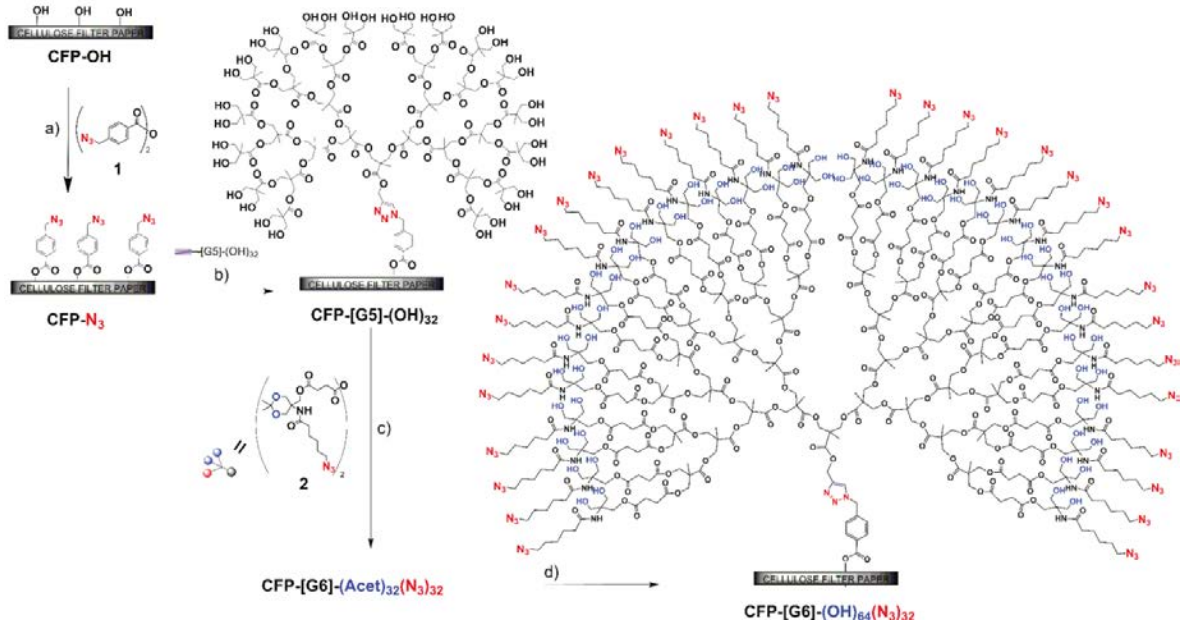

Figure 28: Schematic drawing of a biofunctional cellulose surface grafted with dendrons of fifth generation with 32 azido groups at the periphery.[53].

2.6. Cellulosic polyelectrolytes by CuAAC click chemistry

Polysaccharide-based polyelectrolytes have become very important in formulation of aqueous solutions for a wide range of applications. Today, food and health care industries largely rely on their particular properties in solution and in particular on their strong thickening effect at very low polymer concentration owing to the polyelectrolyte effect.

As firstly shown by Liebert et al., CuAAC click chemistry offered new pathways to original cellulosic polyelectrolytes.[23] Unlike cellulosic esters polyelectrolytes, these new polyelectrolyte were stable towards hydrolysis owing to the high stability of the triazole linkers between cellulose and the ionic side groups.

In a first work, 6-azido-6-deoxycelluloses with DS_{azide} ranging from 0.88 to 0.99 were grafted with an alkyne-functionalised carboxylic acid methyl ester and 2-ethynylaniline (Fig.

29) [23]. Both molecular reagents were considered as precursors for anionic and cationic groups, respectively, after appropriate modification of the grafted cellulose derivatives. High degree of substitution (0.86) was obtained for the carboxylic acid methyl ester in very mild conditions (25°C/molar ratio of 1 with respect to the azido groups). The efficient grafting of 2-ethynylaniline required much higher temperature (70°C) and a large excess in molecular reagent (3 equiv.). Both cellulosic derivatives were soluble in DMF or DMSO. Their modification with strong base or acid led to anionic and cationic cellulosic polyelectrolytes, respectively.

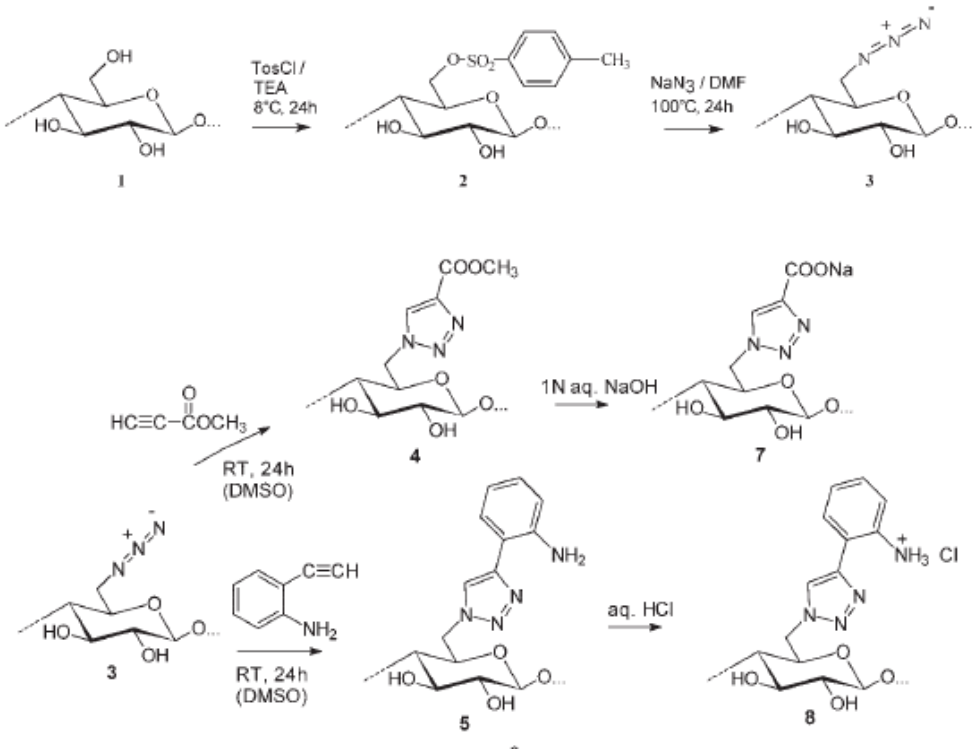

Figure 29: Preparation of anionic and cationic cellulosic polyelectrolytes by CuAAC click chemistry and further modification by strong base or acid [23].

In another work by the same team, this approach was transposed to the grafting of acetylenedicarboxylic acid dimethyl ester by means of click chemistry followed by saponification of the ester side groups.[54] The CuAAC click reaction of 6-azido-6-deoxycellulose with the alkyne-functionalised diester was performed with a grafting rate of 62% and enabled to increase greatly the number of anionic groups obtained after saponification compared to that of the first work. Furthermore, the later anionic cellulosic polylectrolytes displayed tensio-active properties and formed interesting ionotropic gels by precipitation in aqueous solutions containing multivalent ions (Ca^{2+}, Al^{3+}) or a cationic polyelectrolyte (poly(diallyldimethyl ammonium) chloride (polyDADMAC)).

Another interesting approach to novel cationic cellulosic polyelectrolytes based on azido-cellulose and alkyne-functionalised ionic liquids was reported by Gonsior and Ritter.[55] Cellulose is known to be soluble in a few ionic liquids including 1-ethyl-3-methyl imidazolium acetate (emim)(ac) but its viscosity is fairly high in these particular solvents. In the later work, 6-azido 6-deoxy cellulose with a DS_{azido} of ca. 1 was grafted with three different alkyne-functionalised ionic liquids (i.e. 1-methyl, 1-butyl, and 1-benzyl 3- propargyl imidazolium bromides) in DMSO/H_2O by CuAAC click chemistry at 25°C for 48 h (Fig. 30). Almost quantitative grafting was reached in these conditions with very high degrees of substitution for the grafted ionic liquids. Rheology experiments were carried out for virgin cellulose and the corresponding cationic polyelectrolytes in the ionic liquid 1-ethyl-3-methyl imidazolium acetate used as a solvent. The results showed that cellulose grafting with ionic liquids decreased solution viscosity by at least one order of magnitude compared to that of virgin cellulose. Furthermore, the solution viscosity decreased with the size of the alkyl substituent on the imidazolium ionic liquids, the methyl substituent thus providing the lowest solution viscosity.

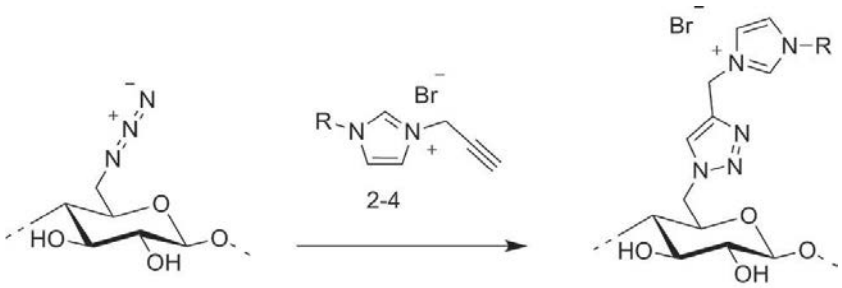

Figure 30: Preparation of cationic polyelectrolytes by grafting of azido-cellulose with alkyne-functionalised imidazolium ionic liquids.[55] R = Methyl, butyl or benzyl.

2.7. Advanced cellulose (nano)materials by CuAAC surface modification

Surface modification of cellulose has been developed for a long time and a few recent bibliographic reviews have pointed out the new progress made for its control by various techniques.[22, 24, 45-47]. The modification of nanocelluloses is another important emerging issue for advanced biomaterials and biocomposites.[56-60] Compared to other modification techniques, CuAAC click chemistry has been rarely used for (nano)cellulose surface modification so far. Nevertheless, recent works in this field show that this click chemistry offers a tremendous potential for designing original materials with very different properties and functionalities from nano to macro-scales.

2.7.1. Advanced materials by cellulose surface modification

Adapting a procedure reported by Hafrén et al. for cellulose paper grafting with a fluorescent probe,[61] Krouit et al. grafted cellulose Avicel powder by an aliphatic polyester in heterogeneous conditions.[62] The cellulosic powder was first functionalised with alkyne side groups with relatively long spacers in C_{11} for improving grafting efficiency. The "grafting onto" was then performed with a α,ω-diazido-polycaprolactone (PCL) by CuAAC click chemistry in mild conditions. In addition to surface grafting, the PCL difunctionality may have also led to limited surface crosslinking. These grafted cellulosic powders were considered as interesting precursors for the development of fully biodegradable cellulosic composites.[63]

A combination of controlled radical polymerisation with CuAAC click chemistry was another interesting approach for the *controlled* surface grafting of cellulose. In a first work by Haddleton et al.,[64] an azide-functionalised fluorescent polymethacrylate (PMMA) oligomer with controlled molecular weight was obtained by controlled radical copolymerisation (ATRP) of methyl methacrylate (MMA) and a fluorescent methacrylate comonomer. This fluorescent oligomer with an azido terminal group was then grafted onto an alkyne-functionalised cotton by CuAAC click chemistry. An azido-monomethoxy poly(ethylene glycol) was also grafted onto the same cotton derivative.

A thorough comparison of the methods of "grafting from" and "grafting onto" by CuAAC click chemistry has been recently reported by Hansson et al. for the cellulose surface grafting with PMMA grafts of different lengths.[65] In this work, PMMA was first "grafted from" a cellulose paper bearing initiator groups by controlled radical polymerisation (ARGET ATRP) (Fig. 31). Following a procedure well known for the control of the graft molecular weight by the "grafting from" method, the use of an alkyne-functional sacrificial initiator enabled to obtain free alkyne-functionalised PMMA oligomers with the same molecular weights as those of the PMMA grafts. These alkyne-functional PMMA oligomers were then "grafted onto" an azide-functionalised cellulose paper. A comparison of both surface grafting methods with identical grafts showed that the grafting density on the cellulosic surface was higher for the method of "grafting from", which also enabled a better control of the graft content. The method of "grafting onto" was limited by lower grafting density and efficiency for the longest grafts, mainly owing to the limited accessibility of the alkyne terminal groups of the corresponding PMMA oligomers.

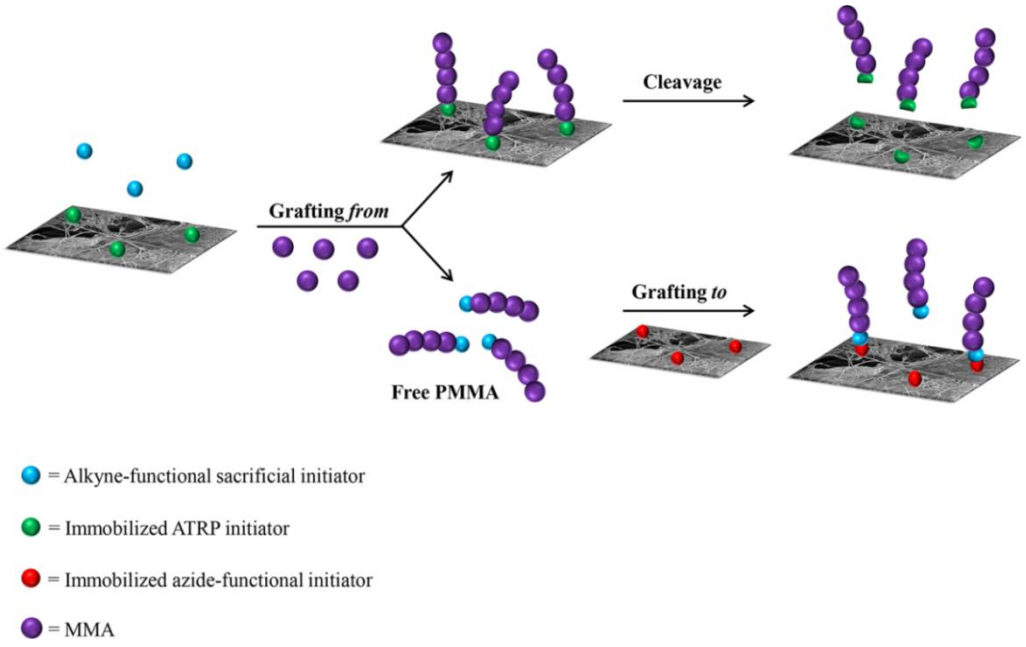

Figure 31: Cellulose surface modification by the methods of "grafting from" and "grafting onto" by CuAAC click chemistry with free alkyne-functional PMMA oligomers obtained during "grafting from" in presence of an alkyne-functional sacrificial initiator.[65].

Recently, Filpponen et al. have proposed a very different strategy for cellulose surface modification based on a combination of adsorption of a "clickable" carboxymethylcellulose on cellulose surface with sequential CuAAC grafting in mild conditions (Fig. 32).[30, 66] In a first step, a carboxymethylcellulose (CMC) modified with azido or alkyne groups was adsorbed on various cellulosic surfaces (*i.e.* regenerated cellulose, cellulose paper, cellulose nanofibrils (CNFs)) by simple coating or dipping in a functionalised CMC aqueous solution. Low CMC degree of substitution (DS_{azide} or DS_{alkyne}) and the presence of electrolytes in the aqueous solution were both important for a good adsorption of the functionalised CMC onto cellulosic surfaces.[66] The grafting of alkyne-functionalised bovine serum albumin (BSA), azido-functionalised fluorescent probe and monomethoxy PEG was then performed in mild conditions by CuAAC click chemistry. The versatility of this approach appears particularly interesting for modifying a variety of cellulosic surfaces.

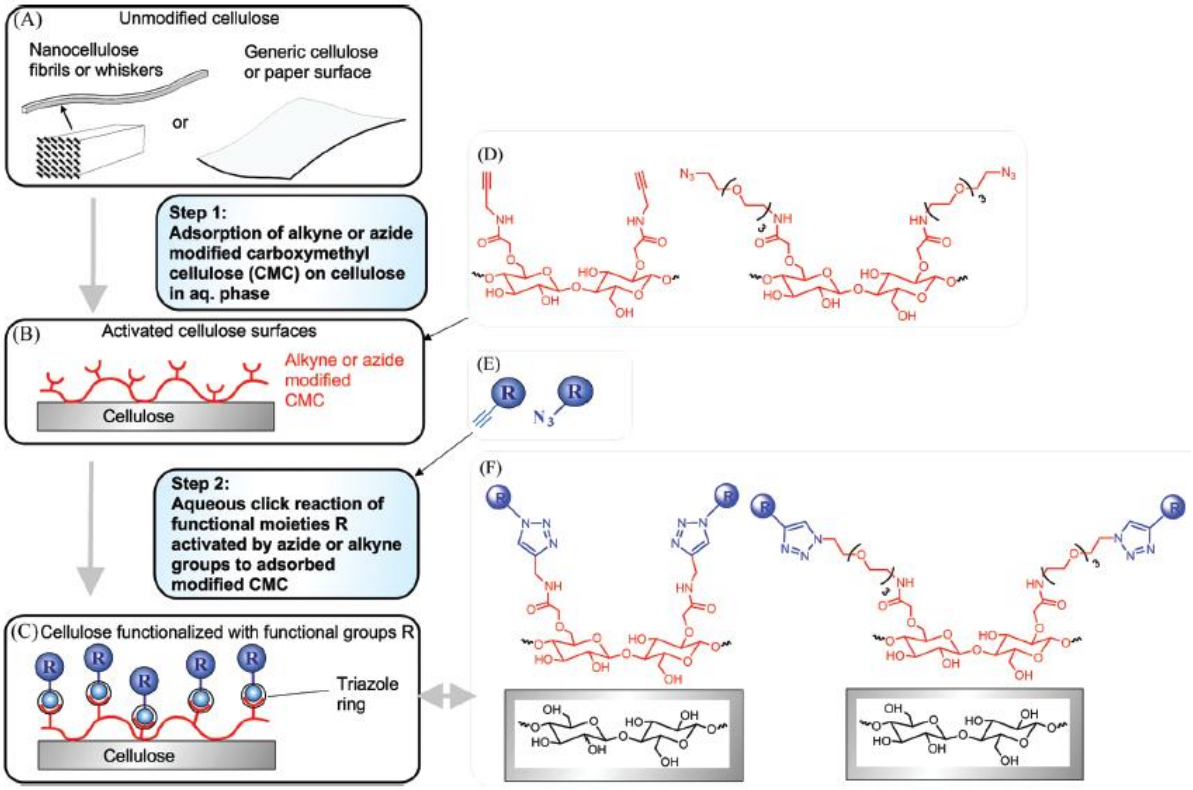

Figure 32: Cellulose surface modification based on a combination of adsorption of a "clickable" carboxymethylcellulose with sequential CuAAC grafting in mild conditions.[30]

2.7.2. Advanced materials by nanocellulose surface modification

Cellulose nanomaterials represent a new class of cellulosic materials (e.g. cellulose nanocrystals (CNC) , nanofibrils (CNF) etc.) with one dimension in the nanometer scale, which offer particularly high prospects for a wide range of applications.[56-59] Taking advantage of their high aspect ratio and outstanding mechanical properties, these renewable cellulosic materials have been mainly used as fillers to reinforce polymer materials in composites. In particular, their incorporation in biopolymers has led to original biocomposites for a sustainable composite industry.[63] Cellulose nanomaterials have also brought new functionalities to cellulose and offered new pathways to advanced materials for the paper, food, health care, cosmetics and pharmaceutical industries.

So far, chemical modification of cellulose nanomaterials has been investigated mainly for improving their compatibility with polymer matrices in composite materials and has been the subject for a few recent reviews.[56, 57, 59, 60] Nevertheless, chemical modification of cellulose nanomaterials by CuAAC click chemistry has been rarely reported so far and has not been reviewed yet.

2.7.2.1. Advanced nanomaterials by cellulose nanocrystals modification

Cellulose nanocrystals (CNCs) are rod-like or whisker nanoparticles with high aspect ratio (typically 3-5 nm in width, 50-500 nm in length) obtained by cellulose acid hydrolysis. Filpponen and Argyropoulos described their surface functionalisation with azido and alkyne groups in two steps.[67] In the first step, hydroxyl groups on the CNC surface were converted into carboxylic acid groups by TEMPO-mediated hypohalite oxidation. In the second step, these carboxylic acid groups were reacted with azido- or alkyne-functionalised amines by ethylcarbodiimide (EDC) coupling in presence of *N*-hydroxy succinimide (NHS). CuAAC click chemistry of the azide and alkyne-surface functionalised CNCs led to the formation of nanoplatelet gels. TEM analysis showed that the nanoplatelets formed after click chemistry retained the rectangular shape of virgin CNCs and that they were the result of a highly regular CNCs packing. The same team further investigated the CuAAC coupling of other azide and alkyne-surface functionalised CNCs for new nanoplatelet gels.[68] TEM analysis showed the importance of solvent polarity for the CNCs packing during nanocellulose gelification induced by CuAAC click chemistry. The CNCs were uniformly oriented in the nanoplatelets prepared in water, while they were rather randomly oriented for those prepared in organic solvent (DMF).

Filpponen et al. also reported smart photoresponsive CNCs obtained by CuAAC grafting with coumarin and anthracene fluorescent probes (Fig.33).[69] Fluorescence microscopy confirmed the fluorescence of the grafted CNCs. Furthermore, UV-photoinduced reversible cycloadditions of coumarin and anthracene resulted in the formation of photoresponsive cellulosic nano-arrays.

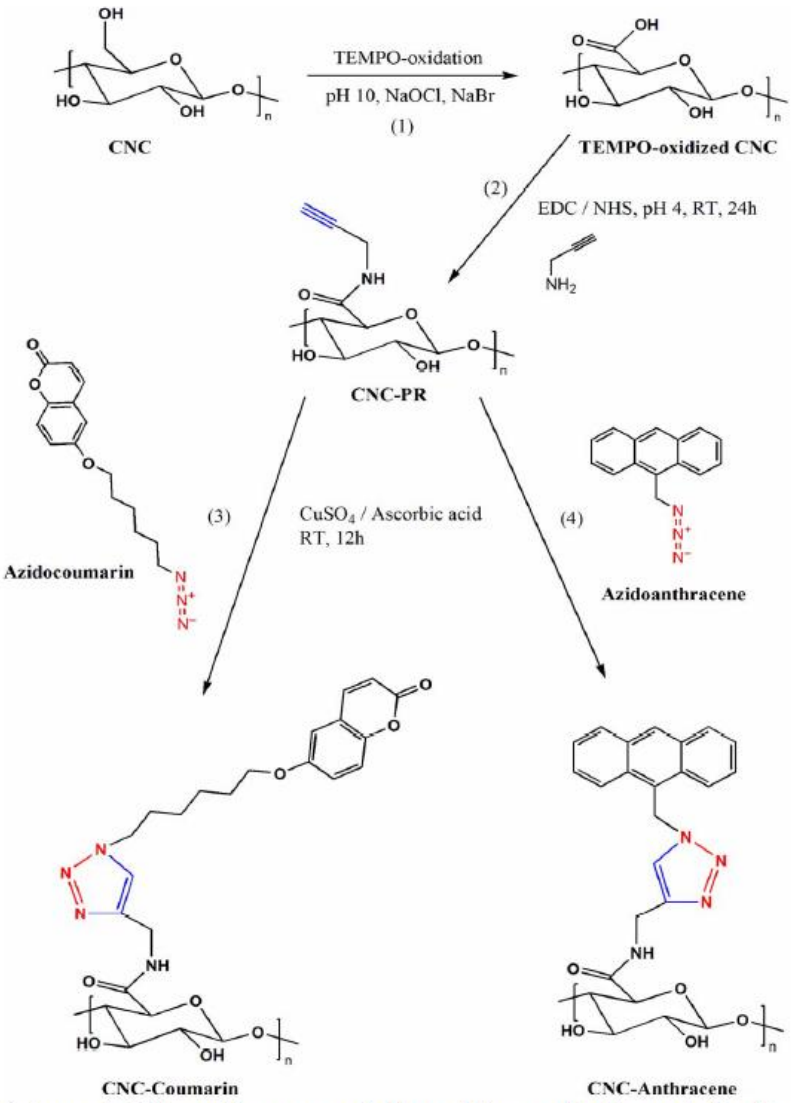

Figure 33: Photoresponsive cellulose nanocrystals (CNCs) obtained by CNC grafting with coumarin and anthracene fluorescent moieties by CuAAC click chemistry.

Taking advantage of another photoresponsive character, Feese et al. developed photobactericidal cellulose nanoparticles by CuAAC grafting of azide-CNCs with an alkyne-functionalised porphyrin.[70] The porphyrin photosensitizer was then activated upon illumination and generated cytotoxic species including singlet oxygen. The resulting photobactericidal effect was the most intense for the bacteria *Staphylococcus aureus*, which represent one of the most dangerous threats to human health. In another work by Eyley and Thielemans, an alkyne-functionalised imidazolium ionic liquid was grafted onto azide-functionalised CNCs for anion exchange applications.[71] These cellulose nanoparticles grafted with imidazoliuim species could also have interesting bactericidal properties.

Original hybrid CNC-protein nanoparticles have also been reported by Karaaslan et al. recently.[72] In this work, CNCs alkyne-functionalised at their reducing ends were coupled with azido-functionalised β-casein micelles by CuAAC click chemistry in water. AFM and TEM imaging showed a variety of shapes for the CNC/ β-casein conjugates obtained in these conditions. Such hybrid polysaccharide-protein nanoparticles could be interesting building blocks for new biomaterials.

2.7.2.2. Advanced nanomaterials by cellulose nanofibrils modification

Cellulose nanofibrils (CNFs) can be prepared from a variety of cellulose sources.[56, 57] These nano-objects have outstanding mechanical properties with a Young's modulus similar to that of Kevlar. Owing to their original properties, CNFs can also, in particular conditions, lead to optically transparent cellulosic paper very different from the white paper obtained from common cellulose (Fig. 34).

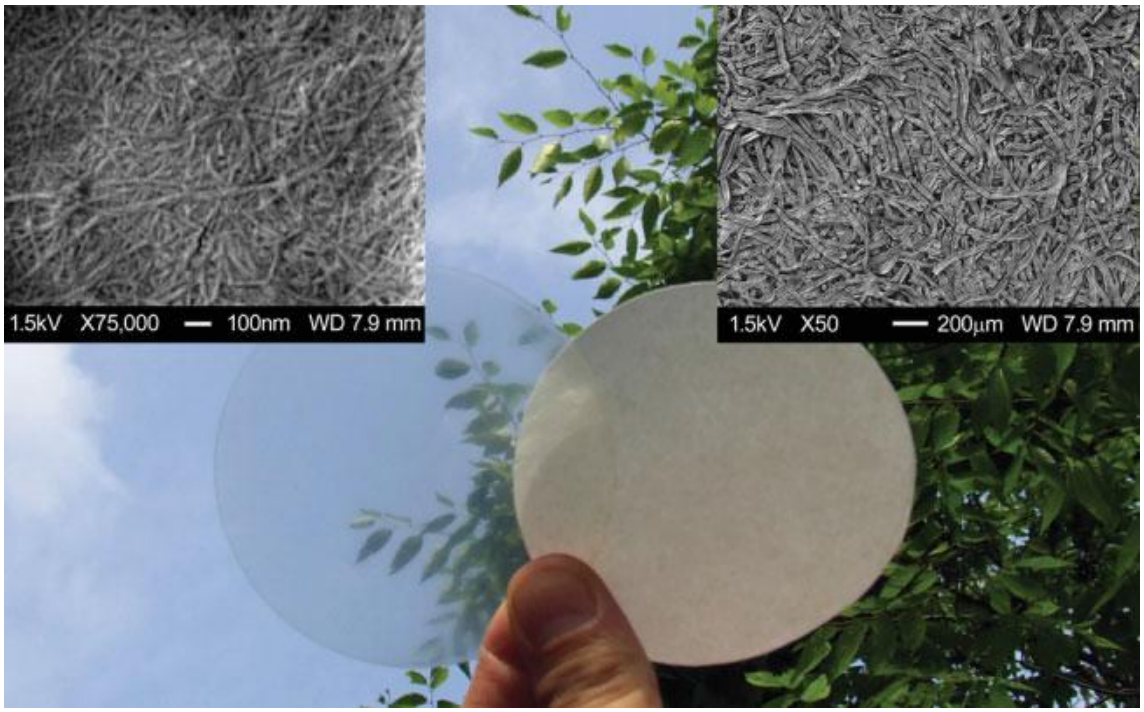

Figure 34: Optically transparent nanofiber paper (left) composed of 15 nm cellulose nanofibers (upper left, scale bar in inset: 100 nm) and conventional cellulose paper (right) composed of 30 µm pulp fibers (upper right, scale bar in inset: 200 µm).[73].

Smart pH-responsive or fluorescent cellulose nanofibrils (CNFs) have been obtained by CNF surface modification by CuAAC click chemistry in mild conditions in aqueous media.[74] The CNF surface was first functionalised with azido groups by reaction with 1-azido-2,3-

epoxypropane in presence of sodium hydroxyde. The azido-CNFs were then used as a nano-platform for introducing amino or fluorescent side groups. Fig. 35 showed an image for a fluorescent pale yellow-green CNF film obtained after grafting of a fluorescent probe. AFM images confirmed that the nanofibrillated structure was well maintained after surface functionalisation. Furthermore, the CNFs with amine side groups displayed pH-responsive rheological properties. The addition of acetic acid to their aqueous suspension led to lower viscosity and a very strong decrease in the storage and loss moduli. In that case, amine protonation was responsible for strong ionic repulsions and a collapse of the CNF network.

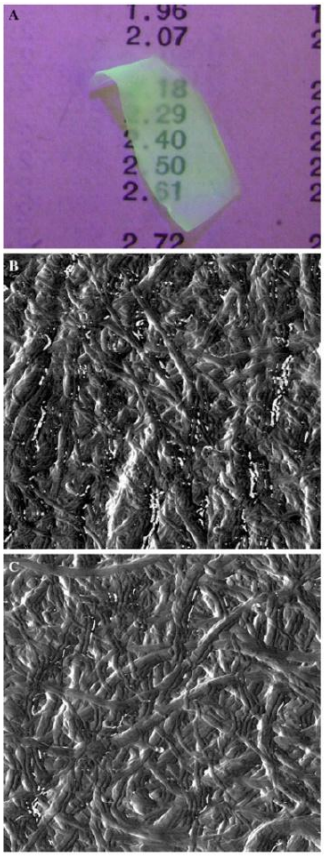

Figure 35: (a) Image of a fluorescent pale yellow-green CNF film obtained after surface grafting of a fluorescent dye by CuAAC click chemistry. AFM phase-images of (b) unmodified and (c) azide-functionalised NFC with scan size of 2 µm.[74]

CNFs functionalised by amine groups by CuAAC click chemistry were also reported by Luong et al. for the development of graphene/cellulose nanocomposite papers with high electrical and mechanical performance.[75] These nanocomposites were obtained by filtering stable dispersions of reduced graphite oxide and amine-functionalised CNFs. The very good dispersion of graphene obtained in this work was partially due to the nucleophilic addition of

the CNFs amine groups with epoxy groups present on graphene. CNFs functionalisation by CuAAC click chemistry provided an efficient compatibilisation system for graphene contents up to 10 wt%. A strong enhancement of the mechanical properties was already observed after addition of graphene in very low amount (0.3 wt%). Furthermore, the electrical conductivity of the graphene/CNF nanocomposite papers strongly increased from 4.79 10^{-4} to 71.8 S m^{-1} with their graphene content from 0.3 to 10 wt%. The high flexibility, stability, mechanical and electrical conductivity performance of the new graphene/CNF nanocomposites offer interesting prospects for portable electronics and electromagnetic shielding devices.

3. Conclusion

Over the past few years, CuAAC click chemistry has offered new ways of modifying cellulose and its derivatives in particular mild conditions and with hydrolytically stable triazole linkers. Its high reliability, efficiency and tolerance of different functional groups have contributed to developing great structural and functional variety for cellulosic materials.

A wide range of copolymer architectures have been easily obtained from azido or alkyne-functionalised cellulosic derivatives: structural or hydrogel crosslinked networks, block and graft copolymers and dendronised celluloses. New cationic and anionic polyelectrolytes have also been easily prepared with greatly improved hydrolytic stability compared to former polyelectrolyte cellulosic esters. The recent progress made on cellulose nanomaterials modification have shown another great potential for the developement of new cellulosic materials for advanced applications from nano to macro-scale.

CuAAC click chemistry has also brought a new range of functionalities to cellulose and its derivatives. Thermo, pH, and photo-responsive cellulosic (nano)materials have been obtained by simple grafting of responsive moieties in homogeneous or heterogeneous conditions. Fluorescent and (photo) bactericidal properties were also easily provided to cellulosic (nano)materials by CuAAC click chemistry.

Within the frame of sustainable chemistry, CuAAC click chemistry will certainly contribute to greatly extend the scope and functionality of cellulose-based materials for a wide range of applications in smart packaging, advanced food, health care, drug delivery, biomaterials, biocomposites, biosensors, bactericidal materials, and biofunctional films.

4. Acknowledgements

The authors would like to thank the ELEMENT Erasmus Mundus Programme for the PhD scholarship awarded to Mrs Faten Hassan Hassan Abdellatif.

5. References

[1] H.C. Kolb, M.G. Finn, and K.B. Sharpless, Click chemistry: Diverse chemical function from a few good reactions, Angewandte Chemie International Edition, 40 (2001) 2004-2021.

[2] C. Barner-Kowollik, F.E. Du Prez, P. Espeel, C.J. Hawker, T. Junkers, H. Schlaad, and W. Van Camp, "Clicking" polymers or just efficient linking: What is the difference, Angewandte Chemie International Edition, 50 (2011) 60–62.

[3] J.F. Lutz and Z. Zarafshani, Efficient construction of therapeutics, bioconjugates, biomaterials and bioactive surfaces using azide–alkyne "click" chemistry, Advanced Drug Delivery Reviews, 60 (2008) 958–970.

[4] W.H. Binder and R. Sachsenhofer, 'Click' chemistry in polymer and material science: An update, Macromolecular Rapid Communications, 29 (2008) 952–981.

[5] A. Sanyal, Diels–Alder cycloaddition-cycloreversion: A powerful combo in materials design, Macromolecular Chemistry and Physics, 211 (2010) 1417–1425.

[6] D.C. Hein, X.M. Liu, and D. Wang, Click chemistry, a powerful tool for pharmaceutical sciences, Pharmaceutical Research, 25 (2008) 2216-2230.

[7] J. Moses and A. Moorhouse, The growing applications of click chemistry, Chemical Society Reviews, 2007 (2007) 1249–1262.

[8] N.t. Brummelhuis and H. Schlaad, Radical thiol–X click chemistry. Encyclopedia of Radicals in Chemistry, Biology and Materials, John Wiley & Sons, Ltd, 2012, pp. 1-40.

[9] C. Hoyle and C. Bowman, Thiol–Ene Click Chemistry, Angewandte Chemie International Edition, 49 (2010) 1540-1573.

[10] H.C. Kolb and K.B. Sharpless, The growing impact of click chemistry on drug discovery, Drug Discovery Today, 8 (2003) 1128-1137.

[11] R.A. Evans, The Rise of Azide–Alkyne 1,3-Dipolar 'Click' Cycloaddition and its Application to Polymer Science and Surface Modification, Australian Journal of Chemistry 60 (2006) 384–395

[12] C. Spiteri and J.E. Moses, Copper-catalyzed azide–alkyne cycloaddition: regioselective synthesis of 1,4,5-trisubstituted 1,2,3-triazoles, Angewandte Chemie International Edition, 49 (2010) 31-33.

[13] C.W. Tornoe, C. Christensen, and M. Meldal, Peptidotriazoles on solid phase: [1,2,3]-triazoles by regiospecific copper(I)-catalyzed 1,3-dipolar cycloadditions of terminal alkynes to azides, The Journal of Organic Chemistry, 67 (2002) 3057-3064.

[14] W.H. Binder and R. Sachsenhofer, 'Click' chemistry in polymer and material science, Macromolecule. Rapid Communication., 28 (2007) 15-54.

[15] V.D. Bock, H. Hiemstra, and J.H. van Maarseveen, CuI-catalyzed alkyne–azide "Click" cycloadditions from a mechanistic and synthetic perspective, European Journal of Organic Chemistry, 2006 (2006) 51-68.

[16] M.v. Dijk, D.T.S. Rijkers, R.M.J. Liskamp, C.F. van Nostrum, and W.E. Hennink, Synthesis and Applications of Biomedical and Pharmaceutical Polymers via Click Chemistry Methodologies, Bioconjugate Chemistry, 20 (2009) 2001–2016.

[17] C. Becer, R. Hoogenboom, and U. Schubert, Click Chemistry beyond Metal-Catalyzed Cycloaddition, Angewandte Chemie International Edition, 48 (2009) 4900-4908.

[18] V.V. Rostovtsev, L.G. Green, V.V. Fokin, and K.B. Sharpless, A Stepwise huisgen cycloaddition process: copper(I)-catalyzed regioselective "ligation" of azides and terminal alkynes, Angewandte Chemie International Edition, 41 (2002) 2596-2599.

[19] P. Wu, A.K. Feldman, A.K. Nugent, C.J. Hawker, A. Scheel, B. Voit, J. Pyun, J.M.J. Fréchet, K.B. Sharpless, and V.V. Fokin, Efficiency and fidelity in a click-chemistry route to triazole

dendrimers by the copper(I)-catalyzed ligation of azides and alkynes, Angewandte Chemie International Edition, 43 (2004) 3928–3932.

[20] D. Fournier, R. Hoogenboom, and U.S. Schubert, Clicking polymers: a straightforward approach to novel macromolecular architectures, Chemical Society Reviews, 36 (2007) 1369-1380.

[21] M. Meldal and C.W. Tornoe, Cu-catalyzed azide-alkyne cycloaddition, Chemical Reviews, 108 (2008) 2952–3015.

[22] P.-H. Elchinger, P.-A. Faugeras, B. Boens, F. Brouillette, D. Montplaisir, R. Zerrouki, and R. Lucas, Polysaccharides: The "Click" Chemistry Impact, Polymers, 3 (2011) 1607-1651.

[23] T. Liebert, C. Hänsch, and T. Heinze, Click chemistry with polysaccharides, Macromolecular rapid communications, 27 (2006) 208-213.

[24] M. Tizzotti, A. Charlot, E. Fleury, M. Stenzel, and J. Bernard, Modification of polysaccharides through controlled/living radical polymerization grafting—towards the generation of high performance hybrids, Macromolecular Rapid Communications, 31 (2010) 1751-1772.

[25] A. Uliniuc, M. Popa, T. Hamaide, and M. Dobromir, New approaches in hydrogel synthesis – click chemistry: A review, Cellulose Chemistry and Technology, 46 (2012) 1-11.

[26] P.-A. Faugeras, F. Brouillette, and R. Zerrouki, Crosslinked cellulose developed by CuAAC, a route to new materials, Carbohydrate Research, 356 (2012) 247-251.

[27] T. Heinze, T. Liebert, and A. Koschella, Sulphonic acid esters. Esterification of polysaccharides, Springer Berlin Heidelberg, 2006, pp. 117-128.

[28] M. Pohl and T. Heinze, Novel biopolymer structures synthesized by dendronization of 6-deoxy-6-aminopropargyl cellulose, Macromolecular Rapid Communications, 29 (2008) 1739-1745.

[29] P. Peng, X. Cao, F. Peng, J. Bian, F. Xu, and R. Sun, Binding cellulose and chitosan via click chemistry: Synthesis, characterization, and formation of some hollow tubes, Journal of Polymer Science Part A: Polymer Chemistry, 50 (2012) 5201-5210.

[30] I. Filpponen, E. Kontturi, S. Nummelin, H. Rosilo, E. Kolehmainen, O. Ikkala, and J. Laine, Generic method for modular surface modification of cellulosic materials in aqueous medium by sequential “click” reaction and adsorption, Biomacromolecules, 13 (2012) 736-742.

[31] Q. Li, H. Kang, and R. Liu, Block and hetero ethyl cellulose graft copolymers synthesized via sequent and one-pot ATRP and "click" reactions, Chinese journal of chemistry, 30 (2012) 2169-2175.

[32] W.Z. Xu and J.F. Kadla, Honeycomb Films of Cellulose Azide: Molecular Structure and Formation of Porous Films, Langmuir, 29 (2013) 727-733.

[33] A. Koschella and D. Klemm, Silylation of cellulose regiocontrolled by bulky reagents and dispersity in the reaction media, Macromolecular symposia, 120 (1997) 115-125.

[34] A. Koschella, T. Heinze, and D. Klemm, First synthesis of 3-*O*-functionalized cellulose ethers via 2,6-di-*O*-protected silyl cellulose, Macromolecular bioscience, 1 (2001) 49-54.

[35] S.C. Fox, B. Li, D. Xu, and K.J. Edgar, Regioselective Esterification and Etherification of Cellulose: A Review, Biomacromolecules, 12 (2011) 1956-1972.

[36] D. Fenn, M. Pohl, and T. Heinze, Novel 3-*O*-propargyl cellulose as a precursor for regioselective functionalization of cellulose, Reactive and Functional Polymers, 69 (2009) 347-352.

[37] W.Z. Xu, X. Zhang, and J.F. Kadla, Design of Functionalized Cellulosic Honeycomb Films: Site-Specific Biomolecule Modification via "Click Chemistry" • , Biomacromolecules, 13 (2012) 350-357.

[38] A. Nakagawa, H. Kamitakahara, and T. Takano, Synthesis and thermoreversible gelation of diblock methylcellulose analogues via Huisgen 1,3-dipolar cycloaddition, Cellulose, 19 (2012) 1315-1326.

[39] Y. Enomoto-Rogers, H. Kamitakahara, A. Yoshinaga, and T. Takano, Comb-shaped graft copolymers with cellulose side-chains prepared via click chemistry, Carbohydrate Polymers, 87 (2012) 2237-2245.

[40] H. Kamitakahara, Y. Enomoto, C. Hasegawa, and F. Nakatsubo, Synthesis of diblock copolymers with cellulose derivatives. 2. Characterization and thermal properties of cellulose triacetate-block-oligoamide 15, Cellulose, 12 (2005) 527-541.

[41] P.H. Elchinger, D. Montplaisir, and R. Zerroukia, Starch–cellulose crosslinking—Towards a new material, Carbohydrate Polymers 87 (2012) 1886- 1890.

[42] T. Agag, K. Vietmeier, A. Chernykh, and H. Ishida, Side-chain type benzoxazine-functional cellulose via click chemistry, Journal of applied polymer science, 125 (2012) 1346-1351.

[43] A. Koschella, M. Hartlieba, and T. Heinze, A "click-chemistry" approach to cellulose-based hydrogels, Carbohydrate Polymers 86 (2011) 154- 161.

[44] J. Zhang, X.D. Xu, D.Q. Wu, X.Z. Zhang, and R.X. Zhuo, Synthesis of thermosensitive P(NIPAAm-co-HEMA)/cellulose hydrogels via ''click" chemistry, Carbohydrate Polymers 77 (2009) 583-589.

[45] M. Billy, A. Ranzani Da Costa, P. Lochon, R. Clément, M. Dresch, S. Etienne, J.M. Hiver, L. David, and A. Jonquières, Cellulose acetate graft copolymers with nano-structured architectures: Synthesis and characterization, European Polymer Journal, 46 (2010) 944-957.

[46] E. Malmström and A. Carlmark, Controlled grafting of cellulose fibres – an outlook beyond paper and cardboard, Polymer Chemistry, 3 (2012) 1702-1713.

[47] A. Carlmark, Tailoring cellulose surfaces by controlled radical polymerization methods, Macromolecular Chemistry and Physics, 214 (2013) 1539-1544.

[48] W. Xu, G. Gao, and J. Kadla, Synthesis of antibacterial cellulose materials using a clickable quaternary ammonium compound, Cellulose, 20 (2013) 1187-1199.

[49] K. Negishi, Y. Mashiko, E. Yamashita, A. Otsuka, and T. Hasegawa, Cellulose chemistry meets click chemistry: syntheses and properties of cellulose-based glycoclusters with high structural homogeneity, Polymers 3 (2011) 489-508.

[50] M. Pohl, J. Schaller, F. Meister, and T. Heinze, Selectively dendronized cellulose: synthesis and characterization, Macromolecular Rapid Communications, 29 (2008) 142-148.

[51] M. Pohl, G.A. Morris, S.E. Harding, and T. Heinze, Studies on the molecular flexibility of novel dendronized carboxymethyl cellulose derivatives, European Polymer Journal, 45 (2009) 1098-1110.

[52] M. Pohl, N. Michaelis, F. Meister, and T. Heinze, Biofunctional surfaces based on dendronized cellulose, Biomacromolecules, 10 (2009) 382-389.

[53] M.I. Montanez, Y. Hed, S. Utsel, J. Ropponen, E. Malmstrom, L. Wagberg, A. Hult, and M. Malkoch, Bifunctional dendronized cellulose surfaces as biosensors, Biomacromolecules, 12 (2011) 2114-2125.

[54] A. Koschella, M. Richter, and T. Heinze, Novel cellulose-based polyelectrolytes synthesized via the click reaction, Carbohydrate research 345 (2010) 1028-1033.

[55] N. Gonsior and H. Ritter, Rheological Behavior of Polyelectrolytes Based on Cellulose and Ionic Liquids Dissolved in 1-Ethyl-3-methyl Imidazolium Acetate, Macromolecular Chemistry and Physics, 212 (2011) 2633−2640.

[56] I. Siro and D. Plackett, Microfibrillated cellulose and new nanocomposite materials: a review, Cellulose, 17 (2010) 459-494.

[57] R.J. Moon, A. Martini, J. Nairn, J. Simonsen, and J. Youngblood, Cellulose nanomaterials review: structure, properties and nanocomposites, Chemical Society Reviews, 40 (2011) 3941-3994.

[58] J. Seppälä, Editorial corner – a personal view, Nanocellulose – a renewable polymer of bright future, Express Polymer Letters 6 (2012) 257.

[59] J.P. Silva, F.K. Andrade, and F.M. Gama, Bacterial cellulose surface modifications, in M. Gama, P. Gatenholm, and K.D. Paul (Eds.). Perspectives in Nanotechnology. Bacterial NanoCellulose: A sophisticated Multifunctional Material, CRC Press, Taylor & Francis Group, Boca Raton, London, New York, 2013, pp. 91-111.

[60] Y. Habibi, Key advances in the chemical modification of nanocelluloses, Chemical Society Reviews, 43 (2014) 1519-1542.

[61] J. Hafrén, W. Zou, and A. Cordova, Heteregeneous "Organoclick" Derivatization of Polysaccharides, Macromolecular Rapid Communications, 27 (2006) 1362-1366.

[62] M. Krouit, J. Bras, and M.N. Belgacem, Cellulose surface grafting with polycaprolactone by heterogeneous click-chemistry, European polymer journal, 44 (2008) 4074-4081.

[63] A. Dufresne and M.N. Belgacem, Cellulose-reinforced Composites: From Micro-to Nanoscale, Polimeros-Ciencia E Tecnologia, 23 (2013) 277-286.

[64] G. Chen, L. Tao, G. Mantovani, V. Ladmiral, D.P. Burt, J.V. Macpherson, and D.M. Haddleton, Synthesis of azide/alkyne-terminal polymers and application for surface functionalisation through a [2 + 3] Huisgen cycloaddition process,''click chemistry'', Soft Matter, 3 (2007) 732-739.

[65] S. Hansson, V. Trouillet, T. Tischer, A.S. Goldmann, A. Carlmark, C. Barner-Kowollik, and E. Malmstr m, Grafting Efficiency of Synthetic Polymers onto Biomaterials: A Comparative Study of Grafting-from versus Grafting-to, Biomacromolecules, 14 (2013) 64-74.

[66] K. Junka, I. Filpponen, L.S. Johansson, E. Kontturi, O.J. Rojas, and J. Laine, A method for the heterogeneous modification of nanofibrillar cellulose in aqueous media, Carbohydrate Polymers, 100 (2014) 107-115.

[67] I. Filpponen and D.S. Argyropoulos, Regular linking of cellulose nanocrystals via click chemistry: Synthesis and formation of cellulose nanoplatelet gels, Biomacromolecules, 11 (2010) 1060-1066.

[68] H. Sadeghifar, I. Filpponen, S.P. Clarke, D.F. Brougham, and D.S. Argyropoulos, Production of cellulose nanocrystals using hydrobromic acid and click reactions on their surface, Journal of Materials Science, 46 (2011) 7344-7355.

[69] I. Filpponen, H. Sadeghifar, and D. Argyropoulos, S., Photoresponsive cellulose nanocrystals, Nanomaterials and nanotechnology, 1 (2011) 34-43.

[70] E. Feese, H. Sadeghifar, H.S. Gracz, D.S. Argyropoulos, and R.A. Ghiladi, Photobactericidal Porphyrin-Cellulose Nanocrystals: Synthesis, Characterization, and Antimicrobial Properties, Biomacromolecules, 12 (2011) 4177-4179.

[71] S. Eyley and W. Thielemans, Imidazolium grafted cellulose nanocrystals for ion exchange applications, Chemical Communications, 47 (2011) 4177-4179.

[72] M.A. Karaaslan, G.Z. Gao, and J.F. Kadla, Nanocrystalline cellulose/beta-casein conjugated nanoparticles prepared by click chemistry, Cellulose, 20 (2013) 2655-2665.

[73] M. Nogi, S. Iwamoto, A.N. Nakagaito, and H. Yano, Optically transparent nanofiber paper, Advanced Materials, 21 (2009) 1595-1598.

[74] N. Pahimanolis, U. Hippi, L.-S. Johansson, T. Saarinen, N. Houbenov, J. Ruokolainen, and J. Seppälä, Surface functionalization of nanofibrillated cellulose using click-chemistry approach in aqueous media, Cellulose, 18 (2011) 1201-1212.

[75] N.D. Luong, N. Pahimanolis, U. Hippi, J.T. Korhonen, J. Ruokolainen, L.-S. Johansson, J.-D. Nam, and J. Seppala, Graphene/cellulose nanocomposite paper with high electrical and mechanical performances, Journal of Materials Chemistry, 21 (2011) 13991-13998.

Chapter 2

PLA grafting onto cellulose acetate by "click" chemistry. Application to new bio-based membranes for ethyl tert-butyl ether (ETBE) bio-fuel purification by pervaporation.

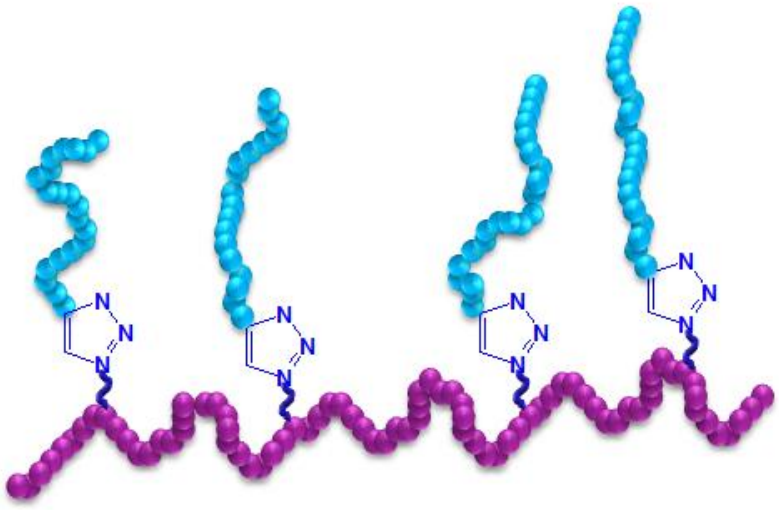

CA-*g*-PLA

PLA grafting onto cellulose acetate by "click" chemistry. Application to new bio-based membranes for ethyl *tert*-butyl ether (ETBE) bio-fuel purification by pervaporation.

Faten HASSAN HASSAN ABDELLATIF[a)], Jérôme BABIN[a)], Carole ARNAL-HERAULT[a)], Cécile NOUVEL[a)], Jean-Luc SIX[a)], Laurent DAVID[b)], Anne JONQUIERES[a)]*

[a)] *Laboratoire de Chimie Physique Macromoléculaire, LCPM UMR CNRS–Université de Lorraine 7375, ENSIC, 1 rue Grandville, BP 20451, 54 001 Nancy Cedex, France.*

[b)] *Laboratoire IMP@Lyon1, Université Claude Bernard Lyon 1, Université de Lyon, CNRS UMR 5223, 15 Bd. André Latarjet, 69622 Villeurbanne Cedex, France.*

Keywords: Cellulose acetate membranes; PLA graft, pervaporation; ethyl *tert*-butyl ether; bio-fuel; polymer grafting; click chemistry.

Abstract : Ethyl *tert*-butyl ether (ETBE) is a fuel octane enhancer considered as a major bio-fuel in Europe. Blended with gasoline fuels, ETBE improves fuel combustion and reduces toxic hydrocarbon emissions. ETBE industrial synthesis lead to an azeotropic mixture EtOH/ETBE (20/80 wt%), which cannot be separated by simple distillation. According to former works, cellulose acetate membranes were extremely selective with a permeate EtOH content of 100% but their flux was much too low for ETBE purification by the pervaporation (PV) membrane process. The affinity of the bio-based polylactide (PLA) for ethanol has also been reported for poly(vinyl pyrrolidone)/PLA blends for this application. In this work, new bio-based membranes were obtained by grafting cellulose acetate with controlled PLA amounts by a “grafting onto” strategy using "click" chemistry. These copolymers were characterized by ATR-FTIR, ^{1}H NMR, DSC, and SAXS. The membrane properties were investigated in terms of structure-morphology-property relationships for the sorption and pervaporation of the targeted mixture. PLA grafting onto cellulose acetate strongly improved the flux (×12) while the ethanol permeate content remained in the very high range (C' > 90 wt%) for ETBE purification by pervaporation.

---

1. Introduction

Membrane separation processes have taken their place among the most important industrial and research topics today and they are currently widely used in gas and liquid separations, waste water treatment and water desalination. Compared to conventional processes such as liquid-liquid extraction or distillation, the membrane processes offer many advantages like modularity, energy saving, and lower environmental impact. Furthermore, the membrane separation processes usually require relatively simple and non-harmful materials, offer greater separation efficiency, higher purity, mild operating conditions and avoid or reduce the using of solvents [1-3]. In all of these processes, the membrane is a key factor and its optimization is essential.

On the other hand, the formulation of fuels with lower environmental impact and the production of new bio-fuels are two main issues for sustainable development but they currently require highly energy-intensive separation steps. Therefore, the search for new cost-effective separation techniques is becoming a key issue for the bio-fuel industry. Compared to conventional organic-organic separation processes (*i.e.* azeotropic distillation, liquid-liquid extraction or extractive distillation), the pervaporation (PV) membrane process alone or in hybrid processes, could offer a very good alternative and greatly contribute to the future development of bio-fuels [4-6].

Among the major bio-fuels in the European Union (EU), ethyl *tert*-butyl ether (ETBE) is an attractive bio-ether used as oxygenated fuel additive to improve fuel combustion and reduce toxic hydrocarbon emissions. It has also contributed to limit the cars environmental impact by replacing the carcinogenic lead derivatives formerly used in the EU. Nevertheless, during the ETBE industrial synthesis, the separation of the azeotropic mixture EtOH/ETBE (20/80 wt%) involves a highly energy-intensive ternary distillation process [7]. This separation process could be advantageously replaced by a PV or PV/distillation hybrid process with an efficient organoselective membrane for ethanol removal [4, 5].

Membrane efficiency is mainly dependent on the membrane composition and structure. A wide range of polymeric materials has been reported for membrane preparation. However, several of these polymer membranes have drawbacks such as poor mechanical properties, thermal stability and swelling resistance, which influence the membrane performance during PV. These drawbacks could be avoided by the synthesis of novel polymeric materials or modifying existing polymers by grafting or blending with other polymers and fillers [8-10].

ETBE purification by PV has been relatively rarely investigated so far [7, 11, 12]. Most of these studies were based on polymeric membranes *i.e.* cellulosic membranes, segmented

copolymers, and poly(vinyl pyrrolidone) (PVP)-based copolymers and blends. The investigation of a cellulose acetate membrane for ETBE purification by PV revealed that cellulose acetate has nearly infinite separation factor with a permeate ethanol content of 100% but its total flux of 0.08 kg/m^2 h at 40°C for a reference membrane thickness of 5 µm was very low [13]. Several approaches have been reported for improving the flux of cellulose acetate membrane while its extremely high selectivity was maintained or only slightly reduced. Permeability and selectivity usually vary in opposite ways and the former results appeared very encouraging in this field [13]. Blending of cellulosic esters improved the total flux in the range of 0.6-3 kg/m^2 h with permeate ethanol contents of 0.907-0.967 at 40°C [14]. Cellulosic semi-interpenetrated networks and graft copolymers with PEO-based polymethacrylate also offered improved membrane properties for the targeted separation [1, 13, 15, 16]. Very recently, we have also reported the grafting of cellulose acetate by three different ionic liquids having the same bromide anion and different cations (imidazolium, pyridinium and ammonium) for ETBE purifcation by PV [17]. The ammonium ionic liquid displayed the best hydrogen bonding acceptor ability (β) and led to the best membrane properties with a normalized flux of 0.182 kg/h m^2 for a reference membrane thickness of 5 µm, a permeate ethanol content of 100% corresponding to an outstanding infinite membrane separation factor at 50°C.

In other respect, polylactide (PLA) has been recognized as a bio-based polyester derived from renewable source such as corn starch [18]. This polymer has a wide range of applications in medical field *e.g.* drug delivery, tissue engineering, and orthopedic devices. PLA is also used in packaging applications due to its high barrier properties, which are strongly influenced by PLA crystallinity [19]. In addition, PLA has been reported for gas permeation of small molecules like He, O_2, CO_2, CH_4 of great interest. A recent study on O_2 permeability through PLA/polypropylene (PP) blends and clay nanocomposites showed that O_2 permeability was strongly dependent on the film composition and that PLA enabled to control the barrier properties of PP-based films with interesting prospects for packaging applications [20].

However, the separation of liquid mixtures by PLA membranes has been very rarely reported so far [12, 18, 21]. The permeability of ethanol through PLA films was investigated by Shinkawa et al. using the PV membrane process. In the latter work, the ethanol flux was mainly dependent on the water flux, which was indicative for strong mass transfer coupling, and the water diffusion coefficient was 1000 times higher than that of ethanol. Even more closely related to this work, PLA/PVP blends have also been reported for the separation of two azeotropic mixtures ethanol/cyclohexane and ethanol/ETBE by PV [12, 21]. The latter

works confirmed the interesting features of PLA for removing ethanol from liquid organic mixtures in particular for ETBE purification.

Over the past few years, an increasing number of publications has also addressed the blending of cellulose and cellulose derivatives with PLA oligomers [22-27]. Compared to PLA blending, the grafting of cellulose and cellulose derivatives with PLA has been rarely reported [28-31]. A series of microcrystalline amphiphilic cellulose-g-PLA (MCC-g-PLA) copolymers was synthesized homogenously by graft copolymerization of cellulose and L-lactide in butyl methyl imidazolium chloride ionic liquid with stannous octanoate catalyst. The resulting copolymers were investigated by fluorescence probe, which showed that MCC-g-PLA can self-assemble in aqueous solution into spherical micelles (10−50 nm)[28]. Using a similar strategy, cellulose acetate-*g*-PLA copolymers were synthesized in ‘‘one pot’’ homogeneous ring opening polymerization using 1-allyl-3-methylimidazolium chloride ionic liquid as reaction media and 4-dimethylaminopridine (DMAP) as the catalyst. The CA-*g*-PLA copolymers had better thermo mechanical properties than those of pure PLA in the temperature range of 60–130°C [29]. Bio-degradable cellulose-based fibers were also obtained by *in-situ* graft copolymerization of L-lactide onto cellulose by reactive extrusion and then the blend melt was directly spun. The resulting fibers revealed better surface morphology and introduced plasticity to cellulose-based fibers [30]. Another related reactive processing strategy was successfully developed for preparing cellulose acetate-*g*-PLA using ring opening graft copolymerization [31]. To the best of our knowledge, the few methods reported so far for the grafting of cellulose and cellulose derivatives with PLA were thus based on "grafting from" method using ring opening polymerization technique.

For the first time, this paper reports cellulose acetate modification by a “grafting onto” strategy of low molecular weight PLA oligomers by using the copper(I) catalyzed Huisgen 1,3-dipolar cycloaddition of azides and alkynes (CuAAC) "click" chemistry. The chemical structure and morphology of the grafted cellulosic copolymers were investigated by ATR-FTIR, ^{1}H NMR, DSC, and SAXS. The sorption and pervaporation performances of the new bio-based membranes were then assessed for the separation of azeotropic mixture EtOH/ETBE (20/80 wt %). The influence of the PLA content on the membrane properties is analyzed on the basis of structure-properties relationships revealing the key membrane features for ETBE purification.

2. Material and methods

2.1. Materials

Cellulose acetate (CA, acetyl 39.7 wt%, M_W = 50000 g/mol), 6-bromohexanoic acid (97%), stannous octoate ($SnOct_2$, 92.5-100.0%), copper bromide (CuBr, 99.99%), propargyl alcohol (99%), 4-dimethylaminopyridine (DMAP, ≥ 99%), and sodium azide (NaN_3 ≥ 99.99%) *N,N,N',N'',N'''*-pentamethyldiethylenetetramine (PMDETA, 99%) were purchased from Sigma-Aldrich. ^{1}H NMR analysis confirmed the acetyl content of cellulose acetate, corresponding to 2.46 of acetyl groups and 0.54 of hydroxyl groups per glycosidic ring. The degrees of substitution (DS) of the side groups were commonly defined as the number of side groups per glycosidic ring. 1-(3-Dimethylaminopropyl)-3-ethylcarbodiimide hydrochloride (EDC.HCl, > 98%) was purchased from TCI Company and dimethyl sulfoxide (DMSO, 99.7%) was purchased from Fisher Scientific. These reagents were used as received without further purification. D,L-Lactide was purchased from Lancaster and it was recrystallized in dry toluene twice and dried under vacuum before using. Toluene was refluxed, distilled over calcium hydride (CaH_2) and then added in the reaction media via cannula under nitrogen atmosphere. The solvents, dichloromethane (DCM, ≥ 99.9 %), tetrahydrofuran (THF, 99.7%), were dried over molecular sieves before using. To avoid contamination by atmospheric moisture, all reagents and solvents were stored under nitrogen atmosphere.

2.2. CA functionalization and grafting

2.2.1. Synthesis of 6-azidohexanoic acid

A mixture of 20 g (0.103 mol) of 6-bromohexanoic acid in 250 mL of DMSO and 8.18 g (0.126 mol) of sodium azide was stirred for 4 hours at room temperature. The solvent was evaporated under reduced pressure and the product was recovered by extraction in DCM and water. The collected organic phases were dried over $MgSO_4$, filtered and concentrated by rotator evaporator to give 6-azidohexanoic acid as yellow oil (94%).

^{1}HNMR spectrum ($CDCl_3$, 300 MHz): 3.27 ppm (t, 2H, H_f); 2.35 ppm (t,2H, H_b); 1.57 ppm (m, 4 H, H_c, H_e); 1.46ppm (m, 2H, H_d).

2.2.2. Synthesis of α-alkyne PLA_{1640}

The controlled ring opening polymerization (ROP) of D,L-Lactide was carried out according to Laville *et.al.* procedure [32]. The PLA oligomer with alkyne terminal function (M_n= 1640 g/mol) was directly obtained using a functional initiator containing an alkyne group (*i.e.* propargyl alcohol). In Schlenk tube under nitrogen flow, 11.2 g (77.7 mmol) of dry D,L-

lactide was dissolved in 50 mL of toluene at 100°C. Both 0.435 g (7.77 mmol) of propargyl alcohol (7.77 mmol) and 0.0944 g (0.0233 mmol) of $SnOct_2$ were separately dissolved in 3 mL of dry toluene. These solutions were then carefully transferred to the D,L-lactide solution through dry cannula. The polymerization reaction was continued for 18h at 100°C. The polymerization reaction was quenched and the α-alkyne PLA was recovered by precipitation twice in cold hexane.

^{1}H NMR spectrum ($CDCl_3$, 300 MHz): 5.14ppm (m, 1H, H_c); 4.74 ppm (d 2H, H_b); 4.4 ppm (m, 1H, H_e); 2.5 ppm (s, 1H, H_a), 1.5 ppm (m, 6H, H_d, H_f);

2.2.3. Modification of CA with azide side groups

In three necks round bottom reactor, 15 g of virgin cellulose acetate (corresponding to 56.54 mmol of glycosidic rings and 30.53 of hydroxyl groups) were dissolved in 300 mL of dry THF under argon flow and vigorous stirring at room temperature. A solution of 4 g (25.48 mmol) of 6-azidohexanoic acid and 0.373 g (2.29 mmol) of DMAP in 150 mL of dry DCM were added to the CA solution. After cooling the mixture at 5°C, 4.84 g (25.24 mmol) of EDC.HCl were added to the reaction medium and stirred for 48 hours at room temperature. The crude polymer was precipitated in 2 L of ethanol (96%), washed twice in ethanol, filtered and dried under vacuum at 60°C overnight. The polymer was obtained as white solid fibers with a yield of 88% The degree of substitution of cellulose acetate by azide groups DS_{azido} = 0.39 was estimated by ^{1}H NMR in $CDCl_3$ using equation (1) :

$$\frac{2DS_{Azido}}{3DS_{Acetyl}+2DS_{Azido}} = \frac{A_{1.3}}{A_{1.7}+A_{2.2}} \quad (1)$$

where $A_{1.3}$ *is* the area of the peak at 1.3 ppm corresponding to 2 methylene protons in the anchor, $A_{1.7}$ *is* the area of the peak at 1.7 ppm corresponding to 3 protons of the acetyl side groups, and $A_{2.2}$ *is* the area of the peak at 2.2 ppm corresponding to methylene protons in the anchor (see main text).

2.2.4 Grafting of the azido CA by "click" chemistry with α-alkyne PLA_{1640}

α-Alkyne PLA_{1640}, in varying ratio, was grafted onto azido-functionalized CA using CuAAC “click” chemistry. As way of example the following procedure describes the synthesis of the cellulose acetate grafted with 40.5 wt% of PLA. In a Schlenk tube, 1 g of azido-functionalized CA (corresponding to 3.13 mmol of glycosidic rings and 1.22 mmol of azide groups) and 0.788 g (0.4807 mmol) of clickable PLA were dissolved in 30 mL of DMSO under argon atmosphere. A theoretical degree of substitution of CA with PLA grafts DS_{PLA}^{theo} =

0.156 was targeted. After complete dissolving of the two polymers, the solution was degassed with argon for several times. 68.9 mg (0.4807mmol) of copper bromide and 2 mg of copper powder dendritic "Cu^0" were added under argon flow to the reaction mixture. The tube was sealed under argon atmosphere and stirred for 24 hours at room temperature. After the completion of reaction, the grafted CA was obtained by precipitation in ethanol in presence of 10 eq. of PMDETA as copper ligand. The precipitated fibers were washed twice in ethanol, filtered and dried at 60°C under vacuum overnight. All grafted polymers were characterized by ATR-FTIR and ^{1}H NMR and (see main text). Experimental degree of substitution of CA with PLA grafts $\mathrm{DS}_{\mathrm{PLA}}^{\mathrm{exp}}$ = 0.1351 were calculated from equation 2.

$$DS_{PLA}^{exp} = \frac{A_{7.6}}{A_{4.8}} \qquad (2)$$

where $A_{7.6}$ *is* the area of the peak at 7.6 ppm corresponding to the H_g proton of the triazole ring formed by CuAAC "click" chemistry and $A_{4.8}$ *is* the area of the peak at 4.8 ppm corresponding to the H_2 proton belonging to the glycosidic rings.

2.2.5. Physicochemical characterization

IR Spectra were recorded for thin polymeric films on a Bruker Tensor 127 FTIR spectrometer equipped with liquid nitrogen cooled MCT detector. The standard sample cell in the FT-IR is a Pike Miracle single-bounce attenuated total reflectance (ATR) cell equipped with a Ge crystal.

^{1}H NMR spectra were recorded on a Bruker Avance 300 spectrometer operating at 300MHz. All NMR experiments used polymer solutions in $CDCl_3$. The chemical shifts were referenced to TMS and were calculated using the residual isotopic impurities of the deuterated solvent. The peak integrations were used to calculate the degrees of substitution of the different side groups or polymer grafts.

The number and weight average molecular weights were estimated by size exclusion chromatography (SEC) using multi-angle laser light scattering detector (MALLS; Mini Dawn Treos, Wyatt), differential refractometer detector (OPTILab Rex, Wyatt), HPLC pump (Waters 515), degazer AF (Waters In-Line), and three PLgel 5µl (10^5, 10^3, and 100 Å) columns (300 x 7.5 mm^2) were used. THF was used as eluent at 40°C with an elution rate of 0.7 mL per min. Polymer solutions (30 mg/mL) were prepared using HPLC-grade THF and were filtered through PTFE membranes (Alltech, average pore diameter: 0.2 µm) prior injection. A refractive index increment (dn/dc) of 0.054 was used for PLA [33].

Thermal analysis was performed by standard Differential Scanning Calorimetry (DSC) using a TA Instruments DSC Q2000. Polymer samples of ca. 10 mg were used for analysis under a continuous flow of nitrogen. Two cycles of measurements from 0 to 210 °C were performed with heating and cooling rates of 10 °C/min. The thermal transitions corresponding to the first and second heating scans differed significantly and showed the strong influence of thermal history. The data reported in this work corresponded to the glass transition temperatures for the second heating scan for better comparison.

The nano-scale morphology of virgin cellulose acetate and cellulose acetate grafted with different PLA contents was determined by means of small X-ray scattering using polymer membranes with thicknesses of ca. 200 µm, which were obtained in the same way as for sorption experiments. Small angle X-ray scattering (SAXS) experiments were carried out at room temperature, without any additional thermal treatment, using synchrotron radiation at the European Synchrotron Radiation Facility (ESRF, Grenoble, France). The SAXS experiments were performed on the BM2-D2AM beamline at an incident energy of 16 keV. A 2D X-ray camera was used (Roper Scientific), and the data were corrected from the dark image, normalization with flat field and tapper camera distortion. Finally, radial average around the incident beam center were calculated. Silver Behenate was used for the channel-q calibration. The background (empty cell) was subtracted in the radial average profiles, after the measurement of the attenuation coefficients.

2.3. Membrane preparation for pervaporation and sorption experiments

The different polymer materials were dissolved in DMF (pure for synthesis) to obtain a polymer concentration of 2.5 % w/v. The solutions were then cast on a PTFE mold. They were carefully removed from the mold after DMF evaporation at 45°C and dried under vacuum overnight. The pervaporation membrane thicknesses ranged from 60-70 µm and the difference in thickness between two membrane points did not exceed 6 µm.

The procedure for sorption membrane casting was similar as that for pervaporation membranes except for polymer concentration, which was increased to 5% w/v in order to obtain membrane thicknesses of ca. 200 µm. The sorption membranes were then carefully dried at 60°C under vacuum for 24 hours before sorption experiments.

2.4. Sorption experiments

For sorption experiments, the dried polymer membranes were weighted and then immersed in the azeotropic mixture EtOH/ETBE (20/80 wt%) in hermetically closed bottles. These bottles were kept at 30°C in a thermostated oven. After one week, the membranes

were taken out the bottles and quickly wiped with paper tissue and weighted in a closed tare bottle. The membranes were regularly weighted until they reached constant swelling weight. At the end of each sorption experiment, the membranes were dried under vacuum and weighted again. The results obtained with the different sorption membranes showed that no polymer dissolution had occurred during the sorption experiments. The total swelling, S (wt%), was calculated from equation (3) :

$$S = \frac{w_S - w_D}{w_D} \times 100 \qquad (3)$$

where w_S and w_D were the membrane weights after and before sorption experiment. The average experimental error for the total swelling S was ± 0.2 wt%.

For determining the composition of the absorbed mixture, the swollen membranes at equilibrium were soaked for 1 night at ambient temperature into 10 mL of diethylether, which is a non solvent for the membrane polymers and a good solvent for both ethanol and ETBE. The desorption solution was then analyzed by gas chromatography using a Shimadzu GC-8A chromatograph with a Porapak Q column, a thermal conductivity detector and hydrogen as carrier gas. The ethanol weight fraction C_s in the desorbed mixture was calculated from the area of the EtOH and ETBE peaks on the basis of a former calibration. The average experimental error for the ethanol weight fraction C^S_{EtOH} was ± 0.005.

Sorption separation factor were then calculated from equation (4) where C_S and C are the ethanol weight fractions in the sorption mixture and the azeotropic mixture EtOH/ETBE, respectively. The symbol for the sorption separation factor was that recently proposed by Baker *et al. [3]*.

$$\beta_S = \frac{C^S_{EtOH}}{1 - C^S_{EtOH}} / \frac{C}{1 - C} \qquad (4)$$

2.5. Pervaporation experiments

Pervaporation experiment was performed for the azeotropic mixture ETOH/ETBE at 50°C using a pervaporation set-up described elsewhere [11]. The downstream pressure of was maintained at less than 0.04 KPa using a vacuum pump. The permeate was collected continuously after condensation by liquid nitrogen using parallel traps. The permeate flux was calculated using equation (5) :

$$Permeate\ \ flux = \frac{W_p}{\Delta t \times A} \qquad (5)$$

where w_p is the permeate sample weight collected during a permeation time Δt and A is the active membrane area.

To do a comparison between different membranes with close but non-equal thicknesses, normalized fluxes, J, were reported for a reference membrane thickness of 5 µm (equation (6)). This reference thickness was chosen because it is easily reached for dense polymer layers on top of asymmetric membranes.

$$J = \frac{Membrane\,\text{thickness}}{5} Permeate\ \ flux \qquad (6)$$

The permeate ethanol weight fraction, C', was determined by gas chromatography in the same conditions as for sorption experiments. The pervaporation separation factor, β_{PV} , was calculated by analogy with the sorption separation factor according to equation (7). The experimental errors were less than 5% for the total fluxes and ± 0.005 for the ethanol weight fractions.

$$\beta_{PV} = \frac{C'_{EtOH}}{1-C'_{EtOH}} / \frac{C}{1-C} \qquad (7)$$

The fairly complex procedure for permeability calculation in pervaporation has already been reported for the separation of the azeotropic mixture EtOH/ETBE [17].

3. Results and discussion

3.1. Synthesis and characterization of cellulose acetate grafted with PLA

Over the last few years, CuAAC "click" chemistry has been widely used as a new way for the modification of cellulose and cellulose derivatives to produce advanced cellulosic materials for a wide range of applications [34] *e.g. i)* crosslinked networks for structural materials and hydrogels [35-37], *ii)* block and graft copolymers [38-41], and *iii)* dendronised celluloses [42-45]. In this work, the cellulose acetate-*g*-PLA membrane materials have been obtained in two steps by a "grafting onto" strategy based on CuAAC "click" chemistry.

3.1.1. Synthesis of azido cellulose acetate

Pre-click modification of cellulose and cellulose is a well known pre-requisite derivatives to introduce azide or alkyne side groups for CuAAC "click" chemistry. This functionalization is usually achieved after the activation of the hydroxyl side groups *e.g.* by tosylation. [35, 46]. In the present paper, cellulose acetate with azide side groups was

obtained through an esterification reaction adapted from a previous study of Neises and Steglich (Fig. 1) [47].

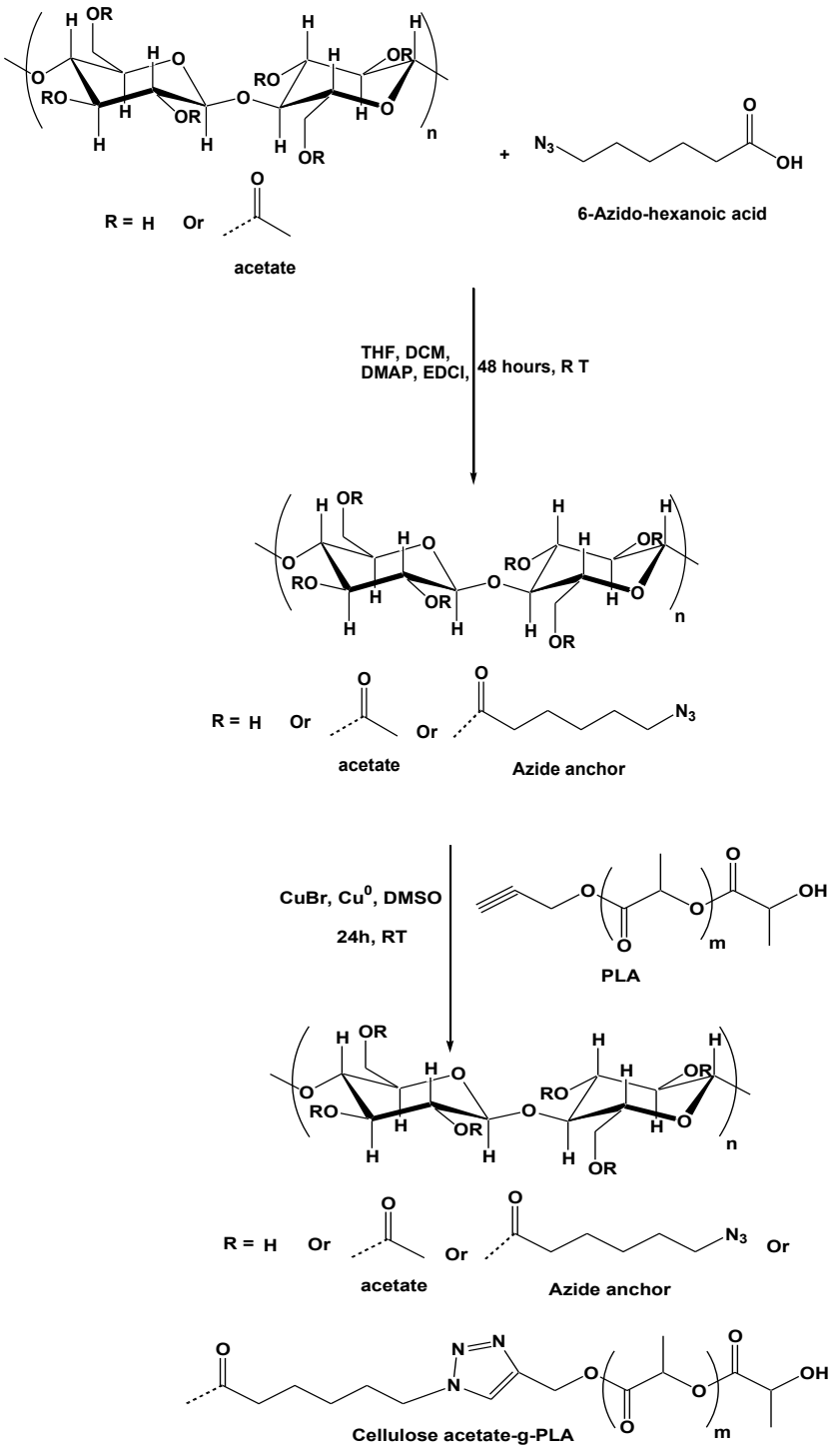

Figure 1: General reaction scheme for the grafting of PLA onto CA by 'click' chemistry

In the first step, 6-azido hexanoic acid was prepared and isolated in good yield (Fig. S1). Then, azido functionalities were introduced along the cellulose acetate chains by esterification of the hydroxyl side groups (DS_{OH}= 0.54) in a mixture of THF/CH_2Cl_2 using EDC.HCl as coupling agent and DMAP as catalyst at room temperature. ATR-FTIR spectrum of azido cellulose acetate (Fig. 2) showed a band around 2100 cm^{-1} corresponding to the azide group. A theoretical degree of substitution of the azido groups equal to 0.45 was targeted. ^{1}H NMR spectrum of azido cellulose acetate (Fig. 3) showed new peaks assigned to the azido hexanoate group in the range of 1.3 ppm to 1.7 ppm (H_c, H_d, H_e), at 2.4 ppm (H_b) and at 3.3 ppm (H_f). An experimental degree of substitution DS_{azido} = 0.39 was evaluated according to equation (1). It was in good agreement with the targeted one given the ^{1}H NMR error for polymer analysis and the well-known limitation in hydroxyl modification in polysaccharide chemistry. The corresponding substitution rate for the hydroxyl groups (86.9%) was typical for high hydroxyl substitution for cellulosic derivatives [34].

3.1.2. Synthesis of α-alkyne PLA

The alkyne PLA oligomer was synthesized in a single step from D,L-lactide by controlled ROP according to Laville *et al.* synthesis [32] using $SnOct_2$ as a catalyst and propargyl alcohol as an alkyne-functionalized initiator. The number average polymerization degree ($\overline{Xn}$) of the functional PLA was calculated using ^{1}H NMR (Fig. 3) from the H_b (initiator) and H_c (lactide) protons at 4.7 and 5.2 ppm, respectively. The $\overline{Xn}$ obtained by ^{1}H NMR was 22 ($\overline{Mn}^{NMR}$ = 1640 g/mol) in good agreement with the $\overline{Mn}$ value obtained from SEC ($\overline{Mn}^{SEC}$= 2000 g/mol, Đ= 1.27). The presence of the terminal alkyne group was also confirmed by AT-FTIR (Fig. 2) with the appearance of two characteristic signals at $\nu_{C\equiv C}$ = 2130 cm^{-1} (weak) and at ν_{C-H} = 3277 cm^{-1} (broad, medium).

3.1.3. Synthesis and characterization of cellulose acetate grafted with PLA

Cellulose acetate-*g*-poly(D,L-lactide) (CA-*g*-PLA) glycopolymers were obtained by the "grafting onto" method depicted in Fig. 1. Azido-functionalized cellulose acetate (N_3-CA, DS_{azido} = 0.39) was grafted with different amounts of α-alkyne PLA by an Huisgen-type Copper(I)-catalyzed Azide-Alkyne Cycloaddition (CuAAC) 'click' chemistry reaction in dry DMSO with CuBr catalyst in presence of Cu^0 at RT for 24h under argon atmosphere. In this way, the PLA content could be easily varied over a broad range with a good control of the copolymer architecture. Such glycopolymers are called CA-*g*-wt%PLA, where wt% is the weight fraction of grafted PLA.

ATR-FTIR spectrometry was used to follow the grafting reaction. Fig. 2 shows stacked spectra of α-alkyne PLA, N_3-CA and CA-*g*-40.5 PLA corresponding to the maximum targeted degree of substitution for the PLA grafts. Due to the absence of a common invariable band in the three spectra, their normalization was impossible and the AT-FTIR spectometry analysis remained qualitative. After performing the "click" reaction between N_3-CA and α-alkyne PLA, the formation of the triazole ring proving the covalent grafting was shown by the appearance of a new signal at 1670 cm^{-1} ($\nu_{C=N}$, medium). At 2100 cm^{-1}, a low intensity band was still observed and can be assigned to residual azido groups as expected from the maximum targeted degree of substitution for the PLA grafts.

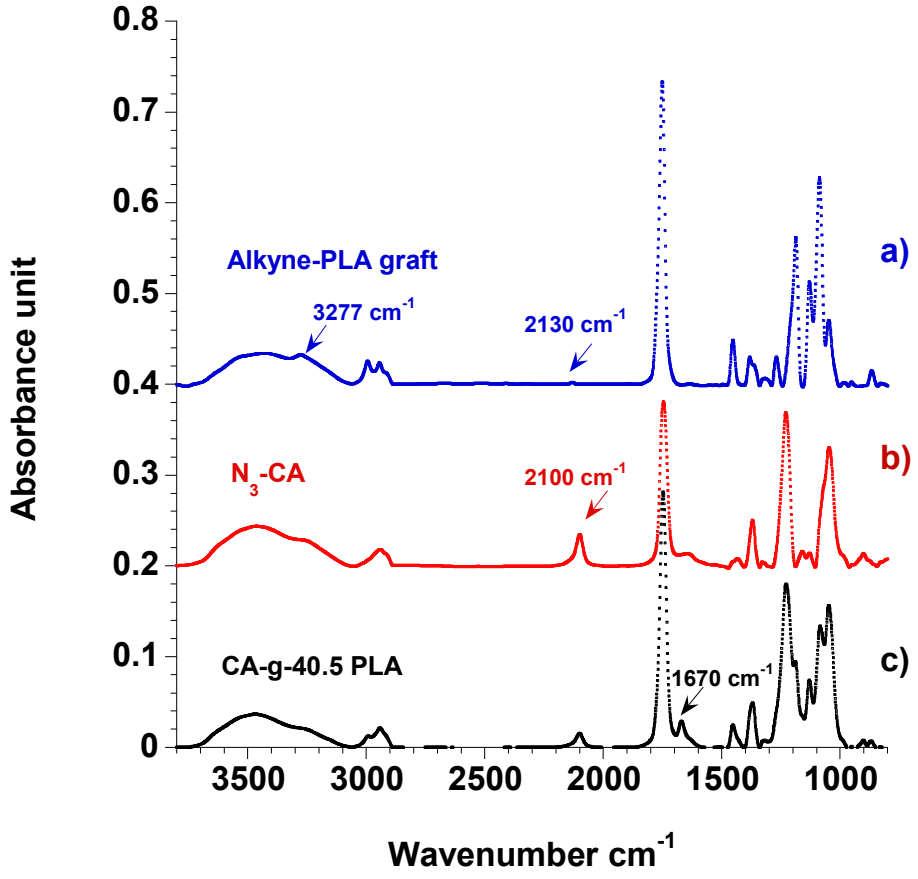

Figure 2: ATR-FTIR spectra for a) the alkyne PLA, b) N_3-CA and c) the CA–g-40.5 PLA.

Similarly as for the ATR-FTIR analysis, Fig. 3 shows a comparison of ^{1}H NMR spectra before and after modifications of CA in $CDCl_3$. The ^{1}H NMR spectrum of CA-g-40.5 PLA showed typical signals of both parts, especially the methyl protons peaks at 1.5 ppm attributed to the PLA grafts and the glucosidic (3-5 ppm) protons peaks from the cellulose acetate backbone. The covalent link of PLA onto N_3-CA was confirmed by the appearing of the H_g proton at 7.6 ppm characteristic of the triazole ring and the corresponding decrease in

the H_f signal at 3.3 ppm adjacent to the azido group. The experimental degrees of substitution of CA with PLA grafts (DS_{PLA}^{exp}) were calculated from equation (2) using the integration of the H_g and H_2 signals at 7.6 ppm and 4.8 ppm, respectively. The weight fraction of PLA in the grafted copolymers was calculated from equation (8).

$$\text{PLA wt\%} = \frac{DS_{PLA}^{exp} \times Mwt_{PLA}}{Mwt_{N_3CA} + DS_{PLA}^{exp} \times Mwt_{PLA}} \quad (8)$$

For each glycopolymer, the data of DS_{PLA}^{theo}, DS_{PLA}^{exp}, grafting rate and weight fraction in PLA are reported in Table 1. As expected, the CuAAC "click" chemistry allowed to access to high grafting rates in the range of 87% to 90% and a good control of the architecture of the copolymers (*i.e.* molecular weight and degree of substitution for the grafts) was easily obtained by the "grafting onto" strategy. The PLA content was varied between 0 and 40.5 wt%. The maximum grafting rate for PLA was limited to less than 50 wt% to maintain cellulose acetate as the principal component in the grafted copolymers. This limitation was decided to ensure a good mechanical withstanding of the different membranes in the PV operating conditions.

Table 1 Results of the ^{1}H NMR characterization of the grafted copolymers CA-g-PLA: theoretical and experimental degrees of substitution for the PLA grafts, grafting rates and PLA weight contents in the grafted copolymers.

Copolymer	$\mathbf{DS_{PLA}^{theo}}$	$\mathbf{DS_{PLA}^{exp}}$	**Grafting rate %**	**PLA wt%**
CA-g-23 PLA	0.065	0.058	89%	23
CA-g-31.5 PLA	0.1	0.087	87%	31.5
CA-g-40.5 PLA	0.15	0.135	90%	40.5

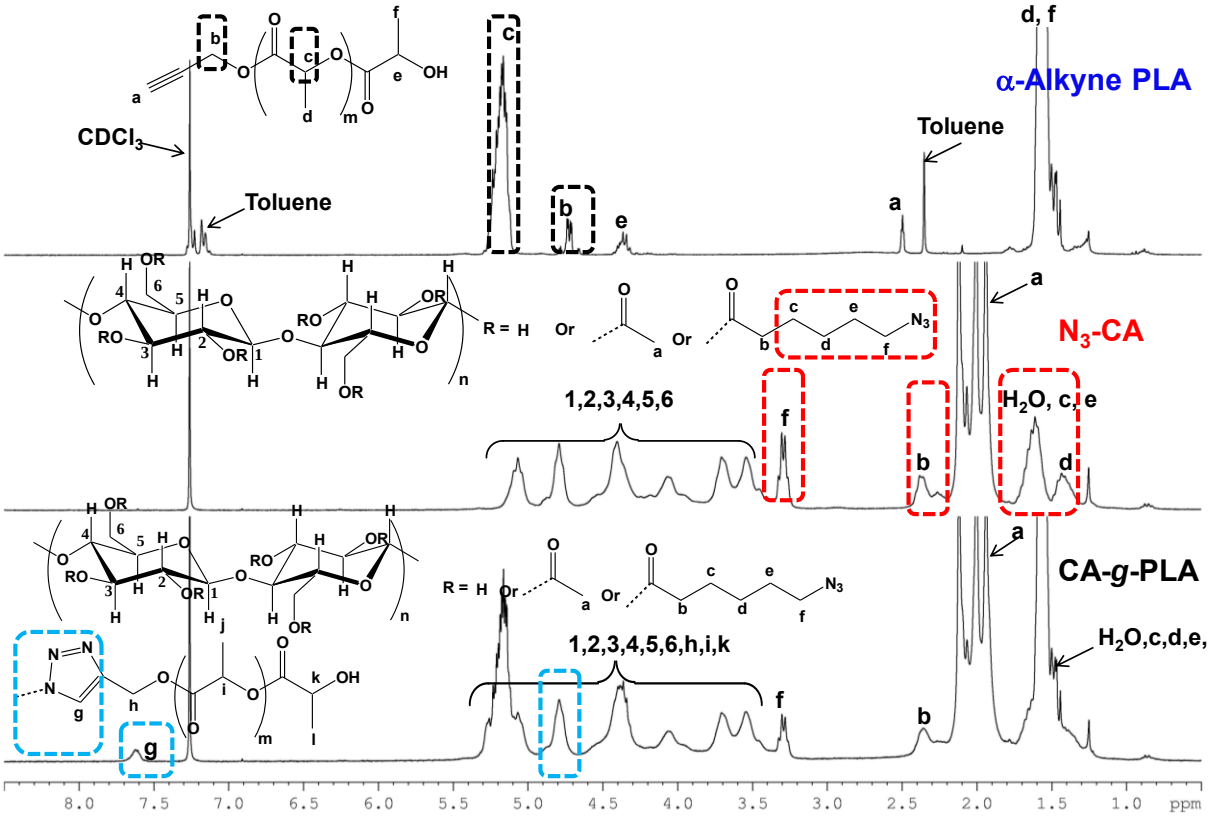

Figure 3: ^{1} H NMR characterization for the alkyne PLA, azido cellulose acetate and the grafted copolymer CA–g-40.5 PLA.

The cellulosic membrane materials were investigated by DSC standard technique and synchrotron SAXS measurements to assess the influence of PLA content on membrane T_g and morphology in relation to the performances obtained during the PV separation process for ETBE purification. In a former related work of our team, cellulose acetate was modified with short or long PEO-containing polymethacrylate grafts to assess the influence of copolymer architecture on the membrane properties for ETBE purification. It was shown that the best membrane properties (J = 0.87 kg/h m^2 for 5 µm, C' = 94 wt% at 50°C) were obtained for the copolymer with the highest amount of short grafts, which displayed a fairly high T_g, homogeneous morphology and no crystallinity [11].

In this work, the thermograms of the dry membranes revealed a single glass transition temperature and no endothermic melting peaks irrespective of their PLA content. Fig. 4 showed that the grafting of cellulose acetate (T_g = 184°C) with 23 wt% of PLA (T_g = 13°C) was responsible for a strong T_g decrease (T_g = 118°C) indicative for a strong plasticizing effect of the PLA grafts in the cellulosic material. By increasing the PLA content to 31.4 wt%,

the plasticizing effect was much stronger (T_g = 69°C) but it tended to level off above 31.4 wt% of PLA in the percolation threshold range. In any case, DSC results showed that the PLA grafting greatly increased the segmental mobility and plasticization of the rigid cellulose acetate chains, which are both expected to contribute to improve the membrane flux.

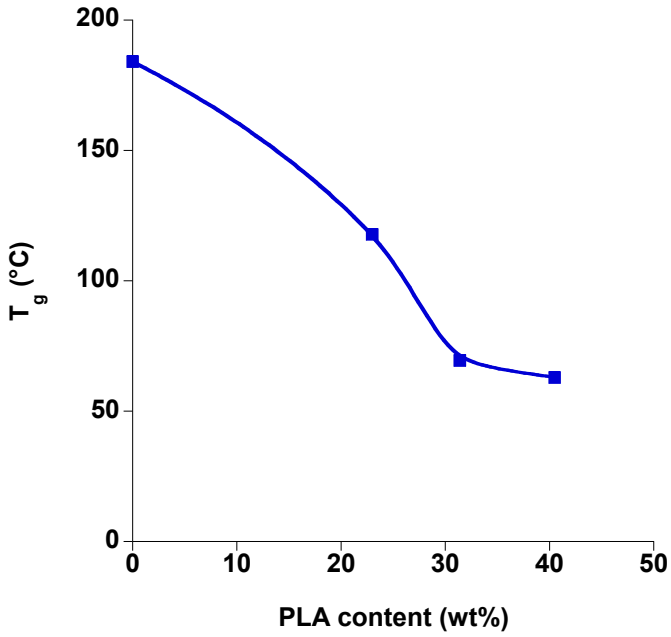

Figure 4: Influence of PLA weight content on the glass transition temperature (T_g) of the grafted copolymers CA-*g*-PLA.

Further insights into the morphology of the grafted cellulosic materials were obtained by synchrotron SAXS measurements. Fig. 5 shows the SAXS patterns of the virgin CA, the modified N_3-CA and the grafted copolymers CA-*g*-PLA with increasing PLA contents from 23 to 40.5 wt%. SAXS experiments were carried out on fairly thick membranes (*ca.* 200 µm). The weak and complex scattering pattern obtained for virgin cellulose acetate was characteristic for large electronic density fluctuations with characteristic sizes larger than 50 nm. Previous works have shown the presence of intermolecular aggregation and heterogeneities in cellulose acetate solutions, which subsisted in the dry membranes after solvent evaporation [48-50]. The PLA grafting onto cellulose acetate changed the scattering pattern significantly. The scattering laws $I(q) \sim q^{-3}$ in the scattering vector *q* range from 10^{-2} to 4 10^{-2} $Å^{-1}$ showed the disappearance of the CA heterogeneities associated with a more homogeneous structure at the nanoscale, but with possible larger scale fluctuations at the micron-range. Furthermore, the absence of any correlation peak after PLA grafting showed the absence of phase separation for the PLA grafts and the homogeneity of the grafted copolymer membranes at the nanoscale.

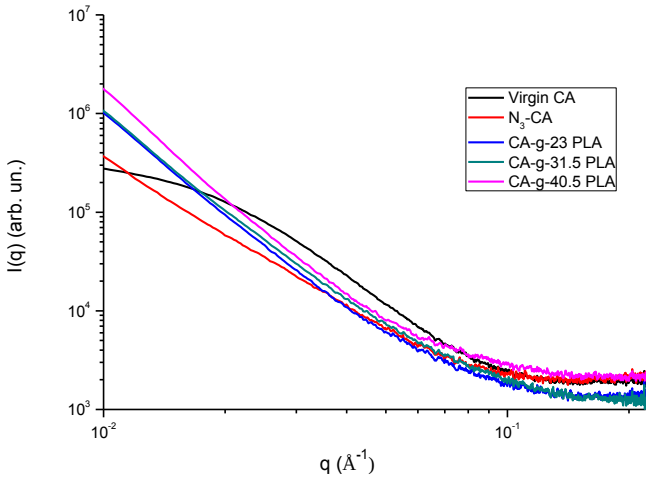

Figure 5: Synchrotron SAXS patterns for virgin CA, N_3-CA and the grafted copolymers CA-*g*-PLA.

3.2. Sorption properties of cellulose acetate grafted with PLA for ETBE purification

According to the sorption-diffusion model [51], permeation of a liquid mixture through dense membranes involves two sequential steps. The first step corresponds to the sorption of a part of the liquid mixture at the membrane upstream side. This step is usually selective and contributes to the feed and permeate enrichments. The second step corresponds to the diffusion of the absorbed molecules through the polymeric membrane material. Determining the sorption properties was thus considered as a first step towards the understanding of the overall membrane separation features.

Sorption properties were investigated for virgin cellulose acetate and cellulose acetate with increasing contents of grafted PLA (Table 2). The experiments were carried out for the azeotropic mixture EtOH/ETBE (20/80 wt %) at 30°C for safety reasons. The presence of hydroxyl side groups (DS_{OH} = 0.54) in virgin cellulose acetate led to very high sorption separation factor β_s= 129 due to their very high affinity for ethanol but the polymer chains rigidity strongly limited the membrane swelling (S= 4.2 wt%). Nevertheless, the cellulosic membranes with increasing PLA contents from 23 to 40.5 wt% showed a moderate linear increase in the swelling S from 7.5 to 11 wt% (Fig. 6). At the same time, the increase in the PLA content was accompanied by the decrease in the copolymer affinity for ethanol and the sorption separation factor decreased from 129 for virgin cellulose acetate to 4.5 for the membrane with the highest grafting rate (CA-g-40.5 PLA). Nonetheless, all grafted

copolymer membranes were still selective towards ethanol during the sorption step, as shown by the ethanol content in the absorbed mixture (≥ 53 wt%) always largely exceeding that of the azeotropic mixture EtOH/ETBE (20 wt%). Therefore, the sorption step systematically induced a first enrichment of the feed mixture in ETBE, which was a strong advantage for ETBE purification.

Table 2 Sorption results for the azeotropic mixture EtOH/ETBE (20/80 wt%) for virgin cellulose acetate and the grafted copolymers CA-*g*-PLA at 30°C.

Membrane	W_{PLA} (wt.%)	S (wt.%)	C^s_{EtOH} (wt.%)	β_s
Virgin CA	0	4.2	97	129
CA-g-23 PLA	23	7.5	65	7.4
CA-g-31.5 PLA	31.5	9	61	6.25
CA-g-40.5 PLA	40.5	11	53	4.5

W_{PLA}: PLA weight fraction in the grafted cellulose acetate; S: total swelling at sorption equilibrium; C^s_{EtOH}: ethanol content in the absorbed mixture; β_s: sorption separation factor

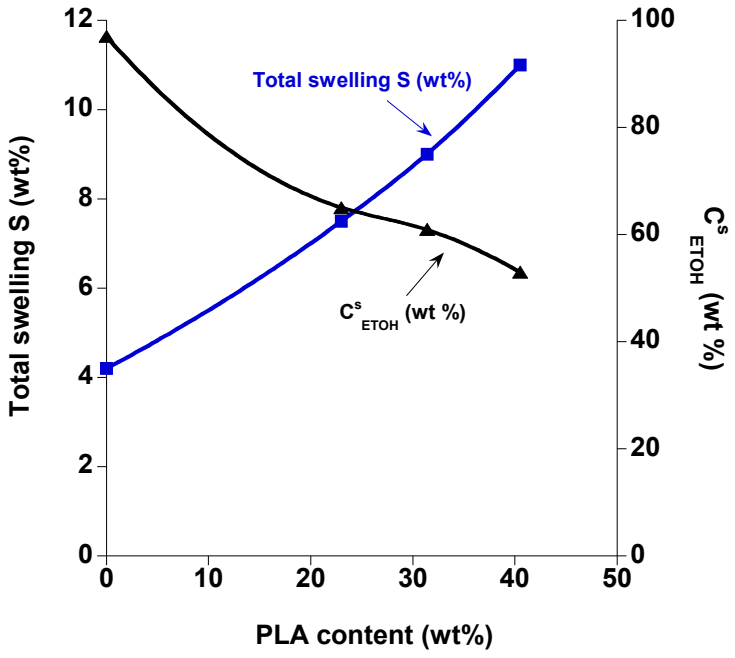

Figure 6: Influence of the PLA content on the total swelling and ethanol content in the absorbed mixture for the sorption of the azeotropic mixture EtOH/ETBE (20/80 wt%) for virgin cellulose acetate and the grafted copolymers CA-*g*-PLA at 30°C.

3.3. Pervaporation properties of cellulose acetate grafted with PLA for ETBE purification

The pervaporation experiments were carried out at 50°C instead of 30°C formerly used for the sorption measurements [11] to improve the fluxes and facilitate the comparison between the different membranes. Furthermore, we have already shown that this change in temperature has a negligible influence on sorption properties, due to the fact that the ethanol and ETBE activity coefficients are almost constant between 30°C and 50°C as confirmed by the corresponding thermodynamic NRTL calculations [11].

Table 3 reports the pervaporation results for the separation of the azeotropic mixture EtOH/ETBE with virgin cellulose acetate and cellulose acetate with increasing contents of grafted PLA.

For virgin cellulose acetate, the permeate contained ethanol only (C'= 100 wt%), which corresponded to an outstanding infinite pervaporation separation factor β_{PV}, but the flux was low (J = 0.023 kg/h m^2). These results were consistent with the pervaporation properties also reported by Nguyen *et al.* for this separation (J = 0.08 kg/h m^2 and C' = 100 wt% at 40°C) [13]. Despite the higher temperature (50°C), the slightly decreased flux obtained in this work may be ascribed to the much higher molecular weight of the cellulose acetate used in this work and to different membrane casting procedures.

Table 3 Pervaporation results for the azeotropic mixture EtOH/ETBE (20/80 wt%) for virgin cellulose acetate and the grafted copolymers CA-*g*-PLA at 50°C.

Membrane	J (kg/h m^2)	C' (wt.%)	β_{PV}	β_D	P_{EtOH} x 1000 (kg µm/h m^2 kPa)	P_{ETBE} x 1000 (kg µm /h m^2 kPa)
Virgin CA	0.023	100	∞	-	2.22	0
CA-g-23 PLA	0.165	99	396	53.3	15.8	0.17
CA-g-31.5 PLA	0.22	97	129	20.67	20.6	0.66
CA-g-40.5 PLA	0.27	93	46	10.19	24.3	1.9

W_{PLA}: PLA weight fraction in the grafted cellulose acetate; J: total flux normalized for a reference membrane thickness of 5 µm; C': ethanol content in permeate; β_{pv}: pervaporation separation factor; β_D: diffusion separation factor; P_i: partial permeability of species i.

Similarly as for membrane swelling, the cellulose acetate flux was increased by nearly 7-fold by grafting 23 wt% of PLA oligomer (Fig. 7). By further increasing the PLA content up to 40.5 wt%, corresponding to the maximum grafting rate, the PV flux further increased up to 12 times compared to that of virgin cellulose acetate. After copolymer grafting, the ethanol permeate content C' decreased very slightly from 100 to 99 wt% for PLA contents increasing up to 23 wt%. When the PLA content was further increased up to 40.5 wt%, the ethanol permeate content gradually decreased to 93 wt% but still remained in the very high range for this application. Therefore, the different membranes CA-*g*-PLA were highly selective to ethanol (C' > 90 wt%) and corresponded to high pervaporation separation factor β_{PV} as shown in Table 3 entry 4.

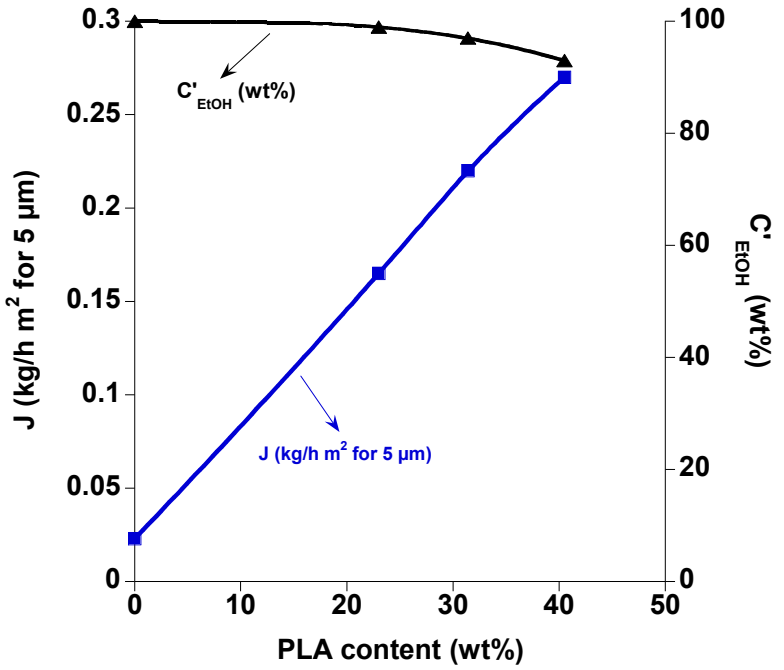

Figure 7: Influence of the PLA content on the total flux and ethanol content in the permeate for the pervaporation of the azeotropic mixture EtOH/ETBE (20/80 wt%) for virgin CA and the grafted copolymers CA-*g*-PLA at 30°C at 50°C.

For a better understanding of the membrane performances, partial permeability data were then considered as *intrinsic* membrane properties, which only reflected the influence of polymer material and permeating species without the effect of the operating conditions [52] (Table 3). These partial permeability data were simply calculated as the ratio of partial flux over the corresponding driving force for mass transfer [53]. For the virgin CA membrane, the partial permeability of ethanol was 2.22 10^{-3} kg µm /h m^2 kPa with infinite PV separation

factor β_{PV} and nil ETBE permeability. Fig. 8 shows that the grafting of PLA onto cellulose acetate increased the partial permeability of both ethanol and ETBE (Fig. 8). Nevertheless, the permeability increase was much stronger for ethanol (×11) than for ETBE (×2) for the maximum PLA content of 40.5 wt%. According to the sorption-diffusion model, this strong difference resulted from the contributions of both sorption and diffusion steps during the global PV mass transfer.

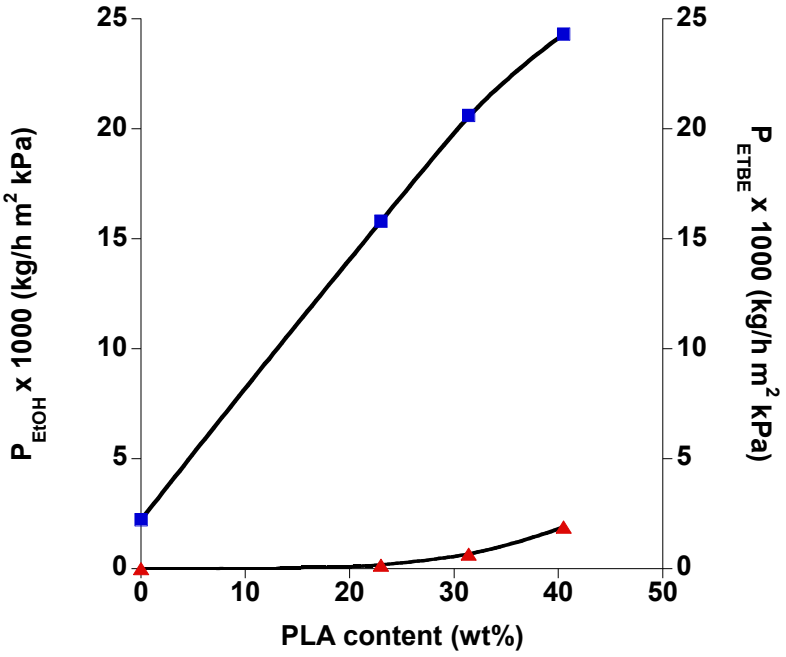

Figure 8: Influence of the PLA content on the partial permeability of ethanol and ETBE for the pervaporation of the azeotropic mixture EtOH/ETBE (20/80 wt%) for virgin CA and the grafted copolymers CA-*g*-PLA at 50°C.

For a better understanding of the respective role of the sorption and diffusion steps on the membrane PV properties, the sorption and diffusion separation factors β_S and β_D were then compared for virgin CA and the grafted copolymers membranes (Fig. 9). The sorption and PV separation factors β_S and β_{PV} were first estimated from the results of the sorption and PV experiments with equations (4) and (7), respectively. The corresponding diffusion separation factors β_D were then calculated from equation (9) according to the assumptions of the sorption-diffusion model [51].

$$\beta_{PV} = \beta_S \times \beta_D \qquad (9)$$

As explained earlier, the sorption and pervaporation experiments were carried out at different temperatures of 30 and 50°C, respectively. Nevertheless, this change in temperature had a negligible influence on the sorption properties due to the fact that the ethanol and ETBE activity coefficients were almost constant between 30°C and 50°C [11]. Therefore, the sorption separation factors calculated for 30°C were assumed quasi-identical at 50°C for calculating the diffusion separation factors β_D. The highest sorption separation factor β_s (129) was found for virgin cellulose acetate and it was much greater than those of the grafted copolymers CA-*g*-PLA. In addition, the pervaporation separation factor β_{PV} of virgin cellulose acetate reached the infinite, leading to an infinite diffusion separation factor β_D. For this reason, the corresponding separation factor data were not be plotted in Fig. 9, which was limited to the grafted copolymers. For all of them, the diffusion separation factor was systematically higher than the sorption separation factor. Therefore, the diffusion step was mainly contributing to the PV separation factor. When the PLA content increased in Fig. 9, the sorption and diffusion steps were less and less selective due to a simultaneous decrease in the copolymers H-bonding ability and rigidity, which favored the simultaneous permeation of the bulky ETBE molecules. Nevertheless, the grafted copolymers membranes still remained highly selective for ETBE purification as shown by the very high ethanol permeate contents (C'>90 wt%) obtained in this work.

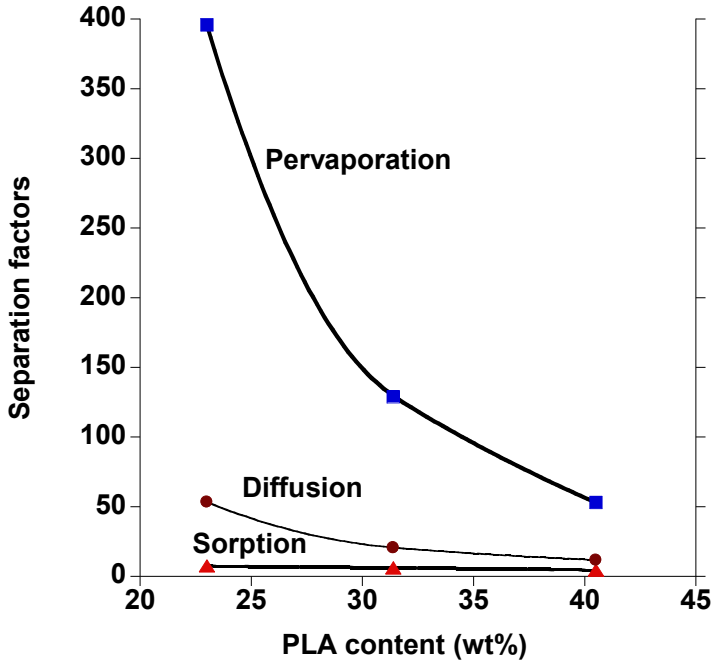

Figure 9: Influence of the PLA content on sorption, diffusion and pervaporation separation factors for the grafted copolymers CA-*g*-PLA.

4. Conclusion

A new strategy for PLA grafting onto cellulose acetate was developed for high performance bio-based membranes for ETBE purification by the pervaporation process. A short α-alkyne PLA oligomer was first synthesized by controlled ROP. This functional PLA oligomer was then grafted onto an azido cellulose acetate by CuAAC "click" chemistry. The grafting rate was easily controlled and the PLA content was varied from 0 to 40.5 wt%. In this study, the maximum PLA content was limited to less than 50 wt% to ensure the mechanical withstanding of the different membranes in the pervaporation conditions.

During the sorption of the azeotropic mixture EtOH/ETBE, the total swelling increased almost linearly with the PLA content while the ethanol content in the absorbed mixture and the sorption separation factor decreased with the PLA content. Nevertheless, the new membranes absorbed ethanol selectively and ensured a first enrichment of the targeted mixture during the sorption step. During pervaporation, the flux increased strongly with the PLA content and the maximum flux was nearly 12 times that of virgin cellulose acetate. The ethanol permeate content decreased slightly with the PLA content but still remained in the very high range (C'>90 wt%) for this application. An analysis based on the sorption-diffusion model revealed that the diffusion step mainly contributed to the very high membrane selectivity obtained with the new grafted copolymers.

The "grafting onto" strategy developed in this work could be extended to other polysaccharides and polymer grafts to provide another way of optimizing membrane properties for challenging separations of the bio-fuels and petroleum industries.

5. References

[1] E.M.V. Hoek and V.V. Tarabara, eds. *Encyclopedia of Membrane Science and Technology*. 2013, John Wiley & Sons.

[2] E. Drioli and L. Giorno, eds. *Comprehensive Membrane Science and Engineering*. 2010, Elsevier Science.

[3] R.W. Baker, Membrane technology and applications, 2nd ed, John Wiley & Sons, Chichester, 2004.

[4] A. Jonquieres, C. Arnal-Herault, and J. Babin, Pervaporation, in: E.M.V. Hoek, V.V. Tarabara (Eds.) Encyclopedia of Membrane Science and Technology, Wiley, volume 3 (2013) pp. 1533-1559.

[5] H. Noureddini, Ethyl tert-butyl ether and methyl tert-butyl ether: status, review, and alternative use. Exploring the environmental issues of mobile, recalcitrant compounds in gasoline, ACS Symposium Series, 799 (2002) 107-124.

[6] F. Lipnizki, Membrane process opportunities and challenges in the bioethanol industry, Desalination, 250 (2010) 1067–1069.

[7] M. Wang, C. Arnal-Herault, C. Rousseau, A.I. Palenzuela, J. Babin, L. David, and A. Jonquieres, Grafting of multi-block copolymers: A new strategy for improving membrane

separation performance for ethyl tert-butyl (ETBE) bio-fuel purification by pervaporation, Journal of Membrane Science, 469 (2014) 31-42.

[8] Y. Zhang, N. Wang, S. Ji, R. Zhang, C. Zhao, and J.-R. Li, Metal-organic framework/poly(vinyl alcohol) nanohybrid membrane for the pervaporation of toluene/n-heptane mixtures, Journal of Membrane Science, 489 (2015) 144-152.

[9] M. Jain, D. Attarde, and S.K. Gupta, Removal of thiophene from n-heptane/thiophene mixtures by spiral wound pervaporation module: Modelling, validation and influence of operating conditions, Journal of Membrane Science, 490 (2015) 328-345.

[10] G. Zhang, J. Li, N. Wang, H. Fan, R. Zhang, G. Zhang, and S. Ji, Enhanced flux of polydimethylsiloxane membrane for ethanol permselective pervaporation via incorporation of MIL-53 particles, Journal of Membrane Science, 492 (2015) 322-330.

[11] M. Billy, A. Ranzani Da Costa, P. Lochon, R. Clement, M. Dresch, and A. Jonquieres, Cellulose acetate graft copolymers with nano-structured architectures: Application to the purification of bio-fuels by pervaporation, Journal of Membrane Science, 348 (2010) 389-396.

[12] S. Zereshki, A. Figoli, S.S. Madaeni, F. Galiano, and E. Drioli, Pervaporation separation of ethanol/ETBE mixture using poly(lactic acid)/poly(vinyl pyrrolidone) blend membranes, Journal of Membrane Science, 373 (2011) 29-35.

[13] Q.-T. Nguyen, C. Léger, P. Billard, and P. Lochon, Novel membranes made from a semi-interpenetrating polymer network for ethanol–ETBE separation by pervaporation, Polymers for Advanced Technologies, 8 (1997) 487-495.

[14] G.S. Luo, M. Niang, and P. Schaetzel, Pervaporation separation of ethyl tert-butyl ether and ethanol mixtures with a blended membrane, Journal of Membrane Science, 125 (1997) 237-244.

[15] Q.-T. Nguyen, R. Clément, I. Noezar, and P. Lochon, Performances of poly(vinylpyrrolidone-co-vinyl acetate)-cellulose acetate blend membranes in the pervaporation of ethanol diethyl tert-butyl ether mixtures: Simplified model for flux prediction, Separation and Purification Technology, 13 (1998) 237-245.

[16] G.S. Luo, M. Niang, and P. Schaetzel, A high performance membrane for sorption and pervaporation separation of ethyl tert-butyl ether and ethanol mixtures, Separation Science and Technology, 34 (1999) 391-401.

[17] F. Hassan Hassan Abdellatif, J. Babin, C. Arnal-Herault, L. David, and A. Jonquieres, Grafting of cellulose acetate with ionic liquids for biofuel purification by a membrane process : Influence of the cation, Carbohydrate Polymers, (2015) submitted (corresponding to the second part of PhD chapter 3).

[18] Y. Shinkawa, Y. Hayashi, S. Sato, and K. Nagai, Permeability of ethanol solution through poly(lactic acid) film, Journal of Applied Polymer Science, 132 (2015) n/a-n/a.

[19] K. Hamad, M. Kaseem, H.W. Yang, F. Deri, and Y.G. Ko, Properties and medical applications of polylactic acid: A review, Express Polymer Letters, 9 (2014) 435-455.

[20] H. Ebadi-Dehaghani, M. Barikani, H.A. Khonakdar, S.H. Jafari, U. Wagenknecht, and G. Heinrich, On O2 gas permeability of PP/PLA/clay nanocomposites: A molecular dynamic simulation approach, Polymer Testing, 45 (2015) 139-151.

[21] S. Zereshki, A. Figoli, S.S. Madaeni, S. Simone, J.C. Jansen, M. Esmailinezhad, and E. Drioli, Poly(lactic acid)/poly(vinyl pyrrolidone) blend membranes: Effect of membrane composition on pervaporation separation of ethanol/cyclohexane mixture, Journal of Membrane Science, 362 (2010) 105-112.

[22] Y. Teramoto and Y. Nishio, Cellulose diacetate-graft-poly(lactic acid)s: synthesis of wide-ranging compositions and their thermal and mechanical properties, Polymer, 44 (2003) 2701-2709.

[23] H. Dong, Q. Xu, Y. Li, S. Mo, S. Cai, and L. Liu, The synthesis of biodegradable graft copolymer cellulose-graft-poly(l-lactide) and the study of its controlled drug release, Colloids and Surfaces B: Biointerfaces, 66 (2008) 26-33.

[24] S. Salmieri, F. Islam, R. Khan, F. Hossain, H.M. Ibrahim, C. Miao, W. Hamad, and M. Lacroix, Antimicrobial nanocomposite films made of poly(lactic acid)-cellulose nanocrystals (PLA-CNC) in food applications: part A-effect of nisin release on the inactivation of Listeria monocytogenes in ham, Cellulose, 21 (2014) 1837-1850.

[25] R. Quintana, O. Persenaire, Y. Lemmouchi, L. Bonnaud, and P. Dubois, Grafted d/l-lactide to cellulose acetate by reactive melt processing: Its role as CA/PLA blend compatibilizer, European Polymer Journal, 57 (2014) 30-36.

[26] J. Dlouha, L. Suryanegara, and H. Yano, Cellulose nanofibre-poly(lactic acid) microcellular foams exhibiting high tensile toughness, Reactive and Functional Polymers, 85 201-207.

[27] N. Peelman, P. Ragaert, K. Ragaert, B. De Meulenaer, F. Devlieghere, and L. Cardon, Heat resistance of new biobased polymeric materials, focusing on starch, cellulose, PLA, and PHA, Journal of Applied Polymer Science, 132 (2015) n/a-n/a.

[28] Y. Guo, X. Wang, X. Shu, Z. Shen, and R.-C. Sun, Self-Assembly and Paclitaxel Loading Capacity of Cellulose-graft-poly(lactide) Nanomicelles, Journal of Agricultural and Food Chemistry, 60 (2012) 3900-3908.

[29] Y. Luan, J. Wu, M. Zhan, J. Zhang, J. Zhang, and J. He, "One pot" homogeneous synthesis of thermoplastic cellulose acetate-graft-poly(l-lactide) copolymers from unmodified cellulose, Cellulose, 20 (2013) 327-337.

[30] Y. Zhang, X. Li, Y. Yang, A. Lan, X. He, and M. Yu, In situ graft copolymerization of l-lactide onto cellulose and the direct melt spinning, RSC Advances, 4 (2014) 34584-34590.

[31] R. Quintana, O. Persenaire, Y. Lemmouchi, L.l. Bonnaud, and P. Dubois, Grafted d/l-lactide to cellulose acetate by reactive melt processing: Its role as CA/PLA blend compatibilizer, European Polymer Journal, 57 (2014) 30-36.

[32] M. Laville, J. Babin, I. Londono, M. Legros, C. Nouvel, A. Durand, R. Vanderesse, M. Leonard, and J.-L. Six, Polysaccharide-covered nanoparticles with improved shell stability using click-chemistry strategies, Carbohydrate Polymers, 93 (2013) 537-546.

[33] C. Nouvel, P. Dubois, E. Dellacherie, and J.-L. Six, Controlled synthesis of amphiphilic biodegradable polylactide-grafted dextran copolymers, Journal of Polymer Science Part A: Polymer Chemistry, 42 (2004) 2577-2588.

[34] F. Hassan Hassan Abdellatif, J. Babin, C. Arnal-Herault, and A. Jonquieres, Chapter 25 : Grafting of cellulose and cellulose derivatives by CuAAC click chemistry, in V.K. Thakur (Ed.). Cellulose-based Graft Copolymers : Structure and Chemistry, CRC Press Taylor & Francis Publisher, 2015, pp. 563-591.

[35] P.-H. Elchinger, P.-A. Faugeras, B. Boens, F. Brouillette, D. Montplaisir, R. Zerrouki, and R. Lucas, Polysaccharides: The "Click" Chemistry Impact, Polymers, 3 (2011) 1607-1651.

[36] T. Liebert, C. Hänsch, and T. Heinze, Click chemistry with polysaccharides, Macromolecular rapid communications, 27 (2006) 208-213.

[37] A. Uliniuc, M. Popa, T. Hamaide, and M. Dobromir, New approaches in hydrogel synthesis – click chemistry: A review, Cellulose Chemistry and Technology, 46 (2012) 1-11.

[38] Q. Li, H. Kang, and R. Liu, Block and hetero ethyl cellulose graft copolymers synthesized via sequent and one-pot ATRP and "click" reactions, Chinese journal of chemistry, 30 (2012) 2169-2175.

[39] W.Z. Xu and J.F. Kadla, Honeycomb Films of Cellulose Azide: Molecular Structure and Formation of Porous Films, Langmuir, 29 (2013) 727-733.

[40] W. Xu, G. Gao, and J. Kadla, Synthesis of antibacterial cellulose materials using a clickable quaternary ammonium compound, Cellulose, 20 (2013) 1187-1199.

[41] K. Negishi, Y. Mashiko, E. Yamashita, A. Otsuka, and T. Hasegawa, Cellulose chemistry meets click chemistry: syntheses and properties of cellulose-based glycoclusters with high structural homogeneity, Polymers 3 (2011) 489-508.

[42] M. Pohl, J. Schaller, F. Meister, and T. Heinze, Selectively dendronized cellulose: synthesis and characterization, Macromolecular Rapid Communications, 29 (2008) 142-148.

[43] M. Pohl, N. Michaelis, F. Meister, and T. Heinze, Biofunctional surfaces based on dendronized cellulose, Biomacromolecules, 10 (2009) 382-389.

[44] M. Pohl, G.A. Morris, S.E. Harding, and T. Heinze, Studies on the molecular flexibility of novel dendronized carboxymethyl cellulose derivatives, European Polymer Journal, 45 (2009) 1098-1110.

[45] M.I. Montanez, Y. Hed, S. Utsel, J. Ropponen, E. Malmstrom, L. Wagberg, A. Hult, and M. Malkoch, Bifunctional dendronized cellulose surfaces as biosensors, Biomacromolecules, 12 (2011) 2114-2125.

[46] P.-A. Faugeras, F. Brouillette, and R. Zerrouki, Crosslinked cellulose developed by CuAAC, a route to new materials, Carbohydrate Research, 356 (2012) 247-251.

[47] B. Neises and W. Steglich, Simple Method for the Esterification of Carboxylic Acids, Angewandte Chemie International Edition, 17 (1978) 522–524.

[48] E. Fleury, J. Dubois, C. Léonard, J.P. Joseleau, and H. Chanzy, Microgels and ionic associations in solutions of cellulose diacetate, Cellulose, 1 (1994) 131-144.

[49] K.D. Goebel, G.C. Berry, and D.W. Tanner, Properties of cellulose acetate. III. Light scattering from concentrated solutions and films. Tensile creep and desalination studies on films Journal of Polymer Science: Polymer Physics Edition, 17 (1979) 917-937.

[50] H. Suzuki, Y. Muraoka, M. Satio, and K. Kamide, Light-scattering study on cellulose diacetate in 2-butanone, European Polymer Journal, 18 (1982) 831-837.

[51] J.G. Wijmans and R.W. Baker, The solution-diffusion model: a review, Journal of Membrane Science, 107 (1995) 1-21.

[52] R.W. Baker, J.G. Wijmans, and Y. Huang, Permeablity, permeance and selectivity: A preferred way of reporting pervaporation performance data, Journal of Membrane Science, 348 (2010) 346-352.

[53] J.G. Wijmans, Process performance = membrane properties + operating conditions, Journal of Membrane Science, 220 (2003) 1-3.

Supporting information

Synthesis of 6-azido hexanoic acid

In 500 mL round bottom reactor, 8.18 g (0.126 mol) of sodium azide were dissolved in 250 mL of DMSO. 20 g (0.103 mol) of 6-bromo hexanoic acid were added to the mixture. This mixture was stirred for 4 hours at room temperature. The product was recovered by extraction in DCM for three times and concentrated by rotator evaporator. The yield was 94%.

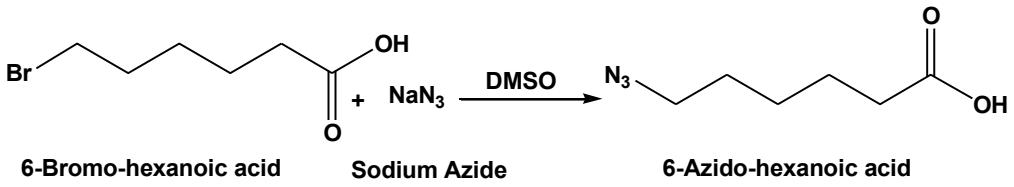

Figure S1: Synthesis of 6 azido hexanoic acid

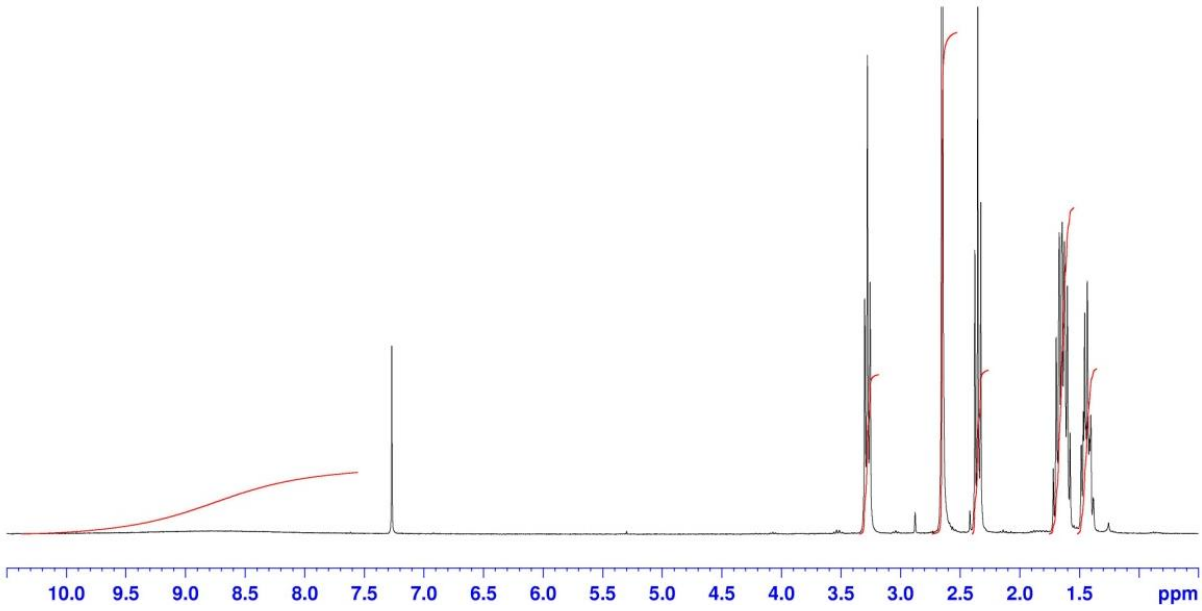

Figure S2: ^{1}H NMR characterization for 6-azido hexanoic acid

Chapter 3

Grafting of cellulose acetate with ionic liquids for biofuel purification by a membrane process

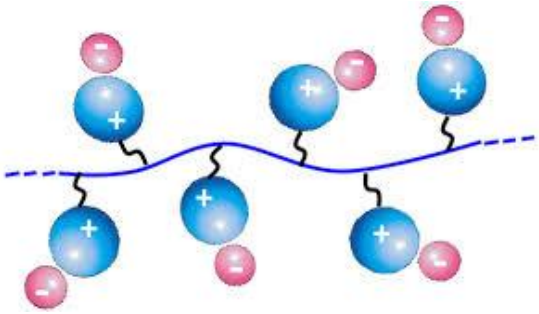

Chapter 3 Part 1

Grafting of cellulose acetate with ionic liquids using click chemistry

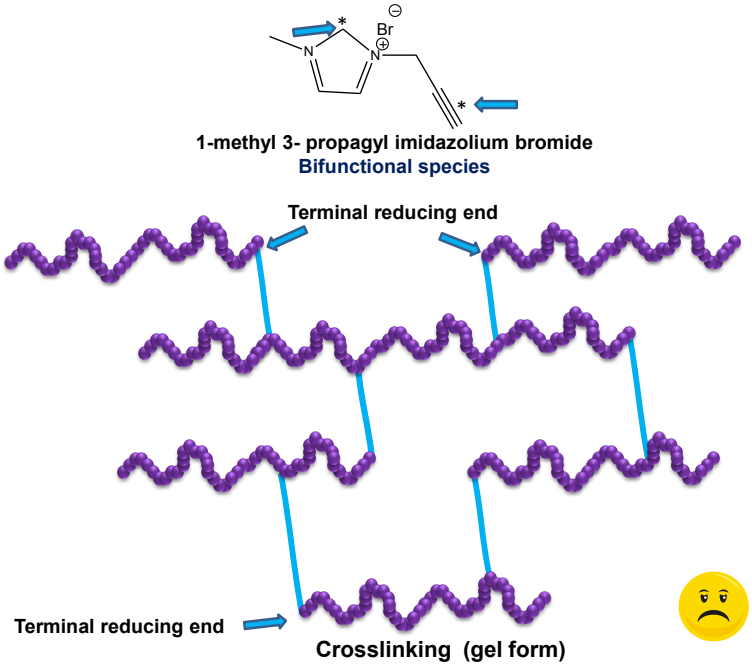

1. Introduction

Ionic liquids (ILs) were first reported in 1888 by S. Gabriel and J. Weiner [1]. ILs are defined as low melting point organic salts which contain permanent charges [2]. They consist of a bulky organic cation and an inorganic or organic anion (Figure 1). The large size of the organic cation permits the charge delocalization and decrease the ILs lattice energy and melting temperature [3].

The ILs unique physical properties (*e.g.* high thermal and chemical stability, negligible vapor pressure and low flammability [4] offer new "green" alternatives to classical volatile organic solvents. Moreover, ILs revealed further advantages compared to volatile organic solvents like easy recovery and recycling. They were also used as specialty solvents for dissolving biopolymers like cellulose, as co-catalysts/initiators in polymerization reactions and as polymer additives for the development of functional polymers [5].

Another ILs great advantage is the variety of combinations for their cation and anion, which allows good control of their physical and chemical properties in a wide range of applications (Figure 1) [4].

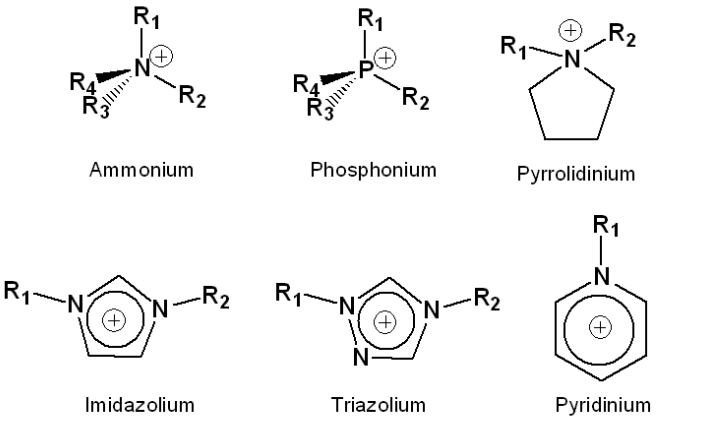

Figure 1: Examples for the variety of cations and anions of the ionic liquids

ILs are generally synthesized in three steps as shown in Figure 2 for imidazolium ILs taken as examples. The first step is the synthesis of an alkyl halide salt by nucleophilic substitution with an alkyl halide RX. The second step corresponds to an anion exchange and the last step is the removal of metal halides side products. The facility of this method helps in

the synthesis of large number of ionic liquids but the complete removal of the inorganic byproducts and water from the desired ILs, especially for hydrophilic ILs, is particularly difficult. Other halide/water free methods have been reported to avoid the former purification problems by using common alkylating reagents but unfortunately several of these alkylating reagents were unstable, toxic and highly expensive [6]. Recently, Kim *et al.* have introduced a new promising water free method for the synthesis of halide and halide-free ILs using orthoesters. The byproducts in this method are alcohols and esters, which are readily evaporated during or after the reaction [6].

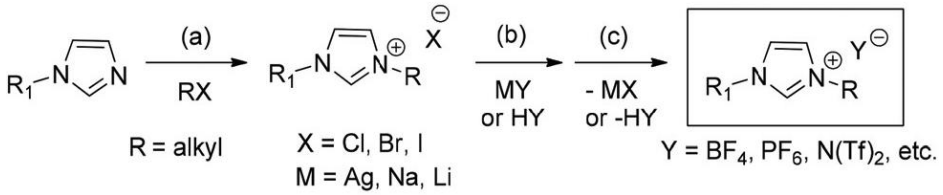

Figure 2: The most common synthesis method for ionic liquids : Example of imidazolium ionic liquids [6].

ILs have been attracted great interest due to their specific properties and the variety of the related applications including organic synthesis, catalysis, separations, and material preparation [7-9]. They can be used as novel and safe electrolytes for advanced devices *e.g.* fuel cells, lithium batteries, electrochemical membranes for capacitors and electromechanical transduction devices for actuators and sensors. ILs, such as for example 1-butyl-3-methyl-imidazoliumtetrafluoroborate, have also been used in the preparation of biosensors [10] and biocatalysis [11] with an increase in enzymatic activity and stability by increasing the ILs concentration. Phosphonium-based ionic liquids have also been reported as efficient catalysts for metal-solvent free cycloaddition reactions with high performance [12]. In addition, amphiphilic ILs enabled the surface modification of the hydrophobic graphene and made it water soluble without losing its excellent electronic conductivity [13].

On the other hand and more closely related to this PhD work, ionic liquids have also been widely used in different areas of separation technology, especially in the field of supported liquid membranes (SLMs) where ionic liquids were immobilized into porous membrane supports [14, 15]. Their negligible vapor pressure and high stability qualified them for gas separation. Over the past decade, ionic liquids have led to a real breakthrough in CO_2 separation from N_2 and CH_4 streams [16]. The removal of CO_2 from industrial gases avoided corrosion of industrial installations and the obtaining of pure CO_2 was also useful for lot of

chemical reactions [17, 18]. Another major current issue is the capture of CO_2 with respect to the greenhouse effect. Supported ILs membranes have also been reported for the separation of sulfur compounds from petroleum and natural gas products. This application is also of great interest as the United States Environmental Protection Agency (EPA) recommended in 2007 to reduce their sulfur compounds to 15 ppm [19]. Generally, the gas permeability and selectivity depended on the nature of the ILs anions more than that of their cations. Therefore, most studies used alkyl methyl imidazolium as model cation and different anions like bis(trifluoromethylsulfonyl) imide (Tf_2N^-), tetrafluoroborate (BF_4^-), hexafluorophosphate (PF_6^-), dicyanamide (dca^-), trifluoromethanesulfone ($CF_3SO_3^-$) and bis((perfluoroethyl)sulfonyl) imide ($BETI^-$) [3, 20].

Compared to gas separation, ionic liquid containing membranes have been much less investigated for the separation of liquid mixtures. Organophilic supported ILs membranes were mainly developed for the extraction of volatile organic solvents from aqueous solutions *e.g.* for the acetone-butanol-ethanol (ABE) fermentation process used for biobutanols production [21, 22]. The selective removal of acetone and butan-1-ol by polydimethylsiloxane was improved by membrane impregnating with two different ionic liquids (1-ethenyl-3-ethyl-imidazolium hexafluorophosphate and tetrapropylammonium tetracyanoborate) [23]. These ILs accelerated the separation of butan-1-ol from model solutions of butan-1-ol and water due to a much higher diffusion coefficient of butan-1-ol in IL-PDMS compared to that in the virgin PDMS membrane [24].

Ethyl *tert*-butyl ether (ETBE) is another promising bio-fuel mainly used in Europe. Since the interdiction of the former toxic lead derivatives, it is used as an alternative to methyl tert-butyl ether (MTBE) as one of the oxygenated additives for gasoline fuels to improve fuel combustion and air quality. ETBE also increases the octane number of gasoline fuels and contributes to the fuels quality. This ether is prepared from bio-ethanol [25-28] through the reaction of isobutene with an excess of ethanol (EtOH) that is obtained from biomass thanks to inciting European policies. An azeotropic mixture ETBE/EtOH (80/20 wt %) is produced from this reaction [27, 29]. But to be blended with gasoline fuels, ETBE has to be purified from its azeotropic mixture. ETBE purification from its azeotropic mixture is impossible by conventional distillation and a highly costly ternary distillation process is currently used for this separation [29, 30]. As reported in chapter II, the pervaporation membrane process has been used effectively for the separation of ETBE/EtOH azeotropic mixture and it can also be operated at mild temperature with interesting energy savings [31].

Moreover, we have already observed in our laboratory that several ionic liquids have a strong affinity for ethanol and much less for ETBE [32]. In 2006, Arce *et al.* have taken advantage of these ILs features for ETBE separation from its azeotropic mixture with EtOH by using 1-ethyl-3-methylimidazolium ethylsulfate ([emim][$EtSO_4$]) as an extraction solvent for liquid–liquid extraction and as an azeotrope breaker for extractive distillation [30]

In this PhD work, we have attempted different strategies for permanent immobilization of ILs by grafting them onto cellulose acetate, *i.e.* a polysaccharide derivative with extremely high selectivity but low flux for ETBE purification. Our main objective was to avoid the ILs extraction in the targeted azeotropic mixture during membrane separation and further extends the scope of ionic liquid-containing membranes to the challenging separation of purely organic mixtures, in which these ionic liquids were soluble.

In this first part of chapter III, we report our first attempt of ILs grafting by "click" chemistry following of our first successful experience with "click" chemistry in chapter II.

2. Experimental

2.1. Materials

A new azido cellulose acetate was used in this part for the grafting of ionic liquids by "click" chemistry. Compared to the azido cellulose acetate used in chapter II, the new azido cellulosic derivative had the same overall chemical structure but a lower degree of substitution for the azide groups (DS_{Azide}= 0.17). This choice was made in an attempt to avoid the systematic gelification occurring during the grafting of ionic liquids for a higher degree of substitution of the azide groups. Furthermore, 1-methylimidazole (99%), copper bromide (CuBr, 99.99%), were purchased from Sigma-Aldrich and used without further purification. Propargyl bromide was purchased from TCI (80% in solution in toluene).

2.2. Methods

2.2.1. Synthesis of 1- methyl-3-propargyl imidazolium bromide

In a round bottom reactor under argon flow, 5 g (0.061 mol) of 1-methyl imidazole were dissolved in 150 mL of diethylether under stirring at room temperature. 13.6 mL of a solution of dry propargyl bromide at 80 wt% in toluene (corresponding to 10.9 g (0.0916 mol) of propargyl bromide) were added drop wisely to the reaction mixture. The resulting mixture was stirred for 4 days at room temperature. The resulting solid was collected by filtration, washed several times with diethyl ether and dried under vacuum for 1 night (yield : 62%).

^{1}H NMR (300 MHz, DMSO-d_6) δ ppm: 9.28 (s, 1H, N-**CH_2**-N); 7.77(d, 2H, N-C-**H);** 5.22(s, 2H, C-**H_2);** 3.88(s, 3H, C-**H_3**); 3.83(s, 1H, C-**H**).

2.2.2. Grafting of imidazolium ionic liquid onto cellulose acetate by "click" chemistry

In Schlenk tube, 1 g of azido cellulose acetate with a DS_{Azide} of 0.17 (corresponding to 3.46 mmol of glycosidic rings and 0.588 mmol of azide groups) and 0.1182 g (0.588 mmol) of 1- methyl-3-propargyl imidazolium bromide were stirred in 30 mL of DMSO under argon atmosphere. After complete dissolution, the solution was purged carefully and backfilled with argon for several times. 84.3 mg (0.588 mmol) of copper bromide and 3 mg of copper powder dendritic "Cu^0" were then added under argon flow. The reaction mixture was purged again to ensure the inert atmosphere. The reaction was continued for 24 hours at room temperature and led to the systematic gelation of the reaction medium.

3. Results and discussion

Following the successful experience with "click" chemistry for PLA grafting onto cellulose acetate in chapter II, we attempted to transpose the former approach to the grafting of ionic liquids from an azido cellulose acetate derivative. Therefore, an imidazolium liquid ionic bearing a complementary alkyne group for the "click" chemistry was first obtained by nucleophilic substitution of propargyl bromide with 1-methyl imidazole in high yield (62%) (Figure 3).

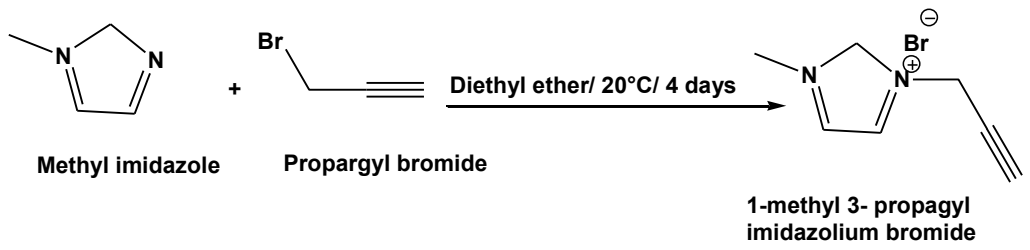

Figure 3: Synthesis of 1- methyl-3-propargyl imidazolium bromide.

The grafting of the alkyne-functionalized imidazolium ionic liquid was then achieved onto an azido cellulose acetate derivative by CuAAC "click" chemistry. Compared to chapter II, the degree of substitution of the azide groups was decreased to 0.17 in an attempt to avoid the systematic gelation of the reaction medium but without any success (Figure 4). Further experiments showed that the gelled medium could not be dissolved in aprotic dipolar solvents (DMF, DMSO), which were expected to be good solvents for the initially expected

grafted polymer chains. Therefore, the grafting of the alkyne imidazolium ionic liquid onto azido cellulose acetate led to a systematic cross-linking of the polymer chains.

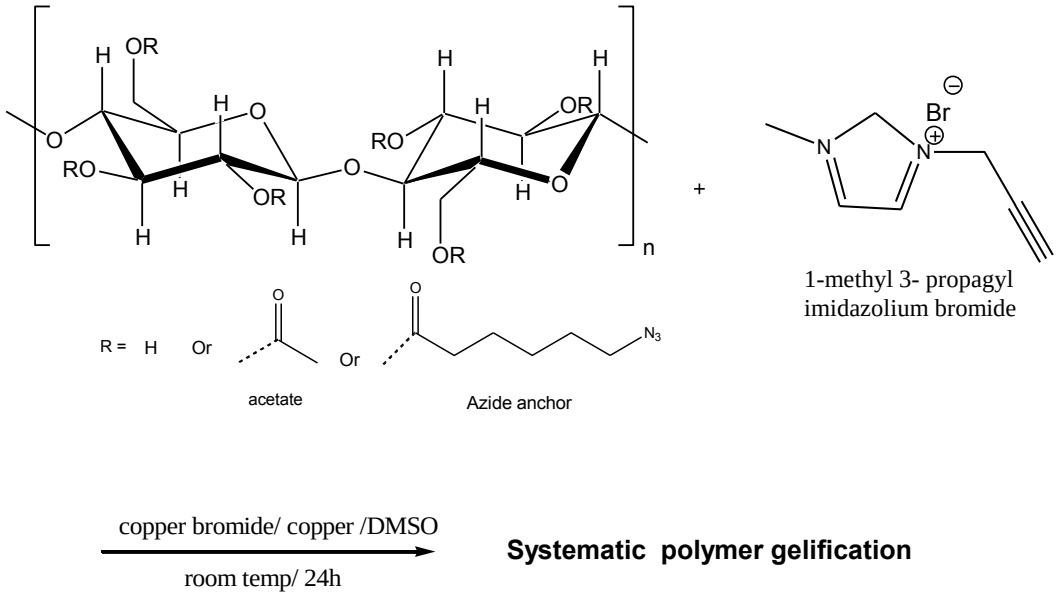

Figure 4: Ionic liquid grafting onto cellulose acetate by CuAAC "click" chemistry.

What were the reasons for the systematic chemical cross-linking occurring during the ionic liquid grafting? A complementary bibliographic study brought the answers to this critical question. In 2002, Aggarwal *et al.* showed that, under basic conditions, butylmethylimidazolium ionic liquids were easily deprotonated at C-2 position due to the acidic character of the corresponding proton, therefore leading to species reactive with electrophiles [33]. Even more interesting for our work, in 2008, Rosenau *et al.* used an imidazolium ionic liquid isotopically labeled at C-2 position ([2-^{13}C-BMIM][OAc]) to probe its side reactions with cellulose in two different conditions (room temperature for 7 days or room temperature for 2 h in presence of 3% triethylamine) [34, 35]. In the later work, ^{13}C NMR analysis revealed that the ^{13}C-labeled imidazolium IL reacted with the anomeric carbon of the cellulose reducing ends through an electrophilic addition involving the C-2 of the ionic liquid in *both* neutral and basic conditions. These first observations were confirmed by using a fluorescent imidazolium ionic liquid in order to enhance the corresponding detection of this

side reaction in the same work. The former results clearly showed that imidazolium ionic liquids can react with the reducing ends of cellulose as shown in Figure 5.

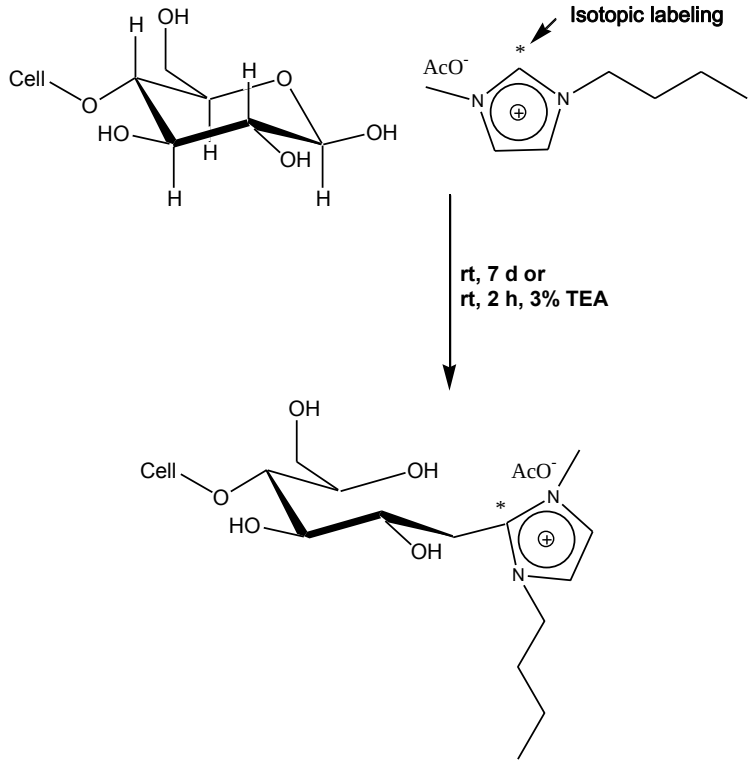

Figure 5: Reaction of a butylmethylimidazolium ionic liquid ^{13}C-labeled specifically at position C-2 with cellulose [34].

Coming back to the grafting of cellulose acetate by the alkyne-functionalized imidazolium ionic liquid of interest in this work, the same reaction of imidazolium C-2 position most likely occurred with the reducing end of the cellulosic chains although it could not be evidenced by ^{13}C NMR due to the lack of specific ^{13}C-labeling unlike the former work of Rosenau *et al.* At the same time, the alkyne group present on the imidazolium ionic liquid for "click" chemistry reacted with the azido groups present as side groups on the cellulose acetate derivative. In these conditions, the alkyne-functionalized imidazolium ionic liquid turned out to be a bi-functional reactant during grafting. Therefore, it acted as an efficient cross-linking agent, making covalent bridges between the polymer chains and leading to the systematic gelation of the system (Figure 6).

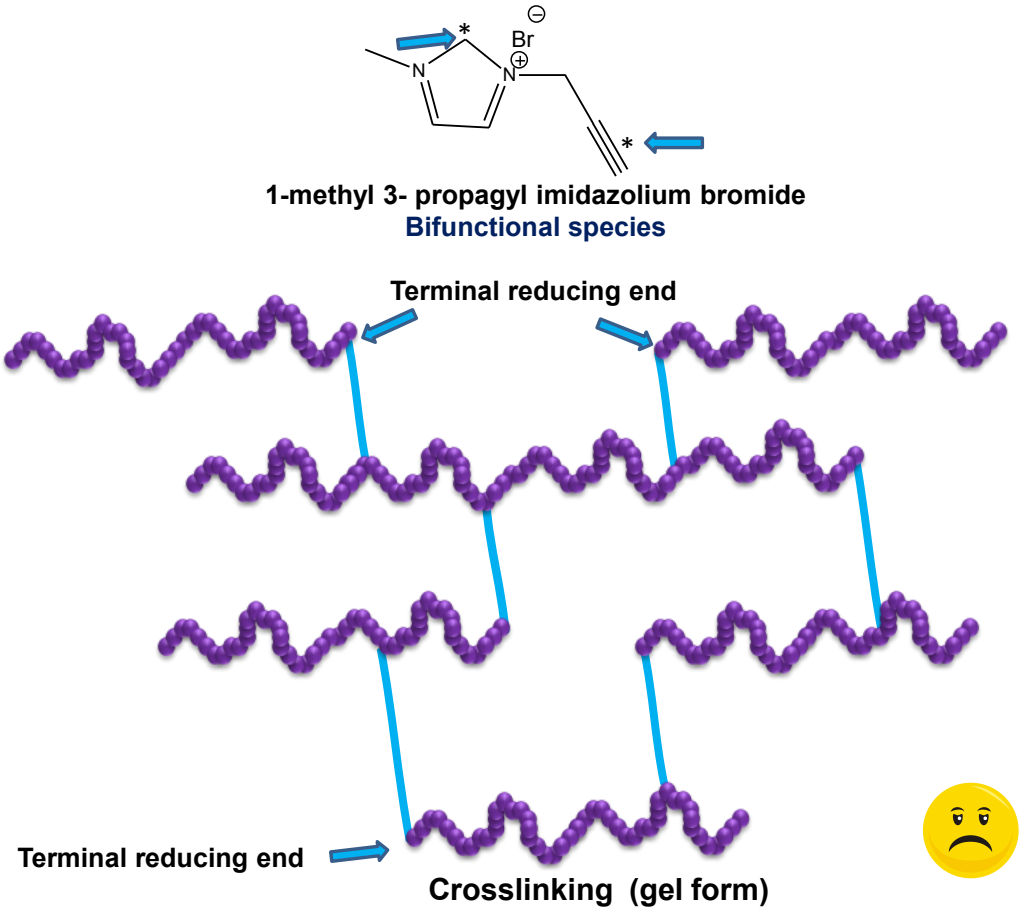

Figure 6: The particular behavior of 1- methyl-3-propargyl imidazolium bromide during the grafting of azido cellulose acetate leading to cross-linking and systematic gelation.

4. Conclusion

The bi-functionality of the alkyne-functionalized imidazolium ionic liquid towards the azido cellulosic chains led to the failure of the "click" strategy initially developed for grafting ionic liquids onto cellulose acetate. Systematic cross-linking and gelation of the reaction medium were not compatible with the targeted membrane application, although it could be acceptable for other applications such as bactericidal cellulosic gels for example.

In the following parts of chapter III, we will explore a new strategy for grafting ionic liquids onto cellulose acetate successfully. This new strategy overcame the former limitations and ensured the permanent ionic liquid immobilization without gelation as required for the membrane application. Therefore, the second part of chapter III will first report on cellulose acetate grafting with ionic liquids containing different cations and the same bromide anion.

The third and last part will then focus on anion exchange for varying the anion structure of the grafted ionic liquid.

5. References

[1] S. Gabriel and J. Weiner, Ueber einige Abkömmlinge des Propylamins, Berichte der deutschen chemischen Gesellschaft, 21 (1888) 2669-2679.

[2] M.D. Green and T.E. Long, Designing Imidazole-Based Ionic Liquids and Ionic Liquid Monomers for Emerging Technologies, Journal of Macromolecular Science Part C: Polymer Reviews, 49 (2009) 291–314.

[3] J.J. Close, K. Farmer, S.S. Moganty, and R.E. Baltus, CO2/N2 separations using nanoporous alumina-supported ionic liquid membranes: Effect of the support on separation performance, Journal of Membrane Science, 390-391 (2012) 201-210.

[4] U.H. Choi, M. Lee, S. Wang, W. Liu, K.I. Winey, H.W. Gibson, and R.H. Colby, Ionic Conduction and Dielectric Response of Poly(imidazolium acrylate) Ionomers, Macromolecules, 45 (2012) 3974-3985.

[5] D. Mecerreyes, Polymeric ionic liquids: Broadening the properties and applications of polyelectrolytes, Progress in Polymer Science 36 (2011) 1629-1648.

[6] D.J. Kim, K.H. Oh, and J.K. Park, A general and direct synthesis of imidazolium ionic liquids using orthoesters, Green Chemistry, 16 (2014) 4098-4101.

[7] Y. Cao, J. Wu, J. Zhang, H. Li, Y. Zhang, and J. He, Room temperature ionic liquids (RTILs): A new and versatile platform for cellulose processing and derivatization, Chemical Engineering Journal, 147 (2009) 13-21.

[8] A. Lewandowski and A. Swiderska, New composite solid electrolytes based on a polymer and ionic liquids, Solid State Ionics, 169 (2004) 21-24.

[9] J. Lu, F. Yan, and J. Texter, Advanced applications of ionic liquids in polymer science, Progress in Polymer Science, 34 (2009) 431-448.

[10] X. Lu, Q. Zhang, L. Zhang, and J. Li, Direct electron transfer of horseradish peroxidase and its biosensor based on chitosan and room temperature ionic liquid, Electrochemistry Communications, 8 (2006) 874-878.

[11] W.-y. Lou, M.-h. Zong, and H. Wu, Enhanced activity, enantioselectivity and stability of papain in asymmetric hydrolysis of d,l-p-hydroxyphenylglycine methyl ester with ionic liquid, Biocatalysis and Biotransformation, 22 (2004) 171-176.

[12] D. Wei-Li, J. Bi, L. Sheng-Lian, L. Xu-Biao, T. Xin-Man, and A. Chak-Tong, Functionalized phosphonium-based ionic liquids as efficient catalysts for the synthesis of cyclic carbonate from expoxides and carbon dioxide, Applied Catalysis A: General, 470 (2014) 183-188.

[13] X. Lu, X. Wang, J. Jin, Q. Zhang, and J. Chen, Electrochemical biosensing platform based on amino acid ionic liquid functionalized graphene for ultrasensitive biosensing applications, Biosensors and Bioelectronics, 62 (2014) 134-139.

[14] S. Paul, E.V. Ann, H.D. James, D.R. Robin, A.K. Carl, L.D. Dan, and D.N. Richard, Supported Ionic Liquid Membranes and Facilitated Ionic Liquid Membranes. Ionic Liquids, American Chemical Society, 2002, (818), pp. 69-87.

[15] D. Han and K.H. Row, Recent Applications of Ionic Liquids in Separation Technology, Molecules, 15 (2010) 2405.

[16] E. Torralba-Calleja, J. Skinner, and D. Gutiérrez-Tauste, CO2 Capture in Ionic Liquids: A Review of Solubilities and Experimental Methods, Journal of Chemistry, 2013 16.

[17] S.D. Hojniak, A.L. Khan, O. Holloczki, B. Kirchner, I.F.J. Vankelecom, W. Dehaen, and K. Binnemans, Separation of Carbon Dioxide from Nitrogen or Methane by Supported Ionic Liquid Membranes (SILMs): Influence of the Cation Charge of the Ionic Liquid, The Journal of Physical Chemistry B, 117 (2013) 15131-15140.

[18] S.D. Hojniak, I.P. Silverwood, A.L. Khan, I.F.J. Vankelecom, W. Dehaen, S.G. Kazarian, and K. Binnemans, Highly Selective Separation of Carbon Dioxide from Nitrogen and Methane by Nitrile/Glycol-Difunctionalized Ionic Liquids in Supported Ionic Liquid Membranes (SILMs), The Journal of Physical Chemistry B, 118 (2014) 7440-7449.

[19] G.O. Yahaya, F. Hamad, A. Bahamdan, V.V.R. Tammana, and E.Z. Hamad, Supported ionic liquid membrane and liquid-liquid extraction using membrane for removal of sulfur compounds from diesel/crude oil, Fuel Processing Technology, 113 (2013) 123-129.

[20] R.D. Noble and D.L. Gin, Perspective on ionic liquids and ionic liquid membranes, Journal of Membrane Science, 369 (2011) 1-4.

[21] A. Plaza, G. Merlet, A. Hasanoglu, M. Isaacs, J. Sanchez, and J. Romero, Separation of butanol from ABE mixtures by sweep gas pervaporation using a supported gelled ionic liquid membrane: Analysis of transport phenomena and selectivity, Journal of Membrane Science, 444 (2013) 201-212.

[22] H.R. Cascon and S.K. Choudhari, 1-Butanol pervaporation performance and intrinsic stability of phosphonium and ammonium ionic liquid-based supported liquid membranes, Journal of Membrane Science, 429 (2013) 214-224.

[23] P. Izak, W. Ruth, Z. Fei, P.J. Dyson, and U. Kragl, Selective removal of acetone and butan-1-ol from water with supported ionic liquid-polydimethylsiloxane membrane by pervaporation, Chemical Engineering Journal, 139 (2008) 318-321.

[24] P. Izak, K. Friess, V. Hynek, W. Ruth, Z. Fei, J.P. Dyson, and U. Kragl, Separation properties of supported ionic liquid-polydimethylsiloxane membrane in pervaporation process, Desalination, 241 (2009) 182-187.

[25] H. Noureddini, Ethyl tert-butyl ether and methyl tert-butyl ether: status, review, and alternative use. Exploring the environmental issues of mobile, recalcitrant compounds in gasoline, ACS Symposium Series, 799 (2002) 107-124.

[26] E. Weber de Menezes and R. Cataluna, Optimization of the ETBE (ethyl tert-butyl ether) production process, Fuel Processing Technology, 89 (2008) 1148-1152.

[27] K.F. Yee, A.R. Mohamed, and S.H. Tan, A review on the evolution of ethyl tert-butyl ether (ETBE) and its future prospects, Renewable and Sustainable Energy Reviews, 22 (2013) 604-620.

[28] M. Wang, C. Arnal-Herault, C. Rousseau, A.I. Palenzuela, J. Babin, L. David, and A. Jonquieres, Grafting of multi-block copolymers: A new strategy for improving membrane separation performance for ethyl tert-butyl (ETBE) bio-fuel purification by pervaporation, Journal of Membrane Science, 469 (2014) 31-42.

[29] M. Billy, A. Ranzani Da Costa, P. Lochon, R. Clement, M. Dresch, and A. Jonquieres, Cellulose acetate graft copolymers with nano-structured architectures: Application to the purification of bio-fuels by pervaporation, Journal of Membrane Science, 348 (2010) 389-396.

[30] A. Arce, H. Rodriguez, and A. Soto, Use of a green and cheap ionic liquid to purify gasoline octane boosters, Green Chemistry, 9 (2007) 247-253.

[31] A. Jonquieres, C. Arnal-Herault, and J. Babin, Pervaporation, in: E.M.V. Hoek, V.V. Tarabara (Eds.) Encyclopedia of Membrane Science and Technology, Wiley, volume 3 (2013) pp. 1533-1559.

[32] A.B. Pereiro, J.M.M. Araújo, J.M.S.S. Esperança, I.M. Marrucho, and L.P.N. Rebelo, Ionic liquids in separations of azeotropic systems: A review, The Journal of Chemical Thermodynamics, 46 (2012) 2-28.

[33] V.K. Aggarwal, I. Emme, and A. Mereu, Unexpected side reactions of imidazolium-based ionic liquids in the base-catalysed Baylis-Hillman reaction, Chemical Communications, (2002) 1612-1613.

[34] G. Ebner, S. Schiehser, A. Potthast, and T. Rosenau, Side reaction of cellulose with common 1-alkyl-3-methylimidazolium-based ionic liquids, Tetrahedron Letters, 49 (2008) 7322-7324.

[35] S. Michael, E. Gerald, L. Falk, B. Ernst, P. Antje, and R. Thomas, Side Reactions in the System Cellulose/1-Alkyl-3-methyl-imidazolium Ionic Liquid. Cellulose Solvents: For Analysis, Shaping and Chemical Modification, American Chemical Society, 2010, (1033), pp. 149-164.

Chapter 3 Part 2

Grafting of cellulose acetate with ionic liquids for biofuel purification by a membrane process: Influence of the cation.

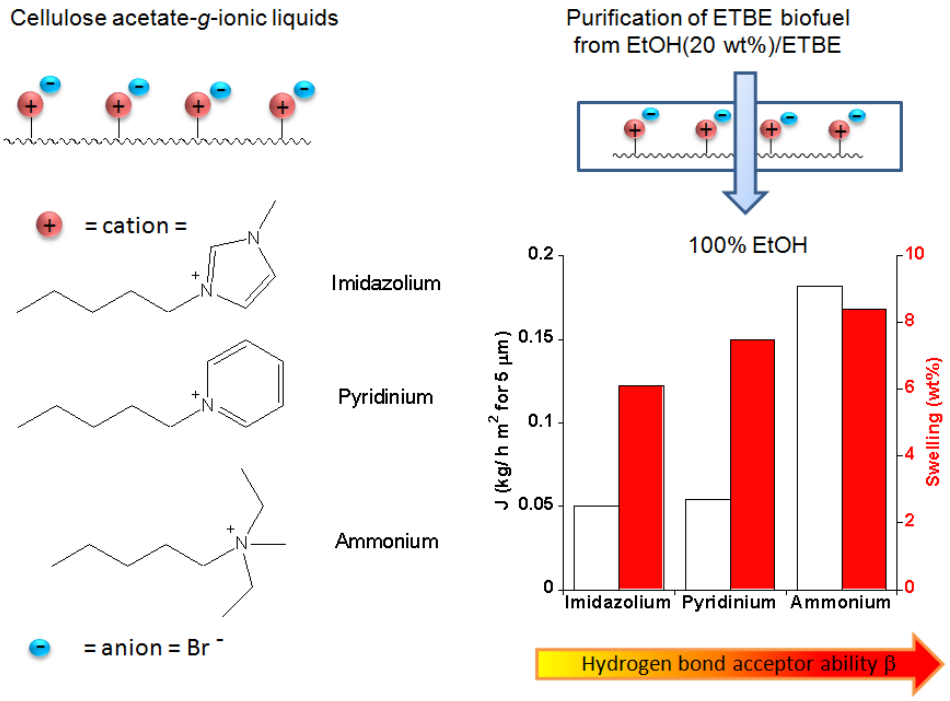

Grafting of cellulose acetate with ionic liquids for biofuel purification by a membrane process: Influence of the cation.

Faten HASSAN HASSAN ABDELLATIF[a)], Jérôme BABIN[a)],
Carole ARNAL-HERAULT[a)], Laurent DAVID[b)], Anne JONQUIERES[a)]*

[a)] *Laboratoire de Chimie Physique Macromoléculaire, LCPM UMR CNRS–Université de Lorraine 7375, ENSIC, 1 rue Grandville, BP 20451, 54 001 Nancy Cedex, France.*

[b)] *Laboratoire IMP@Lyon1, Université Claude Bernard Lyon 1, Université de Lyon, CNRS UMR 5223, 15 Bd. André Latarjet, 69622 Villeurbanne Cedex, France.*

Keywords: polysaccharide modification; ionic liquids; membranes; biofuel; ethyl *tert*-butyl ether; structure-property relationships.

Abstract. During its industrial production, ethyl *tert*-butyl ether (ETBE) biofuel forms an azeotropic mixture containing 20 wt% of ethanol. Compared to the ternary distillation currently used for ETBE purification, the pervaporation membrane process could offer an interesting alternative and important energy savings. Cellulosic membranes have been mainly reported for this application and the selectivity of cellulose acetate was outstanding but its flux was too low. On the other hand, ionic liquid-containing membranes have led to an important breakthrough for gas permeation and, to a much less extent, for the separation of hydro-organic mixtures by pervaporation. This work further extends the scope of ionic liquid-containing membranes to the challenging separation of purely organic mixtures, in which these ionic liquids are soluble. A new strategy has been developed for grafting ionic liquids onto cellulose acetate in order to improve its membrane properties and avoid ionic liquid extraction during ETBE purification. The ionic liquids contained the same bromide anion and different cations (imidazolium, pyridinium and ammonium) with increasing polar feature. The membrane properties were analyzed in terms of structure-property relationships revealing the influence of the ionic liquid content, chemical structure and chemical physical parameters α, β, π* in the Kamlet-Taft polarity scale. The ammonium ionic liquid with the best hydrogen bonding acceptor ability (β) led to the best normalized flux of 0.182 kg/h m^2 for a reference membrane thickness of 5 µm, a permeate ethanol content of 100% corresponding to an outstanding infinite membrane separation factor at 50°C.

---

* Corresponding author. Email address: anne.jonquieres@univ-lorraine.fr, tel: +33 3 83 17 50 29, fax: +33 3 83 37 99 77.

1. Introduction

Membrane separation processes are widely used worldwide for water treatment, gas and liquid separations. Compared to other separation processes such as distillation, adsorption and liquid-liquid extraction, membrane processes offer important energy savings, modularity and lower environmental impact [1-3]. In these separation processes, membrane optimization is essential for industrial success. In addition to being resistant to operating conditions, the membrane material should be both highly permeable and selective. Nevertheless, permeability and selectivity usually vary in opposite ways and the corresponding permeability/selectivity trade-off is a real challenge for membrane designers [1, 2, 4, 5].

In this work, a membrane separation process is considered for the purification of the ethyl *tert*-butyl (ETBE) biofuel, which is one of the major European biofuels. This ether is an oxygenated additive used in gasoline fuels to improve fuel combustion and air quality. Its main industrial synthesis process involves the reaction of isobutene with bio-ethanol and leads to an azeotropic mixture EtOH/ETBE (20/80 wt%), whose current separation by a "ternary" distillation process is highly energy intensive [6-8]. The pervaporation membrane process (PV), alone or in hybrid processes with simple distillation, could offer important energy savings for this separation [7, 9-11].

Nevertheless, ETBE purification by pervaporation is quite challenging and requires *organoselective* membranes capable of extracting ethanol from the targeted azeotropic mixture [6, 7, 11, 12]. The relatively rare PV membranes reported for ETBE purification so far, *i.e.* cellulosic membranes, poly(vinyl pyrrolidone) blends and segmented copolymers, have already been reviewed over the past few years [8, 13, 14]. Cellulosic membranes have been mainly investigated for this separation. In particular, a cellulose acetate (CA) membrane was highly selective with a permeate ethanol content of 100% but the reported flux of 0.08 kg/m^2 h for a reference membrane thickness of 5 µm was too low at 40°C [15]. Cellulosic esters blends enabled to vary the PV fluxes over a broad range 0.6 - 3 kg/m^2 h with permeate ethanol contents in the high range 0.967 - 0.907 at 40°C [16]. Cellulosic semi-interpenetrated networks and graft copolymers with polymethacrylate grafts have also been reported as promising ways for improving cellulosic membrane properties for ETBE purification [13, 15, 17, 18]. In particular, the grafting of cellulose acetate with short polymethacrylate grafts greatly improved membrane flux up to 0.87 kg/m^{2}h while the permeate ethanol content (94%) remained in the very high range at 50°C [13].

In other respects, ionic liquids (ILs) have been recognized as potential environmentally benign alternatives to classical volatile organic solvents due to their thermal stability, non-volatility, negligible vapor pressure and capacity to dissolve a large range of organic compounds [19, 20]. Beyond their use as “green solvents”, ILs have also recently opened new perspectives in the development of materials for energy and industrial separation applications [21-27]. In the latter cases, ILs have been reported for the extraction of interesting bio-products [28, 29], outstanding properties in gas separations [25, 26, 30-33] and, to a much less extent, liquid separation by PV [29, 34-40].

A great advantage of ILs for membrane separations is the variety of combinations for their cation and anion, which allows a good control of their physical chemical properties (Figure 1) [19, 20, 41, 42]. In particular, more or less polar ILs can be obtained depending on their cation and anion structures.

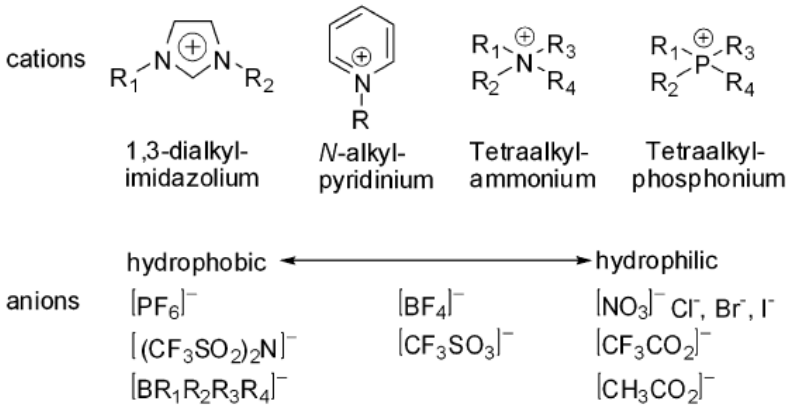

Figure 1: Typical examples for the variety of ionic liquids [41].

Nevertheless, the separation of liquid mixtures by IL containing membranes is particularly challenging and has been reported rarely so far [29, 34-40]. With this respect, the selective recovery of butanol biofuels from aqueous solutions with *organophilic* IL containing membranes has been mostly addressed [29, 34-37, 39, 40, 43]. The separation of other volatile organic compounds (ethanol, isopropyl alcohol, toluene etc.) by IL containing membranes has been reported to a much less extent compared to that of the butanol isomers [29, 44, 45]. In the former references, the introduction of ILs in PV membranes usually led to a significant flux improvement while the membrane selectivity was maintained or slightly reduced. The corresponding membranes were either supported liquid membranes (SLMs) or IL polymer “composites". Recently, the permanent IL immobilization in PDMS

membranes has also been reported for improving membrane stability during butanol recovery [43].

In this work, a new strategy for grafting ILs onto cellulose acetate is proposed for improving its membrane properties for ETBE purification. We have already observed that quaternary ammonium ILs have great affinity for ethanol and are usually soluble in the azeotropic mixture EtOH/ETBE [46]. Recently, an imidazolium IL has also been reported as an interesting extraction solvent for ETBE purification by liquid-liquid extraction and extractive distillation [47]. By offering IL permanent immobilization, the original grafting strategy developed in this work avoided IL extraction in the targeted azeotropic mixture during membrane separation and further extended the scope of ionic liquid-containing membranes to the challenging separation of purely organic mixtures, in which these ionic liquids are soluble.

To the best of our knowledge, the grafting of ionic liquids onto cellulose acetate has not been reported yet and goes beyond the use of ionic liquids as polysaccharide solvents or processing aids. However, copper-catalyzed click chemistry has been reported twice for grafting ionic liquids onto cellulose [48, 49]. Compared to the former grafting by click chemistry, the original strategy developed in this work involved two steps only and avoided handling copper species always difficult to remove from the modified cellulosic materials.

Therefore, the first part of this work reports the grafting of cellulose acetate with ionic liquids containing the same bromide anion and different cations (imidazolium, pyridinium and ammonium) with increasing polar feature. The chemical structure and morphology of the new membrane materials are characterized on the basis of complementary techniques (^{1}H NMR, DSC, SAXS).

The second part focuses on their sorption and PV properties for the separation of the azeotropic mixture EtOH/ETBE. The influence of the IL content and structure on the membrane properties is analyzed on the basis of structure-properties relationships, which reveal the key features of these systems for overcoming the common permeability/selectivity trade-off for ETBE purification.

2. Experimental

2.1. Materials

Cellulose acetate (CA, acetyl 39.7 wt%, M_W = 50,000 g/mol), 6-bromohexanoic acid (97%), 1-methylimidazole (99%), *N,N*-diethylmethylamine (97%), pyridine (99.8%), 4-dimethylaminopyridine (DMAP, ≥ 99%) were purchased from Sigma-Aldrich. ^{1}H NMR

analysis confirmed the acetyl content of cellulose acetate, corresponding to 2.46 of acetyl groups and 0.54 of hydroxyl groups per glycosidic ring. The degrees of substitution (DS) of the side groups were commonly defined as the number of side groups per glycosidic ring. 1-(3-Dimethylaminopropyl)-3-ethylcarbodiimide hydrochloride (EDC.HCl, > 98%) was purchased from TCI Company. All reagents were used as received. All solvents, dichloromethane (DCM, ≥ 99.9 %), tetrahydrofuran (THF, 99.7%), acetonitrile (≥ 99.9%), and dimethylformamide (DMF, ≥ 99.8 %), were dried over molecular sieves before using. In order to prevent contamination by atmospheric moisture, all reagents and solvents were stored under nitrogen atmosphere.

2.2. Synthesis and characterization of cellulose acetate grafted with different ionic liquids

2.2.1. Synthesis of a bromo-cellulose acetate derivative

In three necks round bottom reactor under argon flow, 15 g of cellulose acetate (corresponding to 56.54 mmol of glycosidic rings and 30.53 mmol of hydroxyl groups) were dissolved in 300 mL of dry THF under vigorous stirring at room temperature. 150 mL of dry DCM, 6 g of bromohexanoic acid (30.76 mmol), and 0.373 g of DMAP (3.05 mmol) were added to the reaction mixture. The reaction mixture was cooled at 5°C and 6.44 g of EDC.HCl (33.59 mmol) were added. The resulting mixture was stirred for 48 hours at room temperature. The crude polymer was precipitated in 2 L of ethanol (96%), washed twice in ethanol, filtered and dried under vacuum at 60°C overnight. The polymer was obtained as white solid fibers with a yield of 90% with a DS_{Br} of 0.5 according to ^{1}H NMR analysis.

^{1}H NMR (300 MHz, $CDCl_3$) δ ppm: 5.06-3.54 (m, 7H, H_1, H_2, H_3, H_4, H_5, H_6); 3.44 (m,2H, H_f); 2.38 (m, 2H, H_b); 2.12-1.94 (m, 5H, H_a, H_e); 1.65-1.51 (m, 4H, H_c, H_d)

2.2.2. Reaction of bromo-cellulose acetate with different nucleophiles for cellulose acetate grafting by different ionic liquids

The reaction of bromo-cellulose acetate was carried out with different nucleophiles (*i.e.* 1-methylimidazole, pyridine, *N,N*-diethylmethylamine) to lead to grafted ionic liquids with different cations and the same bromide anion. As way of example, the following procedure describes the reaction of bromo-cellulose acetate (DS_{Br} = 0.5) with one equivalent of methylimidazole. In a Schlenk tube under argon atmosphere, 0.232 g of methylimidazole (2.83 mmol) were added to a solution of 2g of bromo-cellulose acetate (corresponding to 5.65 mmol of glycosidic rings and 2.83 mmol of bromide atoms) in 60 mL of dry acetonitrile. The Schlenk tube was sealed under argon atmosphere and placed at 60°C for 2 days. The

modified cellulose acetate was obtained by precipitation in diethylether, washed twice in diethylether, filtered and dried at 60°C in vacuum oven during one night. All grafted polymers were characterized by ^{1}H NMR (see main text).

2.2.3. Polymer characterization

^{1}H NMR spectra were recorded on a Bruker Avance 300 spectrometer at 300MHz for cellulose acetate and bromo-cellulose acetate from $CDCl_3$ solutions. DMSO-d_6 solvent was used for characterizing the samples of cellulose acetate grafted with different ionic liquids. The chemical shifts were referenced to TMS and were calculated using the residual isotopic impurities of the deuterated solvent. The peak integrations were used to calculate the degree of substitution of the different side groups.

Thermal analysis was performed by standard Differential Scanning Calorimetry (DSC) using a TA Instruments DSC Q2000. Dried polymer samples of ca. 10 mg were used for analysis under a continuous flow of nitrogen. Two cycles of measurements from 20 to 210 °C were performed with heating and cooling rates of 10 °C/min. The thermal transitions corresponding to the first and second heating scans differed significantly and showed the strong influence of thermal history. The data reported in this work corresponded to the glass transition temperatures for the second heating scan for better comparison.

The nano-scale morphology of virgin cellulose acetate and cellulose acetate grafted with different ILs was determined by means of X-ray scattering using polymer membranes with thicknesses of ca. 200 µm, which were obtained in the same way as for sorption experiments. Small angle X-ray scattering (SAXS) experiments were carried out at room temperature, without any additional thermal treatment, using synchrotron radiation at the European Synchrotron Radiation Facility (ESRF) in Grenoble. All the SAXS experiments were performed on the BM2-D2AM beamline at an incident energy of 16 keV. A 2D X-ray camera was used (Roper Scientific), and the data were corrected from the dark image, normalization with flat field and tapper camera distortion. Finally, radial average around the incident beam center were calculated. Silver Behenate was used for the channel-*q* calibration. The background (empty cell) was subtracted in the radial average profiles, after the measurement of the attenuation coefficients.

2.3. Membrane preparation for pervaporation and sorption experiments

The different polymer materials were dissolved in DMF (pure for synthesis) to obtain a polymer concentration of 3.5 % w/v. The solutions were then cast on a PTFE mold. They were carefully removed from the mold after DMF evaporation at 45°C. The pervaporation

membrane thicknesses ranged from 85 to 100 µm and the difference in thickness between two membrane points did not exceed 10 µm.

The procedure for sorption membrane casting was similar as that for pervaporation membranes except for polymer concentration, which was increased to 5% w/v in order to obtain membrane thicknesses of ca. 200 µm. The sorption membranes were then carefully dried at 60°C for 24 hours before sorption experiments.

2.4. Sorption experiments

For sorption experiments, the dried polymer membranes were weighted and then immersed in the azeotropic mixture EtOH/ETBE (20/80 wt%) in hermetically closed bottles. These bottles were kept at 30°C in a thermostated oven. This sorption temperature was chosen for experimental reason. After one week, the membranes were taken out the bottles and quickly wiped with paper tissue and weighted in a closed tare bottle. The membranes were regularly weighted until they reached constant swelling weight. At the end of each sorption experiment, the membranes were dried under vacuum and weighted again. The results obtained with the different sorption membranes showed that no polymer dissolution had occurred during the sorption experiments. The total swelling, S (wt%), was calculated from equation (1) :

$$S = \frac{w_S - w_D}{w_D} \times 100 \qquad (1)$$

where wS and wD were the membrane weights after and before sorption experiment. The average experimental error for the total swelling S was ± 0.2 wt%.

For determining the composition of the absorbed mixture, the swollen membranes at equilibrium were soaked for 1 night at ambient temperature into 10 mL of diethyl ether, which is a non solvent for the membrane polymers and a good solvent for both ethanol and ETBE. The desorption solution was then analyzed by gas chromatography using a Shimadzu GC-8A chromatograph with a Porapak Q column, a thermal conductivity detector and hydrogen as carrier gas. The ethanol weight fraction Cs in the desorbed mixture was calculated from the area of the EtOH and ETBE peaks on the basis of a former calibration. The average experimental error for the ethanol weight fraction CSEtOH was ± 0.005.

Sorption separation factor were then calculated from equation (2) where CSEtOH and C are the ethanol weight fractions in the sorption mixture and the azeotropic mixture EtOH/ETBE, respectively. The symbol for the sorption separation factor was that recently proposed by Baker et al. [50].

$$\beta_S = \frac{C^S_{EtOH}}{1 - C^S_{EtOH}} / \frac{C}{1 - C} \quad (2)$$

2.5. Pervaporation experiments

Pervaporation experiments were performed for the azeotropic mixture EtOH/ETBE at 50°C using a pervaporation set-up described elsewhere [13]. The downstream pressure of the PV cell was maintained at less than 0.04 kPa using a vacuum pump. The permeate was collected continuously after condensation by liquid nitrogen using two parallel traps. The permeate flux was calculated using equation (3) :

$$Permeate\ \ flux = \frac{w_p}{\Delta t \times A} \quad (3)$$

where w_p is the permeate sample weight collected during a permeation time Δt and A is the active membrane area.

To do a comparison between different membranes with close but non-equal thicknesses, normalized fluxes, J, are reported for a reference membrane thickness of 5 µm (equation (4)). This reference thickness was chosen because it is easily reached for dense polymer layers on top of asymmetric membranes.

$$J = \frac{Membrane\ thickness}{5} Permeate\ \ flux \quad (4)$$

The permeate ethanol weight fraction, C', was determined by gas chromatography in the same conditions as for sorption experiments. The pervaporation separation factor, β_{PV} , was calculated by analogy with the sorption separation factor according to equation (5). The experimental errors were less than 5% for the total fluxes and ± 0.005 for the ethanol weight fractions.

$$\beta_{PV} = \frac{C'_{EtOH}}{1 - C'_{EtOH}} / \frac{C}{1 - C} \quad (5)$$

The fairly complex procedure for permeability calculation in pervaporation and the corresponding data are presented in Appendix A.

3. Results and discussion

3.1. Synthesis and characterization of cellulose acetate grafted with different ionic liquids

3.1.1. Synthesis of cellulose acetate grafted with different ionic liquids

The different membrane materials (cellulose acetate-*g*-ionic liquids) were obtained by a two-step synthetic strategy. In the first step, bromide side groups were introduced onto cellulose acetate to act as ionic liquid precursors in the second step (Figure 1). Therefore, the hydroxyl side groups of cellulose acetate (DS_{OH}= 0.54) were first reacted with one equivalent of 6-bromo hexanoic acid in presence of the EDC coupling agent and DMAP catalyst by adapting an esterification method reported by Neises and Steglich [51] (Figure 2).

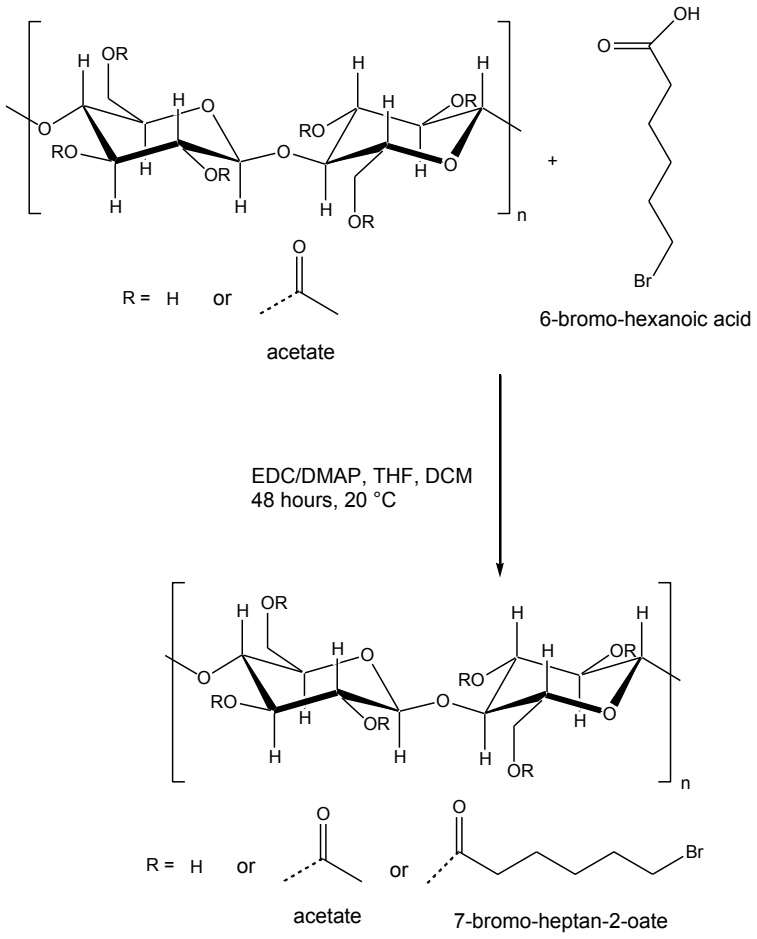

Figure 2: Synthesis of the bromo-cellulose acetate derivative.

^{1}H NMR analysis of the bromo-cellulose acetate derivative was carried out in $CDCl_3$ for good spectral resolution (Appendix B) and showed a substitution rate of 92% for the hydroxyl groups. This substitution rate was typical for high hydroxyl modification in polysaccharide

chemistry [52] and corresponded to a degree of substitution for the bromide side atoms DS_{Br} of 0.5.

In the second step, a solution of the bromo-cellulose acetate was reacted with one of the following nucleophiles : 1-methylimidazole, pyridine, *N,N*-diethylmethylamine (Figure 3). By nucleophilic substitution of the bromide atoms, cellulose acetate was simply grafted with three ionic liquids with different cations (*i.e.* imidazolium, pyridinium, ammonium) and the same bromide anion.

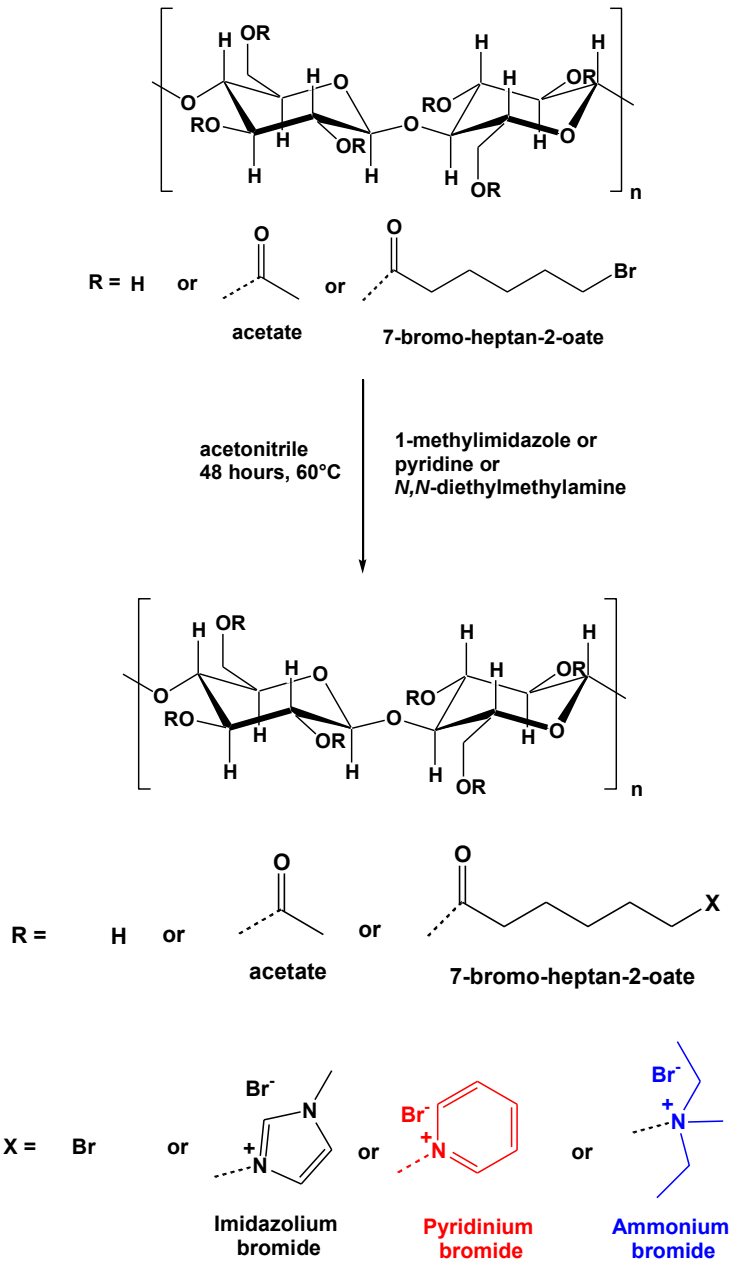

Figure 3: Grafting of cellulose acetate with ionic liquids containing different cations and the same anion [Br^-].

3.1.2. Characterization of cellulose acetate grafted with different ionic liquids

The cellulosic membrane materials with different grafted ionic liquids were characterized by ^{1}H NMR to confirm their chemical structures and to estimate their ionic liquid grafting rates quantitatively (Figure 4). All spectra were recorded in DMSO-d_6 at 300 K except for cellulose acetate grafted with the ammonium bromide ionic liquid. In the latter case, the temperature for ^{1}H NMR analysis had to be increased to 353 K to strongly improve spectral resolution and the grafting rate calculations. After nucleophilic substitution of the bromide atoms, all the spectra showed new peaks, which were characteristic for the different grafted ionic liquids. The integrations of these characteristic peaks enabled to calculate the grafting rate of each ionic liquid as a function of the molar ratio $n_{Nucleophile}/n_{Br}$ in the reaction medium (Figure 5).

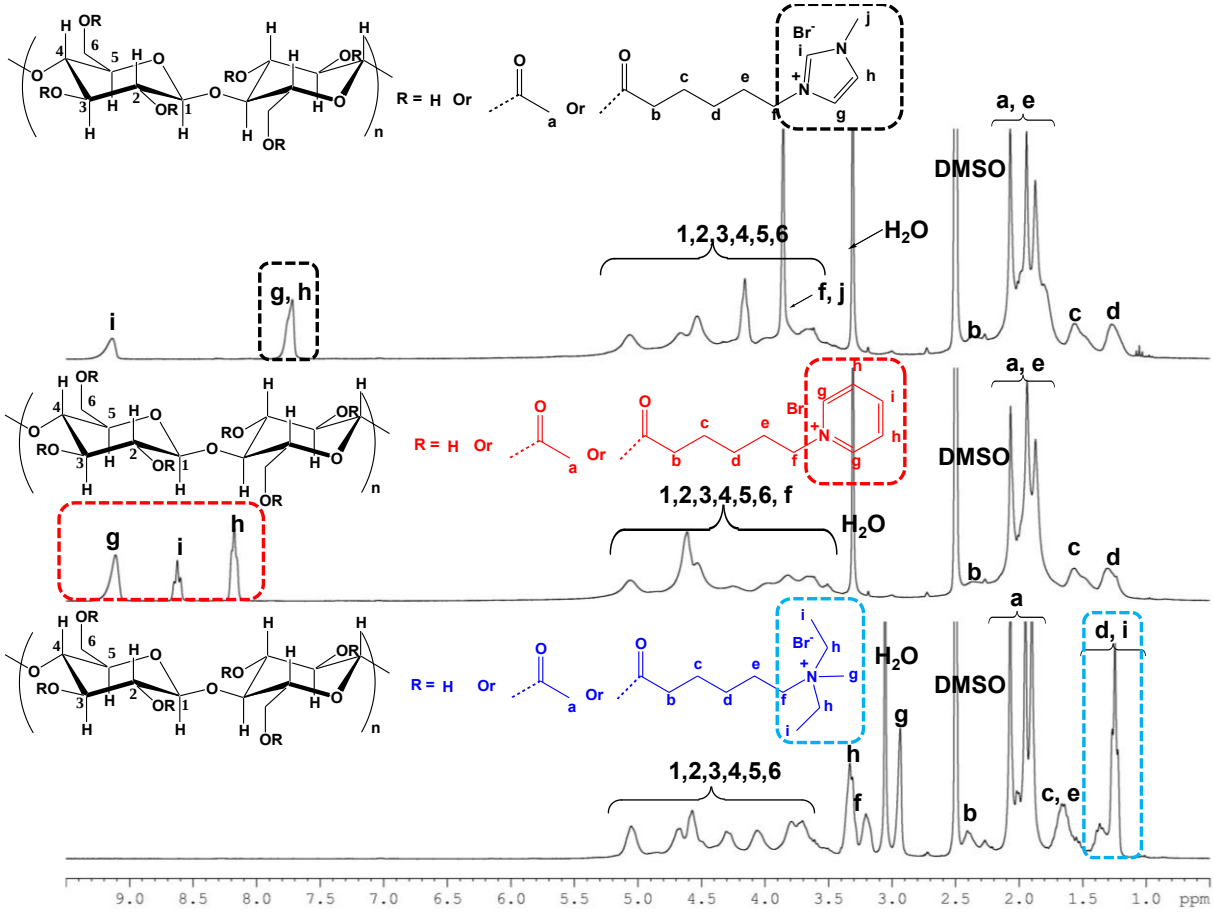

Figure 4: ^{1}H NMR characterization of cellulose acetate with grafted ionic liquids with different cations and the same anion [Br^-] in DMSO-d_6.

Figure 5 shows that the grafting rate of each ionic liquid was varied over a very broad range by increasing the nucleophile amount in the reaction medium. The grafting rate was easily controlled for *N,N*-diethylmethylamine, which reacted almost quantitatively over the whole composition range up to a maximum of 87% corresponding to a high grafting rate for polysaccharide modification. Nevertheless, the reactivity of 1-methylimidazole and pyridine was much lower than that of *N,N*-diethylmethylamine and pyridine was even slightly less reactive than 1-methylimidazole in the acetonitrile solvent. Mc Clelland *et al.* also reported the same type of variation for the related reactivity of pyridine and 1-methylimidazole with an organometallic cation in acetonitrile [53]. The reactivity of the different amines used in our work increased with their nucleophilic character in the following order : pyridine < 1-methylimidazole << *N,N*-diethylmethylamine [54]. Consequently, very large excesses (8 to 10 equivalents) of pyridine and 1-methylimidazole were required to achieve high grafting rates for the corresponding ionic liquids. Even so, the highest grafting rates of 83% and 77% for the imidazolium and pyridinium ionic liquids, respectively, remained lower than that obtained for the ammonium ionic liquid (87%).

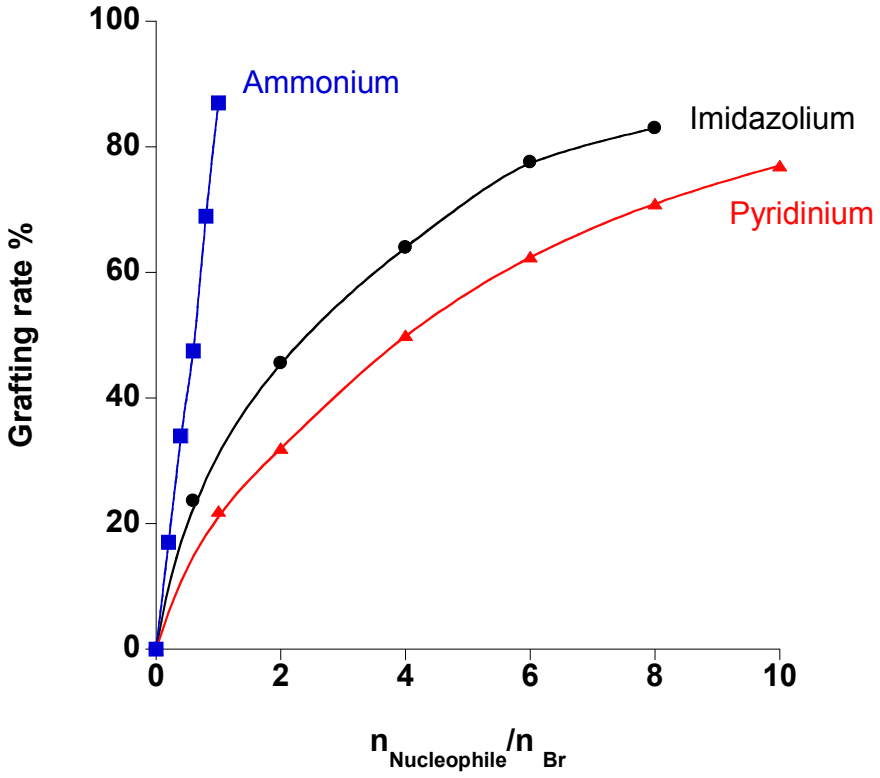

Figure 5: Grafting rate obtained for the different ionic liquids as a function of the molar ratio $n_{nucleophile}/n_{Br}$.

Complementary DSC and synchrotron SAXS measurements were then carried out on the new membranes to assess the ionic liquid influence on membrane glass transition temperature (T_g), crystallinity and morphology. This characterization was made for membranes made from virgin cellulose acetate and cellulose acetate grafted with very close ionic liquid amounts ($W_{IL} \cong 17\%$) corresponding to the highest grafting rates for the three series of membranes with imidazolium, pyridinium and ammonium cations.

All the thermograms of the dry membranes revealed a single glass transition temperature and no endothermic melting peaks. Figure 6 shows the glass transition temperature of the grafted cellulose acetate membranes in comparison with that of the virgin cellulose acetate membrane. The grafting of cellulose acetate by the different ionic liquids induced a systematic T_g decrease, which strongly depended on the ionic liquid cation. The strongest T_g decrease corresponded to the best plasticizing effect. Therefore, membrane plasticizing in the *dry* state increased in the following order of the ionic liquid cations : ammonium ($\triangle T_g = -25°C$) < pyridinium ($\triangle T_g = -42°C$) < imidazolium ($\triangle T_g = -63°C$).

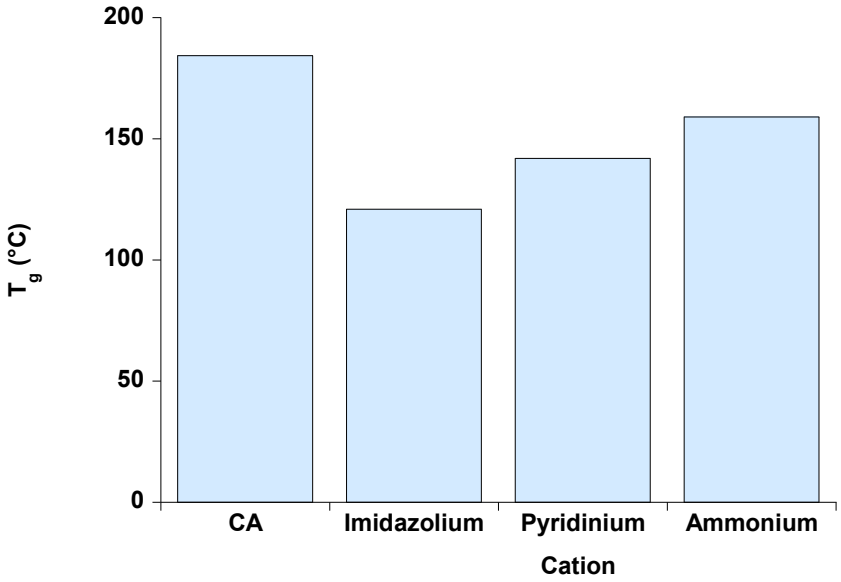

Figure 6: Influence of the ionic liquid cation on the membrane glass transition temperature for very close ionic liquid amounts ($W_{IL} \cong 17\%$) corresponding to the maximum grafting rates.

The plasticizing effect of the grafted ionic liquids increased when the ionic liquid melting temperature (T_m) decreased as shown by the melting data of the corresponding molecular ionic liquids : *N*,*N*,*N*-diethylmethylpentyl ammonium bromide (T_m = 142°C) < 1-

pentylpyridinium bromide ($T_m \cong 66°C$, estimated from a correlation reported by Iken *et al.* for closely related 1-alkylpyridinium bromides [55]) < 1-pentyl-3-methylimidazolium bromide (T_m < 20°C, liquid at room temperature [56]). Therefore, the plasticizing effect on the *dry* membranes increased with the mobility of the related molecular ionic liquids, which was well reflected by the inverse variation of their melting temperature.

The short scale morphology of virgin cellulose acetate and cellulose acetate grafted with the different ionic liquids was then assessed by synchrotron SAXS experiments. One of the underlying questions was related to the dispersion state of the grafted ionic liquids in the membrane materials. Were the grafted ionic liquids finely dispersed or aggregated into nano-structures, which would have a very strong impact on the separation properties as shown by our former work on other grafted cellulose acetate membranes [13] ?

Figure 7 shows that the greatest intensity variation was obtained for virgin cellulose acetate with a 100-fold intensity decrease as a function of the scattering vector *q* over a range of several decades from 8 10^{-3} $Å^{-1}$ to 0.2 $Å^{-1}$. The corresponding weak and complex scattering pattern could not be analyzed through standard procedures used for assessing characteristic scales. Nevertheless, the obtained results showed that the electron density fluctuations inducing SAXS in the virgin cellulose acetate membrane were large with characteristic sizes larger than 50 nm. The complexity of the structural organization of cellulose acetate solutions is well recognized through several studies of intermolecular aggregation in different solvents [57-59]. Light scattering measurements and size exclusion chromatography evidenced microgels rich in cellulose triacetate blocks (partly crystalline microregions) [59]. Such heterogeneities were likely to develop as concentration increased during membrane formation and subsisted in the final membrane morphology [57]. The grafting of cellulose acetate with ionic liquids containing different cations induced a strong reduction in the scattered intensity with similar intensity profiles. The plasticizing effect of the grafted ionic liquids on the dry membranes was most likely responsible for the strong decrease in the electronic density fluctuations, which was characteristic for homogeneous polymer materials. Furthermore, the absence of any diffraction peak for the grafted ionic liquids showed that they were finely dispersed in the polymer membranes irrespective of their cation structure.

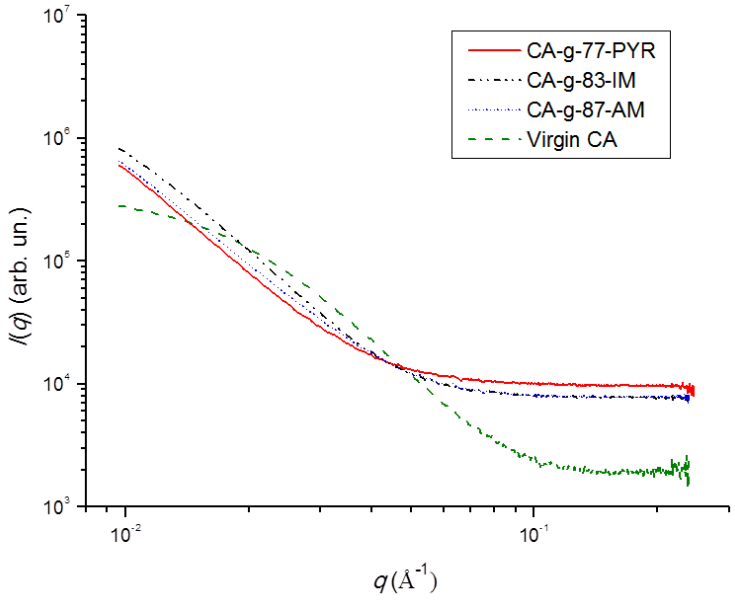

Figure 7: Synchrotron small angle X-ray scattering (SAXS) of virgin cellulose acetate, and cellulose acetate grafted with very close amounts ($W_{IL} \cong 17\%$) of the different ionic liquids corresponding to the maximum grafting rates.

3.2. Membrane properties for ETBE biofuel purification by pervaporation

In the pervaporation membrane process, the separation of a liquid mixture involves three successive steps according to the sorption-diffusion model [60]. The first step corresponds to some liquid sorption at the membrane upstream side. This step is usually selective and already contributes to pervaporation selectivity. The second step corresponds to the diffusion of the absorbed molecules through the pervaporation membrane, whose downstream side is kept under vacuum to ensure the driving force for mass transfer. The third step is the molecules desorption at the membrane downstream side. The latter step is usually considered very rapid and non limiting for mass transfer. Therefore, the membrane properties are generally governed by the sorption and diffusion steps only. In this part, the sorption and pervaporation properties of the cellulose acetate-*g*-ionic liquid membranes are analyzed in terms of structure-property relationships to reveal the influence of the ionic liquid content and cation on the membrane performances for ETBE purification.

3.2.1. Sorption properties of cellulose acetate grafted with different ionic liquids

3.2.1.1. Influence of the ionic liquid content on sorption properties

Sorption experiments were carried out with the azeotropic mixture EtOH/ETBE (20/80 wt %) at 30°C for experimental reasons. The whole series of cellulosic membranes with

increasing grafting rates of imidazolium and ammonium ionic liquids were first investigated. For the pyridinium ionic liquid, only the membrane with the highest grafting rate was investigated due to the low flux values obtained with this membrane serie.

For comparison, Table 1 first reports the sorption results obtained for virgin cellulose acetate and cellulose acetate with increasing contents of grafted *imidazolium* ionic liquid. Virgin cellulose acetate led to fairly low total swelling S (4.2 wt%) and very high sorption separation factor (129) due to the stiffness of the polymer chains and the presence of hydroxyl side groups having very high affinity with ethanol. The cellulosic membranes with increasing grafted imidazolium contents from 0 wt% to 16.4 wt% showed a weak swelling increase (+45%) from 4.2 wt% to 6.1 wt%, still corresponding to low swelling similar as that of virgin cellulose acetate. However, in the same conditions, the sorption separation factor β_S of the grafted cellulose acetate membranes increased very strongly from 53 to 396 and even exceeded that of virgin cellulose acetate (129) for imidazolium grafting rates of at least 50%. Therefore, all the cellulosic membranes with grafted imidazolium ionic liquid were highly selective towards ethanol during the sorption step with ethanol content in the absorbed mixture increasing from 93 wt% up to 99 wt% for the membrane with the highest ionic liquid grafting rate.

Table 1 Influence of the imidazolium ionic liquid content in the grafted cellulose acetate membranes on the sorption and PV properties for the separation of the azeotropic EtOH/ETBE mixtures. *CA-g-X-IM corresponds to cellulose acetate with a grafting rate of X for the imidazolium ionic liquid.*

Membrane	**W_{IL} (wt.%)**	**S (wt.%)**	**C^S_{EtOH} (wt.%)**	**β_s**	**J (kg/hm^2 for 5 µm)**	**C' (wt%)**	**β_{PV}**	**β_D**
Cellulose acetate	0	4.2	0.97	129	0.023	100	∞	-
CA-*g*-23.6-IM	5	4.9	0.93	53	0.053	99.8	1996	37.7
CA-*g*-45.6-IM	9.4	5.5	0.97	129	0.050	100	∞	-
CA-*g*-64-IM	12.9	5.8	0.98	196	0.043	100	∞	-
CA-*g*-83-IM	16.4	6.1	0.99	396	0.050	100	∞	-

W_{IL}: ionic liquid weight fraction in the grafted cellulose acetate; S: total swelling at sorption equilibrium; C^s_{EtOH}: ethanol content in the absorbed mixture; β_s: sorption separation factor; J: total flux normalized for a reference membrane thickness of 5 µm; C': ethanol content in permeate ; β_{pv}: pervaporation separation factor.

For the second series of cellulosic membranes with increasing contents of grafted *ammonium* ionic liquid from 0 to 17.7 wt% (Table 2), the sorption properties followed the same general trends as those found with the grafted imidazolium ionic liquid but the increase in total swelling S was 4-fold stronger. Nevertheless, the membranes with the grafted ammonium ionic liquid were slightly less selective with sorption separation factors β_S increasing from 29 to 156, which still corresponded to very high ethanol contents (≥95%) in the absorbed mixture for the highest ionic liquid contents.

Table 2 Influence of the ammonium ionic liquid content in the grafted cellulose acetate membranes on the sorption and PV properties for the separation of the azeotropic EtOH/ETBE mixtures. *CA-g-X-AM corresponds to cellulose acetate with a grafting rate of X for the ammonium ionic liquid.*

Membrane	W_{IL} (wt.%)	S (wt.%)	C^S_{EtOH} (wt.%)	β_s	J(kg/hm^2 for 5 µm)	C' (wt%)	β_{PV}	β_D
Cellulose acetate	0	4.2	97	129	0.023	100	∞	-
CA-*g*-17-AM	3.8	5.4	88	29	0.069	99		
CA-*g*-34.7-AM	7	6.5	92	40	0.104	100	∞	-
CA-*g*-47.5-AM	10	7.2	95	76	0.166	99.8	1996	21
CA-*g*-60-AM	12.4	7.6	97	129	0.171	100	∞	-
CA-*g*-87-AM	17.7	8.4	98	156	0.182	100	∞	-

W_{IL}: ionic liquid weight fraction in the grafted cellulose acetate; S: total swelling at sorption equilibrium; C^S_{EtOH}: ethanol content in the absorbed mixture; β_s: sorption separation factor; J: total flux normalized for a reference membrane thickness of 5 µm; C': ethanol content in permeate ; β_{pv}: pervaporation separation factor.

3.2.1.2. Influence of the ionic liquid cation on sorption properties

The results reported in Table 3 showed the influence of the ionic liquid cation on the sorption properties for cellulose acetate grafted with very close ionic liquid amounts ($W_{IL} \cong$ 17%) corresponding to the highest grafting rates for the three series of membranes with imidazolium, pyridinium and ammonium cations.

By increasing the polar character from the imidazolium to the ammonium cation, the total swelling S increased from 6.1 wt% to 8.4 wt% (+38%) while the ethanol content in the

absorbed mixture slightly decreased from 99 wt% to 97.5 wt%. The higher membrane swelling induced by the ammonium ionic liquid increased membrane plasticizing in the *swollen* state and facilitated simultaneous ETBE sorption. The corresponding sorption synergy resulted in a slight decrease in the ethanol content of the liquid mixture absorbed by this membrane during the sorption step. For this composition range, the results reported in Table 3 showed that the sorption separation factor β_S was very sensitive to any change in composition of the absorbed mixture and strongly decreased from 396 to 156 for imidazolium and ammonium cations, respectively.

Table 3 Influence of the ionic liquid cation (*i.e.* imidazolium IM, pyridinium PYR and ammonium AM) on the sorption and PV properties of the grafted cellulose acetate membranes with the highest grafting rates

Membrane	W_{IL} (wt.%)	S (wt.%)	C^S_{EtOH} (wt.%)	β_s	J (kg/hm^2 for 5 µm)	C' (wt%)	β_{PV}	β_D
Cellulose acetate	0	4.5	97		0.023	100	∞	-
CA-g-83-IM	16.4	6.1	99	396	0.05	100	∞	-
CA-g-77-PYR	16.6	7.5	98.5	262	0.054	100	∞	-
CA-g-87-AM	17.7	8.4	97.5	156	0.1815	100	∞	-

W_{IL}: ionic liquid weight fraction in the grafted cellulose acetate; S: total swelling at sorption equilibrium; C^s_{EtOH}: ethanol content in the absorbed mixture; β_s: sorption separation factor; J: total flux normalized for a reference membrane thickness of 5 µm; C': ethanol content in permeate ; β_{pv}: pervaporation separation factor.

3.2.2. Pervaporation properties of cellulose acetate grafted with different ionic liquids

3.2.2.1. Influence of the ionic liquid content on pervaporation properties

The temperature chosen for the pervaporation experiments was 50°C instead of 30°C formerly used for the sorption measurements. This change in temperature had a negligible influence on sorption properties due to the fact that the ethanol and ETBE activity coefficients were almost constant between 30°C and 50°C as confirmed by the corresponding thermodynamic NRTL calculations [13]. Nevertheless, a temperature of 50°C can easily be reached in industrial pervaporation modules and the membrane fluxes of the new

membranes were also strongly improved at 50°C, which also facilitated a comparison between the different membranes.

Table 1 reports the pervaporation results for the separation of the azeotropic mixture EtOH/ETBE with virgin cellulose acetate and cellulose acetate with increasing contents of grafted *imidazolium* ionic liquid.

The pervaporation properties of virgin cellulose acetate were consistent with the data formerly reported by Nguyen *et al.* for this separation (J = 0.08 kg/m²/h and C' = 100 wt% at 40°C) [15] although the pervaporation flux obtained in this work (J = 0.023 kg/m²/h) was slightly inferior despite the higher temperature (50 °C). This slightly lower flux may be due to the much higher average molecular weight of the cellulose acetate investigated in this work (50,000 g/mol) compared to that reported in the former work (29,000 g/mol). Differences in membrane casting procedures may also have slightly affected the membrane flux of this glassy polymer. In this work also, the permeate contained ethanol only (C' = 100 wt%) in good agreement with the former results reported by Nguyen *et al.* for virgin cellulose acetate [15].

The results reported in Entry 6 of Table 1 showed that the cellulose acetate flux was increased nearly 2-fold by grafting 5 wt% of imidazolium ionic liquid. However, by further increasing the grafted imidazolium content up to the maximum grafting rate of 16.4 wt%, the normalized pervaporation flux did not change significantly and remained low for the targeted application (*ca.* 0.05 kg/m^2 h). Surprisingly, the imidazolium content did not seem to have any influence on membrane permeability during this separation (Figure 8). The reason for this very particular behavior is not well understood. Furthermore, the permeate samples contained at least 99.8 wt% of ethanol and, for most membranes, ETBE could not be detected by GC analysis. All of these membranes were thus extremely selective to ethanol and the corresponding separation factors β_{PV} usually tended to infinity.

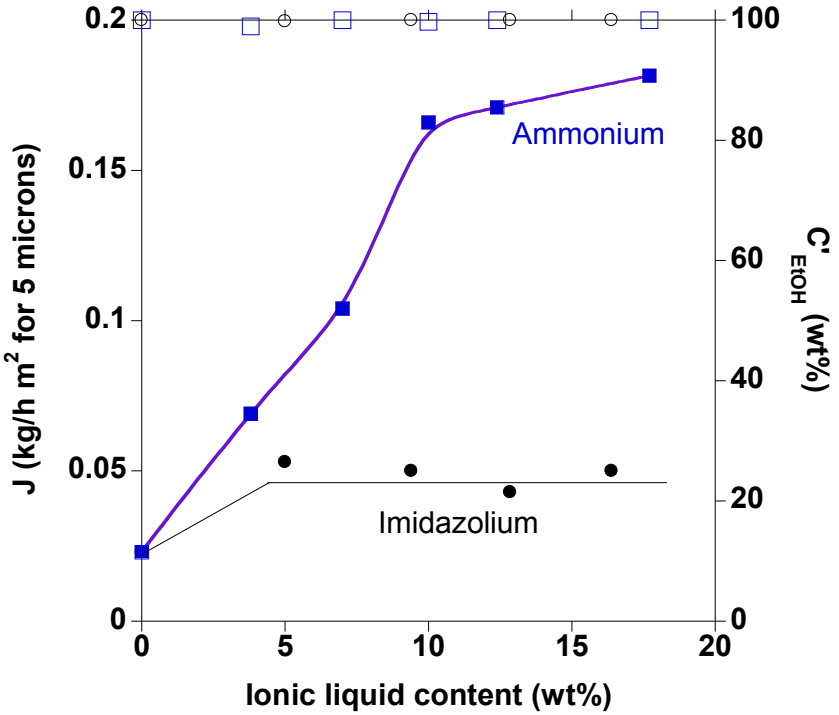

Figure 8: Influence of the ionic liquid content in the grafted cellulose acetate membranes on the PV properties for the separation of the azeotropic mixture EtOH (20 wt%)/ETBE at 50°C: Y1 axis : Total flux J for imidazolium (●) and ammonium (■) ionic liquids; Y2 axis: Ethanol permeate content C'_{EtOH} for imidazolium (○) and ammonium (□) ionic liquids.

Cellulose acetate grafting with increasing amounts of the *ammonium* ionic liquid led to even better pervaporation results for ETBE purification (Table 2). Figure 8 shows that the pervaporation flux increased up to a factor 8 with ammonium content varying in the range of 0 to 17.7 wt%. This flux increase was very strong for the low ammonium contents and tended to level off above 10 wt% of ionic liquid. All of these membranes were also extremely selective with permeate samples containing at least 99 wt% of ethanol.

3.2.2.2. Influence of the ionic liquid cation on the pervaporation properties

The results reported in Table 3 showed the influence of the different ionic liquid cations on the membrane flux by comparison with their swelling for cellulose acetate grafted with very close ionic liquid amounts ($W_{IL} \cong 17\%$) corresponding to the highest grafting rates.

The maximum grafting of cellulose acetate with imidazolium and pyridinium ionic liquids almost doubled the pervaporation flux while the total swelling was only slightly increased in these conditions. Nevertheless, the flux remained low for the targeted application. Therefore, the whole series based on the pyridinium ionic liquid was not further investigated in this work.

The improvement in membrane properties was much higher with the ammonium ionic liquid with a 8-fold flux increase. By far, the ammonium ionic liquid led to the best normalized pervaporation flux (0.182 kg/h m^2) partially due to the best membrane swelling obtained with this ionic liquid, which doubled in these conditions. Nevertheless, for the ammonium ionic liquid, the improvement in flux was almost 4-fold stronger than that of swelling. This difference showed the key role played by the diffusion step in the pervaporation mass transfer. The highest membrane swelling obtained with this particular ionic liquid induced the strongest plasticizing effect on the *swollen* membranes during pervaporation. In these conditions, the diffusion of ethanol molecules was strongly improved and highly contributed to the pervaporation flux.

Furthermore, all of the membranes with maximum contents in different ionic liquids were extremely selective to ethanol and ETBE was not detected in the corresponding permeate samples. Therefore, the maximum grafting of cellulose acetate with different bromide ionic liquids led to outstanding infinite separation factors for ETBE purification by pervaporation.

3.2.3. Chemical physical analysis of the membrane properties based on ionic liquid polarity parameters

To get a better understanding of the membrane properties for ETBE purification, a chemical physical analysis was then made on the basis of Kamlet and Taft polarity parameters. These parameters accounted for the ionic liquid chemical physical features in terms of hydrogen bonding donor ability (α), hydrogen bonding acceptor ability (β) and polarizability (π*) [61]. The Kamlet-Taft parameters are known to depend upon the solvatochromic probes used for their determination [62]. In this work, attention has been paid to consider only Kamlet-Taft parameters determined with the same set of probes (*N,N*-diethyl-4-nitroaniline/4-nitroaniline) to allow a proper comparison of the different ionic liquids. Nevertheless, the polarity parameters of the ionic liquids of interest have not been reported yet and their measurement at a common temperature would be very difficult owing to the very high melting temperature of the corresponding ammonium bromide (T_m = 142°C). For this reason, the Kamlet-Taft polarity parameters of closely related ionic liquids [62-64] have been considered in this work to assess the influence of the ionic liquid cation in a *homologous* series and rank the different ionic liquids of interest in the Kamlet and Taft polarity scale accordingly (Figure 9).

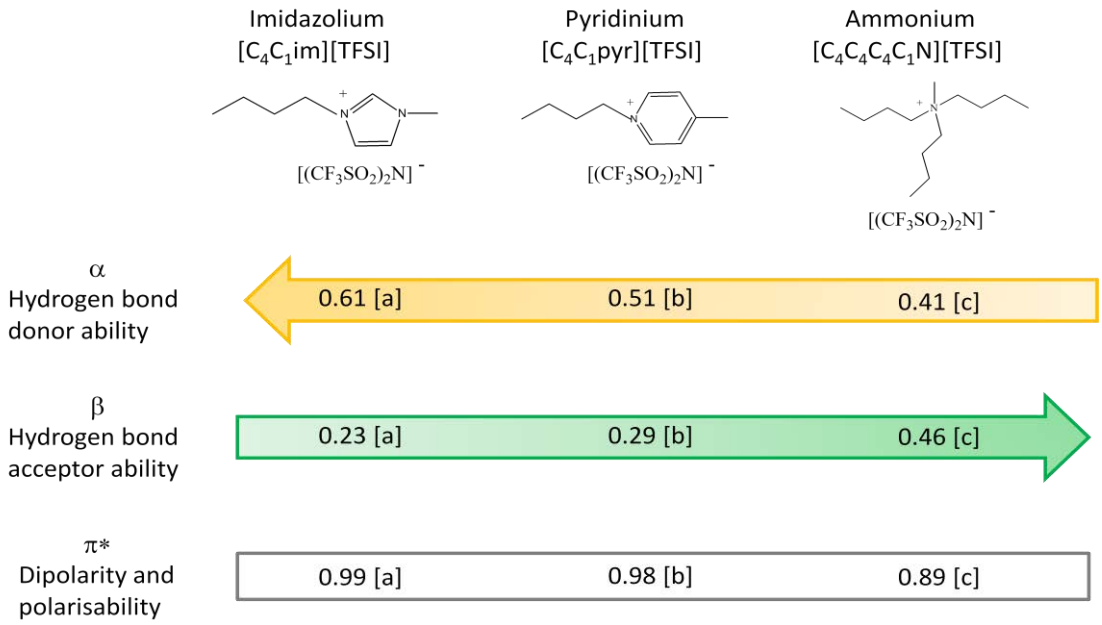

Figure 9: Kamlet-Taft chemical physical parameters of related ionic liquids used for the structure-property relationship analysis of the membrane properties according to [a] [62], [b] [63] and [c] [64].

As shown in Figure 9, the related ionic liquids contained the same bis(trifluoromethanesulfone)imide (Tf_2N^-) anion and the different cations of interest. The Tf2N$^-$ anion was responsible for their much lower melting temperatures compared to those obtained with the bromide anion, which corresponded to a pre-requisite for determining the Kamlet-Taft parameters. As expected for this type of compounds, the parameters α and β reflecting the hydrogen bonding acceptor and donor ability, respectively, varied in opposite ways. Therefore, the hydrogen bonding acceptor ability β increased in the following cation order : imidazolium < pyridinium < ammonium. The π* polarisability parameters of the imidazolium and pyridinium ionic liquids were very close while that of ammonium ionic liquid was significantly decreased.

Figure 10 makes a comparison of the sorption and pervaporation properties for cellulose acetate grafted with ionic liquids containing imidazolium, pyridinium and ammonium cations, which were ranked in the order of increasing hydrogen bonding acceptor ability β. It shows that membrane sorption strongly increased with the hydrogen bonding ability β of the grafted ionic liquid. A better hydrogen acceptor ability most likely favored strong interactions with ethanol, which is a strong hydrogen bonding donor (α = 0.83 [61]). Therefore, the ionic liquid with the ammonium cation led to the highest membrane swelling, resulting in the strongest membrane plasticization and sorption synergy. Finally, the pervaporation flux was

also strongly improved by increasing the hydrogen bonding ability of the grafted ionic liquid. This improvement resulted from the combination of a better membrane swelling/plasticization with an easier ethanol diffusion.

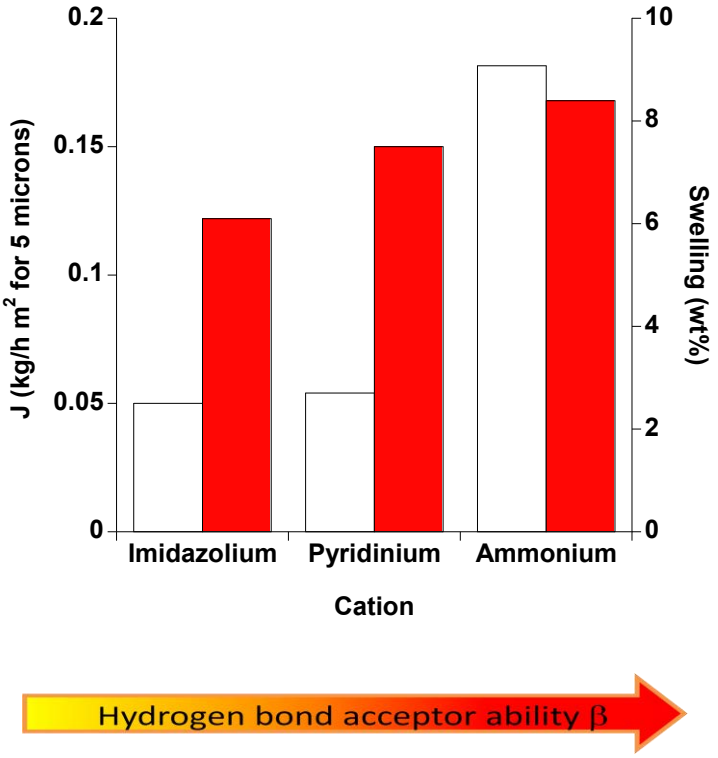

Figure 10: Chemical physical analysis of the membrane properties based on the Kamlet-Taft parameter β characteristic for hydrogen acceptor ability. Influence of the ionic liquid cation on the normalized total flux J (kg/h m^2) (white bars) and total swelling (wt%) (dark bars) for the separation of the azeotropic mixture EtOH(20 wt%)/ETBE.

4. Conclusion

A simple method was developed for grafting cellulose acetate with ionic liquids containing the same bromide anion and different cations. The new grafting strategy enabled to vary the ionic liquid structure and content over a wide composition range in the membrane materials. The covalent grafting avoided the extraction of the ionic liquids in the azeotropic mixture EtOH/ETBE and led to stable membrane properties during ETBE purification by pervaporation.

The ammonium ionic liquid with the best hydrogen bonding acceptor ability combined the best membrane swelling with the strongest plasticizing effect for the swollen membranes during pervaporation. These particular features resulted in the best membrane properties

with a normalized flux of 0.182 kg/h m^2 for reference membrane thickness of 5 µm and a permeate ethanol content of 100% corresponding to an infinite membrane separation factor at 50°C.

Last but not least, this work further extended the scope of ionic liquid-containing membranes to the challenging separation of purely organic liquid mixtures, in which these ionic liquids were soluble. This first work revealed the strong influence of the ionic liquid cation on the membrane properties for ETBE purification. In the future, it will be interesting to assess the influence of the counter anions, which will offer new opportunities to further improve the membrane properties. More generally, the strategy of ionic liquid grafting onto polysaccharides could be applied to other types of polymer membranes and greatly expand the scope of ion-containing membranes to other challenging separations.

5. Acknowledgements

The authors would like to thank the ELEMENT Erasmus Mundus Programme for the PhD scholarship and the corresponding extension offered to Mrs Faten HASSAN HASSAN ABDELLATIF.

6. References

[1] R.W. Baker, Membrane technology and applications, 2nd ed, John Wiley & Sons, Chichester, 2004.

[2] E. Drioli and L. Giorno, eds. *Comprehensive Membrane Science and Engineering*. 2010, Elsevier Science: Kidlington (UK).

[3] E.M.V. Hoek and V.V. Tarabara, eds. *Encyclopedia of Membrane Science and Technology*. 2013, John Wiley & Sons.

[4] Encyclopedia of Membrane Science and Technology, E.M.V. Hoek and V.V. Tarabara (Ed.), John Wiley & Sons, 2013.

[5] L.M. Robeson, The upper bound revisited, Journal of Membrane Science, 320 (2008) 390-400.

[6] E. Weber de Menezes and R. Cataluna, Optimization of the ETBE (ethyl tert-butyl ether) production process, Fuel Processing Technology, 89 (2008) 1148-1152.

[7] K.F. Yee, A.R. Mohamed, and S.H. Tan, A review on the evolution of ethyl tert-butyl ether (ETBE) and its future prospects, Renewable and Sustainable Energy Reviews, 22 (2013) 604-620.

[8] M. Wang, C. Arnal-Herault, C. Rousseau, A.I. Palenzuela, J. Babin, L. David, and A. Jonquieres, Grafting of multi-block copolymers: A new strategy for improving membrane separation performance for ethyl tert-butyl (ETBE) bio-fuel purification by pervaporation, Journal of Membrane Science, 469 (2014) 31-42.

[9] M.S. Chen, R.M. Eng, J.L. Glazer, and C.G. Wensley, Pervaporation process for separating alcohols from ethers, Pervaporation process for separating alcohols from ethers US patent 7,774,365, 1988.

[10] C. Streicher, Institut Francais du Pétrole, Ethyl tertio-butyl ether purification process combining a membrane method and distillation, Ethyl tertio-butyl ether purification process combining a membrane method and distillation US Patent 5607557, 1997.

[11] A. Jonquieres, C. Arnal-Herault, and J. Babin, Pervaporation, in: E.M.V. Hoek, V.V. Tarabara (Eds.) Encyclopedia of Membrane Science and Technology, Wiley, volume 3 (2013) pp. 1533-1559.

[12] A. Jonquieres, R. Clement, P. Lochon, M. Dresch, and B. Chrétien, Industrial state of the art of pervaporation and vapor permeation in the Western countries, Journal of Membrane Science, 206 (2002) 87-117.

[13] M. Billy, A. Ranzani Da Costa, P. Lochon, R. Clement, M. Dresch, and A. Jonquieres, Cellulose acetate graft copolymers with nano-structured architectures: Application to the purification of bio-fuels by pervaporation, Journal of Membrane Science, 348 (2010) 389-396.

[14] S. Zereshki, A. Figoli, S.S. Madaeni, F. Galiano, and E. Drioli, Pervaporation separation of ethanol/ETBE mixtures using poly(lactic acid)/poly(vinyl pyrrolidone) blend membranes, Journal of Membrane Science, 373 (2011) 29-35.

[15] Q.T. Nguyen, C. Leger, and P.L. P. Billard, Novel membranes made from a semi-interpenetrating polymer network for ethanol-ETBE separation by pervaporation, Polymers for Advanced Technologies, 8 (1997) 487-495.

[16] G.S. Luo, M. Niang, and P. Schaetzel, Pervaporation separation of ethyl tert-butyl ether and ethanol mixtures with a blended membrane, Journal of Membrane Science, 125 (1997) 237-244.

[17] Q.T. Nguyen, R. Clement, I. Noezar, and P. Lochon, Performances of poly(vinylpyrrolidone-co-vinyl acetate)- cellulose acetate blend membranes in the pervaporation of ethanol-ethyl tert-butyl ether mixtures. Simplified model for flux prediction, Separation and Purification Technology, 13 (1998) 237-245.

[18] G.S. Luo, M. Niang, and P. Schaetzel, A high performance membrane for sorption and pervaporation separation of ethyl tert-butyl ether and ethanol mixtures, Separation Science and Technology, 34 (1999) 391-401.

[19] R. Rogers and K. Seddon, eds. *Industrial applications of ionic liquids*. 2002, American Chemical Society Books.

[20] P. Wasserscheid and T. Welton, Ionic liquids in Synthesis, 2nd ed, Wiley-VCH, Weinheim, 2008.

[21] P. Scovazzo, A.E. Visser, J. Davis, H., R. Rogers, D., C. Koval, A., D. DuBois, L., and R.D. Noble, Supported Ionic Liquid Membranes and Facilitated Ionic Liquid Membranes, ACS Symposium Series, 818 (Ionic liquids) (2002) 69-87.

[22] M.D. Green and T.E. Long, Designing Imidazole-Based Ionic Liquids and Ionic Liquid Monomers for Emerging Technologies, Journal of Macromolecular Science Part C: Polymer Reviews, 49 (2009) 291–314.

[23] J. Lu, F. Yan, and J. Texter, Advanced applications of ionic liquids in polymer science, Progress in Polymer Science, 34 (2009) 431-448.

[24] D. Han and K.H. Row, Recent Applications of Ionic Liquids in Separation Technology, Molecules 15 (2010) 2405-2426.

[25] L.J. Lozano, C. Godinez, A.P. de los Rios, F.J. Hernandez-Fernandez, S. Sanchez-Segado, and F.J. Alguacil, Recent advances in supported ionic liquid membrane technology, Journal of Membrane Science, 376 (2011) 1-14.

[26] R.D. Noble and D.L. Gin, Perspective on ionic liquids and ionic liquid membranes, Journal of Membrane Science, 369 (2011) 1-4.

[27] J. Chen, H. Rodríguez, and R.D. Rogers, Editorial Special Issue on Ionic Liquids for Separations, Separation Science and Technology, 47 (2012) 167-168.

[28] C. Roosen, P. Müller, and G. Lasse, Ionic liquids in biotechnology: applications and perspectives for biotransformations, Applied Microbiology and Biotechnology, 81 (2008) 607-614.

[29] P. Izak, K. Friess, and M. Sipek, Chapter 12 : Pervaporation and permeation taking advantage of ionic liquids, in S.V. Gorley (Ed.). Handbook of membrane research: Properties, performances and applications, Nova Science Publishers, New York, 2010, pp. 387-402.

[30] P. Scovazzo, Determination of the upper limits, benchmarks, and critical properties for gas separations using stabilized room temperature ionic liquid membranes (SILMs) for the purpose of guiding future research, Journal of Membrane Science, 343 (2009) 199-211.

[31] S. Hanioka, T. Maruyama, T. Sotani, M. Teramoto, H. Matsuyama, K. Nakashima, M. Hanaki, F. Kubota, and M. Goto, CO2 separation facilitated by task-specific ionic liquids using a supported liquid membrane, Journal of Membrane Science, 314 (2008) 1-4.

[32] J.J. Close, K. Farmer, S.S. Moganty, and R.E. Baltus, CO2/N2 separations using nanoporous alumina-supported ionic liquid membranes: Effect of the support on separation performance, Journal of Membrane Science, 390-391 (2012) 201-210.

[33] S.D. Hojniak, I.P. Silverwood, A.L. Khan, I.F.J. Vankelecom, W. Dehaen, S.G. Kazarian, and K. Binnemans, Highly Selective Separation of Carbon Dioxide from Nitrogen and Methane by Nitrile/Glycol-Difunctionalized Ionic Liquids in Supported Ionic Liquid Membranes (SILMs), The Journal of Physical Chemistry B, 118 (2014) 7440-7449.

[34] G. Fadeev and M.M. Meagher, Opportunities for ionic liquids in recovery of biofuels, Chemical Communications, 3 (2001) 295-296.

[35] P. Izak, W. Ruth, Z. Fei, P.J. Dyson, and U. Kragl, Selective removal of acetone and butan-1-ol from water with supported ionic liquid-polydimethylsiloxane membrane by pervaporation, Chemical Engineering Journal, 139 (2008) 318-321.

[36] M. Matsumoto, Y. Murakami, and K. Kondo, Separation of 1-butanol by pervaporation using polymer inclusion membranes containing ionic liquids, Solvent Extraction Research and Development, 18 (2011) 75-83.

[37] S. Heitmann, J. Krings, P. Kreis, A. Lennert, W.R. Pitner, A. Gorak, and M.M. Schulte, Recovery of n-butanol using ionic liquid-based pervaporation membranes, Separation and Purification Technology, 97 (2012) 108-114.

[38] Garba O. Yahaya, Feras Hamad, Ahmed Bahamdan, Veera V.R. Tammana, and E.Z. Hamad, Supported ionic liquid membrane and liquid–liquid extraction using membrane for removal of sulfur compounds from diesel/crude oil, Fuel Processing Technology 113 (2013) 123-129.

[39] H.R. Cascon and S.K. Choudhari, 1-Butanol pervaporation performance and intrinsic stability of phosphonium and ammonium ionic liquid-based supported liquid membranes, Journal of Membrane Science, 429 (2013) 214-224.

[40] A. Plaza, G. Merlet, A. Hasanoglu, M. Isaacs, J. Sanchez, and J. Romero, Separation of butanol from ABE mixtures by sweep gas pervaporation using a supported gelled ionic liquid membrane: Analysis of transport phenomena and selectivity, Journal of Membrane Science, 444 (2013) 201-212.

[41] J. Yuan and M. Antonietti, Poly(ionic liquid)s: Polymers expanding classical property profiles, Polymer, 52 (2011) 1469-1482.

[42] P.C.H. Anthony E. Somers, Douglas R. MacFarlane and Maria Forsyth, A Review of Ionic Liquid Lubricants, Lubricants, 1 (2013) 3-21.

[43] N.L. Mai, S.H. Kim, S.H. Ha, H.S. Shin, and Y.-M. Koo, Selective recovery of acetone-butanol-ethanol from aqueous mixture by pervaporation using immobilized ionic liquid polydimethylsiloxane membrane, Korean Journal of Chemical Engineering, 30 (2013) 1804-1809.

[44] M. Kohoutova, A. Sikora, A. Hovorka, A. Randova, J. Schauer, M. Tiama, K. Setnia□kova, R. Petria□kovia□, S. Guernik, N. Greenspoon, and P. Izak, Influence of ionic liquid content on properties of dense polymer membranes, European Polymer Journal, 45 (2009) 813-819.

[45] K. Takekoshi, T. Miyata, and T. Uragami, Benzene-permselectivity of Poly(methylmethacrylate)-Poly(dimethylsiloxane) graft-copolymer membranes containing ionic liquid, Pacifichem 2010 Conference, Honolulu, USA, December 15-20, (2010) MATNANO-385.

[46] A. Jonquieres, M. Awkal, R. Clément, and P. Lochon, New ion-containing polyimides for the purification of bio-fuels by a membrane separation process, in K.L. Mittal (Ed.). Polyimides and High Temperature Polymers: Synthesis, Characterization and Applications, Koninklijke Brill NV Edition, Leiden, 2009, (5), pp. 339-351.

[47] A. Arce, H. Rodriguez, and A. Soto, Use of a green and cheap ionic liquid to purify gasoline octane boosters, Green Chemistry, 9 (2007) 247-253.

[48] N. Gonsior and H. Ritter, Rheological Behavior of Polyelectrolytes Based on Cellulose and Ionic Liquids Dissolved in 1-Ethyl-3-methyl Imidazolium Acetate, Macromolecular Chemistry and Physics, 212 (2011) 2633−2640.

[49] W.Z. Xu, G. Gao, and J.F. Kadla, Synthesis of antibacterial cellulose materials using a "clickable" quaternary ammonium compound, Cellulose, 20 (2013) 1187-1199.

[50] R.W. Baker, J.G. Wijmans, and Y. Huang, Permeablity, permeance and selectivity: A preferred way of reporting pervaporation performance data, Journal of Membrane Science, 348 (2010) 346-352.

[51] B. Neises and W. Steglich, Simple Method for the Esterification of Carboxylic Acids, Angewandte Chemie International Edition, 17 (1978) 522–524.

[52] F. Hassan Hassan Abdellatif, J. Babin, C. Arnal-Herault, and A. Jonquieres, Chapter 25 : Grafting of cellulose and cellulose derivatives by CuAAC click chemistry, in V.K. Thakur (Ed.). Cellulose-based Graft Copolymers : Structure and Chemistry, CRC Press Taylor & Francis Publisher, 2015, pp. 563-591.

[53] R.A. McClelland, V.M. Kanagasabapathy, N.S. Banait, and S. Steenken, Reactivities of diarylmethyl and triarylmethyl cations with primary amines in aqueous acetonitrile solutions. The importance of amine hydration, Journal of the American Chemical Society, 114 (1992) 1816-1823.

[54] H. Mayr and M. Patz, Scales of nucleophilicity and electrophilicity : A system for ordering polar organic and organometallic reactions, Angewandte Chemie International Edition, 33 (1994) 938-957.

[55] H. Iken, F. Guillen, H. Chaumat, M.-R. Mazières, J.-C. Plaquevent, and T. Tzedakis, Scalable synthesis of ionic liquids: comparison of performances of microstructured and stirred batch reactors, Tetrahedron Letters, 53 (2012) 3474-3477.

[56] N. Zhao, L. Liu, F. Biedermann, and O.A. Scherman, Binding Studies on CB[6] with a Series of 1-Alkyl-3-methylimidazolium Ionic Liquids in an Aqueous System, Chemistry – An Asian Journal, 5 (2010) 530-537.

[57] K.D. Goebel, G.C. Berry, and D.W. Tanner, Properties of cellulose acetate. III. Light scattering from concentrated solutions and films. Tensile creep and desalination studies on films Journal of Polymer Science: Polymer Physics Edition, 17 (1979) 917-937.

[58] H. Suzuki, Y. Muraoka, M. Satio, and K. Kamide, Light-scattering study on cellulose diacetate in 2-butanone European Polymer Journal, 18 (1982) 831-837.

[59] E. Fleury, J. Dubois, C. Léonard, J.P. Joseleau, and H. Chanzy, Microgels and ionic associations in solutions of cellulose diacetate, Cellulose, 1 (1994) 131-144.

[60] J.G. Wijmans and R.W. Baker, The solution-diffusion model: a review, Journal of Membrane Science, 107 (1995) 1-21.

[61] M.J. Kamlet and R.W. Taft, The solvatochromic comparison method. I. The .beta.-scale of solvent hydrogen-bond acceptor (HBA) basicities, Journal of the American Chemical Society, 98 (1976) 377-383.

[62] M.A. Ab Rani, A. Brant, L. Crowhurst, A. Dolan, M. Lui, N.H. Hassan, J.P. Hallett, P.A. Hunt, H. Niedermeyer, J.M. Perez-Arlandis, M. Schrems, T. Welton, and R. Wilding, Understanding the polarity of ionic liquids, Physical Chemistry Chemical Physics, 13 (2011) 16831-16840.

[63] J.-M. Lee, S. Ruckes, and J.M. Prausnitz, Solvent polarities and Kamlet-Taft parameters for ionic liquids containing a pyridinium cation, Journal of Physical Chemistry Part B, 112 (2008) 1473-1476.

[64] S. Spange, R. Lungwitz, and A. Schade, Correlation of molecular structure and polarity of ionic liquids, Journal of Molecular Liquids, 192 (2014) 137-143.

[65] J.G. Wijmans, Process performance = membrane properties + operating conditions, Journal of Membrane Science, 220 (2003) 1-3.

[66] R.C. Reid, J.M. Prausnitz, and T.K. Sherwood, The Properties of Gases and Liquids, 3rd edn, McGraw-Hill, New York, 1977.

Appendices

Appendix A. Permeability calculation and data for ETBE purification by pervaporation

According to the sorption-diffusion model [65], the permeability, P_i, of each species *i* was calculated from its partial flux normalized to the reference membrane thickness of 5 μm, J_i, and the corresponding trans-membrane pressure gradient (i.e. driving force for mass transfer) on the basis of equation (A.1) :

$$P_i = \frac{J_i}{\frac{P_{i,feed}^{vapor} - P_{i,permeate}^{vapor}}{5}} \qquad \text{(A.1)}$$

where $P_{i,feed}^{vapor}$ and $P_{i,permeate}^{vapor}$ are the equilibrium partial vapor pressures of species *i* in the feed and permeate, respectively.

$P_{i,feed}^{vapor}$ was calculated from the thermodynamics of the liquid/vapor equilibrium (LVE) corresponding to the azeotropic mixture EtOH/ETBE. For the LVE at the moderate feed pressure used in this work, the equality of the fugacity of species *i* in the liquid and vapor phases led to equation (A.2) [66]:

$$P_{i,feed}^{vapor} \cong \gamma_{i,feed}\, x_{i,feed}\, P_i^{saturated\ vapor} \qquad \text{(A.2)}$$

where $\gamma_{i,feed}$ is the activity coefficient of species *i* in the liquid feed mixture, $x_{i,feed}$ is the molar fraction of species *i* in the liquid feed mixture and $P_i^{saturated\ vapor}$ is the saturated vapor pressure of species *i* at the feed temperature. ETBE and ethanol saturated vapor pressures were calculated from Frost-Thodos equation and Antoine equation, respectively. The activity coefficients of ETBE and ethanol were calculated by the non-random two liquids (NRTL) equations. For the feed mixture EtOH/ETBE (20/80 wt%) at 50 °C, the corresponding equilibrium partial vapor pressures were 49.6 kPa and 51.7 kPa for ETBE and ethanol, respectively.

$P_{i,permeate}^{vapor}$ was simply estimated from the molar fraction of species *i* in the permeate, $y_{i,permeate}$, and the permeate pressure, $P_{permeate}$, by equation (A.3):

$$P_{i,permeate}^{vapor} = y_{i,permeate}\, P_{permeate} \qquad \text{(A.3)}$$

For the very low permeate pressure (less than 0.04 kPa) used in this work, $P_{i,permeate}^{vapor} \ll P_{i,feed}^{vapor}$ for ETBE and ethanol. Therefore, the permeability of each species *i* was simply estimated from the partial flux normalized to the reference membrane thickness of 5 μm, J_i, by equation (A.4) :

$$P_i \cong \frac{J_i}{\frac{P_{i,feed}^{vapor}}{5}} \quad \text{(A.4)}$$

Table A.1 Influence of the imidazolium ionic liquid content in the grafted cellulose acetate membranes on ethanol and ETBE permeability for the separation of the azeotropic EtOH/ETBE mixtures. *CA-g-X-IM corresponds to cellulose acetate with a grafting rate of X for the imidazolium ionic liquid.*

Membrane	**W_{IL} (wt.%)**	P_{EtOH} x 1000 (kg µm/h m^2 kPa)	P_{ETBE} x 1000 (kg µm /h m^2 kPa)
Cellulose acetate	0	2.2	0
CA-*g*-23.6-IM	5	5.1	0.01
CA-*g*-45.6-IM	9.4	4.8	0
CA-*g*-64-IM	12.9	4.2	0
CA-*g*-83-IM	16.4	4.8	0

W_{IL}: ionic liquid weight fraction in the grafted cellulose acetate; P_i: partial permeability of species i.

Table A.2 Influence of the ammonium ionic liquid content in the grafted cellulose acetate membranes on ethanol and ETBE permeability for the separation of the azeotropic EtOH/ETBE mixtures. *CA-g-X-AM corresponds to cellulose acetate with a grafting rate of X for the ammonium ionic liquid.*

Membrane	**W_{IL} (wt.%)**	P_{EtOH} x 1000 (kg µm/h m^2 kPa)	P_{ETBE} x 1000 (kg µm /h m^2 kPa)
Cellulose acetate	0	2.2	0
CA-*g*-17-AM	3.8	6.6	0.07
CA-*g*-34.7-AM	7	10.0	0
CA-*g*-47.5-AM	10	16.0	0.03
CA-*g*-60-AM	12.4	16.5	0
CA-*g*-87-AM	17.7	17.6	0

W_{IL}: ionic liquid weight fraction in the grafted cellulose acetate; P_i: partial permeability of species i.

Table A.3 Influence of the ionic liquid cation (*i.e.* imidazolium IM, pyridinium PYR and ammonium AM) on ethanol and ETBE permeability of the grafted cellulose acetate membranes with the highest grafting rates.

Membrane	**W_{IL} (wt.%)**	P_{EtOH} x 1000 (kg µm/h m^2 kPa)	P_{ETBE} x 1000 (kg µm /h m^2 kPa)
Cellulose acetate	0	2.2	0
CA-g-83-IM	16.4	4.8	0
CA-g-77-PYR	16.6	5.2	0
CA-g-87-AM	17.7	17.6	0

W_{IL}: ionic liquid weight fraction in the grafted cellulose acetate; P_i: partial permeability of species i.

Appendix B. ^{1}H NMR characterization of the bromo-cellulose derivative.

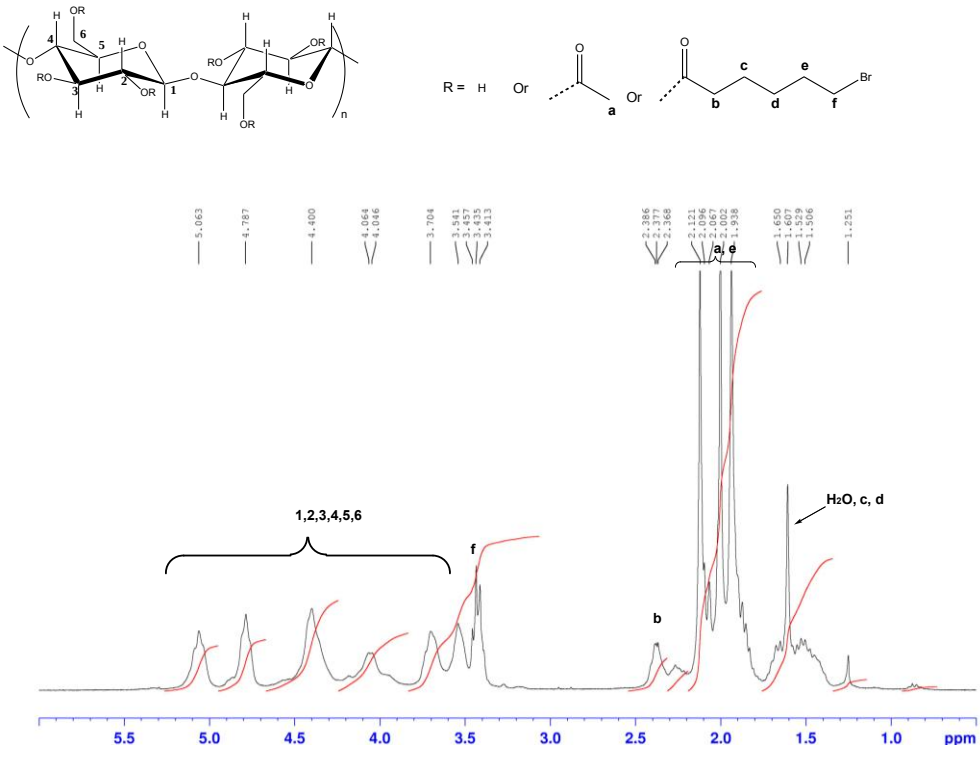

Figure B. 1: ^{1}H NMR characterization of the bromo-cellulose acetate derivative.

Chapter 3 Part 3

Grafting of cellulose acetate with ionic liquids for biofuel purification by a membrane process : Influence of the anion.

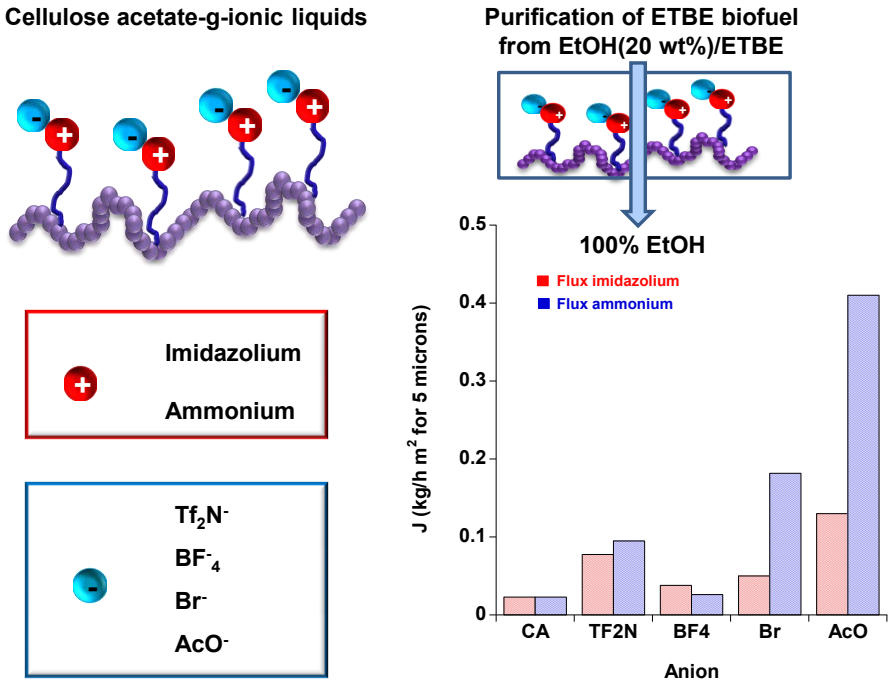

Grafting of cellulose acetate with ionic liquids for biofuel purification by a membrane process : Influence of the anion.

Faten HASSAN HASSAN ABDELLATIF[a)], Jérôme BABIN[a)],
Carole ARNAL-HERAULT[a)], Laurent DAVID[b)], Anne JONQUIERES[a)]*

[a)] *Laboratoire de Chimie Physique Macromoléculaire, LCPM UMR CNRS–Université de Lorraine 7375, ENSIC, 1 rue Grandville, BP 20451, 54 001 Nancy Cedex, France.*

[b)] *Laboratoire IMP@Lyon1, Université Claude Bernard Lyon 1, Université de Lyon, CNRS UMR 5223, 15 Bd. André Latarjet, 69622 Villeurbanne Cedex, France.*

Keywords: polysaccharide modification; ionic liquids; membranes; biofuel; ethyl *tert*-butyl ether; structure-property relationships.

Abstract. Ethyl *tert*-butyl ether (ETBE) is an attractive biofuel currently blended to gasoline fuels to improve combustion and reduce toxic emissions. During ETBE production, this ether forms an azeotropic mixture containing 20 wt% of ethanol, which is removed by ternary distillation. This method is highly energy intensive and the pervaporation membrane process has been proposed as a good alternative for this separation. Following our recent work on cellulose acetate grafting with ionic liquids containing the same bromide anion for ETBE purification by pervaporation, this new work further extends the scope of ionic liquid-containing membranes to the challenging separation of purely organic mixtures, in which these ionic liquids are soluble. Therefore, the bromide anion $Br^-$of imidazolium and ammonium ionic liquids formerly grafted onto cellulose acetate was exchanged by three other anions (Tf_2N^-, BF_4^- and AcO^-) to assess the anion influence on the membrane properties. The sorption and pervaporation properties were analyzed in terms of structure-property relationships showing the influence of the anion chemical structure, molecular size and physico-chemical parameters in the Kamlet-Taft polarity (α, β, π*) scale. The ammonium ionic liquid with the acetate anion combining the highest hydrogen bonding acceptor ability β with big molecular size and led to the best membrane properties with a normalized flux of 0.41 kg/h m^2 (almost 20 times that of virgin cellulose acetate) for a reference membrane thickness of 5 µm and a permeate ethanol content of 100% corresponding to an infinite membrane separation factor at 50°C.

---

1. Introduction

Ethyl *tert*-butyl ether (ETBE) is an attractive bio-ether used in the European Union (EU) as biofuel. ETBE is generally blended with gasoline fuels to reduce toxic hydrocarbon emissions by improving fuel combustion. Due to the biodegradable characteristics of ETBE, it has also been used in replacement of the related methyl *tert*-butyl ether (MTBE) [1, 2]. In the EU, ETBE is usually catalytically synthesised from bio-ethanol and isobutene. During its industrial production, it forms an azeotropic mixture containing 20 wt% of ethanol. This mixture is currently separated by a highly energy intensive ternary distillation process. However, former works have already shown that ETBE could be purified by the pervaporation membrane process, which offers important energy savings, modularity and lower environmental impact compared to ternary distillation [3, 4].

In membrane separation processes, designing of the membrane material is always critical. Ideally, the membrane should be both highly permeable and highly selective. However, in most cases, permeability and selectivity vary in opposite ways thus leading to a permeability/selectivity trade-off [3-6]. Polymeric membranes are generally preferred to inorganic membranes for extracting ethanol from the azeotropic mixture EtOH/ETBE due to their low cost and broad range of compositions but many of these polymer membranes are still limited by the permeability/selectivity trade-off [2, 7-10].

Cellulose acetate is a very good film-forming cellulosic material well known in membrane separation for water purification and gas permeation. This polysaccharide derivative has also been reported for ETBE purification by pervaporation. For this application, cellulose acetate was highly selective with a permeate ethanol weight fraction of 100% but its flux of 0.08 kg/m^2 h for a reference membrane thickness of 5 µm was much too low at 40°C . Cellulosic esters blends enabled to vary the PV fluxes over a broad range from 0.6 kg/m^2 h to 3 kg/m^2 h with permeate ethanol contents varying from 0.967 to 0.907 at 40°C [11] Cellulosic semi-interpenetrated networks and graft copolymers with polymethacrylate grafts have also been reported as promising ways for improving cellulosic membrane properties for ETBE purification [12-14]. In particular, PEO-based polymethacrylate grafting of cellulose acetate greatly improved the membrane flux up to 0.87 kg/m^2 h while the permeate ethanol content (94%) remained in the very high range at 50°C [12].

On the other hand, ionic liquids (ILs) have had a very strong impact in chemistry and physical chemistry over the past decade due to their unique properties. ILs have been used as green alternatives to volatile organic solvents due to their thermal stability, non-volatility, negligible vapor pressure and capacity to dissolve a large range of organic compounds [15,

16]. Their interesting physico-chemical properties can be specifically tailored by selecting the nature of their cation and anion. In particular, ILs have the capability to interact with different solutes via dipolar/dispersion forces and H-bonding interactions depending on the type of their cation and anion [17]. It has been shown that some cations *e.g.* mono alkyl ammonium salts [18] are strong H-bonding donors while other anions *e.g.* acetate and chloride anions [19] are strong H-bonding acceptors capable of interacting strongly with H-bonding donor species like alcohols [17].

Even more closely related to this work, ILs containing membranes have led to a major breakthrough in gas permeation by overcoming the permeability/selectivity trade-off for CO_2 capture [20-25]. Comparatively, ILs containing membranes have been rarely reported for liquid separations so far [26-33]. The former related works focused on the recovery of biofuels from dilute fermentation broths or that of volatile organic compounds (VOCs) from water with *organophilic* membranes.

We have also recently reported the first IL containing *organoselective* membranes for ETBE purification by pervaporation [34]. The later work further extended the scope of ILs containing membranes to the challenging separation of purely organic mixtures, in which these ILs were soluble. These membranes were obtained by grafting cellulose acetate with ILs containing the same bromide anion and different cations (imidazolium, pyridinium and ammonium) with increasing polar features. The membrane properties varied strongly with the IL cation and content. For the highest IL content (ca. 17 wt%), cellulose acetate grafted with the ammonium IL having the best hydrogen bonding acceptor ability led to the highest normalized flux of 0.182 kg/h m^2 for a reference membrane thickness of 5 µm, a permeate ethanol content of 100% and an infinite membrane separation factor at 50°C for the targeted membrane application.

This new work analyzes the influence of the IL anion on the membrane properties of cellulose acetate grafted with ILs for ETBE purification by pervaporation. The first part reports on the variation of the anion chemical structure (Tf_2N^-, BF_4^-, Br^- and AcO^-) by anion exchange from two cellulosic materials grafted with ionic liquids in our previous work. These cellulose acetate derivatives contained very close amounts (ca. 17 wt%) of grafted imidiazolium and ammonium bromides and have shown the most different trends for the targeted application. The structure and morphology of the new cellulosic membrane materials obtained after anion exchange were characterized by complementary techniques (^{1}H NMR, ^{19}F NMR, DSC, SAXS).

In the second part, the sorption and PV properties of the new membranes were analyzed for the separation of the azeotropic mixture EtOH/ETBE on the basis of structure-properties relationships revealing the key anion features for the targeted application.

2. Experimental

2.1. Materials

The two starting cellulosic materials were cellulose acetate grafted with ca. 17 wt% of 1-pentyl-3-methyl-imidazolium bromide [C_5C_1im][Br] or *N,N,N,N*-pentyldiethylmethyl-ammonium bromide [$C_5C_2C_2C_1$N][Br] corresponding to the highest grafting rates obtained in our former work [34]. The corresponding degree of substitution of the grafted ionic liquids (DS_{LI}) was ca. 0.42 for both cellulosic materials. The different salts used for anion exchange (sodium acetate (NaAcO ≥ 99%), sodium tetrafluoroborate ($NaBF_4$, 98%), lithium bis(trifluoromethanesulfonyl)imide ($LiTf_2N$, ≥ 99%)) and the Amberlite® resin A-26 (OH form) were purchased from Sigma-Aldrich and used without further purification. The solvent *N,N*-dimethylformamide (DMF, ≥ 99.8 %, Sigma Aldrich) was purified by fractional distillation over calcium hydride and stored under dry nitrogen atmosphere.

2.2. Synthesis and characterization of cellulose acetate grafted with ionic liquids containing different anions

2.2.1. Synthesis of cellulose acetate grafted with ionic liquids containing acetate anion

As way of example, the bromide to acetate anion exchange is described for cellulose acetate grafted with the imidazolium bromide ionic liquid. In 100 mL round bottom reactor, 2 g of cellulose acetate-g-[C_5C_1im][Br] (corresponding to 2.05 mmol of bromide anions) were dissolved in 60 mL of purified DMF before adding a solution of 1.68 g (10 eq.) of sodium acetate in 5 mL of distilled water. The reaction mixture was left under magnetic stirring for 2 days at room temperature. The solution was filtered to remove the precipitated excess of sodium acetate and the bromide salt. The cellulosic polymer was collected after precipitation in diethyl ether followed by extensive washing with water to remove sodium bromide. The resulting polymer cellulose acetate-g-[C_5C_1im][Ac] was dried in vacuum oven at 60°C. The anion exchange rate was determined by ^{1}H NMR (see main text).

2.2.2. Synthesis of cellulose acetate grafted with different ionic liquids containing Tf_2N– or BF_4^- anions

As way of example, the bromide to fluorinated anion exchange is described for cellulose acetate grafted with the imidazolium bromide ionic liquid. In 100 mL round bottom

reactor, 2 g of cellulose acetate-g-[C_5C_1im][Br] (corresponding to 2.05 mmol of bromide anions) were dissolved in 60 mL of purified DMF before adding 3.53 g (6 eq) of $LiTf_2N$ or 1.35 g (6 eq) of $NaBF_4$ in powder form. After dissolution of the fluorinated inorganic salt, the reaction mixture was left under magnetic stirring for 2 days at room temperature. The resulting polymers were recovered by precipitation in distilled water or in ethanol (96%) for the cellulosic polymers containing the Tf_2N^- or BF_4^- anions, respectively. These products were dried in vacuum oven at 60°C for one night. The anion exchange rates were determined by quantitative ^{19}F NMR using pentafluorophenol as internal standard.

2.2.3. Polymer characterization

^1H NMR and ^{19}F NMR spectra were recorded on a Bruker Avance 300 spectrometer at 300 MHz and 376 MHz, respectively. ^1H NMR for cellulose acetate-g-[C_5C_1im][Br] and cellulose acetate-g-[$C_5C_2C_2C_1N$][Br] and their derivatives with acetate anions were obtained from DMSO-d_6 solution at 300 K except for cellulose acetate grafted with the ammonium bromide ionic liquid. In the latter case, the temperature for ^1H NMR analysis had to be increased to 353 K to strongly improve spectral resolution [34]. The chemical shifts were referenced to TMS and were calculated using the residual isotopic impurities of the deuterated solvent. ^{19}F NMR was used for characterizing the cellulosic derivatives containing the fluorinated anions. The chemical shifts were referenced to trifluoroacetic acid. An internal standard (pentafluorophenol) was used for determining the anion exchange rates. The ^{19}F NMR samples were prepared by dissolving precisely ca. 15 mg of each grafted cellulosic polymer in 0.5 mL of DMSO-d_6 and 0.1 mL of a fresh pentafluorophenol stock solution (26.1 mg/1mL of DMSO-d_6) was then added for quantitative analysis. The detailed procedure for determining the exchange rates for the fluorinated anions in described in Appendix A.

Thermal analysis was performed by standard Differential Scanning Calorimetry (DSC) using a TA Instruments DSC Q2000. Polymer samples of ca. 10 mg were used for analysis under a continuous flow of nitrogen. Two cycles of measurements from 20 to 210 °C were performed with heating and cooling rates of 10 °C/min. The thermal transitions corresponding to the first and second heating scans differed significantly and showed the strong influence of thermal history. The data reported in this work corresponded to the glass transition temperatures for the second heating scan for better comparison.

The nano-scale morphology of virgin cellulose acetate and cellulose acetate grafted with different ILs was determined by means of small X-ray scattering using polymer membranes with thicknesses of ca. 200 µm, which were obtained in the same way as for sorption experiments. Small angle X-ray scattering (SAXS) experiments were carried out at

room temperature, without any additional thermal treatment, using synchrotron radiation at the European Synchrotron Radiation Facility (ESRF, Grenoble, France). The experiments were performed on the BM2-D2AM beamline at an incident energy of 16 keV. A 2D X-ray camera was used (Roper Scientific), and the data were corrected from the dark image, normalized with flat field and tapper camera distortion. Finally, radial average around the incident beam center were calculated. Silver Behenate was used for the channel-*q* calibration. The background (empty cell) was subtracted in the radial average profiles, after the measurement of the attenuation coefficients.

2.3. Membrane preparation for pervaporation and sorption experiments

The different polymer materials were dissolved in DMF (pure for synthesis) to obtain a polymer concentration of 3.5 % w/v. The solutions were then cast on a PTFE mold. They were carefully removed from the mold after DMF evaporation at 45°C. The pervaporation membrane thicknesses ranged from 85 to 100 µm and the difference in thickness between two membrane points did not exceed 10 µm.

The procedure for sorption membrane casting was similar as that for pervaporation membranes except for polymer concentration, which was increased to 5% w/v in order to obtain membrane thicknesses of ca. 200 µm. The sorption membranes were then carefully dried at 60°C for 24 hours before sorption experiments.

2.4. Sorption experiments

For sorption experiments, the dried polymer membranes were weighted and then immersed in the azeotropic mixture EtOH/ETBE (20/80 wt%) in hermetically closed bottles. These bottles were kept at 30°C in a thermostated oven. This sorption temperature was chosen for experimental reason. After one week, the membranes were taken out the bottles and quickly wiped with paper tissue and weighted in a closed tare bottle. The membranes were regularly weighted until they reached constant swelling weight. At the end of each sorption experiment, the membranes were dried under vacuum and weighted again. The results obtained with the different sorption membranes showed that no polymer dissolution had occurred during the sorption experiments. The total swelling, S (wt%), was calculated from equation (1) :

$$S = \frac{w_S - w_D}{w_D} \times 100 \qquad (1)$$

where w_S and w_D were the membrane weights after and before sorption experiment.

For determining the composition of the absorbed mixture, the swollen membranes at equilibrium were soaked for 1 night at ambient temperature into 10 mL of diethyl ether, which is a non solvent for the membrane polymers and a good solvent for both ethanol and ETBE. The desorption solution was then analyzed by gas chromatography using a Shimadzu GC-8A chromatograph with a Porapak Q column, a thermal conductivity detector and hydrogen as carrier gas. The ethanol weight fraction C_s in the desorbed mixture was calculated from the area of the EtOH and ETBE peaks on the basis of a former calibration.

Sorption separation factor were then calculated from equation (2) where C^S_{EtOH} and C are the ethanol weight fractions in the sorption mixture and the azeotropic mixture EtOH/ETBE, respectively. The symbol for the sorption separation factor was that recently proposed by Baker *et al.* [35].

$$\beta_S = \frac{C^S_{EtOH}}{1 - C^S_{EtOH}} / \frac{C}{1 - C} \qquad (2)$$

2.5. Pervaporation experiments

Pervaporation experiments were performed for the azeotropic mixture EtOH/ETBE at 50°C using a pervaporation set-up described elsewhere [12]. The downstream pressure of the PV cell was maintained at less than 0.04 kPa using a vacuum pump. The permeate was collected continuously after condensation by liquid nitrogen using two parallel traps. The permeate flux was calculated using equation (3) :

$$Permeate\ \ flux = \frac{W_p}{\Delta t \times A} \qquad (3)$$

where w_p is the permeate sample weight collected during a permeation time Δt and A is the active membrane area.

To do a comparison between different membranes with close but non-equal thicknesses, normalized fluxes, J, are reported for a reference membrane thickness of 5 µm (equation (4)). This reference thickness was chosen because it is easily reached for dense polymer layers on top of asymmetric membranes.

$$J = \frac{Membrane\ thickness}{5} Permeate\ \ flux \qquad (4)$$

The permeate ethanol weight fraction, C', was determined by gas chromatography in the same conditions as for sorption experiments. The pervaporation separation factor, β_{PV} , was calculated by analogy with the sorption separation factor according to equation (5). The

experimental errors were less than 5% for the total fluxes and ± 0.005 for the ethanol weight fractions.

$$\beta_{PV} = \frac{C'_{EtOH}}{1-C'_{EtOH}} / \frac{C}{1-C} \qquad (5)$$

The fairly complex procedure for permeability calculation in pervaporation has already been reported [34] and the corresponding data are presented in Appendix B.

3. Results and discussion

3.1. Synthesis and characterization of cellulose acetate grafted with different ionic liquids by anion exchange

Figure 1 shows the general procedure used for exchanging the bromide anions in cellulose acetate materials grafted with imidazolium $[C_5C_1im][Br]$ or ammonium $[C_5C_2C_2C_1N][Br]$ ionic liquids. Different anions were usually introduced by using a large excess in different inorganic salts containing the targeted anions and removing the resulting bromide salt. After anion exchange, eight cellulosic materials with imidazolium or ammonium cations and one of the following anions (Tf_2N^-, BF_4^-, Br^- and AcO^-) were available for membrane preparation and characterization. The chemical structures and abbreviations used for the different grafted ionic liquids are given in Appendix C.

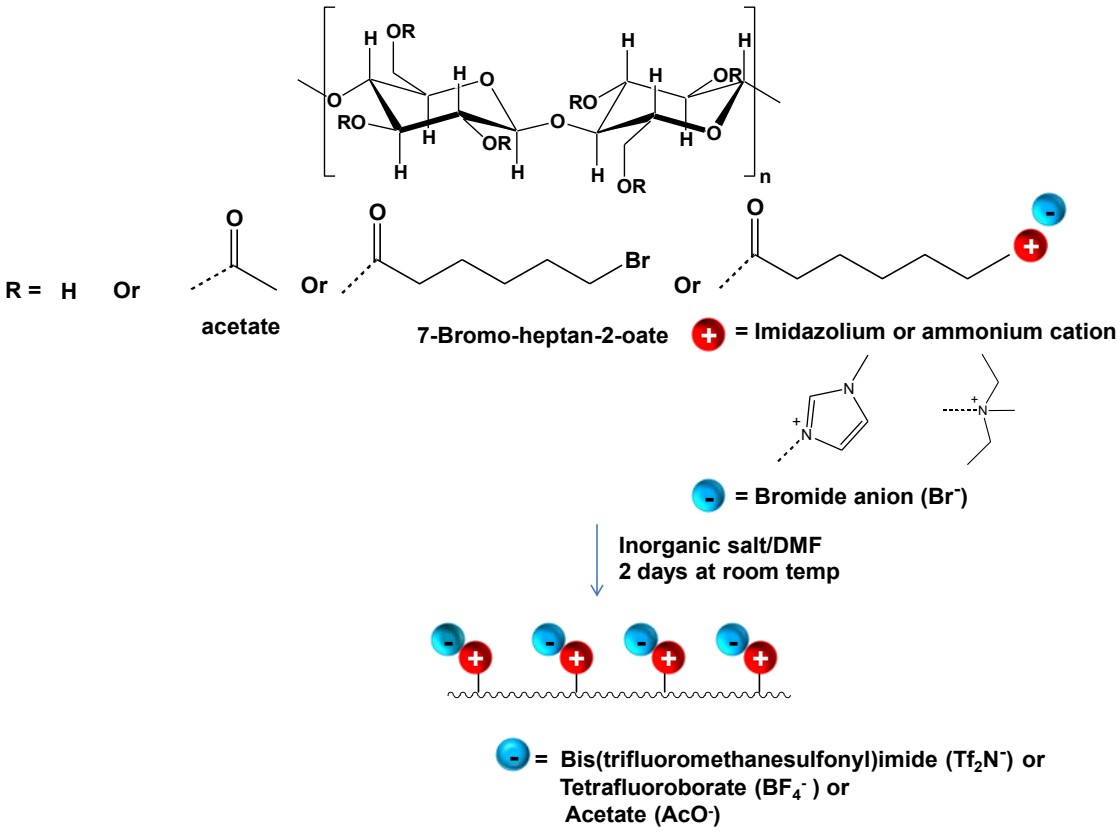

Figure 1: Synthesis of cellulose acetate with grafted ionic liquids with imidazolium or ammonium cations and different anions by anion exchange of cellulosic precursors with bromide counter anions

3.1.1. Cellulose acetate grafted with imidazolium or ammonium ionic liquids with acetate counter anions

One of the best reported methods for exchanging halide anions by the acetate anion in ionic liquids takes advantage of the Amberlite® resin A-26 with hydroxide anions [36]. After a first exchange of the bromide anions by the Amberlite® hydroxide anions, these strongly basic anions are then converted to acetate anions by treating the corresponding ionic liquids with acetic acid. According to the literature [36], this method is highly efficient for molecular ionic liquids with nearly 100% exchange rates. When it was applied to the cellulose acetate samples grafted with imidazolium/ammonium bromide ionic liquids, this anion exchange strategy led to the chemical degradation of the polymer materials. In any case, ^{1}H NMR revealed a strong decrease (– 30%) in their degree of esterification, which was ascribed to the cleavage of the acetate and linker ester groups by the strongly basic hydroxide anions of the Amberlite® resin.

Therefore, the anion exchange was then achieved with acetate salts. Sodium acetate was preferred to silver acetate due to its slightly better solubility in the aprotic dipolar solvent (DMF) used for anion exchange, its lower cost and good stability. Nevertheless, the solubility of the sodium acetate salt was still very limited in DMF and using a water solution of this salt improved its solubility and the anion exchange rate.

^{1}H NMR analysis of both cellulosic materials grafted with imidazolium or ammonium ionic liquids before and after bromide anion exchange confirmed the anion exchange with the appearing of a new peak in the range of 1.4 ppm to 1.7 ppm, which was characteristic for the new acetate counter anions (Figure 2). The integrations of this new peak enabled to calculate the bromide to acetate exchange rate for each ionic liquid. Even with a very large excess (10 eq.) in the sodium acetate salt, the exchange rate of cellulose acetate-g-[C_5C_1im][AcO] and cellulose acetate-g-[$C_5C_2C_2C_1$N][AcO] did not exceed 64% and 66%, respectively. This limitation in the anion exchange rate was most likely due to the heterogeneous conditions imposed by the very low solubility of the acetate salt. Furthermore, ^{1}H NMR showed that there was no change in the degree of esterification and that no chemical degradation occurred after anion exchange with sodium acetate, which is a weak base.

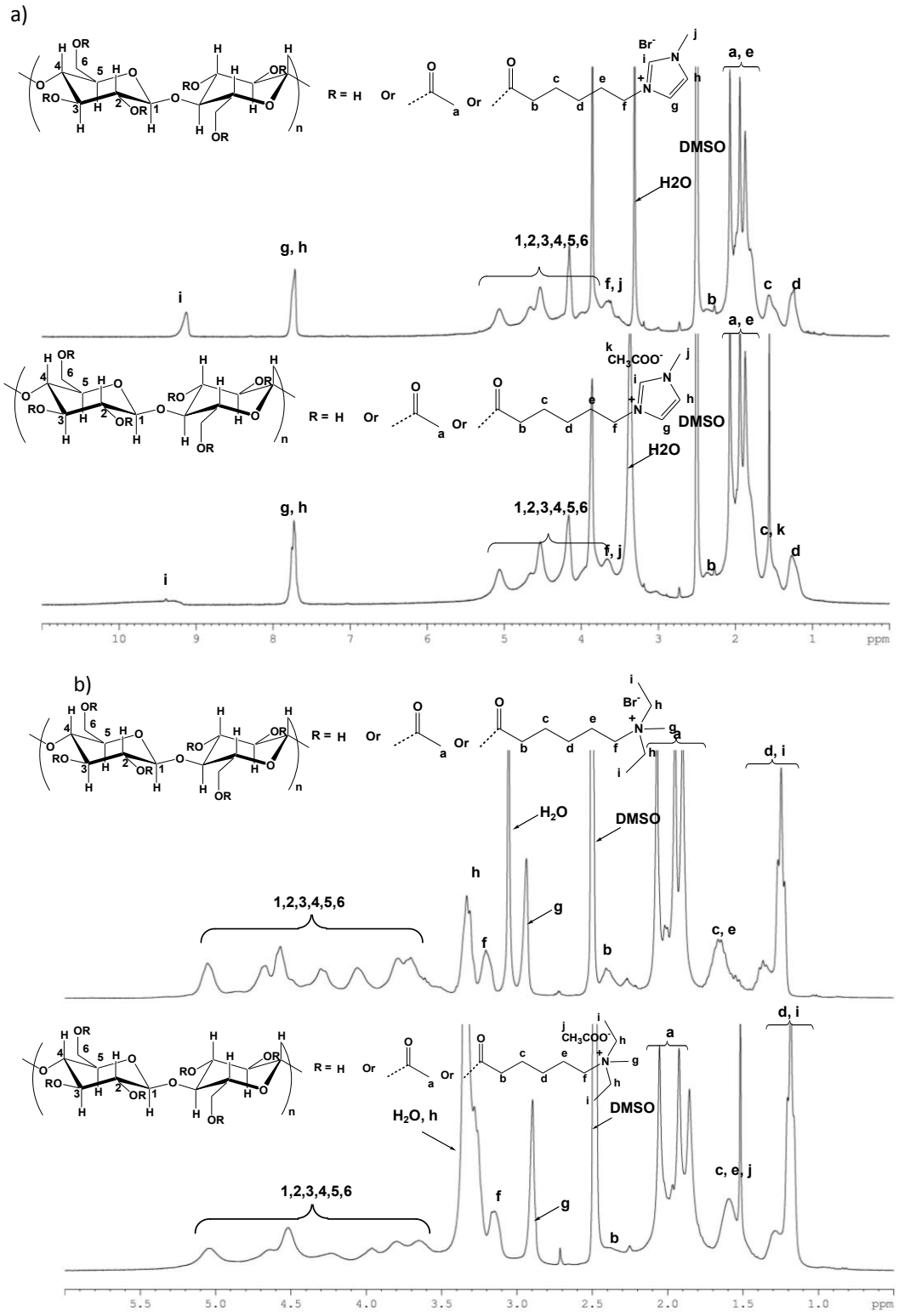

Figure 2: Comparison of the ^{1}H NMR spectra in DMSO-d_6 at 300 MHz before and after anion exchange with sodium acetate for: a) cellulose acetate-g-[C_5C_1im][X] and b) cellulose acetate-g-[$C_5C_2C_2C_1$N][X]

3.1.2. Cellulose acetate grafted with imidazolium and ammonium ionic liquids with fluorinated counter anions

The anion exchange of bromide to fluorinated anions was greatly improved compared to that to the acetate anion due to the much better solubility of both fluorinated salts ($LiTf_2N$ and $NaBF_4$) in DMF. The anion exchange was carried out in homogeneous condition with a large excess in fluorinated salts to ensure complete anion exchange. Precise purification of the resulting polymers was important to avoid the formation of pinholes in the membranes in case of residual inorganic salts.

Furthermore, ^1H NMR analysis showed that the degree of esterification of the cellulosic materials did not change after anion exchange and that no chemical degradation occurred during chemical modification. However, ^1H NMR analysis was not suitable for assessing the anion exchange for the fluorinated anions since they did not contain any protons. Therefore, quantitative ^{19}F NMR analysis was made to confirm the presence of the new fluorinated counter anions in each polymer structure and assess their exchange rates. As the four cellulosic materials with fluorinated anions did not contain any other fluorinated groups, pentafluorophenol was used as an internal standard for determining the anion exchange rate quantitatively for each polymer material according to a procedure detailed in Appendix A.

Figure 3 shows the ^{19}F NMR characterization of both cellulosic materials grafted with imidazolium or ammonium ionic liquids after complete bromide anion exchange with the two fluorinated salts $LiTf_2N$ or $NaBF_4$. For the cellulosic material grafted with *imidazolium* ionic liquid (Figure 3a), using 6 equivalents of the fluorinated salts led to 100% exchange rates for both Tf_2N^- and BF_4^- anions according to quantitative ^{19}F NMR analysis. In the same conditions, the anion exchange with the cellulosic material grafted with the *ammonium* ionic liquid resulted in significantly lower exchange rates of 89% and 80% for the Tf_2N^- and BF_4^- anions, respectively. The anion exchange was thus less efficient with the ammonium ionic liquid compared to the imidazolium likely be due to the hindrance in the ammonium ionic liquid structure. Nevertheless, in the later case, increasing the amount of both fluorinated salts to 10 equivalents enabled 100% anion exchange for both Tf_2N^- and BF_4^- anions (Figure 3b).

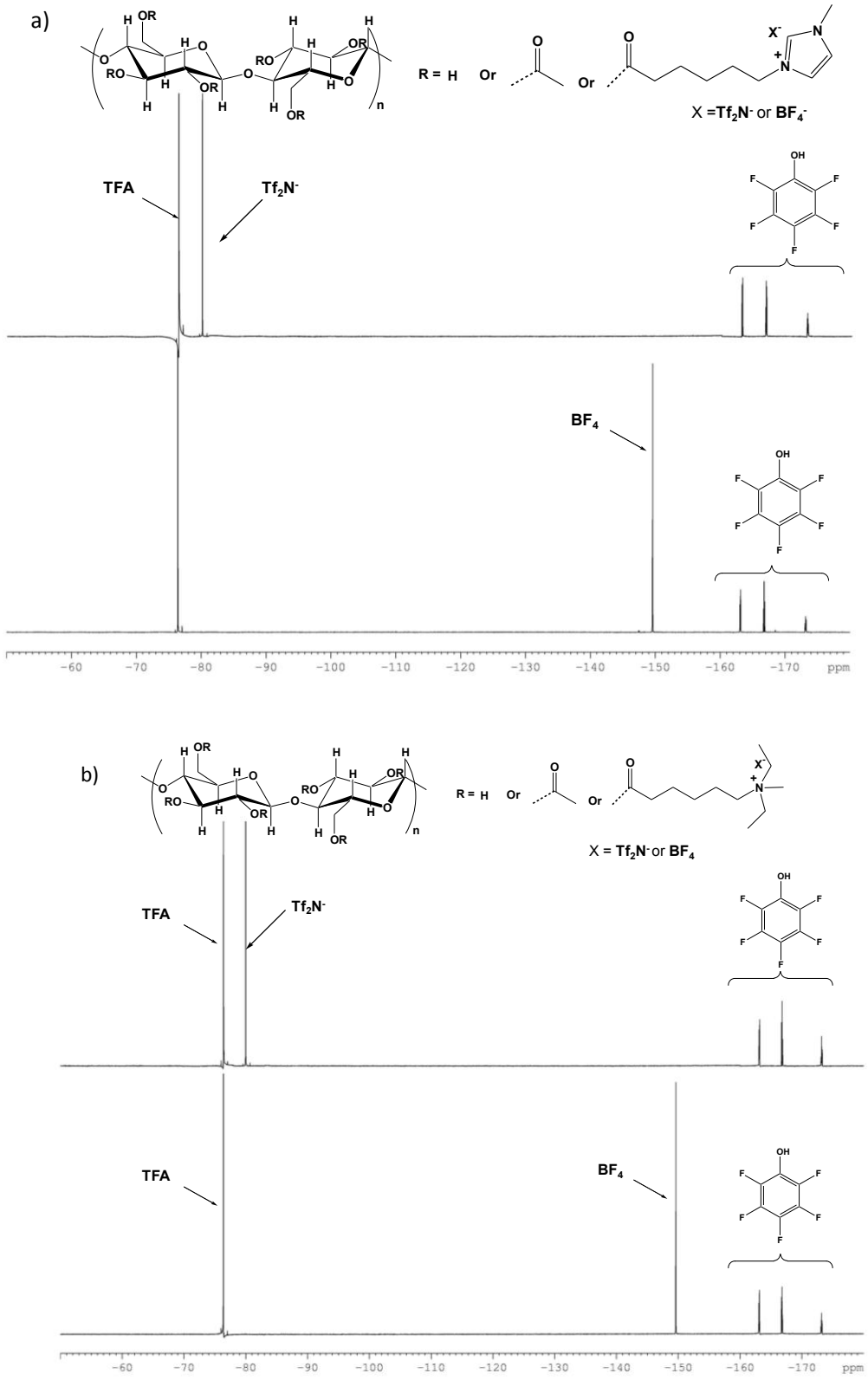

Figure 3: Quantitative ^{19}F NMR characterization in DMSO-d_6 at 376 MHz after anion exchange with two fluorinated salts $LiTf_2N$ or $NaBF_4$ for : a) cellulose acetate-g-$[C_5C_1im][X]$ and b) cellulose acetate-g-$[C_5C_2C_2C_1N][X]$

3.1.3. Morphology characterization of the different cellulosic materials based on DSC and synchrotron SAXS

Our former work has already shown that the grafting of cellulose acetate with nearly identical amounts of ionic liquids containing different cations and the same bromide anion was responsible for a strong decrease in the polymer glass transition temperature (T_g) compared to that of virgin cellulose acetate [34]. In addition, the T_g increased with the ionic liquid melting temperature in the following order : imidazolium < pyridinium < ammonium. In this new work, we focus on the influence of the anion (Tf_2N^- BF_4^-, Br^- and AcO^-) for grafted imidazolium and ammonium ionic liquids. The melting and glass transition temperatures of ionic liquids are known to strongly depend upon their anion structure [36] and it was expected that the anion exchange would also have an influence on polymer glass transition temperature.

DSC analysis for both series of cellulose acetate-g-[C_5C_1im][X] and cellulose acetate-g-[$C_5C_2C_2C_1$N][X] with different anions did not reveal any endothermic melting peaks. Figure 4 revealed a strong influence of the ionic liquid anion on the polymer T_g, which increased in the following anion order : $Tf_2N^- < AcO^- < BF_4^- < Br^-$. The strongest T_g decrease corresponded to the Tf_2N^- anion with the imidazolium ionic liquid. This anion was loosely interacting with the imidazolium cation due to its large size and the low Coulomb interactions between ions [37]. Therefore, the Tf_2N^- anion led to the best membrane plasticization by strongly decreasing the polymer T_g from 184°C to 111°C for virgin cellulose acetate and cellulose acetate-g-[C_5C_1im][TF_2N], respectively.

Unlike what had been observed for ionic liquids with different cations, the influence of the ionic liquid anion on the polymer T_g was not directly correlated to the ionic liquid melting temperature as shown by the corresponding T_m data reported in Table 1 for a series of very close imidazolium ionic liquids [C_4C_1im][X]. Attempts were then made for correlating the polymer T_g with different physico-chemical properties of the ionic liquid T_g, such as density, molecular weight, total molecular volume or molecular volume of their cation or anion (Table 1). A single correlation could be found with the ionic liquid T_g data of closely related imidazolium species. The polymer T_g decreased with the ionic liquid T_g for imidazolium with Tf_2N^-, BF_4^- and Br^- anions. Unfortunately, the T_g of the corresponding imidazolium ionic liquid with an acetate anion could not be found in the literature.

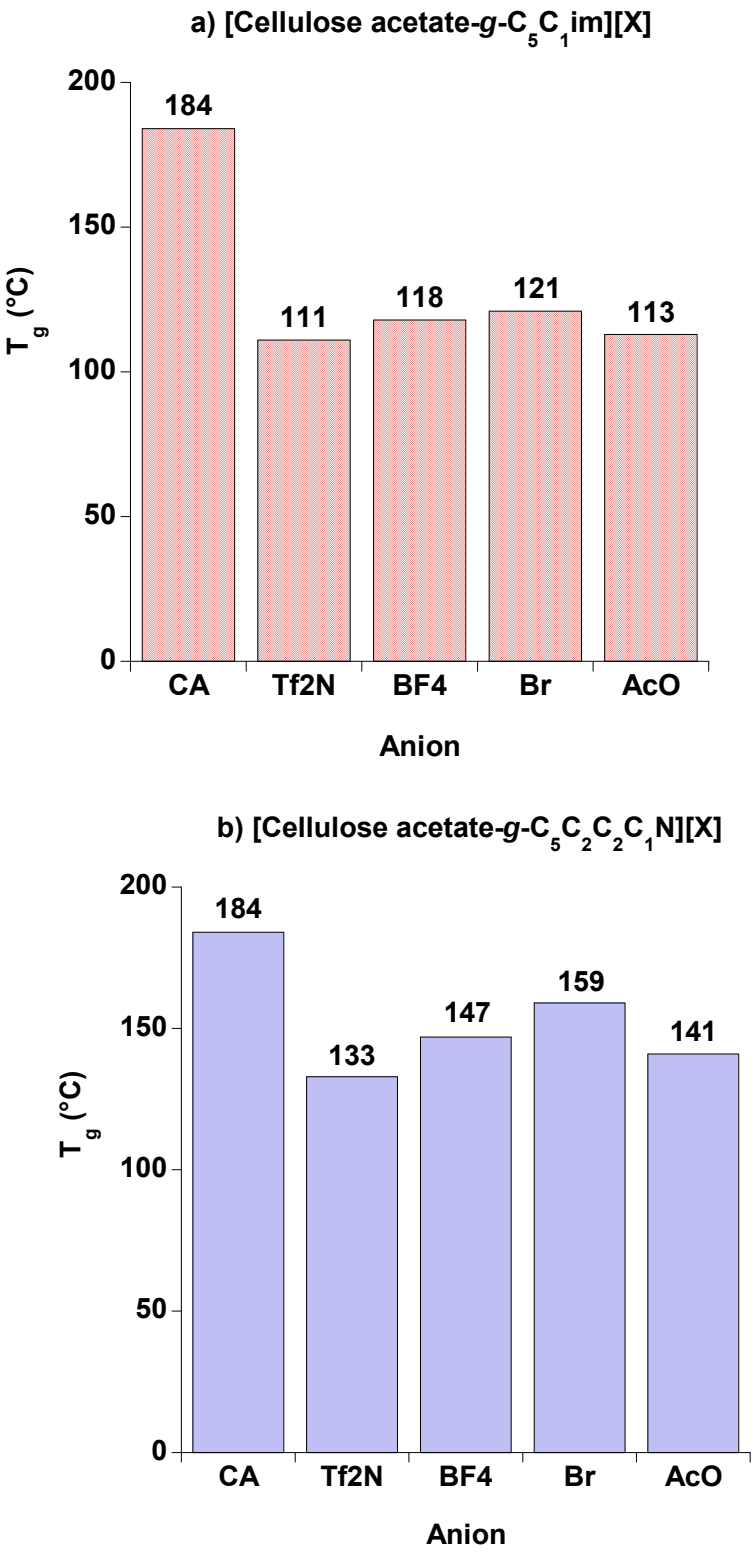

Figure 4: Influence of the ionic liquid anion X^- on the polymer glass transition temperature for nearly identical ionic liquid amounts ($W_{IL} \cong 17$ wt% w/w) for: a) cellulose acetate-g-[C_5C_1im][X] and b) cellulose acetate-g-[$C_5C_2C_2C_1$N][X]

For the second series cellulose acetate-g-[$C_5C_2C_2C_1N$][X], the influence of the ionic liquid anion on polymer T_g followed the same general trend as for the first membrane series but the decrease in the polymer T_g was systematically lower owing to the higher stiffness of the ammonium ionic liquids. The T_g of the corresponding ammonium ionic liquids were not reported in the literature and their correlation with the polymer T_g could not be evidenced in that case.

Table 1 Physico-chemical properties of related ionic liquids [C_4C_1im][X] and [$C_5C_2C_2C_2N$][X] used for the structure-property relationship analysis of the membrane properties

Ionic liquid	T_m (°C)	T_g (°C)	Density ($g/cm^{3)}$	Mwt (g/mol)	V_{cation} ($Å^3$)	V_{anion} ($Å^3$)	V_{IL} ($Å^3$)[a]	V_{IL} ($Å^3$)
[C_4C_1im][TF_2N]	-4	-104[38]	1.429 [39]	419.36	238	230	489	468
[C_4C_1im][BF_4]	-	-71 [40]	1.21 [41]	226.02	238	73	311.29	311
[C_4C_1im][Br]	69 [42]	-50 [43]	1.44 [44]	219.15	238	32	253.36	270
[C_4C_1im][Ac]	<-20 [45]	-	1.055 [45]	198.27	238	75	313	313
[$C_5C_2C_2C_2N$][TF2N] [46]	-	-	-		332	230	-	562
[$C_5C_2C_2C_2N$][BF_4]	-	-	-		332	73	-	405
[$C_5C_2C_2C_2N$][Br]	-	-	-		332	32	-	364
[$C_5C_2C_2C_2N$][Ac]	-	-	-		332	75	-	407

T_m: melting temperature; T_g: glass transition temperature; Mwt: molecular weight, V_{cation}: cation molecular volume, V_{anion}: anion molecular volume; [a)]Total molecular volume of ionic liquid calculated from the corresponding density, [b)] Total molecular volume of ionic liquid calculated from the molecular volume of both cation and anion reported by Kobrak et al. [46].

The short scale morphology of virgin cellulose acetate and cellulose acetate grafted with imidazolium and ammonium ionic liquids containing the different anions Tf_2N^-, BF_4^-, Br^- and AcO^- was then assessed by synchrotron SAXS experiments to assess the dispersion state of the grafted ionic liquids in the membrane materials. Previous studies have evidenced that the dispersion state of the grafts (*i.e.* finely dispersed or aggregated into nano-structures) has a strong impact on the separation properties of grafted cellulose acetate membranes [12].

Figure 5 shows the scattered intensity of virgin cellulose acetate and both series of cellulose acetate-g-IL as a function of the scattering vector *q* over a range from 10^{-2} $Å^{-1}$ to 0.2 $Å^{-1}$. Virgin cellulose acetate exhibited the scattering pattern of a nano-heterogeneous particulate system with gyration radius close to 9 nm, typical of the size of cellulose acetate crystallites. The complexity of the structural organization of cellulose acetate solutions is well recognized through several studies of intermolecular aggregation in different solvents [47-49]. Light scattering measurements and size exclusion chromatography have evidenced microgels rich in cellulose triacetate blocks (partly crystalline microregions) [47]. Such heterogeneities were likely to develop as concentration increased during membrane formation and obviously subsisted in the final membrane morphology [48]. In this work, the grafting of cellulose acetate with different ILs induced a change in the scattering regime (in the scattering vector range from 10^{-2} to 2-4 10^{-2} $Å^{-1}$) with a scattering law $I(q) \sim q^{-3}$ associated with more homogeneous structures at the nanoscale. The new scattering data showed the disappearance of the cellulose acetate crystallites, but with possible larger scale fluctuations at the micron-range. The scattering pattern of both series of cellulose acetate-g-IL could not be analyzed in details through standard procedures since the characteristic sizes were larger than 50 nm. Furthermore, the absence of any correlation peak for the grafted ionic liquids showed that they were homogeneously dispersed in the polymer membranes irrespective of their cation and anion structure.

a) Cellulose acetate-g-[C_5C_1im][X]

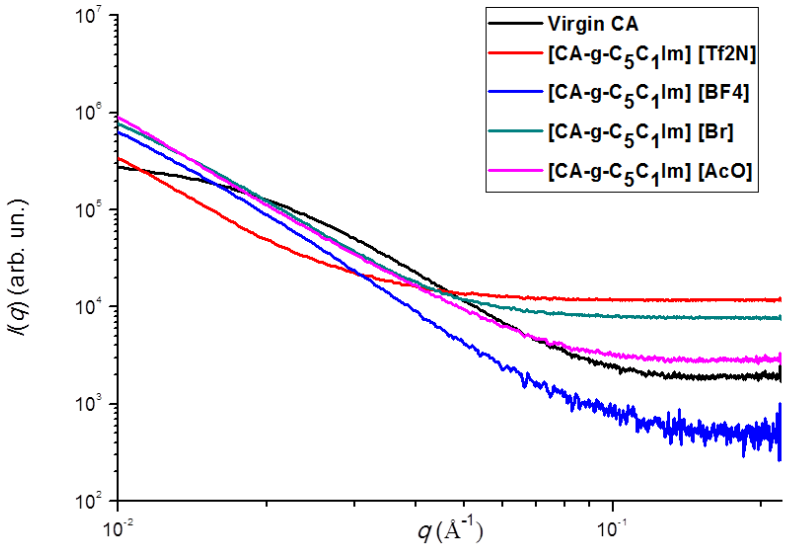

b) Cellulose acetate-g-[$C_5C_2C_2C_1N$][X]

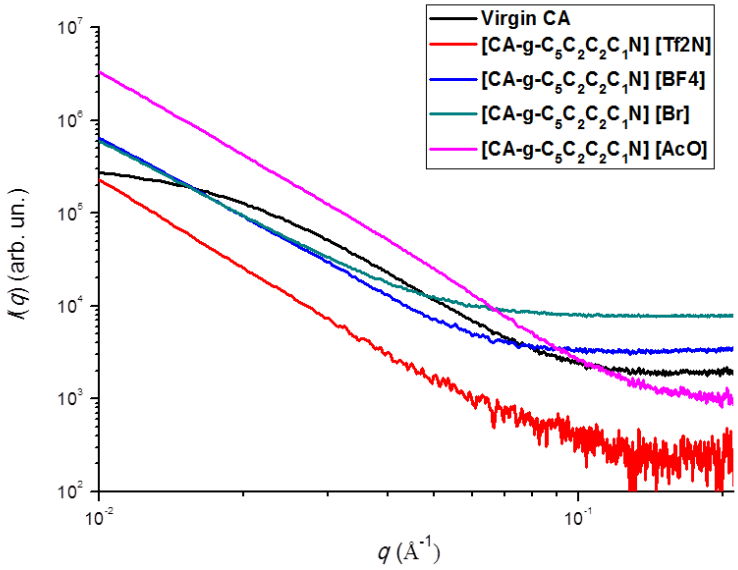

Figure 5: Influence of the ionic liquid anion X^- on synchrotron small angle X-ray scattering (SAXS) for nearly identical ionic liquid amounts ($W_{IL} \cong 17$ wt%) for : a) cellulose acetate-g-[C_5C_1im][X] and b) cellulose acetate-g-[$C_5C_2C_2C_1N$][X] in comparison with virgin cellulose acetate

3.2. Sorption properties of cellulose acetate grafted with ionic liquids containing different anions for ETBE purification

The sorption-diffusion model states that the permeation of a liquid mixture through a dense membrane is mainly governed by two sequential steps. The first step corresponds to some liquid absorption at the membrane upstream side. This sorption step is usually selective and contributes to the pervaporation selectivity. The second step is the diffusion of the absorbed molecules through the dense membrane. In the following part of this work, the sorption properties of cellulose acetate grafted with ionic liquids containing different anions will be analyzed in terms of structure-property relationships to reveal the influence of the ionic liquid anion on the first step of pervaporation mass transfer.

3.2.1 Influence of the ionic liquid anion on sorption properties of cellulose acetate grafted with different ionic liquids for ETBE purification

Sorption experiments were carried out for the azeotropic mixture EtOH/ETBE (20/80 wt %) at 30°C for experimental reasons. Both series of cellulose acetate-g-[C_5C_1im][X] and cellulose acetate-g-[$C_5C_2C_2C_1$N][X] with very close ionic liquids contents (ca. 17 wt%) but different anions (Tf_2N^- BF_4^-, Br^- and AcO^-) were investigated.

Table 2 shows the sorption results obtained for the different membranes in comparison with cellulose acetate. The virgin polysaccharide derivative led to fairly low total swelling S (4.2 wt%) and very high sorption separation factor (129) due to the polymer stiffness and the presence of hydroxyl side groups having very high affinity with ethanol. After grafting of cellulose acetate with *imidazolium* ionic liquids with different anions, the total swelling decreased or increased depending on the anion structure. The fluorinated anions led to slightly lower total swelling of 4 wt% and 3 wt% and sorption separation factors of 62 and 76 for Tf_2N^- and BF_4^-, respectively. However, it was initially surprising that the most fluorinated anion (Tf_2N^-) led to a slightly increased total swelling compared to the less fluorinated one (BF_4^-). This particular behavior will be better understood on the basis of the Kamlet-Taft analysis of the membrane properties reported in the last section. In contrast, the hydrophilic anions (Br^- and AcO^-) improved the total swelling compared to virgin cellulose acetate by +45% and +114%, respectively, with very high ethanol sorption separation factors of 396 and 196.

For cellulose acetate grafted with *ammonium* ionic liquids containing different anions, the anion influence on the sorption data generally followed the same trends as for the first series based on the imidazolium ionic liquids. Nevertheless, for a given anion, the total swelling was systematically slightly higher and the sorption separation factor significantly

decreased with the ammonium cation. This decrease in sorption selectivity was ascribed to an increase in sorption synergy due to a better membrane plasticization after total swelling increase as discussed in our former work on the cation influence [34].

Table 2 Sorption properties for the separation of the azeotropic mixture EtOH/ETBE with cellulose acetate-g-[C_5C_1im][X] and cellulose acetate-g-[$C_5C_2C_2C_1$N][X] with nearly identical ionic liquid amounts ($W_{IL} \cong 17$ wt%) in comparison with virgin cellulose acetate.

Anion	Imidazolium cation			Ammonium cation		
	S (wt.%)	C^s_{EtOH} (wt.%)	β_s	S (wt.%)	C^s_{EtOH} (wt.%)	β_s
CA	4.2	0.97	129	4.2	0.97	129
Tf_2N^-	4	0.94	62	5.3	0.91	40
BF_4^-	3	0.95	76	4	0.94	62
Br^-	6.1	0.99	396	8.4	0.975	156
AcO^-	9	0.98	196	11	0.96	96

W_{IL}: ionic liquid weight fraction in the grafted cellulose acetate; S: total swelling at sorption equilibrium; C^s_{EtOH}: ethanol content in the absorbed mixture; β_s: sorption separation factor

3.3. Pervaporation properties of cellulose acetate grafted with different ionic liquids for ETBE purification

The temperature of the pervaporation experiments was 50°C instead of 30°C formerly used for the sorption measurements [12]. A temperature of 50°C can be easily reached in industrial pervaporation modules and the fluxes were improved, which also facilitated comparison between the different membranes. Table 3 reports the pervaporation results for the separation of the azeotropic mixture EtOH/ETBE with virgin cellulose acetate and cellulose acetate grafted with imidazolium or ammonium ionic liquids differing in their anions. Ionic liquid grafting generally improved the pervaporation flux and this improvement strongly depended upon the cation and anion structures. Furthermore, the membranes of both series, whatever the type of the anion, were extremely selective with permeate samples containing 100 wt% of ethanol corresponding to infinite separation factors.

Table 3 Pervaporation properties for the separation of the azeotropic mixture EtOH/ETBE with cellulose acetate-g-[C_5C_1im][X] and cellulose acetate-g-[$C_5C_2C_2C_1$N][X] with nearly identical ionic liquid amounts ($W_{IL} \cong 17$ wt%) in comparison with virgin cellulose acetate at 50°C.

Anion	Imidazolium cation			Ammonium cation		
	J (kg/h m^2)for 5µm	C' (wt%)	β_{PV}	J (kg/h m^2)for 5µm	C' (wt%)	β_{PV}
CA	0.023	100	∞	0.023	100	∞
Tf_2N^-	0.078	100	∞	0.095	100	∞
BF_4^-	0.038	100	∞	0.026	100	∞
Br^-	0.05	100	∞	0.1815	100	∞
AcO^-	0.13	100	∞	0.41	100	∞

J: total flux normalized for a reference membrane thickness of 5 µm; C': ethanol content in permeate ; β_{pv}: pervaporation separation factor; β_D: diffusion separation factor.

The pervaporation properties of virgin cellulose acetate were consistent with the data formerly reported by Nguyen *et al.* for this separation (J = 0.08 kg/m²/h and C' = 100 wt% at 40°C) [13] although the pervaporation flux obtained in this work (J = 0.023 kg/m²/h) was slightly inferior despite the higher temperature (50 °C). This slightly lower flux may be due to the much higher average molecular weight of the cellulose acetate investigated in this work (50,000 g/mol) compared to that reported in the former work (29,000 g/mol). Differences in membrane casting procedures may also have slightly affected the membrane flux of this glassy polymer. In this work also, the permeate contained ethanol only (C' = 100 wt%) in good agreement with the former results reported by Nguyen *et al.* for virgin cellulose acetate [13].

For the *imidazolium* series, the pervaporation flux was increased by nearly 3.4 fold with the most fluorinated Tf_2N^- anion whereas it increased by 1.6 fold only with the less fluorinated BF_4^- anion. Similarly as for sorption, for the fluorinated anions, the Tf_2N^- anion led to the best flux due to better membrane swelling and plasticization. The hydrophilic bromide anion improved the flux by nearly 2 fold, which still remained lower than that obtained with Tf_2N^-, although the corresponding total swelling was higher (+152%). This particular behavior was

ascribed to the weaker plasticizing effect of the grafted ionic liquid in that case, as shown by the highest polymer glass transition temperature found with the bromide anion. Nevertheless, by exchanging the bromide anion for the AcO^- anion, the flux strongly improved by nearly 5.7 fold due to better membrane plasticization and swelling.

For the *ammonium* series, the pervaporation fluxes were even more improved with all anions except for BF_4^- compared to those of the first imidazolium series. Compared to virgin cellulose acetate, the flux were increased by 4 fold for the Tf_2N^- anion. The hydrophilic anions (Br^- and AcO^-) led to the best flux improvement by nearly 8 and 18 fold, respectively, due to improved membrane swelling and plasticization. The best pervaporation properties (J = 0.41 kg/h m^2 for 5 µm and infinite separation factor) were thus achieved with cellulose acetate grafted with the ammonium ionic liquid containing the acetate counter anion.

3.4. Kamlet-Taft analysis of the membrane properties based on ionic liquid polarity parameters

According to the best of our knowledge, very little is known about the influence of ionic liquid anion on membrane properties for liquid separations due to the lack of systematic studies involving homologous series of ionic liquids with several anions. Nevertheless, a few authors working on thermodynamic or membrane properties for gas permeation have already mentioned that this influence is particularly complex [50-53]. To have a better understanding of this influence on the membrane properties, a structure-property relationship analysis was then made on the basis of physico-chemical parameters in the Kamlet and Taft polarity scale [54]. This scale is commonly used to estimate solvation properties and physico-chemical features in terms of hydrogen bonding donor ability (α), hydrogen bonding acceptor ability (β) and polarizability (π*) for organic solvents and molecular ionic liquids [55].

3.4.1. Choice of the Kamlet-Taft parameters used for the physico-chemical analysis

Kamlet-Taft parameters are known to depend on the molecular probes used for determining them. Therefore, Kamlet-Taft parameters determined using the same molecular probes (*i.e. N*,*N*-diethyl-4-nitroaniline/4-nitroaniline) have been selected in this work for allowing a proper comparison. The Kamlet-Taft parameters of the ionic liquids of interest have not been reported yet and their measurement at a common temperature would be very difficult owing to the very high melting temperature of the corresponding ammonium bromide (T_m = 142°C). For this reason, the Kamlet-Taft parameters α, β, and π* have been considered for a series of closely related imidazolium ionic liquids $[C_4C_1im][Tf_2N]$, $[C_4C_1im][BF_4]$, $[C_4C_1im][AcO]$ and $[C_6C_1im][Br]$ in Table 4. Because of the high melting

temperature ($T_m \cong 65°C$) of the ionic liquid [C_4C_1im][Br] [44], which is not appropriate for these measurements, the Kamlet-Taft parameters of a closely related ionic liquid ([C_6C_1im][Br]) which is a liquid at room temperatue [56] were used to assess the influence of the bromide anion on the membrane properties. According to the work of Spange *et al.* having correlated the ionic liquid polarity parameters with their molecular structure, the Kamlet-Taft parameters of [C_6C_1im][Br] should not differ significantly from those of [C_4C_1im][Br] [57].

In Table 4, the hydrogen bonding donor ability α of the imidazolium ionic liquids with the hydrophobic anions (Tf_2N^-, BF_4^-) was higher than that obtained with the hydrophilic anions (Br^-, AcO^-). On the other hand, their hydrogen bonding acceptor ability β increased with the hydrophilic character of the ionic liquid anions in the following order $Tf_2N^- < BF_4^- < Br^- < AcO^-$. The π^* polarizability parameters were nearly the same for TF_2N^-, BF_4^- and Br^- while that of AcO^- was significantly lower. Kamlet-Taft parameters for the related ammonium ionic liquids have not been reported in the literature. Nevertheless, according to former works [34], their Kamlet-Taft parameters are expected to vary with the anion in the same way as that reported for the imidazolium ionic liquids.

Table 4 Kamlet-Taft parameters of closely related imidazolium ionic liquids used for the structure-property relationship analysis of the membrane sorption and pervaporation properties.

Ionic liquid	**α**	**β**	**π^***
[C_4C_1im][TF_2N][a]	0.61	0.23	0.984
[C_4C_1im][BF_4][a]	0.63	0.37	1.05
[C_6C_1im][Br][b]	0.45	0.74	1.09
[C_4C_1im][Ac][c]	0.57	1.18	0.89
Ethanol	0.83	0.75	0.51

[a] Ref:[58], [b] Ref [59],[c] Ref[60]

3.4.2. Kamlet-Taft analysis of the sorption and pervaporation properties

Figure 6 makes a comparison of the *sorption* properties of both series of cellulose acetate grafted with imidazolium or ammonium ionic liquids containing different anions X^-. In this Figure, the anions were ranked in the order of increasing hydrogen bonding donor ability β of the grafted ionic liquid, showing that the total swelling usually increased with the hydrogen bonding ability of the grafted ionic liquid. A better hydrogen acceptor ability most likely favored strong interactions with ethanol, which is a strong hydrogen bonding donor (α = 0.83 [61].

Nevertheless, the Tf_2N^- anion led to an interesting significant swelling increase compared to the BF_4^- anion for both membrane series, although the corresponding hydrogen bonding acceptor ability β was higher. These results evidenced that at least another parameter was contributing to the sorption behavior of these membranes. The anion molar volume (Br^- << BF_4^- ≅ AcO^- << Tf_2N^- (Table 1)) also played a role in membrane swelling. Increasing the anion size was responsible for weakening the interactions between the cation and anion, finally allowing slightly better interactions with the azeotropic mixture for both hydrophobic and hydrophilic anions. This influence was particularly obvious for the biggest hydrophobic fluorinated anion (Tf_2N^-) but it certainly also participated to the best swelling obtained with the biggest hydrophilic anion (AcO^-).

For both membranes series, the ethanol weight fraction of the absorbed mixture C^S_{EtOH} was very high and followed the same general trend irrespective of the ionic liquid cation. As expected for these EtOH selective membranes, it increased with the hydrogen bonding acceptor ability β of the grafted ionic liquids for the following anions Tf_2N^- < BF_4^- < Br^-. The AcO^- anion led to a slightly reduced C^S_{EtOH} compared to what would be expected from the former trend. The highest swelling obtained with this particular anion for both membrane series induced the strongest solvent induced plasticization and facilitated simultaneous ETBE absorption. This sorption synergy eventually led to a small decrease in sorption selectivity.

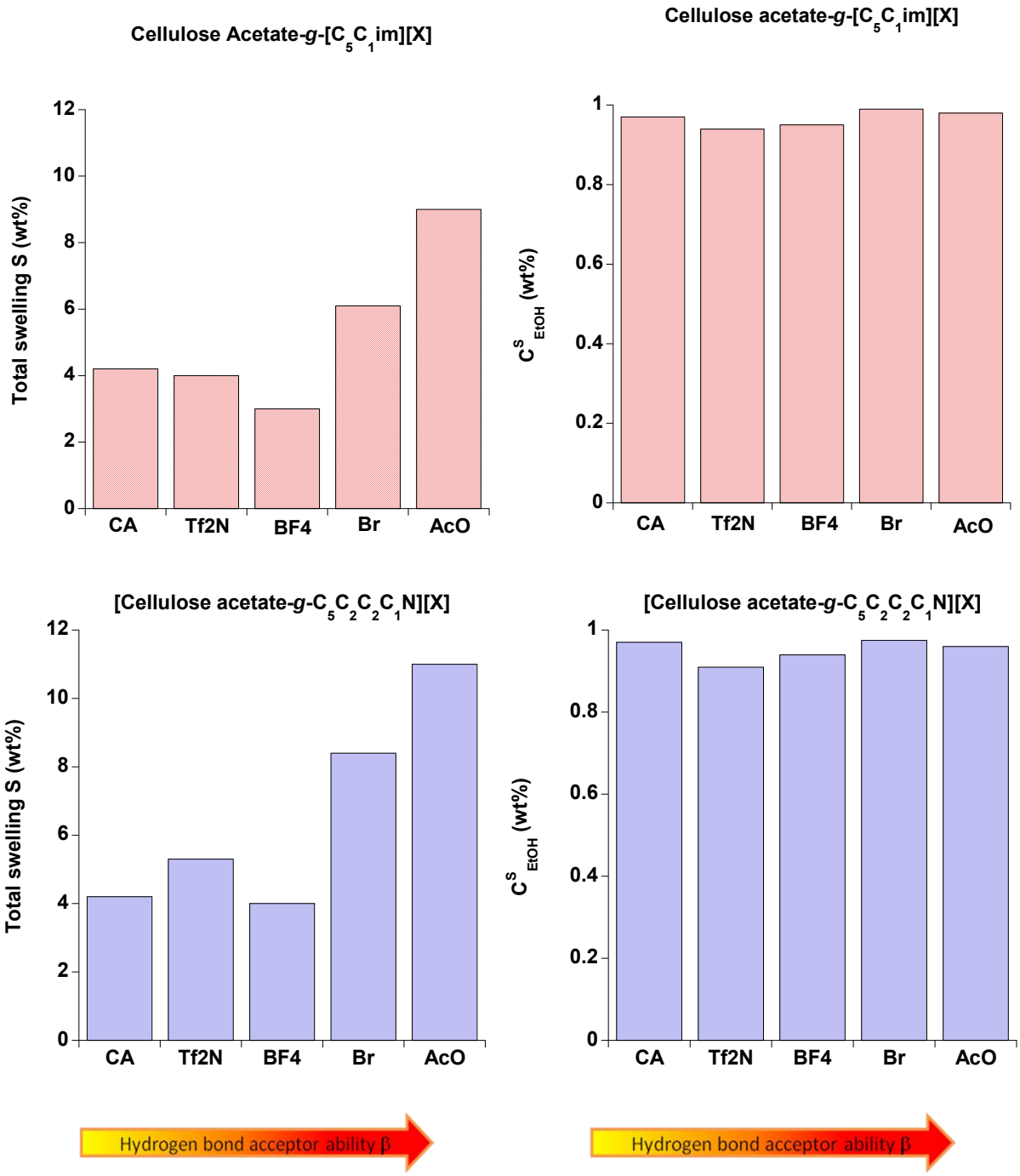

Figure 6: Influence of the ionic liquid anion on the sorption properties for the separation of the azeotropic mixture EtOH/ETBE with cellulose acetate-g-[C_5C_1im][X] and cellulose acetate-g-[$C_5C_2C_2C_1$N][X] with nearly identical ionic liquid amounts (W_{IL} ≅ 17 wt%) in comparison with virgin cellulose acetate.

In *pervaporation*, the permeate samples contained ethanol only and the pervaporation separation factors were infinite for both membrane series. Therefore, the total pervaporation flux was an ethanol flux in each case. Figure 7 showed that the pervaporation flux followed

the same general trends as the total swelling as a function of the hydrogen bonding acceptor ability β of the grafted ionic liquids but this influence was much stronger on the flux. The anion size obviously also played a role on membrane permeability. The biggest hydrophobic and hydrophilic anions (Tf_2N^- and AcO^-) favored permeation by improving membrane swelling, induced plasticization and solvent diffusion in an even better way than solvent sorption as expected from the free volume theories.

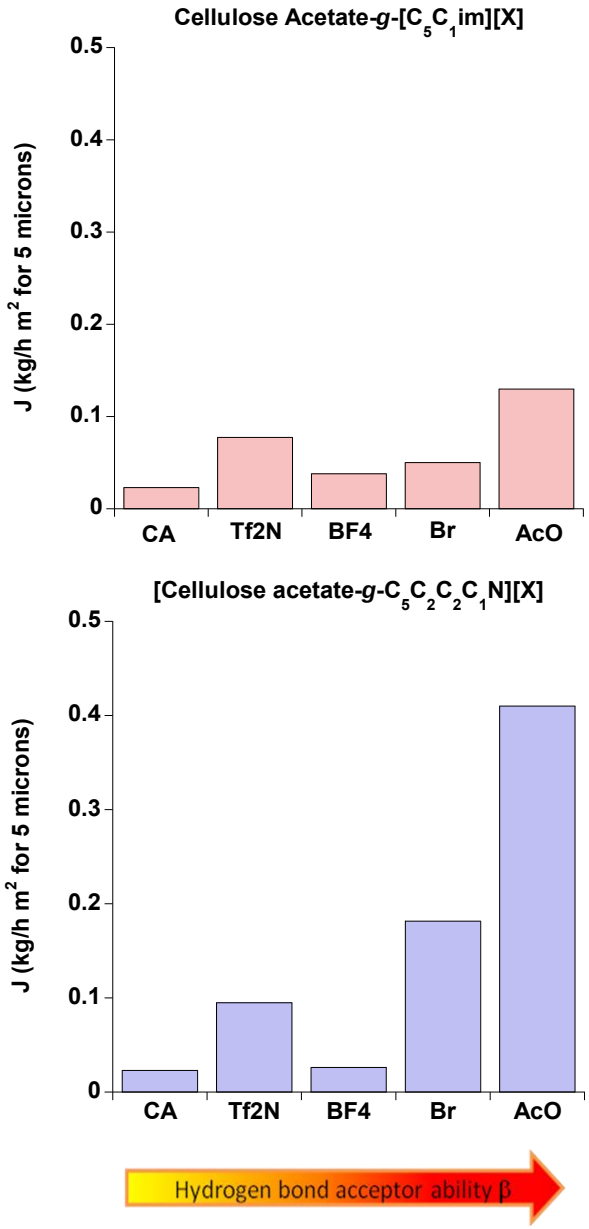

Figure 7: Influence of the ionic liquid anion on the pervaporation flux for the separation of the azeotropic mixture EtOH/ETBE with cellulose acetate-g-[C_5C_1im][X] and cellulose acetate-g-[$C_5C_2C_2C_1$N][X] with nearly identical ionic liquid amounts (W_{IL} ≅ 17 wt%) in comparison with virgin cellulose acetate.

These theories indeed consider that solvent diffusion coefficients vary exponentially with the membrane solvent content. Therefore, according to these theories, an increase in membrane swelling leads to an even better improvement of solvent diffusion. Finally, the membrane with the ionic liquid combining the best hydrogen bonding acceptor ability β with big cation and anion sizes (*i.e.* $[C_5C_2C_2C_1N][AcO]$) led to the best separation performance for ETBE purification by pervaporation.

4. Conclusion

Two cellulose acetate polymers grafted with nearly identical amounts ($W_{IL} \cong 17$ wt%) of bromide imidazolium and ammonium ionic liquids were used as precursors for anion exchange with various salts. Using large salt excesses led to quantitative exchange for the fluorinated anions (Tf_2N^- and BF_4^-) as shown by ^{19}F NMR analysis. The exchange of bromide for the AcO^- anion was really challenging given the degradation of cellulose acetate in basic conditions and the very poor solubility of common acetate salts in cellulose acetate solvents, finally limiting the exchange rate to 66% for this anion. Nevertheless, 8 membranes made of cellulose acetate grafted with imidazolium and ammonium ionic liquids differing in their anions (Tf_2N^- BF_4^-, Br^- and AcO^-) enabled the first physico-chemical analysis of the anion influence in homologous membrane series for liquid separation.

During sorption of the azeotropic mixture EtOH/ETBE, the total swelling increased with the hydrogen bonding acceptor ability β of the grafted ionic liquid and the anion size, which both favored membrane interactions with ethanol. The very high sorption selectivity also increased with the hydrogen bonding acceptor ability β of the grafted ionic liquid but this increase was partially compensated by sorption synergy for the highest swelling obtained with the best anion (AcO^-). During pervaporation, all of these membranes permeated ethanol only. The pervaporation flux followed the same general trends as the total swelling but the flux improvement was even stronger than that of swelling as expected from the free volume theories accounting for solvent diffusion through dense polymer membranes.

Finally, the ammonium ionic liquid with the acetate anion combined the highest hydrogen bonding acceptor ability β with big molecular size and led to the best membrane properties with a normalized flux of 0.41 kg/h m^2 (almost 20 times that of virgin cellulose acetate) for a reference membrane thickness of 5 µm and a permeate ethanol content of 100% corresponding to an infinite membrane separation factor at 50°C.

5. Acknowledgements

The authors would like to thank the ELEMENT Erasmus Mundus Programme for the PhD scholarship and the corresponding extension offered to Mrs Faten HASSAN HASSAN ABDELLATIF.

6. References

[1] H. Noureddini, Ethyl tert-butyl ether and methyl tert-butyl ether: status, review, and alternative use. Exploring the environmental issues of mobile, recalcitrant compounds in gasoline, ACS Symposium Series, 799 (2002) 107-124.

[2] K.F. Yee, A.R. Mohamed, and S.H. Tan, A review on the evolution of ethyl tert-butyl ether (ETBE) and its future prospects, Renewable and Sustainable Energy Reviews, 22 (2013) 604-620.

[3] E. Drioli and L. Giorno, eds. *Comprehensive Membrane Science and Engineering*. 2010, Elsevier Science.

[4] E.M.V. Hoek and V.V. Tarabara, eds. *Encyclopedia of Membrane Science and Technology*. 2013, John Wiley & Sons.

[5] R.W. Baker, Membrane technology and applications, 2nd ed, John Wiley & Sons, Chichester, 2004.

[6] L.M. Robeson, The upper bound revisited, Journal of Membrane Science, 320 (2008) 390-400.

[7] J. Chen, J. Zhang, Y. Feng, J. Wu, J. He, and J. Zhang, Synthesis, characterization, and gas permeabilities of cellulose derivatives containing adamantane groups, Journal of Membrane Science, 469 (2014) 507-514.

[8] E. Weber de Menezes and R. Cataluna, Optimization of the ETBE (ethyl tert-butyl ether) production process, Fuel Processing Technology, 89 (2008) 1148-1152.

[9] A. Jonquieres, C. Arnal-Herault, and J. Babin, Pervaporation, in: E.M.V. Hoek, V.V. Tarabara (Eds.) Encyclopedia of Membrane Science and Technology, Wiley, volume 3 (2013) pp. 1533-1559.

[10] A. Jonquieres, R. Clement, P. Lochon, M. Dresch, and B. Chrétien, Industrial state of the art of pervaporation and vapor permeation in the Western countries, Journal of Membrane Science, 206 (2002) 87-117.

[11] G.S. Luo, M. Niang, and P. Schaetzel, Pervaporation separation of ethyl tert-butyl ether and ethanol mixtures with a blended membrane, Journal of Membrane Science, 125 (1997) 237-244.

[12] M. Billy, A. Ranzani Da Costa, P. Lochon, R. Clement, M. Dresch, and A. Jonquieres, Cellulose acetate graft copolymers with nano-structured architectures: Application to the purification of bio-fuels by pervaporation, Journal of Membrane Science, 348 (2010) 389-396.

[13] Q.T. Nguyen, C. Leger, P. Billard, and P. Lochon, Novel membranes made from a semi-interpenetrating polymer network for ethanol-ETBE separation by pervaporation, Polymers for Advanced Technologies, 8 (1997) 487-495.

[14] Q.T. Nguyen, R. Clement, I. Noezar, and P. Lochon, Performances of poly(vinylpyrrolidone-co-vinyl acetate)- cellulose acetate blend membranes in the pervaporation of ethanol-ethyl tert-butyl ether mixtures. Simplified model for flux prediction, Separation and Purification Technology, 13 (1998) 237-245.

[15] R. Rogers and K. Seddon, eds. *Industrial applications of ionic liquids*. 2002, American Chemical Society Books.

[16] P. Wasserscheid and T. Welton, Ionic liquids in Synthesis, 2nd ed, Wiley-VCH, Weinheim, 2008.

[17] R. Bini, O. Bortolini, C. Chiappe, D. Pieraccini, and T. Siciliano, Development of Cation/Anion "Interaction" Scales for Ionic Liquids through ESI-MS Measurements, The Journal of Physical Chemistry B, 111 (2007) 598-604.

[18] J.D. Holbrey and R.D. Rogers, Physicochemical Properties, in P. Wasserscheid and T. Welton (Eds.). Ionic Liquids in Synthesis, Wiley-VCH Verlag GmbH & Co. KGaA, 2008, pp. 57-174.

[19] Y. Fukaya, H. Ohno, and S.T. Hirasawa, Chapter 8 - Energy-Saving Biomass Processing with Polar Ionic Liquids. Research Approaches to Sustainable Biomass Systems, Academic Press, Boston, 2014, pp. 205-223.

[20] L.J. Lozano, C. Godinez, A.P. de los Rios, F.J. Hernandez-Fernandez, S. Sanchez-Segado, and F.J. Alguacil, Recent advances in supported ionic liquid membrane technology, Journal of Membrane Science, 376 (2011) 1-14.

[21] R.D. Noble and D.L. Gin, Perspective on ionic liquids and ionic liquid membranes, Journal of Membrane Science, 369 (2011) 1-4.

[22] P. Scovazzo, Determination of the upper limits, benchmarks, and critical properties for gas separations using stabilized room temperature ionic liquid membranes (SILMs) for the purpose of guiding future research, Journal of Membrane Science, 343 (2009) 199-211.

[23] S. Hanioka, T. Maruyama, T. Sotani, M. Teramoto, H. Matsuyama, K. Nakashima, M. Hanaki, F. Kubota, and M. Goto, CO_2 separation facilitated by task-specific ionic liquids using a supported liquid membrane, Journal of Membrane Science, 314 (2008) 1-4.

[24] J.J. Close, K. Farmer, S.S. Moganty, and R.E. Baltus, CO_2/N_2 separations using nanoporous alumina-supported ionic liquid membranes: Effect of the support on separation performance, Journal of Membrane Science, 390-391 (2012) 201-210.

[25] S.D. Hojniak, I.P. Silverwood, A.L. Khan, I.F.J. Vankelecom, W. Dehaen, S.G. Kazarian, and K. Binnemans, Highly Selective Separation of Carbon Dioxide from Nitrogen and Methane by Nitrile/Glycol-Difunctionalized Ionic Liquids in Supported Ionic Liquid Membranes (SILMs), The Journal of Physical Chemistry B, 118 (2014) 7440-7449.

[26] P. Izak, K. Friess, and M. Sipek, Chapter 12 : Pervaporation and permeation taking advantage of ionic liquids, in S.V. Gorley (Ed.). Handbook of membrane research: Properties, performances and applications, Nova Science Publishers, New York, 2010, pp. 387-402.

[27] G. Fadeev and M.M. Meagher, Opportunities for ionic liquids in recovery of biofuels, Chemical Communications, 3 (2001) 295-296.

[28] P. Izak, W. Ruth, Z. Fei, P.J. Dyson, and U. Kragl, Selective removal of acetone and butan-1-ol from water with supported ionic liquid-polydimethylsiloxane membrane by pervaporation, Chemical Engineering Journal, 139 (2008) 318-321.

[29] M. Matsumoto, Y. Murakami, and K. Kondo, Separation of 1-butanol by pervaporation using polymer inclusion membranes containing ionic liquids, Solvent Extraction Research and Development, 18 (2011) 75-83.

[30] S. Heitmann, J. Krings, P. Kreis, A. Lennert, W.R. Pitner, A. Górak, and M.M. Schulte, Recovery of n-butanol using ionic liquid-based pervaporation membranes, Separation and Purification Technology, 97 (2012) 108-114.

[31] G.O. Yahaya, F. Hamad, A. Bahamdan, V.V.R. Tammana, and E.Z. Hamad, Supported ionic liquid membrane and liquid–liquid extraction using membrane for removal of sulfur compounds from diesel/crude oil, Fuel Processing Technology 113 (2013) 123-129.

[32] H.R. Cascon and S.K. Choudhari, 1-Butanol pervaporation performance and intrinsic stability of phosphonium and ammonium ionic liquid-based supported liquid membranes, Journal of Membrane Science, 429 (2013) 214-224.

[33] A. Plaza, G. Merlet, A. Hasanoglu, M. Isaacs, J. Sanchez, and J. Romero, Separation of butanol from ABE mixtures by sweep gas pervaporation using a supported gelled ionic liquid

membrane: Analysis of transport phenomena and selectivity, Journal of Membrane Science, 444 (2013) 201-212.

[34] F. Hassan Hassan Abdellatif, J. Babin, C. Arnal-Herault, L. David, and A. Jonquieres, Grafting of cellulose acetate with ionic liquids for biofuel purification by a membrane process : Influence of the cation, Carbohydrate Polymers, (2015) submitted (corresponding to the second part of PhD chapter 3).

[35] R.W. Baker, J.G. Wijmans, and Y. Huang, Permeablity, permeance and selectivity: A preferred way of reporting pervaporation performance data, Journal of Membrane Science, 348 (2010) 346-352.

[36] I. Dinares, C. Garcia de Miguel, A. Ibanez, N. Mesquida, and E. Alcalde, Imidazolium ionic liquids: A simple anion exchange protocol, Green Chemistry, 11 (2009) 1507-1510.

[37] E.I. Izgorodina, Towards large-scale, fully ab initio calculations of ionic liquids, Physical Chemistry Chemical Physics, 13 (2011) 4189-4207.

[38] J.G. Huddleston, A.E. Visser, W.M. Reichert, H.D. Willauer, G.A. Broker, and R.D. Rogers, Characterization and comparison of hydrophilic and hydrophobic room temperature ionic liquids incorporating the imidazolium cation, Green Chemistry, 3 (2001) 156-164.

[39] J.L. Anthony, J.F. Brennecke, J.D. Holbrey, E.J. Maginn, R.A. Mantz, R.D. Rogers, P.C. Trulove, A.E. Visser, and T. Welton, Physicochemical Properties of Ionic Liquids. Ionic Liquids in Synthesis, Wiley-VCH Verlag GmbH & Co. KGaA, 2003, pp. 41-126.

[40] J.D. Holbrey and K.R. Seddon, The phase behaviour of 1-alkyl-3-methylimidazolium tetrafluoroborates; ionic liquids and ionic liquid crystals, Journal of the Chemical Society, Dalton Transactions, (1999) 2133-2140.

[41] S. Zhang, N. Sun, X. He, X. Lu, and X. Zhang, Physical Properties of Ionic Liquids: Database and Evaluation, Journal of Physical and Chemical Reference Data, 35 (2006) 1475-1517.

[42] S. Xin and L.A. Jennifer, Influences of Side Chain Length of 1-Alkyl-3-methylimidazolium Bromide on Silica Saturation. Ionic Liquids: From Knowledge to Application, American Chemical Society, 2009, (1030), pp. 189-197.

[43] C.P. Fredlake, J.M. Crosthwaite, D.G. Hert, S.N.V.K. Aki, and J.F. Brennecke, Thermophysical Properties of Imidazolium-Based Ionic Liquids, Journal of Chemical & Engineering Data, 49 (2004) 954-964.

[44] L.M. Ramenskaya, E.P. Grishina, A.M. Pimenova, and M.S. Gruzdev, The influence of water on the physicochemical characteristics of 1-butyl-3-methylimidazolium bromide ionic liquid, Russian Journal of Physical Chemistry A, Focus on Chemistry, 82 (2008) 1098-1103.

[45] K.G. Bogolitsyn, T.E. Skrebets, and T.A. Makhova, Physicochemical properties of 1-butyl-3-methylimidazolium acetate, Russian Journal of General Chemistry, 79 (2009) 125-128.

[46] M.N. Kobrak, The relationship between solvent polarity and molar volume in room-temperature ionic liquids, Green Chemistry, 10 (2008) 80-86.

[47] E. Fleury, J. Dubois, C. Léonard, J.P. Joseleau, and H. Chanzy, Microgels and ionic associations in solutions of cellulose diacetate, Cellulose, 1 (1994) 131-144.

[48] K.D. Goebel, G.C. Berry, and D.W. Tanner, Properties of cellulose acetate. III. Light scattering from concentrated solutions and films. Tensile creep and desalination studies on films Journal of Polymer Science: Polymer Physics Edition, 17 (1979) 917-937.

[49] H. Suzuki, Y. Muraoka, M. Satio, and K. Kamide, Light-scattering study on cellulose diacetate in 2-butanone, European Polymer Journal, 18 (1982) 831-837.

[50] P.J. Carvalho and J.A.P. Coutinho, The polarity effect upon the methane solubility in ionic liquids: a contribution for the design of ionic liquids for enhanced CO_2/CH_4 and H_2S/CH_4 selectivities, Energy & Environmental Science, 4 (2011) 4614-4619.

[51] J.L. Anthony, J.L. Anderson, E.J. Maginn, and J.F. Brennecke, Anion Effects on Gas Solubility in Ionic Liquids, The Journal of Physical Chemistry B, 109 (2005) 6366-6374.

[52] J.E. Bara, Ionic Liquids in Gas Separation Membranes. Encyclopedia of Membrane Science and Technology, John Wiley & Sons, Inc., 2013.

[53] A.B. Pereiro, J.M.M. Araujo, J.M.S.S. Esperanca, I.M. Marrucho, and L.P.N. Rebelo, Ionic liquids in separations of azeotropic systems - A review, The Journal of Chemical Thermodynamics, 46 (2012) 2-28.

[54] M.J. Kamlet and R.W. Taft, The solvatochromic comparison method. I. The .beta.-scale of solvent hydrogen-bond acceptor (HBA) basicities, Journal of the American Chemical Society, 98 (1976) 377-383.

[55] C. Reichardt, Polarity of ionic liquids determined empirically by means of solvatochromic pyridinium N-phenolate betaine dyes, Green Chemistry, 7 (2005) 339-351.

[56] http://www.tcichemicals.com/eshop/en/us/commodity/H1227/.

[57] S. Spange, R. Lungwitz, and A. Schade, Correlation of molecular structure and polarity of ionic liquids, Journal of Molecular Liquids, 192 (2014) 137-143.

[58] M.A. Ab Rani, A. Brant, L. Crowhurst, A. Dolan, M. Lui, N.H. Hassan, J.P. Hallett, P.A. Hunt, H. Niedermeyer, J.M. Perez-Arlandis, M. Schrems, T. Welton, and R. Wilding, Understanding the polarity of ionic liquids, Physical Chemistry Chemical Physics, 13 (2011) 16831-16840.

[59] A. Jelicic, N. Garcia, H.-G. Lohmannsroben, and S. Beuermann, Prediction of the Ionic Liquid Influence on Propagation Rate Coefficients in Methyl Methacrylate Radical Polymerizations Based on Kamlet-Taft Solvatochromic Parameters, Macromolecules, 42 (2009) 8801-8808.

[60] T.V. Doherty, M. Mora-Pale, S.E. Foley, R.J. Linhardt, and J.S. Dordick, Ionic liquid solvent properties as predictors of lignocellulose pretreatment efficacy, Green Chemistry, 12 (2010) 1967-1975.

[61] M.J. Kamlet, J.-L.M. Abboud, M.H. Abraham, and R.W. Taft, Linear solvation energy relationships. 23. A comprehensive collection of the solvatochromic parameters, π*, α and β, and some methods for simplifying the generalized solvatochromic equation, Journal of Organic Chemistry, 48 (1983) 2877-2887.

Appendix

Appendix A. Quantitative determination of the exchange rate for the fluorinated anions

^{19}F NMR was used for characterizing the cellulosic derivatives containing the fluorinated anions. The chemical shifts were referenced to trifluoroacetic acid added to the NMR samples in very tiny amount. An internal standard (pentafluorophenol) was used for determining the anion exchange rates. The ^{19}F NMR samples were prepared by dissolving precisely ca. 15 mg of each grafted cellulosic polymer in 0.5 mL of DMSO-d_6 and 0.1 mL of a fresh pentafluorophenol stock solution (26.1 mg/1mL of DMSO-d_6) was then added for quantitative analysis.

After anion exchange with $LiTf_2N$, the mole number of the Tf_2N^- anions in the polymer chains was estimated from the integrated areas of the ^{19}F NMR peaks at 80.0 and 166.79 ppm corresponding to the 6 fluorine nuclei of the Tf_2N^- anions and two fluorine nuclei of the pentafluorophenol internal standard, respectively :

$$\frac{6n_{Tf_2N}}{2n_{internal\ standard}} = \frac{A_{80}}{A_{166.79}} \qquad \text{(A.1)}$$

The exchange rate of Tf_2N^- anions was then calculated from the following equation:

$$\frac{n_{Tf_2N}}{n_{anion\ (calculated)}} \times 100 \qquad \text{(A.2)}$$

where $n_{anion\ (calculated)}$ is the mole number of Tf_2N^- anions corresponding to 100% exchange for the known amount of polymer sample dissolved in the ^{19}F NMR tube.

The exchange rate of BF_4^- was estimated similarly from the mole number of the BF^-_4 anions in the polymer chains after anion exchange. Its calculation was made from the integrated areas of the ^{19}F NMR peaks at 149.0 and 166.79 ppm, corresponding to the four fluorine nuclei of the BF^-_4 anions and to two fluorine nuclei of the pentafluorophenol internal standard, respectively :

$$\frac{4n_{BF_4}}{2n_{internal\ standard}} = \frac{A_{149}}{A_{166.79}} \qquad \text{(A.3)}$$

Appendix B. Permeability data for ETBE purification by pervaporation

This Appendix reports the partial permeability data of ethanol and ETBE as *intrinsic* membrane properties, which only reflect the influence of polymer material and permeating species without the effect of the operating conditions. These partial permeability data were simply calculated as the ratio of partial flux over the corresponding driving force for mass transfer by a procedure we have already described [34].

Table A.1 Partial permeability of ethanol and ETBE for the separation by pervaporation of the azeotropic mixture EtOH/ETBE with cellulose acetate-g-[C_5C_1im][X] and cellulose acetate-g-[$C_5C_2C_2C_1$N][X] with nearly identical ionic liquid amounts ($W_{IL} \cong$ 17 wt%) in comparison with virgin cellulose acetate at 50°C.

Counter ion	**Imidazolium cation**		**Ammonium cation**	
	P_{EtOH} x 1000 (kg/h m^2 kPa)	P_{ETBE} x 1000 (kg/h m^2 kPa)	P_{EtOH} x 1000 (kg/h m^2 kPa)	P_{ETBE} x 1000 (kg/h m^2 kPa)
CA	2.22	0	2.22	0
Tf_2N^-	7.49	0	9.19	0
BF^-_4	3.67	0	2.5	0
Br^-	4.8	0	17.6	0
AcO^-	12.57	0	39.65	0

P_i: partial permeability of species i.

Appendix C: Structures and abbreviations for the different ionic liquids grafted onto cellulose acetate

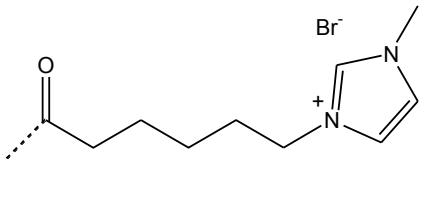

$[C_5C_1im][Br]$

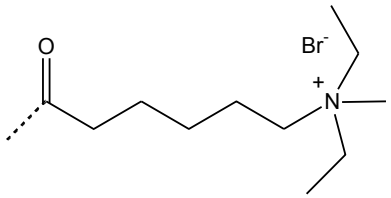

$[C_5C_2C_2C_1N][Br]$

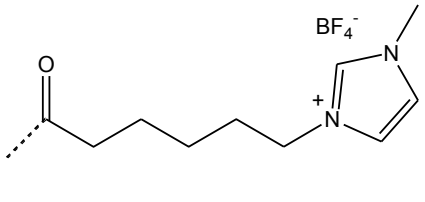

$[C_5C_1im][BF_4]$

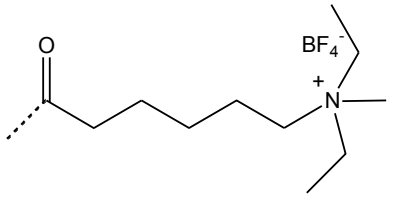

$[C_5C_2C_2C_1N][BF_4]$

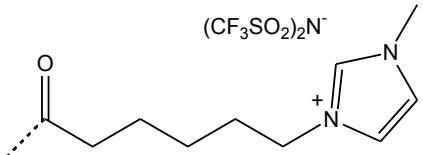

$[C_5C_1im][Tf_2N]$

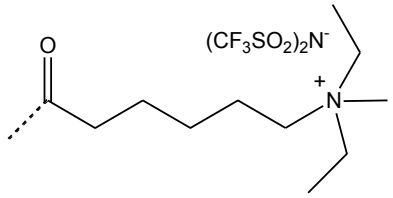

$[C_5C_2C_2C_1N][TF_2N]$

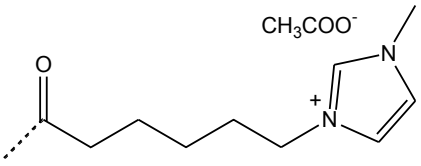

$[C_5C_1im][AcO]$

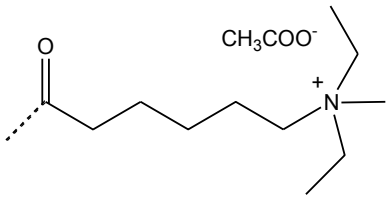

$[C_5C_2C_2C_1N][AcO]$

Conclusion of Chapter 3

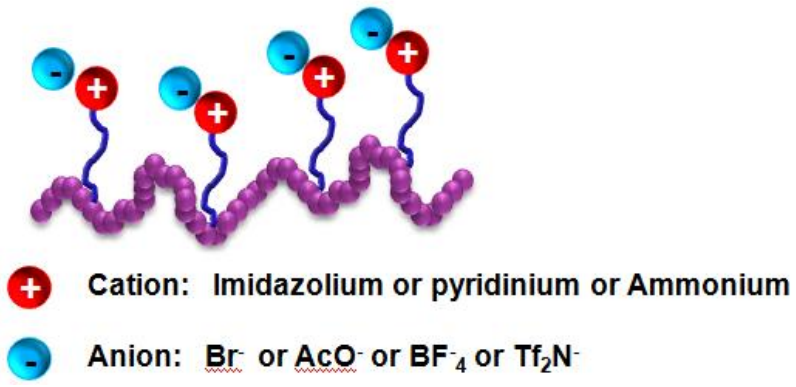

In this chapter, different strategies were reported for ionic liquid "grafting onto" cellulose acetate for *organoselective* membranes for ETBE purification. These grafting strategies extended the scope of ionic liquid-containing membranes to the challenging separation of purely organic mixtures, in which these ionic liquids are soluble.

In the first part of chapter 3, first attempts were made to graft an azido cellulose acetate with an alkyne-functionalized ionic liquid by the CuAAC "click" chemistry. Unfortunately, this strategy failed with the systematic gelation of the reaction medium, which was ascribed to a coupling side reaction involving the C-2 of the imidazolium ionic liquid and the anomeric carbon of the cellulose acetate reducing ends.

In the second part of chapter 3, an original simple strategy was then successfully developed for grafting cellulose acetate with various amounts of ionic liquids containing the same bromide anion and different cations (imidazolium, pyridinium and ammonium). The resulting materials were characterized by complementary techniques (^{1}H NMR, DSC and SAXS). The grafted ionic liquids were homogeneously dispersed in the polymer materials and they were responsible for strong polymer plasticizing, which increased in the following cation order: ammonium < pyridinium < imidazolium.

The sorption and pervaporation membrane features were then investigated for ETBE purification in terms of structure-property relationships. During sorption, both swelling and selectivity increased with the ionic liquid content. For the highest contents in different ionic liquids ($W_{IL} \cong 17$ wt %), swelling increased and sorption selectivity decreased in the following cation order : imidazolium < pyridinium < ammonium. During pervaporation in comparison with virgin cellulose acetate, the flux was increased up to factors 2 and 8 for the imidazolium and ammonium ionic liquids, respectively. The membranes with the maximum ionic liquid contents revealed outstanding infinite pervaporation separation factors with permeate samples containing ethanol only. An analysis of the membrane properties on the basis of the Kamlet and Taft parameters showed that the ammonium ionic liquid with the best hydrogen bonding acceptor ability (β) eventually led to the best membrane properties for ETBE purification with normalized flux of 0.182 kg/h m^2 for a reference membrane thickness of 5 µm and a permeate ethanol content of 100% at 50°C.

In the last part of Chapter 3, a procedure of anion exchange was used to analyze the influence of the anion structure (Tf_2N^-, BF_4^-, Br^- and AcO^-) on the membrane properties for imidazolium and ammonium ionic liquids ($W_{IL} \cong 17$ wt %). It was a real challenge for the AcO^- anion due to cellulose acetate degradation in basic conditions and the very poor solubility of

common acetate salts in cellulose acetate solvents, finally limiting the exchange rate to 66%. The exchange for fluorinated anions (Tf_2N^- and BF_4^-) was much easier and quantitative by using large excess of their corresponding salts.

The sorption and pervaporation properties of 8 membranes made of cellulose acetate grafted with imidazolium and ammonium ionic liquids differing in their anions (Tf_2N^- BF_4^-, Br^- and AcO^-) were then investigated for ETBE purification. During sorption, the swelling increased with the hydrogen bonding donor ability β of the grafted ionic liquid and the anion size, which both favored membrane interactions with ethanol. The very high sorption selectivity also increased with the parameter β but this increase was partially compensated by sorption synergy for the best swelling obtained with acetate anion. During pervaporation, all of these membranes permeated ethanol only. The pervaporation flux followed the same general trends as the swelling but the flux improvement was even better as expected from the free volume theories accounting for solvent diffusion through dense polymer membranes. Finally, the ammonium ionic liquid with the acetate anion combined the highest hydrogen bonding acceptor ability β with big molecular size and finally led to the best membrane properties with a flux of 0.41 kg/h m^2 (almost 20 times that of virgin cellulose acetate) for a reference membrane thickness of 5 µm and a permeate ethanol content of 100% at 50°C.

General Conclusion and Future Prospects

Ethyl *tert*-butyl ether (ETBE) is currently considered as one of the leading European bio-fuels. Widely used in gasoline blends, it improves the fuel octane number, its combustion and consequently air quality by minimizing toxic emissions. During the ETBE production from bio-ethanol and isobutene, ETBE forms an azeotropic mixture containing 20 wt% of ethanol, which is separated by the highly energy-intensive ternary distillation method. The pervaporation membrane process (PV) could offer an interesting alternative for this separation with *organoselective* membranes. Cellulosic membranes have been mainly reported for this application so far. In particular, cellulose acetate was highly selective with a permeate ethanol content of 100% but the flux of 0.023 kg/h m^2 obtained in this work for a reference membrane thickness of 5 µm was too low at 50°C.

In chapter 1, we reviewed the basics of "click" chemistry and the various types of "click" reactions before focusing on the Cu-catalyzed Azide-Alkyne Cycloaddition (CuAAC) of interest in this work. The second part made a thorough review on different CuAAC strategies for modifying cellulose and cellulosic derivatives at the macro, micro and nano-scales. Recently published as a book chapter, this review showed the great prospects offered by CuAAC "click" chemistry for the preparation of a wide range of advanced cellulose-based materials *e.g.* cross-linked networks, block and graft copolymers, dendronised celluloses, polyelectrolytes and functional nano-celluloses.

Relying on the conclusions of chapter 1, **chapter 2** reported the development of bio-based membranes by CuAAC "click" chemistry for ETBE purification. An α-alkyne- polylactide oligomer obtained by controlled ROP was grafted onto an azido cellulose acetate with high efficiency (87%). These copolymers were characterized by ATR-FTIR and ^{1}H NMR, showing that the PLA content was easily varied from 0 to 40.5 wt% in the grafted copolymers. The maximum PLA content was limited to less than 50 wt% to ensure the mechanical withstanding of the different membranes in the pervaporation conditions. According to SAXS, the PLA grafts were homogeneously dispersed and they induced a strong plasticizing of the polymer membranes as shown by DSC. The membrane properties were investigated in terms of structure-morphology-property relationships for the sorption and pervaporation of the targeted mixture. PLA grafting onto cellulose acetate improved the swelling (×2.6) and, to a much greater extent, the flux (×12) while the ethanol permeate content remained in the very high range (C' > 90 wt%) for ETBE purification by pervaporation.

In chapter 3, different strategies were developed for ionic liquid "grafting onto" cellulose acetate for ETBE purification. These strategies extended the scope of ionic liquid-containing membranes to the challenging separation of purely organic mixtures, in which these ionic liquids are soluble. The permanent grafting of these ionic liquids avoided their

extraction in the targeted azeotropic mixture EtOH/ETBE and led to stable membrane properties during pervaporation. Aiming at overcoming the limitations of the CuAAC "click" chemistry for grafting an imidazolium ionic liquid onto cellulose acetate, a new simple 2-step strategy has been developed for grafting ionic liquids efficiently. The first grafted ionic liquids contained the same bromide anion and different cations (imidazolium, pyridinium and ammonium) with increasing polar feature. The grafted ionic liquids led to strong membrane plasticizing in the *dry* state as shown by DSC while SAXS analysis evidenced that the ionic liquids were homogeneously dispersed in the membrane materials. The influence of ionic liquids cation on the membrane properties was analyzed in terms of structure-property relationships revealing the influence of the ionic liquid content, chemical structure and chemical physical parameters α, β, π* in the Kamlet-Taft polarity scale. The ammonium ionic liquid with the best hydrogen bonding acceptor ability (β) led to the best normalized flux of 0.182 kg/h m^2 for a reference membrane thickness of 5 µm and a permeate ethanol content of 100% at 50°C.

According to the best of our knowledge, very little is known about the influence of the ionic liquid anion on membrane properties due to the lack of systematic studies involving homologous series of ionic liquids. In the last part of chapter 3, two cellulose acetate polymers grafted with nearly identical amounts ($W_{IL} \cong 17$ wt %) of bromide imidazolium and ammonium ionic liquids were used as precursors for anion exchange with various anions (AcO^-, Tf_2N^-, and BF_4^-,). An analysis of the sorption and pervaporation properties showed that the anion played a strong and complex role on the membrane properties. The ionic liquid hydrogen bonding acceptor ability (β) and molecular size were identified as two key parameters for optimizing the membrane properties for ionic liquids with different anions.

The ammonium ionic liquid with the acetate anion, combining the highest hydrogen bonding acceptor ability β with big molecular size, finally led to the best membrane properties with a normalized flux of 0.41 kg/h m^2 (almost 20 times that of virgin cellulose acetate) for a reference membrane thickness of 5 µm and a permeate ethanol content of 100% corresponding to an infinite membrane separation factor at 50°C.

In the future, the extension of these "grafting onto" strategies to other types of grafts or polysaccharides could offer interesting prospects for membrane separation processes or a wide range of other applications requiring functional polysaccharide materials.

In particular, the grafting of polar polymer grafts onto a cellulosic derivative could be further explored by varying the types and molecular weights of the grafts for ETBE

purification. These variations would enable to analyze the influence of the grafted copolymer architecture on the membrane properties. Beyond the targeted application, this strategy could also be very useful for developing new high performance membranes for the separation of protic species from aprotic ones or the removal of aromatics from alkanes in the petroleum industry. Varying the type of "click" chemistry could also be interesting to avoid handling copper species always difficult to remove from the final polymer materials.

With respect to the last PhD work, the simple grafting of ionic liquids onto polysaccharides is certainly another issue offering great prospects for a lot of applications including membrane separations. The first results obtained in this PhD have shown that the grafting of molecular ionic liquids onto cellulose acetate greatly extended the scope of ionic liquid-containing membranes to the new field of liquid/liquid separations. In the future, it would be interesting to increase the amount of grafted ionic liquids by grafting poly(ionic liquid)s (PILs). By combining the approaches of chapters 2 and 3, it could be possible to incorporate very large amounts of ionic liquids, which would then be capable of percolating within the polymer membranes for achieving even better separation properties. Beyond the initial target of ETBE purification, this strategy could also offer new prospects for other challenging membrane processes including those related to CO_2 separations and capture. In particular, the problems associated with handling free ionic liquids in gas permeation membranes (like extraction or exudation) could be very well solved by extending the PhD strategy to ILs or PILs grafting. In the biomedical field, the grafting of ILs or PILs onto polysaccharides will keep developing for new bactericidal materials, gels and coatings.

UNIVERSITÉ DE LORRAINE

Autorisation de soutenance de thèse

Arrêté du 7 août 2006 relatif à la formation doctorale

Civilité, Nom, Prénom du doctorant : Madame HASSAN HASSAN ABDELLATIF Faten
École Doctorale : RP2E - Ressources Procédés Produits Environnement
Laboratoire : LCPM - Laboratoire de Chimie Physique Macromoléculaire

COMPOSITION DU JURY FINAL

NOM & PRENOM	ADRESSE COMPLETE (avec Téléphone et e-mail)	QUALITE	LABORATOIRE
JONQUIERES Anne	Laboratoire de Chimie Physique Macromoléculaire 1 rue Grandville BP 20451 54001 NANCY Cedex 54001 NANCY 06 26 46 96 38 anne.jonquieres@univ-lorraine.fr	Directeur de thèse - Professeur A int	Université de Lorraine/ENSIC
ESPUCHE Eliane	Laboratoire Ingénierie des Matériaux Polymères Bâtiment POLYTECH-Lyon 15, boulevard Latarjet 69622 VILLEURBANNE 69622 VILLEURBANNE 04 72 43 27 01 eliane.espuche@univ-lyon1.fr	Rapporteur - Professur A ext	Université de Lyon 1
ROBIN Jean-Jacques	Institut Charles Gerhardt UMR CNRS-UM2 5253 Université Montpellier 2 CC 1700 Place Eugène Bataillon 34095 MONTPELLIER Cedex 5 34095 MONTPELLIER Cedex 5 04 67 14 41 57 jean-jacques.robin@univ-montp2.fr	Rapporteur - Professeur A ext	Université Montpellier 2
ARNAL-HERAULT Carole	Laboratoire de Chimie Physique Macromoléculaire 1 rue Grandville BP 20451 54001 NANCY Cedex 54001 NANCY 03 83 17 52 42 carole.arnal-herault@univ-lorraine.fr	CoDirecteur de thèse - Maître de Conférences B int	Université de Lorraine/ENSIC ACT.

DECISION DE L'ECOLE DOCTORALE :

Au vu de la composition du jury et des rapports favorables, l'école doctorale autorise la soutenance de l'étudiante HASSAN HASSAN ABDELLATIF Faten.

Date le 24/2/16

Favorable

Signature

Stéphane DESOBRY
Directeur de l'École Doctorale n° 410
«Ressources-Procédés-Produits-Environnement»

DECISION DU PRESIDENT :

Au vu de la composition du jury et des rapports favorables, le Président autorise la soutenance de l'étudiante HASSAN HASSAN ABDELLATIF Faten.

Date

03 MARS 2016

Signature

Pour le Président et par délégation,
Le Vice-Président du CS

Frédéric VILLIERAS

Grafted cellulose acetate derivatives for the purification of biofuels by a sustainable membrane separation process

Abstract

During the industrial production of ethyl *tert*-butyl ether (ETBE) biofuel, this ether forms an azeotropic mixture containing 20 wt% of ethanol. Compared to the ternary distillation currently used for ETBE purification, the pervaporation membrane process could offer an interesting alternative and important energy savings. Cellulosic membranes have been mainly reported for this application. In particular, the selectivity of cellulose acetate (CA) was outstanding but its flux was too low. In this work, different grafting strategies were developed for improving the CA membrane properties for ETBE purification. The first strategy used "click" chemistry to graft CA with polylactide oligomers leading to original bio-based membranes for the targeted application. The grafting of ionic liquids onto CA was then investigated first by "click" chemistry (unsuccessful due to side reactions) and then by another two-step strategy implying simple nucleophilic substitution. A second series of cellulosic materials was obtained by grafting different ionic liquids containing the same bromide anion and different cations (imidazolium, pyridinium or ammonium) with increasing polar feature. A third series of new membrane materials was finally developed by exchanging the bromide anion with different anions Tf_2N^-, BF_4^-, and AcO^-. The membrane properties of all grafted CA membranes were finally assessed on the basis of the sorption-diffusion model, which revealed that both sorption and pervaporation properties were improved by the different grafting strategies.

Key words: cellulose acetate, grafting, "click" chemistry, polylactide, ionic liquids, membranes, bio-fuel, permeability, structure-property relationships

Dérivés greffés de l'acétate de cellulose pour la purification d'un biocarburant par un procédé de séparation membranaire dans une politique de développement durable

Résumé

Lors de la production industrielle du biocarburant éthyl *tert*-butyl éther (ETBE), cet éther forme un azéotrope contenant 20 % d'éthanol. Comparé à la distillation ternaire utilisée pour la purification de l'ETBE, le procédé membranaire de pervaporation pourrait offrir une alternative intéressante et d'importantes économies d'énergie. Des membranes cellulosiques ont principalement été décrites pour cette application. En particulier, la sélectivité de l'acétate de cellulose (CA) était extrêmement élevée mais son flux trop faible. Dans cette thèse, différentes stratégies de greffage ont été explorées pour améliorer ses propriétés membranaires. La première a mis en œuvre la chimie "click" pour le greffage d'oligomères polylactide, conduisant à des membranes bio-sourcés originales pour cette application. Le greffage de liquides ioniques (LIs) a ensuite été étudié, initialement par chimie "click" (échec dû à des réactions secondaires) puis par une autre stratégie en 2 étapes impliquant une simple substitution nucléophile. Une seconde série de matériaux cellulosiques a été obtenue avec des LIs contenant un même anion bromure et différents cations (imidazolium, pyridinium ou ammonium) de polarité croissante. Une troisième série de nouveaux matériaux membranaires a ensuite été développée en échangeant l'anion bromure par différents anions Tf_2N^-, BF_4^-, and AcO^-. Les propriétés membranaires de tous les matériaux greffés ont finalement été évaluées sur la base du modèle de sorption-diffusion, révélant que la sorption et la pervaporation étaient conjointement améliorées par les différentes stratégies de greffage développées.

Mots clés : acétate de cellulose, greffage, chimie "click", polylactide, liquides ioniques, membranes, biocarburant, perméabilité, relations propriétés-structures

Laboratoire de Chimie Physique Macromoléculaire UMR CNRS-UL 7375, ENSIC,

1 rue Grandville, BP 20451, 54001 Nancy Cedex.